

**Functional detection of
botulinum neurotoxin serotypes A-F
by monoclonal neoepitope-specific
antibodies**

Inaugural-Dissertation
to obtain the academic degree
Doctor rerum naturalium (Dr. rer. nat.)

submitted to the Department of
Biology, Chemistry and Pharmacy
of Freie Universität Berlin

by

Laura von Berg

2018

This work was carried out from February 2014 to June 2017 at Robert Koch Institute in the Centre for Biological Threats and Special Pathogens unit 3 (ZBS3) “Biological Toxins” guided by Dr. Brigitte G. Dorner.

1. Evaluator: Dr. Brigitte G. Dorner

2. Evaluator: Prof. Dr. Rupert Mutzel

Disputation on 26th March 2019

ACKNOWLEDGMENTS

Many kind people contributed to the success of this work, who I would like to gratefully thank at this point.

Many thanks to Dr. Brigitte Dorner for giving me the opportunity to work on such an interesting topic in her group at RKI, supervising and coordinating my project with such great enthusiasm and helpful advice, and appraising my thesis.

I furthermore thank Dr. Rupert Mutzel from FU Berlin who kindly agreed to appraise my thesis.

I gratefully thank my project partner from RKI Dr. Daniel Stern for his countless advice and helpful tips which tremendously contributed to the success of this work. In addition, I thank Daniel for always motivating me and proposing valuable solutions if results were unexpected and inconclusive.

Many thanks also to Dr. Martin Dorner from RKI for his opinion and excellent council in many technical challenges that came up throughout the thesis.

Furthermore, I would like to thank our collaboration partners from MHH, Dr. Andreas Rummel, Dr. Stefan Mahrhold, and Dr. Jasmin Weisemann for their excellent work in examining and generating the receptor constructs used in this work and their valuable contribution and advice in many vivid discussions on the FuMiBoNT project.

In addition, I am very thankful to Olena Shatohina and Kathrin Grunow for their technical support, which greatly contributed to experimental success and data collection. I also heartily thank Jacek Millert, Ewa Schlereth, Anna Kowalczyk, Dr. Sylvia Worbs, Dr. Bettina Kampa, Dr. Martin Skiba, the other PhD students Maren Krüger, Dr. Eva Hansbauer, Thea Neumann, and all other members from ZBS3 for the nice and friendly working atmosphere and their help in daily laboratory routine, especially during hybridoma screenings.

I genuinely thank my friends and family who always supported me and had an open ear and welcoming home if needed. With all my heart I thank Tom for his loving and motivating words when I was under stress, for supporting me all the time, and for having Jona with me who brought love and happiness into our lives beyond words.

TABLE OF CONTENTS

ACKNOWLEDGMENTS	I
TABLE OF CONTENTS	II
ABBREVIATIONS	VI
1 ABSTRACT	1
2 ZUSAMMENFASSUNG	2
3 INTRODUCTION	4
3.1 General aspects of botulinum neurotoxins	4
3.1.1 Botulism.....	5
3.1.2 Variability of BoNTs	6
3.2 BoNT mode of action	7
3.2.1 Receptor binding	10
3.2.2 Translocation of the LC into the cytoplasm.....	12
3.2.3 Substrate cleavage.....	12
3.3 Detection of BoNT.....	14
3.3.1 Challenges in BoNT detection.....	14
3.3.2 Animal experiments for BoNT testing	16
3.3.3 PCR based detection of <i>Clostridia</i> genes.....	18
3.3.4 Immunological detection methods	18
3.3.5 Endopeptidase activity assays	20
3.3.5.1 <i>Sensitivity of endopeptidase activity assays depends on BoNT</i> <i>substrate cleavage</i>	21
3.3.5.2 <i>Monitoring substrate cleavage by MS & FRET</i>	23
3.3.5.3 <i>Endopeptidase activity assays employing neoepitope specific</i> <i>antibodies (Neo-Abs)</i>	24
3.4 Aims of the thesis.....	27
4 MATERIAL AND METHODS	29
4.1 Materials.....	29
4.1.1 Chemicals and reagents.....	29
4.1.2 Buffers	30
4.1.3 Enzymes and antibodies used in immunological assays	33
4.1.4 Toxins.....	35
4.1.5 Substrate proteins and peptides	36
4.1.6 Animals	39
4.1.7 Cells, cell culture media, and reagents.....	39
4.1.8 Consumables	41
4.1.9 Kits	42
4.1.10 Devices.....	42
4.1.11 Software	44

TABLE OF CONTENTS

4.2	Methods.....	45
4.2.1	Cell culture.....	45
4.2.1.1	<i>Passaging of myeloma and hybridoma cells</i>	45
4.2.1.2	<i>Freezing and thawing of cells</i>	45
4.2.2	Handling of botulinum neurotoxins.....	45
4.2.2.1	<i>Safety issues</i>	45
4.2.2.2	<i>Production of Clostridia supernatants</i>	46
4.2.3	Generation of monoclonal antibodies.....	46
4.2.3.1	<i>Principle of generation of Neo-mAbs</i>	46
4.2.3.2	<i>Immunization of mice</i>	47
4.2.3.3	<i>Testing of antibody titer</i>	48
4.2.3.4	<i>Generation of antibody producing hybridoma cells</i>	48
4.2.3.5	<i>Screening</i>	50
4.2.3.6	<i>Subcloning</i>	50
4.2.3.7	<i>Quality controls</i>	51
4.2.3.8	<i>Antibody production and purification</i>	51
4.2.3.9	<i>Isotyping of monoclonal antibodies by sandwich ELISA</i>	52
4.2.4	Biochemical methods.....	52
4.2.4.1	<i>SDS-PAGE</i>	52
4.2.4.2	<i>Determination of protein concentration</i>	54
4.2.4.3	<i>Assembly of dual-Syt-II-Nanodiscs</i>	54
4.2.4.4	<i>Coupling of glutathione to casein</i>	55
4.2.4.5	<i>Coupling of antibodies or receptor molecules to M270- or M280 paramagnetic dynabeads</i>	55
4.2.4.6	<i>Coupling of substrate molecules to fluorescent magnetic luminex-beads</i>	56
4.2.4.7	<i>Biotinylation of antibodies</i>	57
4.2.4.8	<i>Trypsin digest of BoNT</i>	57
4.2.4.9	<i>Preparation of complex matrices for spiking experiments</i>	58
4.2.5	Immunological methods.....	58
4.2.5.1	<i>Western blotting to analyse specificity of Neo-mAbs</i>	58
4.2.5.2	<i>Surface plasmon resonance (SPR)</i>	59
4.2.5.3	<i>Indirect ELISA</i>	63
4.2.5.4	<i>Enrichment of toxin with paramagnetic beads</i>	64
4.2.5.5	<i>Endopeptidase-ELISA</i>	65
4.2.5.6	<i>Duplex-assay</i>	65
4.2.5.7	<i>Determination of assay performance of endopeptidase assays</i>	67
4.2.6	Optimization of cleavage conditions employing multifactorial Design-of-experiments (DoE).....	67
4.2.6.1	<i>Principle of the “Taguchi DoE” method</i>	67
4.2.6.2	<i>Substrate cleavage</i>	70
4.2.6.3	<i>SDS-PAGE for the analysis of substrate cleavage</i>	71
4.2.6.4	<i>Statistical analysis of Taguchi experiments</i>	72
4.2.6.5	<i>Validation of Taguchi-DoE with control experiments</i>	73
4.2.7	Formulas used for statistical analysis.....	73
5	RESULTS	76

TABLE OF CONTENTS

5.1	Optimization of BoNT substrate cleavage employing statistical experiments	76
5.1.1	Influence of buffer components varies between the different BoNT serotypes ...	76
5.1.2	Statistical analysis of L9 arrays identifies optimal buffer condition for each serotype.....	79
5.1.3	Comparison of optimized buffers with previously described reference buffer	82
5.1.4	Development of a consensus buffer for optimal cleavage of each serotype.....	83
5.2	Generation and characterisation of monoclonal neoepitope specific antibodies	85
5.2.1	Generation of Neo-mAbs.....	85
5.2.2	Characterisation of purified Neo-mAbs.....	89
5.2.2.1	<i>SPR measurements reveal different binding characteristics of Neo-mAbs</i>	89
5.2.2.2	<i>Characterisation by Western blotting and Endopeptidase-ELISA demonstrates exclusive specificity towards cleaved substrate</i>	93
5.2.2.3	<i>Comparison of Neo-mAbs in an endopeptidase activity assay</i>	97
5.2.2.4	<i>Summary of antibody characterisation.....</i>	98
5.3	Development of different assay formats for the detection of catalytically active BoNT by Neo-mAbs	103
5.3.1	Evaluation of an Endopeptidase-ELISA for the detection of catalytically active BoNT/A-F.....	103
5.3.1.1	<i>Endopeptidase-ELISA proves to be a robust assay with high sensitivities for the detection of catalytically active BoNT/A-F.....</i>	104
5.3.1.2	<i>Detection of BoNT activity from complex matrices required toxin enrichment</i>	106
5.3.1.3	<i>Sensitive detection of BoNT/A-F from spiked serum samples with the Endopeptidase-ELISA.....</i>	109
5.3.2	Development of a novel duplex-assay for the simultaneous detection of two distinct serotypes	111
5.3.2.1	<i>Duplex-assay allows for highly sensitive detection of BoNT/A-F.....</i>	113
5.3.2.2	<i>Detection of BoNT from spiked serum samples.....</i>	115
5.3.2.3	<i>Interlaboratory comparison of the BoNT/A + BoNT/B duplex-assay demonstrates robustness and transferability of the assay</i>	116
5.4	Implementation of receptor binding in the duplex-assay for the detection of BoNT/A and B	117
5.4.1	Optimized receptor constructs for the enrichment of BoNT/A and B	118
5.4.2	Sensitive detection of BoNT/A and B in a combined duplex-assay covering receptor binding and enzymatic activity	119
5.4.2.1	<i>Detection of BoNT/A and B from different sample matrices with the combined duplex-assay (receptor enrichment + enzymatic activity).....</i>	121
5.4.3	Subtype recognition of receptor molecules and monoclonal antibodies varies..	123
5.4.3.1	<i>Detection of BoNT from Clostridia supernatants with antibody- and receptor-based enrichment.....</i>	125
6	DISCUSSION	128
6.1	Design of optimized buffer conditions for BoNT/A-F employing statistical DoE.....	128
6.1.1	Previously published results could partially be confirmed by the Taguchi DoE analysis.....	130

TABLE OF CONTENTS

6.2	Generation and comprehensive characterisation of Neo-mAbs	131
6.2.1	Special immunization strategies and stringent screening procedure were required to generate a unique panel of Neo-mAbs	132
6.2.2	Thorough characterisation elucidates prominent features of Neo-mAbs	133
6.2.3	Neo-mAbs exhibit exquisite specificity towards their target cleavage sites	135
6.2.4	Suitability of Neo-mAbs for enzymatic detection of BoNT	135
6.3	Development of different approaches for the functional detection of BoNT	136
6.3.1	Detection of BoNT/A-F enzymatic activity	138
6.3.1.1	<i>Highly sensitive detection of BoNT/A-F by a straightforward Endopeptidase-ELISA</i>	<i>138</i>
6.3.1.2	<i>Implementation of the Luminex™ platform enables multiplex toxin detection.....</i>	<i>138</i>
6.3.1.3	<i>Detection of BoNT from human serum.....</i>	<i>139</i>
6.3.2	Duplex assay combining receptor binding and enzymatic activity for BoNT/A and B	140
6.3.2.1	<i>Suitability of receptor molecules for BoNT enrichment.....</i>	<i>141</i>
6.3.2.2	<i>Sensitive detection of BoNT/A and B from buffer and complex matrices</i>	<i>141</i>
6.4	Conclusion and outlook	143
7	REFERENCES.....	145
8	PUBLICATIONS	157
9	POSTERS AND TALKS	158
10	CURRICULUM VITAE.....	159
11	APPENDIX	160

ABBREVIATIONS

$A_{450-620nm}$	Absorption at 450 nm wavelength minus absorption at 620 nm wavelength
AH	Azaserine/Hypoxanthine
ANOM	Analysis of means
ANOVA	Analysis of variances
APS	Ammonium persulfate
BALB/c	Inbred laboratory mouse strain
BoNT	Botulinum neurotoxin
BSA	Bovine serum albumin
<i>C.</i>	<i>Clostridium</i>
CBPA	Cell based potency assay
CDC	US Centers for Disease Control and Prevention
CM5	Carboxy methyl dextran matrix 5
CM-dextran	Carboxymethyl-dextran
C-terminal	Carboxy-terminal
CV	Coefficient of variation
Da	Dalton [g/mol]
dB	Decibel
DIN	Deutsche Industrie-Norm
DMSO	Dimethyl sulfoxide
DNA	Deoxyribonucleic acid
DoE	Design of experiments
DTT	Dithiothreitol
e.g.	<i>exempli gratia</i> (Latin: for example)
EC50	Half maximal effective concentration
EDC	1-ethyl-3-(3-dimethylaminopropyl)carbodiimide
EDTA	Ethylenediaminetetraacetic acid
ELISA	Enzyme-linked Immunosorbent Assay
EtOH	Ethanol
FACS	Fluorescence-activated cell sorting
Fc	Flow cell
FCS	Foetal calf serum
FDA	US Food and Drug Administration
FRET	Förster resonance energy transfer
<i>g</i>	Acceleration due to gravity
GI	Gastrointestinal
GPG	G-protein purified

ABBREVIATIONS

h	Hour(s)
H6t	His-tag with thrombin cleavage site
HA	Hemagglutinin protein
HBS	HEPES buffered solution
HC	Heavy chain
H _c	C-terminal part of BoNT HC
HDA	Hemi diaphragm assay
HEPES	4-(2-hydroxyethyl)-1-piperazineethanesulfonic acid
H _N	N-terminal part of BoNT HC
HPLC	High performance liquid chromatography
HRP	Horseradish peroxidase
ibid.	<i>ibidem</i> (Latin: in the same place)
IgG	Immunoglobulin
IL-6	Interleukin 6
kDA	Kilo Dalton
KLH	Keyhole limpet hemocyanin
LC	Light chain
LD	Luminal domain
LD50	Lethal dose 50 (dose required to kill half of test animals)
LFA	Lateral flow assay
LOD	Limit of detection
M	Molar [mol/l]
mAb	Monoclonal antibody
MBA	Mouse bioassay
MeOH	Methanol
MFI	Median fluorescence intensity
MHH	Hannover Medical School
MLD50	Minimal lethal dose 50 (minimal dose required to kill half of test animals)
MS	Mass spectrometry
MSP	Membrane scaffold protein
NaCl	Sodium chloride
NAP	Neurotoxin associated protein
ND	Phospholipid-bilayer-nanodiscs
NEM	N-Ethylmaleimide
Neo-Ab	Neoepitope specific antibody
Neo-mAb	Monoclonal neoepitope specific antibody
NHS	N-Hydroxysuccinimide

ABBREVIATIONS

NMRI	Outbred laboratory mouse strain
No.	<i>numero</i> (Latin: number)
N-terminal	Amino-terminal
NTNH	Non-toxic non-hemagglutinin
pAb	Polyclonal antibody
PAGE	Polyacrylamide gel electrophoresis
PBS	Phosphate-buffered saline
PCR	Polymerase chain reaction
PEG	Polyethylene glycol
Pen/Strep	Penicillin/Streptomycin
POD	Peroxidase
PTC	Progenitor toxin complex
PVDF	Polyvinylidene fluoride
RCM	Reinforced Clostridial Medium
RKI	Robert Koch Institute
rpm	Revolutions per minute
RT	Room temperature
RU	Resonance units
S/N-ratio	Signal-to-noise-ratio
SA-PE	Streptavidin-phycoerythrin
SD	Standard deviation
SDS	Sodium dodecyl sulfate
SNAP	Synaptosomal-associated protein
SNARE	Soluble N-ethylmaleimide-sensitive-factor attachment receptor
SPR	Surface plasmon resonance
SV2	Synaptic vesicle glycoprotein 2
Syt	Synaptotagmin
TEMED	Tetramethylethylenediamine
TMAO	Trimethylamine N-oxide dihydrate
TMB	3,3',5,5'-tetramethylbenzidine
TPGY	Trypticase-Peptone-Glucose-Yeast Extract Broth
Tris	Tris(hydroxymethyl)aminomethane
v/v	Volume per volume
VAMP	Vesicle-associated membrane protein
w/o	without
w/v	Weight per volume
WHO	World Health Organization
β-ME	β-Mercaptoethanol

1 ABSTRACT

Botulinum neurotoxins (BoNTs) represent the most poisonous substances known and cause the rare but potentially life-threatening disease botulism. Diagnostics of botulism is a highly challenging task, as minute amounts of more than 40 different BoNT sero- and subtypes must be detected from complex sample matrices. To date, the gold-standard method for BoNT detection is still the ethically controversial mouse bioassay. BoNTs' high toxicity is mediated by an exquisite neurospecificity, determined by specific binding to neuronal receptors, combined with enzymatic cleavage of proteins involved in neurotransmitter release at serotype specific cleavage sites. Thus, enzymatically active BoNT can be monitored by substrate cleavage, while different serotypes can be distinguished by detection of the exact cleavage site.

In this work, functional *in vitro* approaches for highly sensitive detection of all clinically relevant BoNT serotypes A-F were established. To that aim, neoepitope specific antibodies (Neo-mAbs), recognizing the serotype specific cleavage sites of BoNT/A-F on their synaptic substrate molecule, were generated and thoroughly characterized. To achieve maximum sensitivity, cleavage conditions of all BoNT serotypes were optimized by statistical means. High affinity Neo-mAbs as well as optimal cleavage conditions were implemented in two distinct assay platforms enabling detection of BoNT/A-F: An Endopeptidase-ELISA for straightforward toxin detection and a novel Luminex™ duplex-assay for simultaneous detection of two distinct BoNTs. Furthermore, as an additional step of BoNT action, receptor binding was integrated in the duplex-assay for BoNT/A and B. All assays exhibited sensitivities comparable to the mouse bioassay and could detect BoNT from different complex matrices such as serum and foods. The unique tools generated in this work together with the established assay platforms therefore represent a major step forward towards the replacement of the mouse bioassay for botulism diagnostics.

2 ZUSAMMENFASSUNG

Botulinum Neurotoxine (BoNTs) sind die giftigsten bekannten Substanzen und lösen das seltene, aber lebensbedrohliche neurologische Krankheitsbild Botulismus aus. Die Diagnostik von Botulismus stellt eine große Herausforderung dar, da geringe Toxin-Konzentrationen von über 40 verschiedenen BoNT Sero- und Subtypen sicher aus komplexen Matrices erfasst werden müssen. Obwohl der Maus-Bioassay ethisch umstritten ist, wird er daher immer noch in der Routinediagnostik als Goldstandard verwendet. Die hohe Toxizität von BoNT begründet sich durch eine hochspezifische Bindung an neuronale Rezeptoren sowie der enzymatischen Aktivität. Letztere ist durch die Spaltung bestimmter an der Neurotransmitter-Ausschüttung beteiligter Proteine charakterisiert. Dabei spalten alle BoNTs bestimmte Substratproteine Serotyp-spezifisch an einer einzigen Peptidbindung. Die Detektion der spezifischen Spaltstellen auf den jeweiligen Substratproteinen ermöglicht somit zum einen die Unterscheidung einzelner Serotypen und zum anderen die Darstellung der enzymatischen Aktivität von BoNT.

In diesem Zusammenhang wurden in der vorliegenden Arbeit funktionelle *in vitro*-Methoden entwickelt, um alle klinisch relevanten BoNT Serotypen A-F hochsensitiv zu erfassen. Dafür wurden zunächst Neoepitop-spezifische monoklonale Antikörper (Neo-mAK) hergestellt und umfassend charakterisiert. Diese erkennen hochspezifisch durch BoNT geschnittenes Substrat, während ungeschnittene Substrate jeweils nicht erkannt werden. Des Weiteren wurden mit Hilfe eines statistischen Ansatzes erstmals optimale Spaltungsbedingungen für alle BoNT-Serotypen etabliert. Für den Nachweis von katalytisch aktiven BoNT/A-F wurden hochaffine Neo-mAKs sowie optimale Spaltungsbedingungen in zwei unterschiedliche Verfahren implementiert. Zum einen wurde ein Endopeptidase-ELISA entwickelt, der einen technisch einfachen Toxin Nachweis ermöglicht. Zum anderen wurde ein neuer Duplex-Assay, basierend auf der LuminexTM-Technologie etabliert, der erstmalig die parallele Erfassung zwei verschiedener Serotypen mittels Neo-mAK ermöglicht. Um einen weiteren funktionellen Aspekt des BoNT-Wirkungsmechanismus *in vitro* abzubilden, wurde zudem die Bindung von BoNT an seinen natürlichen neuronalen Rezeptor für BoNT/A und B im Duplex-Assay integriert.

Die etablierten Methoden zeigten ähnliche oder deutlich höhere Sensitivitäten wie der Maus-Bioassay. Des Weiteren gelang es mit allen Verfahren, BoNT aus verschiedenen komplexen

ZUSAMMENFASSUNG

Matrices hochsensitiv nachzuweisen. Die in der Arbeit hergestellten einmaligen Reagenzien sowie die neu etablierten Nachweisverfahren leisten daher einen wichtigen Beitrag, um den Maus-Bioassay in der Botulismus-Diagnostik mittelfristig durch ein *in vitro*-Verfahren ersetzen zu können.

3 INTRODUCTION

3.1 General aspects of botulinum neurotoxins

Botulinum neurotoxins (BoNTs) are the most toxic substances known and causative agents of the potentially fatal illness botulism. BoNTs are produced by different strains of anaerobe spore forming bacteria of the genus *Clostridia* (*C. botulinum*, *C. baratii*, and *C. butyricum*), which ubiquitously occur in soil, on plants, in water, and in the intestinal tract of animals [1]. Consequently, various potential sources of the toxin are found in the environment.

Botulism was first described in the early 19th century by the German physician Justinus Kerner, who identified poorly conserved ham as the source of the disease [2]. In 1895 van Ermengen was the first to identify BoNT produced by *Clostridium botulinum* as the disease-causing agent of a botulism outbreak in Belgium [3]. Since then, BoNT gained increasing attention by the medical community as both a highly potent disease-causing toxin as well as a potential therapeutic agent.

The discovery of BoNT's mechanism of action in the middle of the 20th century [4] – the blockage of neurotransmitter release at neuromuscular junctions – as well as the ability to produce pure toxin in considerable amounts paved the way for its application in the treatment of a variety of disorders. Today, BoNT is used to treat over 20 neurological and non-neurological disorders including spasticity, muscle spasms, or pelvic pain [5] and is furthermore used in cosmetics for the reduction of facial wrinkles [6].

Besides its roles as a disease-causing toxin and its effective use as a therapeutic agent, BoNT is, due to its extreme potency, considered as a biological weapon and listed as a category A agent by the US Centers for Disease Control and Prevention (CDC) [7].

In conclusion, all aspects regarding BoNT mentioned above demand for a reliable and sensitive detection of the toxin: The analysis of patient, food, or environmental samples for diagnostic purposes, the potency testing of batches of BoNT containing therapeutics, and finally the analysis of suspect substances in case of a biothreat scenario.

Detection of BoNT for diagnostic purposes is a highly challenging task as minute amounts of different disease-causing toxin variants must be reliably detected from complex sample matrices. Due to the lack of reliable and sensitive *in vitro* methods, the mouse bioassay (MBA) is the gold-standard method for botulism diagnostics requiring approximately 9000 mice per

INTRODUCTION

year (estimation of the RKI) in Germany. To reduce animal testing, a replacement method to the MBA is highly desirable.

3.1.1 Botulism

BoNTs cause the rare but potentially fatal neurological disease Botulism in humans and animals. The disease is characterized by a descending flaccid paralysis involving typical symptoms such as a blurred vision, ptosis, and/or diarrhoea followed by obstipation. In severe cases the disease affects the lungs, ultimately leading to death due to respiratory failure [8]. In Germany according to § 6 of the German Protection against Infection Act (*Infektionsschutzgesetz*) botulism or suspect cases of botulism are subject to registration with about 10 cases per year [9] reported.

Three different major forms of botulism in humans are described, depending on the route of toxin entry. Of those, the most common form in Germany is foodborne botulism, which is caused by the ingestion of contaminated food that contains the pre-formed toxin. Conversely, infant botulism is caused by the ingestion of unprocessed food that contains the spores of *Clostridia* which then germinate in the intestine. Here, colonization of the intestine by *Clostridia* and subsequent toxin production is facilitated due to an immature gut microbiota in infants [10]. Finally, wound botulism is caused by the introduction of *Clostridia* spores into deep wounds, where they germinate and produce toxin. This form of botulism is frequently found in injecting drug users [11, 12]. Another very rare form of botulism is iatrogenic botulism, which is caused upon excessive usage of BoNT for cosmetic or therapeutic purposes [13].

Treatment of botulism generally involves the application of antitoxin combined with supportive care. In cases of wound or infant botulism antimicrobial therapy may be applied. Since antitoxin can only neutralize BoNT as long as it resides in the circulation, a quick administration after intoxication is required. In very severe cases of botulism, intensive care treatment involving mechanical ventilation may be necessary for several weeks or even months. With appropriate treatment, the mortality rate of botulism ranges between 5%–10% [14], if left untreated, it is fatal in 40%–50% of cases [15].

INTRODUCTION

3.1.2 Variability of BoNTs

Since the recognition of BoNT as the disease-causing agent of botulism by van Ermengem in 1896, different BoNT variants have been discovered [3, 16]. Historically, different BoNTs are classified based on their neutralization by different antisera and grouped into seven widely accepted serologically distinct serotypes designated BoNT/A-G [17]. A further recently discovered but not yet classified serotype, is a hybrid between BoNT/A and F and named BoNT/H, BoNT/FA, or BoNT/HA [18-21]. Additionally, BoNT/X and BoNT/En (aka BoNT/J which is in contrast to all other serotypes not produced by *Clostridia* but by *Enterococcus faecium*) have been proposed as novel serotypes recently [22-24].

Botulism in animals is caused by serotypes C and D and its mosaic variants CD and DC, typically affecting husbandry and birds [16, 25, 26]. Contrary, serotypes A, B, E, and rarely F cause botulism in humans [25]. The novel identified serotype BoNT/HA has been associated with a single case of infant botulism so far [18]. No validated cases of human or animal botulism have been reported for BoNT/G, which was isolated from a soil sample [27].

For treatment of botulism, the present serotype has major implications, as antitoxins are only available against serotypes A, B, and E (trivalent antitoxin, GlaxoSmithKline, Middlesex, UK) or serotypes A-G (heptavalent antitoxin, Emergent BioSolutions Inc., Gaithersburg, USA).

Different BoNT serotypes are further divided into subtypes, which can differ remarkably on amino acid level [28, 29]. Amino acid sequences of different subtypes differ up to 16% for BoNT/A, 7% for BoNT/B, 11% for BoNT/E, and with the highest subtype variability with up to 36% for BoNT/F [29]. Until now more than 40 different sero- and subtypes have been identified and the number is expected to be further growing (Figure 1). Despite this large variability, all BoNT sero- and subtypes are structurally similar, employ the same mode of action for intoxication, and consequently induce the same symptoms – a flaccid paralysis – in BoNT sensitive organisms [30].

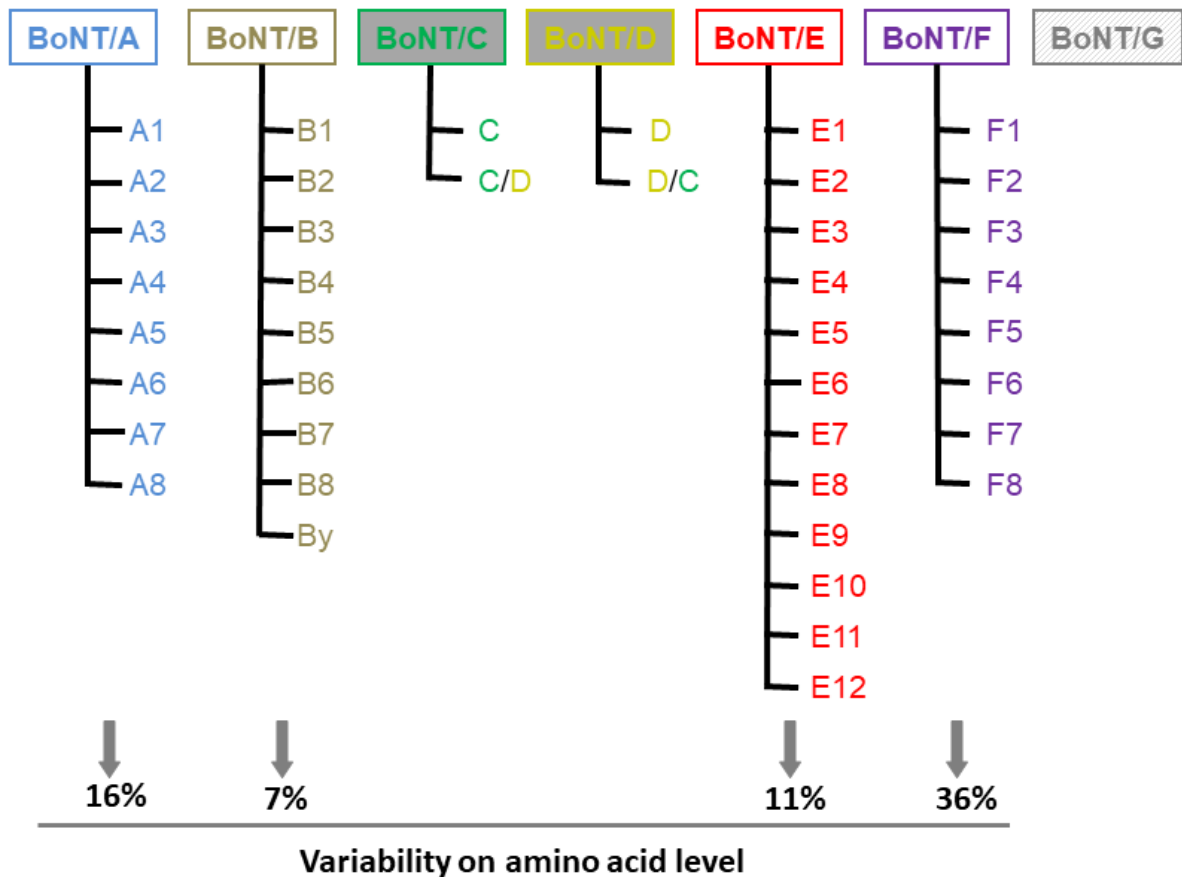


Figure 1: Overview on BoNT sero- and subtypes. Seven widely accepted serologically distinct serotypes designated BoNT/A-G have been identified so far. Each serotype groups a number of different subtypes or mosaic variants as indicated. Serotypes shown with a grey background are pathogenic to animals, whereas serotypes shown with a white background are pathogenic to humans. BoNT/By is a novel subtype isolated at RKI that has not been assigned officially yet. For BoNT/G no confirmed botulism case has been demonstrated yet. Data illustrated here was retrieved from [1, 28, 31-36].

3.2 BoNT mode of action

Intoxication with BoNT occurs most commonly through the ingestion of contaminated food, which contains the pre-formed toxin. Consequently, BoNT is taken up through the gastrointestinal (GI) tract and must pass the intestinal barrier to enter the circulation. To survive the harsh conditions residing in the stomach and GI tract, such as a low pH and host proteases as well as to adsorb to and pass the epithelial gut barrier, BoNT is produced in association with non-toxic neurotoxin associated proteins (NAPs) forming progenitor toxin complexes (PTC) [37]. In the smallest PTC, designated M-PTC, BoNT associates with a non-toxic non-hemagglutinin (NTNH) protein. Larger PTCs (L-PTC) are composed of hemagglutinin proteins (HA-17, HA-33, and HA-70) added to the M-PTC [38] forming a propeller like structure with three arms (Figure 2, A) [39-41]. While NTNH shields BoNT in the GI tract and protects it

INTRODUCTION

from inactivation by low pH and degradation [42], HA-proteins play a role in the adsorption to epithelial cells and subsequent transcytosis of the complex [43]. After crossing the epithelial barrier, BoNT enters the blood stream, dissociates from its accessory proteins, and migrates to motorneurons [44, 45].

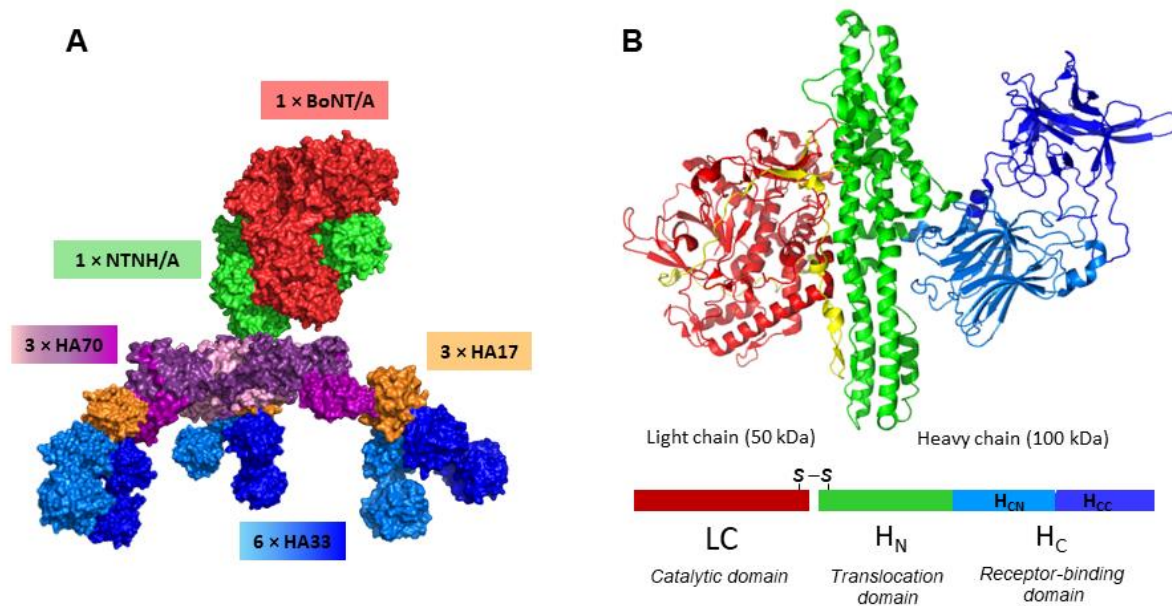


Figure 2: Structures of L-PTC complex (A) and isolated BoNT molecule (B). (A) Organization of the L-PTC in a propeller like structure with BoNT/A1 (red) forming a tight complex with NTN/A1 (green) and associated HA proteins HA-70 (purple), HA-17 (orange) and HA-33 (blue). The image was kindly provided by Maren Krüger, RKI and was modified after Lam and Jin et al [38] (PDB IDs: 3V0A (M-PTC), 4LO4 (HA70), 4LO0 (HA70 and HA33)). (B) Crystal structure of BoNT/B1 (PDB ID: 1EPW [46]) showing the three different domains of the toxin: The enzymatically active LC (red), and the HC consisting of the translocation domain H_N (green) and the receptor binding domain H_C (H_{CN} in light blue and H_{CC} in dark blue). A peptide belt linking the LC to the HC is shown in yellow.

The high potency of BoNT with an approximate lethal dose (LD₅₀) to humans of 1 ng/kg body weight (intravenously or intramuscularly) [47, 48] is primarily determined by its highly selective neurospecificity as well as its catalytic activity both relying on the unique structural characteristics of BoNT molecules.

Despite the large variability of different BoNT molecules, all BoNTs are synthesized as 150 kDa proteins that can be divided into the same structural and functional units: A 50 kDa enzymatically active light chain (LC) and a 100 kDa heavy chain (HC) which are additionally linked via a single inter-chain disulphide bond (Figure 2, B). For enzymatic activity, the LC must be proteolytically cleaved from the HC, which is mediated through clostridial or – in the case of non-proteolytic *Clostridia* strains – host proteases. The HC of the toxin is further divided

INTRODUCTION

into a 50 kDa N-terminal domain termed H_N , which mediates the translocation of the toxin into the cytoplasm, and a 50 kDa C-terminal receptor binding domain, termed H_C , which is composed of an N-terminal (H_{CN}) and a C-terminal (H_{CC}) part [25].

The mechanism of BoNT action involves three major steps (Figure 3, A): First is the binding to selective receptors on presynaptic membranes at neuromuscular junctions, mediated by the H_C and its uptake into recycling synaptic vesicles. Second is the translocation of the LC into the cytoplasm which is facilitated by the H_N and third is the cleavage of proteins involved in synaptic vesicle fusion facilitated by the LC. Said cleavage blocks the release of neurotransmitters into the synaptic cleft. Since BoNT selectively targets motor neurons it induces muscle paralysis by inhibiting acetylcholine mediated signal transmission at neuromuscular junctions [49].

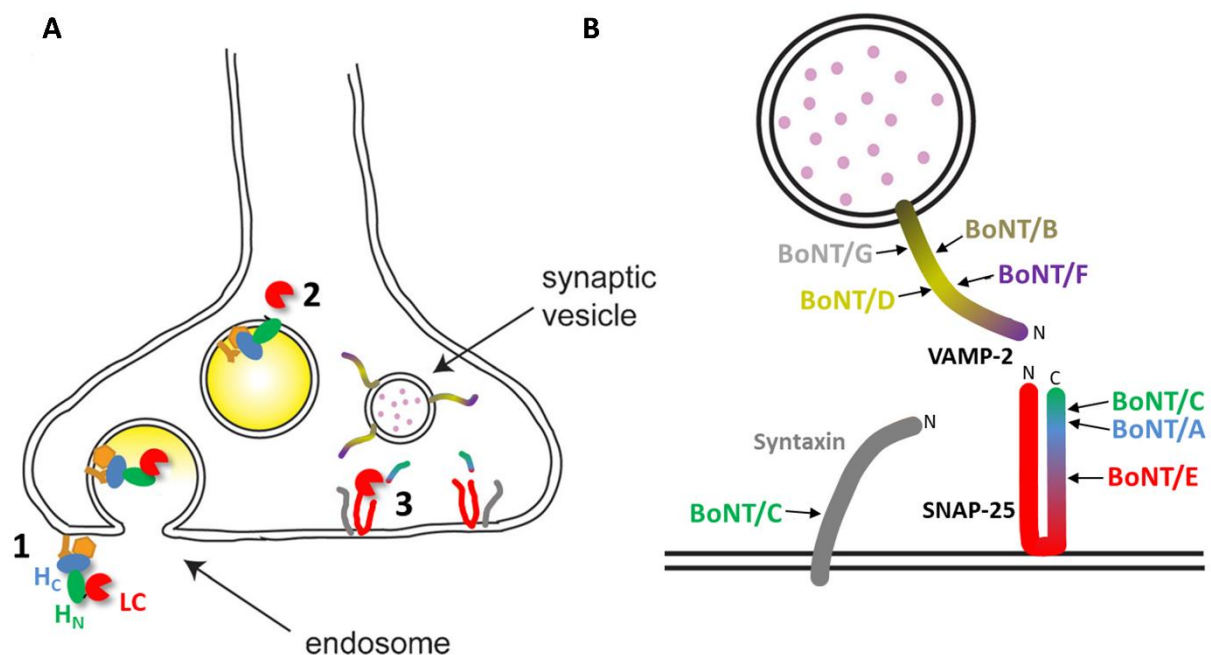


Figure 3: Mechanism of BoNT action. (A) BoNT mechanism of action involves three major steps: The binding of the toxins H_C (blue) to specific receptors (orange) at presynaptic membranes (1). The translocation of the LC (red) into the cytosol (2) and the cleavage of proteins involved in synaptic vesicle recycling by the LC (3). (B) Different BoNT serotypes cleave different proteins of the SNARE-complex. BoNT/A, E, and C cleave SNAP-25, whereas BoNT/B, D, F, and G cleave VAMP. BoNT/C is the only serotype that has two substrates cleaving SNAP-25 and syntaxin. The cleavage site of BoNT/HA as well as BoNT/F5, which is four amino acids upstream of BoNT/F is not shown in this image. The image was modified after [50].

3.2.1 Receptor binding

BoNTs strict selectivity for motor neurons is mediated by the binding to specific receptors on presynaptic membranes at neuromuscular junctions. Since BoNT is usually present in very low concentrations after entering the circulation, a highly efficient uptake mechanism is required for intoxication. To that aim, BoNTs evolved a unique dual-receptor binding mode, which is based on the presence of two independent binding regions in the H_{CC} of the toxin [51]. The current view on BoNT receptor binding proposes an initial interaction with polysialogangliosides such as GD1a or GT1b, followed by a more stable binding to specific neuronal protein receptors [52, 53]. In the course of this work, the classical dual-receptor binding paradigm has been extended by a third lipid-based interaction [54].

Polysialogangliosides consist of a hydrophobic ceramide moiety and a carbohydrate proportion, which is presented on the outer surface of cells [55] and recognized by the H_{CC} of BoNT. The ganglioside-binding motif in the H_{CC} of BoNT/A, B, E, F, and G is conserved, whereas BoNT/C and D exhibit different binding mechanisms [56]. Polysialogangliosides are abundantly present on synaptic membranes and associated together with glycoproteins in membrane microdomains [55]. Therefore, they present an efficient way to accumulate the scarcely present BoNT molecules on synaptic membranes.

After the initial contact to membranes through gangliosides, BoNT additionally interacts with specific neuronal receptors creating a high affinity binding. So far two different neuronal receptors for BoNTs have been identified: Synaptotagmin (Syt) isoforms I and II and synaptic vesicle glycoprotein 2 (SV2) isoforms A, B, and C. Syt and SV2 both are involved in synaptic vesicle cycling and are therefore located in the lumen of synaptic vesicles or, after membrane fusion of vesicles, on the outer surface of neuronal membranes.

Syt is a synaptic vesicle protein that is involved in the regulation of synaptic vesicle exocytosis by sensing intracellular calcium concentrations [57]. It has an intracellular calcium sensing C-terminal domain and a luminal N-terminal domain, which is exposed on cell surfaces upon vesicle fusion with the cell membrane. Both segments are connected through a single transmembrane domain (Figure 4). Syt has been identified as a receptor for BoNT/B, DC, and G [58-61].

Akin to Syt, SV2 is presumably involved in synaptic vesicle cycling by rendering primed synaptic vesicles fully calcium responsive [62, 63]. It contains twelve transmembrane domains with

INTRODUCTION

three cytosolic domains and one highly glycosylated large luminal domain 4 (LD4) (Figure 4). SV2 has been shown to bind BoNT/A and E [64-67]. BoNT/F and D are also believed to bind to SV2 but a direct protein-protein interaction has not yet been demonstrated [68-70].

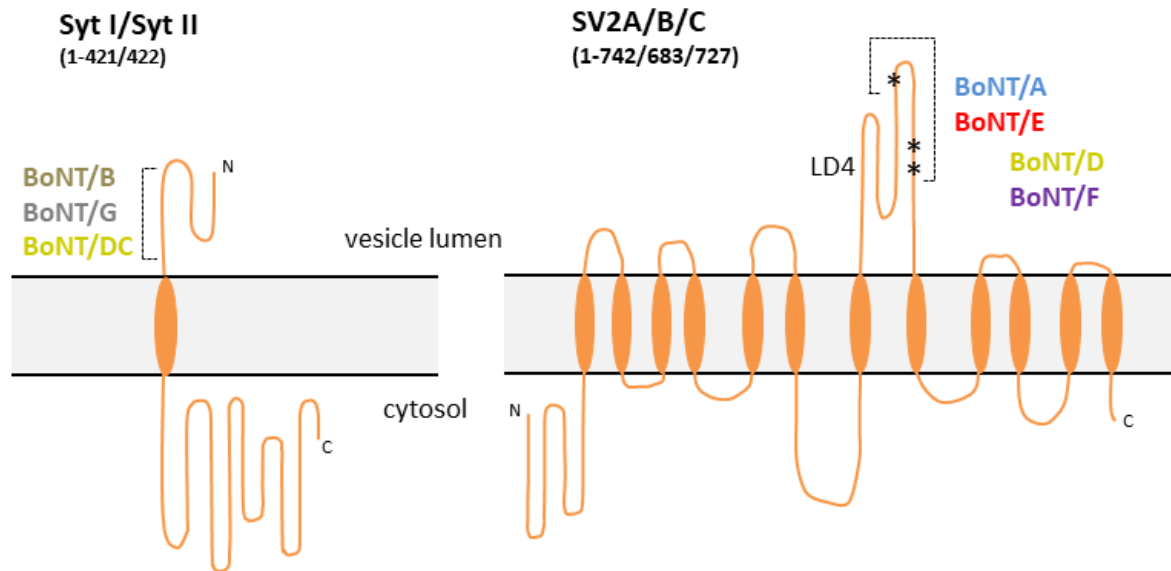


Figure 4: Identified receptors for different BoNT molecules. Syt-I and Syt-II are membrane proteins consisting of 422/421 amino acids. The N-terminal part of the protein faces towards the vesicular lumen and serves as receptor for BoNT/B, G, and presumably also DC (segment mediating binding is shown in brackets). SV2A, SV2B, and SV2C are large (742/683/727 amino acids) membrane glycoproteins harbouring 12 putative transmembrane domains. The LD4 in the C-terminal part of the protein faces towards the vesicular lumen and mediates binding of BoNT/A and E (segment mediating binding is shown in brackets) and presumably also D and F. Asterisks indicate glycosylation sites in the LD4 of SV2.

BoNT/A binds all three isoforms of SV2, having the highest affinity for SV2C. Recently it has been demonstrated that glycosylation of the luminal domain 4 (LD4) of SV2C, particularly at position N559, is crucial for high affinity binding to BoNT/A [71, 72]. Other than BoNT/A, BoNT/E binds to SV2A and SV2B, but does not bind SV2C [70]. It also requires glycosylation at specific residues of SV2A or B for sufficient binding, as no interaction is observed with bacterially expressed SV2 [65]. Compared to BoNT/A and E, data on SV2 binding to BoNT/D and F is scarce and requires further investigation to verify the proposed interactions. It has been demonstrated that BoNT/D co-precipitated SV2A and B from solubilized rat brain extracts [70], whereas BoNT/F co-precipitated with all three SV2 isoforms from synaptic vesicle lysates [68, 69]. For BoNT/C no protein receptor has been identified so far and it presumably solely uses gangliosides as receptor [73, 74].

INTRODUCTION

In summary, BoNTs efficient uptake into neuronal cells is mediated by a dual- or ternary-receptor binding mechanism exploiting gangliosides to accumulate the toxin on neuronal membranes and the specific neuronal receptors Syt or SV2 and putatively also lipids to facilitate high affinity binding and subsequent cellular entry.

3.2.2 Translocation of the LC into the cytoplasm

After receptor binding, BoNT enters the cell by endocytosis through recycling vesicles. To execute its enzymatic activity BoNT LC has to be translocated from the vesicle lumen into the cytosol. The mechanism by which the LC is translocated into the cytosol is not fully understood. The current proposed model suggests that acidification of the vesicular lumen induces substantial conformational changes in BoNTs LC and H_N. This leads to the insertion of the H_N into the membrane facilitating the transport of the LC into the cytosol [25].

Notably, the LC remains connected to the HC via its disulphide bridge for transport until it reaches the cytosol [75]. Reduction takes place after the LC enters the cytosol and is mediated by different cytosolic enzymes. After reduction, the translocation process of the LC is irreversible (ibid.).

3.2.3 Substrate cleavage

The third major step of BoNT action is the enzymatic cleavage of proteins involved in synaptic vesicle recycling mediated by the toxins LC. This step ultimately leads to the blockage of neurotransmitter release at neuromuscular junctions inducing paralysis of the muscle.

Proteins targeted by the different BoNT serotypes are components of the soluble N-ethylmaleimide-sensitive-factor attachment receptor (SNARE) complex. SNARE-complexes are the core machinery for the fusion of neurotransmitter loaded synaptic vesicles with the synaptic membrane, thereby facilitating neurotransmitter release into the synaptic cleft. In neuronal cells, the SNARE-complex is formed by three proteins: vesicle-associated membrane protein (VAMP, also termed synaptobrevin), synaptosomal-associated protein 25 (SNAP-25), and syntaxin 1, all of which harbour a 60–70 amino acid SNARE motif [76]. VAMP and syntaxin 1 are anchored to vesicular membranes, whereas SNAP-25 is linked to the cellular membrane. Through their SNARE motifs the three SNARE proteins can form a tightly associated complex which initiates membrane fusion [76]. The SNARE complex proteins are

INTRODUCTION

essential players in synaptic vesicle cycling including neurotransmitter release and synaptic signalling which can be disturbed through cleavage by BoNT.

Different BoNT serotypes cleave different SNARE proteins at specific sites: BoNT/A, E, and, C cleave SNAP-25, whereas BoNT/B, D, F, and HA cleave VAMP. BoNT/C is the only serotype that has two substrates cleaving SNAP-25 and syntaxin (Figure 3, B and Figure 5) [49, 77]. All subtypes of one serotype share the same unique cleavage positions. Thus, the different BoNT serotypes A-HA, including all known subtypes, can be distinguished by only eight specific cleavage sites. The only exception to this rule is BoNT/F5, which cleaves VAMP four amino acids upstream of all other BoNT/F subtypes [78]. Notably, the novel proposed serotype BoNT/HA has the same cleavage site as BoNT/F5 [19].

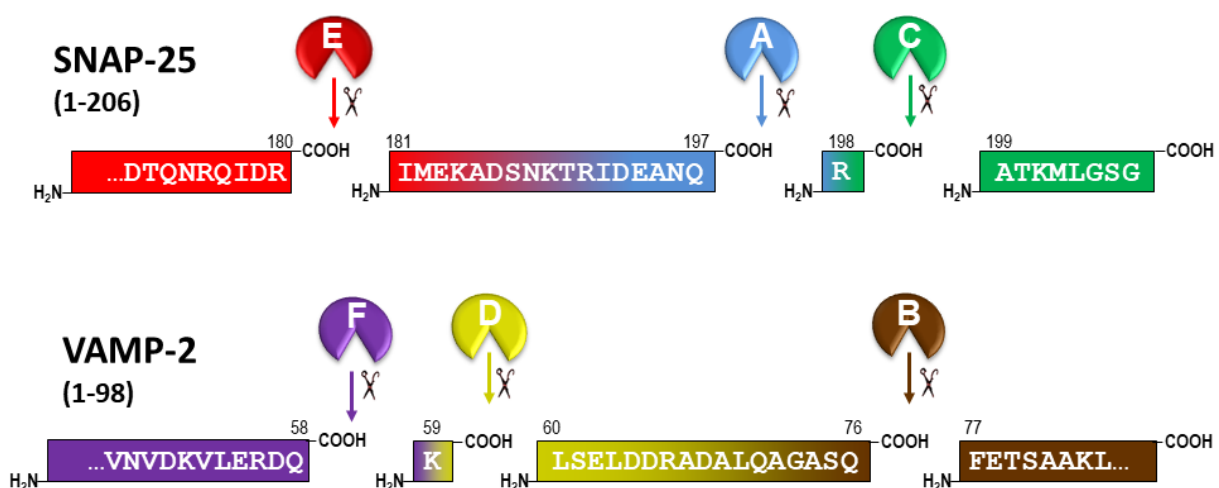


Figure 5: Cleavage sites of different BoNT serotypes on SNAP-25 or VAMP-2. Different BoNT serotypes cleave SNAP-25 or VAMP-2 at specific positions and can therefore be discriminated by their substrate specificity. BoNT/E, A, and C cleave SNAP-25 at positions 180/181, 197/198, and 198/199 respectively. BoNT/F, D, and B cleave VAMP-2 at positions 58/59, 59/60, and 76/77 respectively. Note that cleavage sites of BoNT/A and C as well as BoNT/F and D differ by only a single amino acid. Not shown is the cleavage site of BoNT/HA and BoNT/F5 on VAMP-2 at position 54/55.

SNARE protein cleavage by BoNT LCs is mediated through a conserved Zn^{2+} dependent metalloprotease activity and all BoNT LCs harbour a strictly conserved HExxH motif in their active sites, typically found in metalloproteases [79]. To efficiently cleave their substrate, the specific peptide bond to be hydrolysed must be properly placed near the HExxH motif. This can only be achieved by extensive interactions between LC and SNARE protein. Indeed, besides binding to the active site, crucial interactions between the SNARE proteins and BoNT

INTRODUCTION

LCs have been identified [80]. Said interactions were found to be far distant from both, the cleavage site on the target SNARE protein and the LCs active site. Several, so called exosites, have been found in BoNT LCs, accounting for their exquisite substrate specificity [50, 81].

3.3 Detection of BoNT

3.3.1 Challenges in BoNT detection

Sensitive detection of BoNT is required in two major applications: The detection of BoNT from patient, food, or environmental samples for diagnostics of suspect cases of botulism and the potency testing of BoNT containing products for pharmaceutical or cosmetic purposes [82]. Due to BoNTs high potency, detection methods in both applications need to be extremely sensitive with detection limits in the low pg/mL range whereas other requirements considerably vary (summarized in Table 1).

Detection of BoNT for diagnostic purposes requires the detection of all known and unknown disease-causing sero- and subtypes (see section 3.1.2). Knowledge on the present serotype is crucial for patient treatment, as different antitoxins, with different neutralizing capacities, are available. On the other hand, knowledge on the subtype present may be beneficial to provide epidemiological information about the disease, especially in outbreak situations [88]. The detection of all BoNT sero- and subtypes is a major diagnostic challenge usually requiring an individual assay for each serotype. In contrast, for potency testing of pharmaceutical products, the BoNT subtype present is defined through the production process and known before testing. An adequate assay for detection can be chosen accordingly.

The avoidance of interference with matrix components is another challenge in botulism diagnostics. Depending on the form of botulism, sample matrices can be heterogeneous including patient samples such as serum, feces, intestinal contents, wound swabs, pus, or tissues as well as environmental and food samples [88]. As invariably all assay systems are influenced by various matrix component, the compatibility with different sample matrices must be individually evaluated for each assay. Contrary, pharmaceutical products contain highly pure toxin solutions in a known physiological buffer. Here, matrix interference does not play a role for detection.

INTRODUCTION

To take effective counter-measures after intoxication with BoNT, a rapid diagnosis is important. For a beneficial effect, antitoxin should be administered as soon as possible after intoxication [15]. Hence, in botulism diagnostics the time to result is critical and should be kept to a minimum. This is less relevant for pharmaceutical BoNT products as the production process itself is time-consuming.

For diagnostic purposes, the exact determination of the toxin concentration in a sample is not crucial. The confirmation of the presence of the toxin and the toxin producing organism in combination with a clinical picture and/or an epidemiological context is usually sufficient for positive diagnostics [82, 83]. In contrast, potency testing of BoNT containing products for medical applications requires the exact, statistically valid determination of toxin concentration.

Finally, detection methods for both, diagnostics of botulism as well as potency testing of BoNT, should ideally be able to detect fully functional toxin. However, for botulism diagnostics, a rough estimate of the toxin's functional activity is sufficient. Contrary, the representation of all mechanistic steps of BoNT action is fundamental for pharmaceutical products, as only fully functional toxin has the desired therapeutic effect [84].

Table 1: Comparison of different requirements for the detection of BoNT for diagnostic purposes or potency testing of pharmaceutical products.

Botulism diagnostics	Potency testing of pharmaceutical products containing BoNT
Detection of all sero- and subtypes and all possible toxin complexes	Predefined known sero- and subtype must be detected
Detection from complex matrices (patient samples, food, environmental samples)	Detection from predefined known solution (physiological buffer)
Time to result is critical for therapeutic interventions	Time to result is less critical
Range of toxin concentration is sufficient	Highly precise statistically valid toxin concentration needs to be determined
Rough estimate of toxin's functional activity is sufficient	All steps of BoNT action must be reflected (receptor binding, translocation, enzymatic activity)

INTRODUCTION

Summing up, detection of BoNT for diagnostic purposes requires the detection of all sero- and subtypes from a large variety of different sample matrices in a limited time frame. For potency testing of pharmaceutical products, fully functional toxin of a predefined BoNT subtype needs to be detected from a known physiological buffer with exquisite precision.

Numerous assays for BoNT detection have been developed in the past. These include *in vivo* and *ex vivo* approaches as well as a large variety of different *in vitro* approaches. The latter comprise cell based assays, PCR-based approaches for the detection of toxin genes, immunological methods for direct toxin detection, or functional approaches such as endopeptidase based assays which monitor the toxin's catalytic activity. However, due to the high requirements for BoNT detection in the different applications, the "gold standard" laboratory test is still the MBA.

3.3.2 Animal experiments for BoNT testing

In vivo and *ex vivo* methods have the advantage of only detecting fully functional toxin by depicting all three steps of BoNT action: Receptor binding, translocation of the catalytically active LC into the cytoplasm, and cleavage of target proteins ultimately inducing muscle paralysis. In addition, respective methods usually exhibit a high sensitivity and specificity and can detect all disease-causing sero- and subtypes. The most common approaches are the MBA and the phrenic nerve hemidiaphragm assay (HDA). Other non-lethal *in vivo* methods include assays measuring the local paralysis induced by BoNT, for example digit abduction (DAS assay), hind limb paralysis (locomotor activity assay), grip strength, or toe-spread reflex [82, 83].

Mouse bioassay (MBA)

The MBA was introduced in 1920 and is still the "gold standard method" in botulism diagnostics and the officially accepted method for confirmation of active BoNT by international regulatory agencies (e.g. German Standard DIN10102 or AOAC Official Method 977.26).

In the MBA, a BoNT containing sample is injected intraperitoneally into mice and animals are monitored for symptoms of botulism for up to four days. Typical symptoms include laboured breathing, weakness of limbs, a wasp-like abdomen, and eventually death due to respiratory failure [85]. The assay is highly ethically controversial as it imposes pain and distress on the laboratory mice. In addition, for a comprehensive sample analysis including serotyping by

INTRODUCTION

neutralizing antibodies, and determination of toxin concentration by sample dilutions up to 40 mice per sample are required.

Advantages of the MBA are its high sensitivity with detection limits between 10–100 pg/mL depending on the serotype tested, the presentation of all mechanistic steps of BoNT action, the ability to detect all potentially disease-causing sero- and subtypes including any unknown toxin variants, and the compatibility with most sample matrices including serum, gastric content, wound samples, and bacterial cultures [16, 86].

The MBA also has major drawbacks. Besides the ethical concerns mentioned above, the assay is time-consuming as it can take up to four days to achieve results, which may be critical in diagnostic settings. Additionally, results cannot directly be transferred from mice to human due to variations regarding toxicity in distinct species. This could be explained by e.g. differences in the sequences of target receptors [87]. Furthermore, the MBA is restricted to laboratories with an animal facility and highly trained staff. Finally, the assay requires large sample volumes and exhibits a rather high interlaboratory variability [88].

Phrenic nerve hemidiaphragm assay (HDA)

The HDA is an *ex vivo* test which is performed with preparations of phrenic nerve connected with hemidiaphragm muscle from sacrificed mice or rat [4]. By electrical stimulation of the nerve muscle twitches can be measured which decrease upon the addition of BoNT due to paralysis. Akin to the MBA, the method is very sensitive (with similar detection limits as the MBA), displays all steps of BoNT action, and allows the detection of all sero- and subtypes. Corresponding to the MBA, the usage of neutralizing antibodies allows for serotyping. The HDA can be performed in a much shorter duration than the MBA (< 4 h) and requires fewer animals, as multiple samples can be tested with one preparation. In addition, the pain imposed on animals is greatly reduced compared to the MBA [89].

However, the assay still requires animals and can also only be performed by laboratories with an animal facility and experienced staff. Another disadvantage of the method is that compatibility with different sample matrices has not been thoroughly tested yet. The HDA is therefore only of limited use for botulism diagnostics.

3.3.3 PCR based detection of *Clostridia* genes

PCR-based techniques are a common tool for the detection of pathogens and due to their high sensitivity, short duration, and simplicity widely performed. With regard to botulism diagnostics, PCR-based techniques are used to detect *Clostridia* genes, *bont* genes, and/or complex genes, from patient or food samples or bacterial cultures [82, 83]. The detection of *bont* genes from feces or intestinal contents is of great interest, as they usually contain the bacteria, and other methods aiming at toxin detection often fail due to matrix interferences. The development of multiplex methods employing quantitative real-time PCR (qPCR) techniques enabled the highly sensitive simultaneous detection of multiple BoNT serotypes from a single sample [90-93]. Knowledge on the exact subtype can be achieved by whole genome sequencing, which is increasingly used due to advancements in sequencing technologies and has implications in epidemiological outbreak investigations. Sequence variations of different BoNT subtypes can, however, lead to false negative results in PCR-based techniques, when mutations occur in the primer binding sites. Furthermore, as BoNT alone may cause botulism, irrespective of the presence or absence of the producing organism the sole detection of *C. botulinum* genes is insufficient for diagnostics. In addition, PCR-based techniques are not able to determine toxin concentration or discriminate between intact and silent genes. However, they represent an additional useful tool to complement other diagnostic assays for BoNT detection.

3.3.4 Immunological detection methods

Immunological detection systems for BoNT are by far the most commonly used *in vitro* method and numerous assays have been developed in the past [82, 94, 95]. The general principle of immunological methods is to detect BoNT with a capture antibody that immobilizes the toxin on a surface and a detection antibody conjugated to a suitable reporter for signal read-out. Binding epitopes of capture and detection antibodies must vary. For BoNT detection either polyclonal or monoclonal antibodies may be used. Polyclonal antibodies are antibodies that originate from multiple B-cell lineages in the body and represent a heterogeneous mixture of different antibodies covering multiple epitopes on the target protein. In contrast, monoclonal antibodies originate from a single parental B-cell clone and recognize a unique epitope on the target protein.

INTRODUCTION

Immunological methods have the advantage of being very simple and fast to perform (within one working day), have – depending on the antibodies used – a high sensitivity (comparable to the MBA), are highly reproducible, and compatible with a range of matrices. Assay sensitivity and matrix compatibility markedly depend on the antibodies used for detection. One major drawback of immunological BoNT detection is the risk of false negative results, when certain BoNT subtypes are not recognized. This may be the case when mutations in a specific subtype occur within the binding epitopes of capture or detection antibody. Due to the large variability between different BoNT subtypes (of the same serotype) with up to 36% divergence on amino acid level it is most likely that some subtypes are missed out, especially when monoclonal antibodies are used for detection. Polyclonal antibodies are, however, less suitable for the detection of BoNT from complex matrices than monoclonal antibodies, as they are more prone to provoke false positive results due to matrix interference. Immunodetection of BoNT furthermore has the disadvantage that inactivated toxin might be detected (e.g. after heating), as a discrimination of functional active and inactive toxin is usually not possible by the method. Despite these limitations, immunological methods are very useful for an initial screening of suspect samples, as they deliver fast results and are easy to perform. This is especially convenient, when large sample numbers must be analysed. Still, one should keep in mind that false positive or negative results may occur and always use additional methods for confirmation.

Sandwich Enzyme-linked Immunosorbent Assay (ELISA)

The most common method for immunological detection of BoNT is the classical sandwich ELISA. Here, the capture antibody is immobilized on a plastic microtiter plate with high protein-binding capacity. Toxin containing sample is then added for toxin capture. Finally, signals can be detected by the addition of a detection antibody coupled to a reporter, e.g. horseradish peroxidase (HRP). The reporter converts a chromogenic substrate (in the case of HRP as reporter 3,3',5,5'-tetramethylbenzidine (TMB)), to a coloured product. By the addition of acid (H_2SO_4), conversion is stopped, and the signal intensity can be quantified spectroscopically using a plate reader.

Luminex™ technology

To reduce experimental effort as well as sample and material consumption, bead-based immunoassays using the Luminex™ technology that allow for the analysis of multiple samples

INTRODUCTION

in parallel were developed. In respective assays, the principle of the classical ELISA format is transferred onto magnetic polystyrene beads. Here, the capture antibody is immobilized on beads to capture toxin from solution. Beads with captured toxin can then magnetically be separated from the solution. This principle enables the enrichment of toxin from larger sample volumes as well as an extraction of toxin from complex matrices. For detection, a detection antibody is employed which is either directly or indirectly coupled to a fluorescent reporter molecule. Sample read-out is then facilitated by flow cytometry. The Luminex™ xMAP technology employs beads labelled with different ratios of two (or three) different fluorescent dyes. Bead sets with up to 100 (or 500) differently labelled luminex-beads are available, which can be spectrally discriminated. Diverse capture antibodies can be coupled to differently labelled luminex-beads and thereby different immunoassays, detecting distinct antigens, can be performed in parallel from one sample (assay principle see Figure 6). This system has successfully been used for the development of a highly sensitive pentaplex assay, enabling the simultaneous detection of five different toxins, including BoNT/A and B [96].

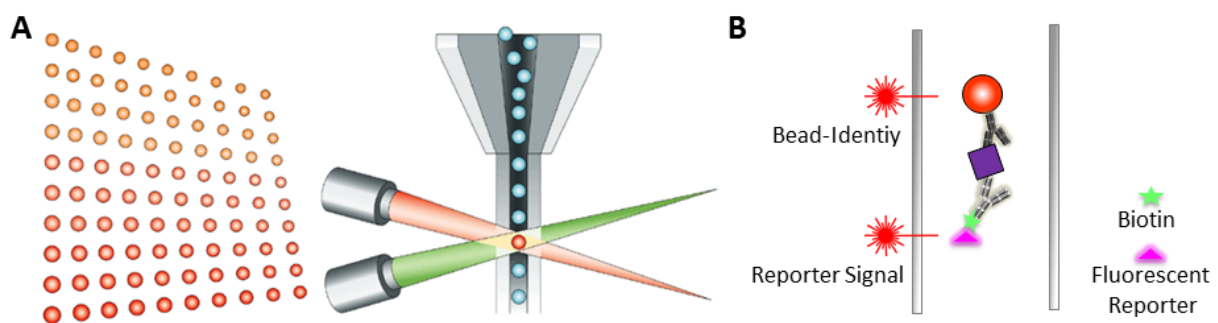


Figure 6: Principle of bead-based immunoassays using the Luminex™ xMAP technology. (A) Beads are differently labelled with a unique ratio of two different fluorescent dyes resulting in a set of 100 different bead regions (sets with 500 different regions are also available). Using specialized flow cytometers (e.g. Bio-Plex® instrument), the differently labelled bead regions can be discriminated spectrally by a laser beam. An additional laser beam is used to analyse the reporter molecule fluorescent signal. Image was taken from [97]. (B) For immune-detection, a capture antibody (dark grey) is coupled to a specific bead region. After capture of the analyte (purple), a detection antibody (light grey) coupled to biotin is used, which is then marked by a fluorescent reporter molecule (e.g. Streptavidin-R-Phycoerythrin). The respective bead region as well as the signal of the reporter molecule are detected by flow cytometry.

3.3.5 Endopeptidase activity assays

Immunological BoNT detection methods mentioned above directly detect the presence of the toxin. Instead, endopeptidase activity assays monitor the last step of BoNT action: the

INTRODUCTION

cleavage of SNARE proteins, mediated by the toxins catalytically active LC. These assays therefore have the advantage of displaying one major step of BoNT action which is the ultimate step conferring toxicity. In combination with an enrichment step via the toxins' HC (through antibodies or receptor molecules) endopeptidase assays can detect the presence of the toxin and its functionality. In addition, endopeptidase assays can yield extremely high sensitivities due to signal amplification through cleavage of multiple substrates by a single BoNT molecule [98]. Furthermore, sensitivity of endopeptidase assays can be modulated by choosing adequate conditions for BoNT substrate cleavage.

3.3.5.1 Sensitivity of endopeptidase activity assays depends on BoNT substrate cleavage

In endopeptidase activity assays, substrate cleavage is used for BoNT detection. Thus, sensitivity of respective assays mainly depends on cleavage efficiency. As the catalytic activity between different BoNT serotypes and subtypes varies [32, 99-102], the achievable assay sensitivity depends on the sero- and subtype present in a sample.

In addition, it has been demonstrated that several other factors have profound influence on cleavage efficiency (summarized in Table 2). Naturally, long cleavage durations improve substrate cleavage, as they allow for a more complete cleaved substrate. Furthermore, a cleavage temperature at 37°C seems to be optimal for serotypes pathogenic to humans [103, 104], whereas BoNT/C and DC, both pathogenic to animals, seem to prefer a slightly elevated temperature of 42°C for efficient cleavage reflecting the higher body temperature in the animals affected such as birds [105]. Regarding *in vitro* endopeptidase assays, several publications demonstrated that the choice of buffer condition as well as substrate molecule has considerable influence on cleavage efficiency. A reducing agent, such as DTT, is a crucial buffer supplement for efficient reduction of the disulphide bond connecting HC and LC. DTT concentrations ranging from 1–20 nM have been proven to be sufficient in different assay formats [101, 106, 107]. Similarly, the presence of Zn²⁺ ions is indispensable to support the metalloprotease activity of BoNT LCs [108]. Interactions between Zn²⁺ and DTT can, however, induce complex formation which has been shown to be inhibitory for LC-A [107]. Other buffer components shown to support or reduce BoNT substrate cleavage include the osmolyte trimethylamine N-oxide (TMAO), having a stabilizing effect on LC structure [109], BSA, NaCl, pH value, or Tween 20 [107, 108, 110-112]. Furthermore, substrate length has an impact on

INTRODUCTION

cleavage efficiency, with short substrates being less efficient [107]. This could be explained by the lack of important exosites in shortened peptide substrates.

Taken together, multiple factors have been shown to either reduce or support substrate cleavage of BoNT. Knowledge on optimal cleavage conditions of the different BoNT serotypes could therefore potentially enhance the achievable sensitivity of cleavage based assays.

Table 2: Factors influencing SNARE protein cleavage by different BoNT LCs based on selected publications.

Factor	LC-Serotype ^a	Effect ^b	Optimal level found ^c	Reference
Temperature	B	n.a.	37°C	[103]
	C	n.a.	42°C	[105]
	D	n.a.	42°C	[105]
	E	n.a.	37°C	[103, 104]
pH	A	n.a.	6.5–7	[101, 110]
	B	n.a.	7–7.4	[101, 108, 110]
	C	n.a.	6.5	[105]
	D	n.a.	7.3	[105]
	E	n.a.	7	[110]
ZnCl ₂	A	+	120 µM	[107]
DTT	A	+	4–5 mM	[107, 110]
	E	+	2.5 mM	[110]
NaCl	A	+	100 mM	[107]
	B	–	n.a.	[108]
	E	–	n.a.	[110]
TMAO	A	+	1.6 M	[109]
	B	+	1.25 M	[109]
	E	+	1.5 M	[109]
BSA	A	+	0.2–2.5 mg/mL	[107, 109, 111]
Tween-20	A	+	0.5%	[110]

^a Either recombinant LCs or BoNT holotoxin was used.

^b + = positive effect; – = negative effect; n.a. = not applicable

^c Optimal concentration found in respective studies (if a concentration range is indicated, varying optimal concentrations were identified in different studies).

INTRODUCTION

3.3.5.2 Monitoring substrate cleavage by MS & FRET

The detection of BoNT cleavage can be achieved by different assay platforms. Of those, FRET and MS have been shown to be efficient tools to detect catalytically active BoNT with high sensitivity. FRET based techniques track cleavage of fluorescently labelled peptide substrates, whereas MS allows for the direct detection of cleavage products based on their mass-to-charge ratio.

FRET based detection of BoNT cleavage

FRET is a widely used technique to study protein-protein interactions and cleavage of peptide bonds. With respect to BoNT detection, FRET is used to monitor the cleavage of peptide substrates thereby detecting the presence of catalytically active toxin. To that aim, short peptide substrates flanked with a fluorescent donor and acceptor molecule are employed. Upon substrate cleavage by BoNT, donor and acceptor molecule become separated which can be detected by an increase in fluorescence intensity.

Using FRET based techniques, sensitivities comparable to the MBA have been achieved for BoNT detection [113-116]. Furthermore, these assays can be easily performed in a brief time frame and commercial kits are available [117] enabling a broad applicability.

A major problem in FRET based assays is the detection of BoNT from complex sample matrices. False positive results are easily generated if peptide substrates are unspecifically cleaved by matrix components. Therefore, a stringent immuno-affinity enrichment step to remove matrix components is required in respective assays. [115, 118]

Furthermore, in FRET based assays all cleavage sites of BoNTs targeting the same substrate (SNAP-25: A, C, and E; VAMP-2: B, D, and F) are within the donor and quencher molecule. A discrimination of serotypes A, C, and E or B, D, and F is not possible. To allow for the discrimination of serotypes E or A/C and B or F/D shortened substrates can be applied. This, however, results in reduced assay sensitivity due to the lack of important exosites [119]. Without further array modifications, serotypes A and C as well as D and F cannot be distinguished as their specific cleavage sites are separated by only one amino acid. For these reasons, FRET based assays are only of limited use for diagnostic purposes.

INTRODUCTION

Endopep-MS assay

In the Endopep-MS assay, BoNT cleaved peptide substrates are monitored by mass spectrometry [120]. Due to the different sizes of cleavage products, this approach enables the identification of the present serotype. Furthermore, by additionally analysing the toxin on the protein level after trypsin digest, the exact subtype can be identified, although this usually requires large toxin amounts. Endopep-MS is a very sensitive method for BoNT detection, greatly exceeding the sensitivity of the MBA with detection limits below 0.04 mouse LD50/mL (for serotypes B and E) [120, 121].

Akin to other endopeptidase assays, the detection of BoNT from complex matrices requires an immuno-affinity enrichment step. But endopep-MS is, due to the unambiguous identification of cleavage products by MS, less prone to false positive results compared to FRET based assays, and detection of BoNT from a variety of sample matrices has been successfully demonstrated [121-124]. For these reasons, endopep-MS is, besides the MBA, the method of choice for botulism diagnostics. However, the method is restricted to expert laboratories, as expensive technical equipment and highly trained laboratory staff is required. Hence, to enable a broad application in routine laboratories, more straightforward methods are required.

3.3.5.3 Endopeptidase activity assays employing neoepitope specific antibodies (Neo-Abs)

Neo-Abs are specialized antibodies that exclusively recognize a newly exposed or modified neoepitope on a protein, whereas the native protein should not be recognized [125]. Regarding BoNT detection, Neo-Abs can be employed to discriminate cleaved and uncleaved substrate. Here, Neo-Abs specifically recognize the newly formed N- or C-terminal neoepitope on SNARE proteins after cleavage by BoNT, whereas they fail to bind to the uncleaved protein. As different BoNT serotypes cleave their substrate at distinct sites (section 3.2.3), they can be distinguished by their substrate specificity. In addition, the cleavage site of one serotype is conserved among the different subtypes. The principle of detecting the exact cleavage site of each BoNT serotype by Neo-Abs therefore enables the detection of catalytically active BoNT molecules, the discrimination of different serotypes, and the detection of all subtypes of so far known serotypes.

Different approaches using different platforms employing polyclonal or monoclonal Neo-Abs have been developed for the detection of serotypes A, B, C, E, and F (summarized in Table 3)

INTRODUCTION

Those include cell based, SPR based, or ELISA based assays. A cell based potency assay (CBPA) for detection of BoNT/A, which is used for potency testing of pharmaceutical products, analyses cell lysates treated with BoNT for cleaved SNAP-25 by sandwich-ELISA with a monoclonal neoepitope specific antibody (Neo-mAb) [126]. Here, an EC₅₀ of 240 pg/mL is achieved for detection from buffer.

Similarly, Neo-mAbs are employed in a novel SPR based approach enabling detection of BoNT/A and E from buffer and serum samples [127-129]. Hereby, cleaved substrate immobilized on a capture chip is detected by injecting the corresponding Neo-mAb (the general principle of measuring protein-protein interactions by SPR is outlined in Figure 10 in the method section). This method yielded impressive sensitivities of 0.06 pg/mL for BoNT/A and 67 pg/mL for BoNT/E thereby outperforming most other *in vitro* approaches.

Recently, novel polyclonal antibodies detecting uncleaved as well as BoNT/B, D, and F cleaved VAMP-2 from cell lysates by Western blotting have been proposed for neurotoxin potency testing [130].

Finally, ELISA based approaches using polyclonal Neo-Abs have been developed for the detection of BoNT/A, B, C, E, and F (see Table 3). Here, SNAP-25 or VAMP-2 is immobilized on plastic microtiter plates and subsequently cleaved by BoNT. Newly exposed neoepitopes can then be detected by Neo-Abs and an HRP-conjugated anti-species antibody. The so called Endopeptidase-ELISA reaches sensitivities in the low pg/mL range [110, 131]. With the incorporation of an immuno-affinity enrichment step, BoNT could be detected from matrices such as food or serum [132-134]. Advantages of the Endopeptidase-ELISA are its high sensitivity combined with its straightforward assay protocol and signal read-out devoid of advanced technical equipment. Still, until now no Endopeptidase-ELISA that utilizes Neo-mAbs has been described.

Polyclonal Neo-Abs are much easier to produce than monoclonal antibodies. However, they have the drawback that they are limited in production, possibly leading to lot-to-lot variations which may restrict assay reproducibility. More importantly, they are more prone to cross-reactivity towards uncleaved substrate and/or neighbouring cleavage sites as they usually recognize multiple epitopes on a protein. For the same reason, they imply a higher risk of false positive results when complex matrices are tested, as unspecifically cleaved substrate or matrix components may be recognized. In contrast, Neo-mAbs are less prone to artefacts as

INTRODUCTION

they solely recognize a single epitope on the target protein. Furthermore, once established, a hybridoma cell line enables the unlimited production of desired monoclonal antibodies in consistent quality. However, production of monoclonal antibodies is laborious, as thousands of hybridoma clones must be screened, followed by an elaborate process including subcloning, expansion of hybridoma cultures, antibody purification, and characterisation (for more details see section 5.1). Until now, Neo-mAbs for the detection of catalytically active BoNT are only available for serotypes A and E [126, 129, 133, 135]. A panel of Neo-mAbs covering all BoNT cleavage sites would enable the development of straightforward and sensitive assays addressing all relevant BoNT serotypes thereby improving botulism diagnostics.

Table 3: Previously described Neo-Abs for the detection of SNARE protein cleavage by BoNT.

Serotype	Specificity ^a	Ab-type ^b	Detection method	Sensitivity (pg/mL) ^c	Reference
A	N	pAb	ELISA	130	[136]
A	N	pAb	ELISA	0.04	[110]
A	N	pAb	ELISA	3.3–5000 ^f	[101]
A	N	mAb	Cell based potency assay	240 ^g	[126]
A	N	pAb	ELISA	0.04/ 0.13 ^{e, f}	[133, 134]
A	N	mAb	SPR	0.06/ 0.075 ^e	[127, 128]
B	C	pAb	ELISA	100–200/5 ^f	[132, 136]
B	C	pAb	ELISA	25 ^f	[101]
B	N	pAb	ELISA	< 1 ^f	[137]
B, D, F ^h	C	pAbs	Western blot	not reported	[130]
C	N/C ^d	pAbs	ELISA	25 /1000 ^d	[131]
E	N	pAb	ELISA	4.8	[110]
E	N	mAb	SPR	66.7	[129]
F	C	pAb	ELISA	25 ^f	[101]

^a N- or C-terminal fragment generated after cleavage of SNAP-25 by BoNT/A, C, or E or VAMP-2 by BoNT/B or F, which is recognized by Neo-Ab

^b Poly- (pAb) or monoclonal (mAb) antibodies.

^c Sensitivity was either reported as limit of detection (LOD) directly in pg/mL or otherwise converted from minimal lethal doses (MLD50) according to the data contained in the respective manuscript.

^d Cleavage of Syntaxin.

^e Detection from serum.

^f With previous enrichment step via receptor binding or antibody.

^g EC50 reported instead of limit of detection.

^h antibodies also detect full-length VAMP-2 and are therefore not truly Neo-Abs

3.4 Aims of the thesis

This thesis was accomplished within the scope of the FuMiBoNT project (*Funktionelle Multiplex-Detektion von Botulinum-Neurotoxinen*) in cooperation with Hannover Medical School (MHH) funded by the BMBF under the call “animal replacement methods”.

The major goal of the FuMiBoNT project was to investigate an innovative *in vitro* approach for the functional detection of all clinically relevant BoNT serotypes BoNT/A-F as a replacement method to the MBA. Here, two important aspects of BoNT action – receptor binding as well as catalytic activity – should be depicted (Figure 7).

Receptor binding included the investigation, design, and generation of suitable receptor molecules mimicking the binding of BoNT to its natural receptor and was studied by the collaboration partner at MHH. The receptor molecules should then be integrated in a novel assay to capture toxin from a sample prior to detection of catalytic activity. For comparison, monoclonal anti-BoNT antibodies (which were already available at RKI by the start of the project) should be employed for BoNT capture for evaluation and benchmarking of receptor structures developed.

The depiction of BoNTs catalytic activity with a novel enzymatic assay was addressed in this work. To ensure optimal *in vitro* substrate cleavage by BoNT, cleavage conditions for the different BoNT serotypes were optimized by a statistical approach. To monitor BoNTs catalytic activity, Neo-mAbs covering the cleavage sites of all clinically relevant BoNT serotypes A-F were generated and thoroughly characterised to ensure exclusive specificity. Furthermore, reagents (receptor molecules or alternatively anti-BoNT antibodies plus Neo-mAbs) were implemented in a highly sensitive suspension array enabling the detection of both specific binding of BoNT/A and B to its neuronal receptor and endopeptidase activity. Alternatively, a highly sensitive assay displaying BoNTs catalytic activity (devoid of receptor binding) was developed for serotypes A-F. The novel assay was evaluated regarding robustness and sensitivity and tested for the detection of BoNT from different complex matrices.

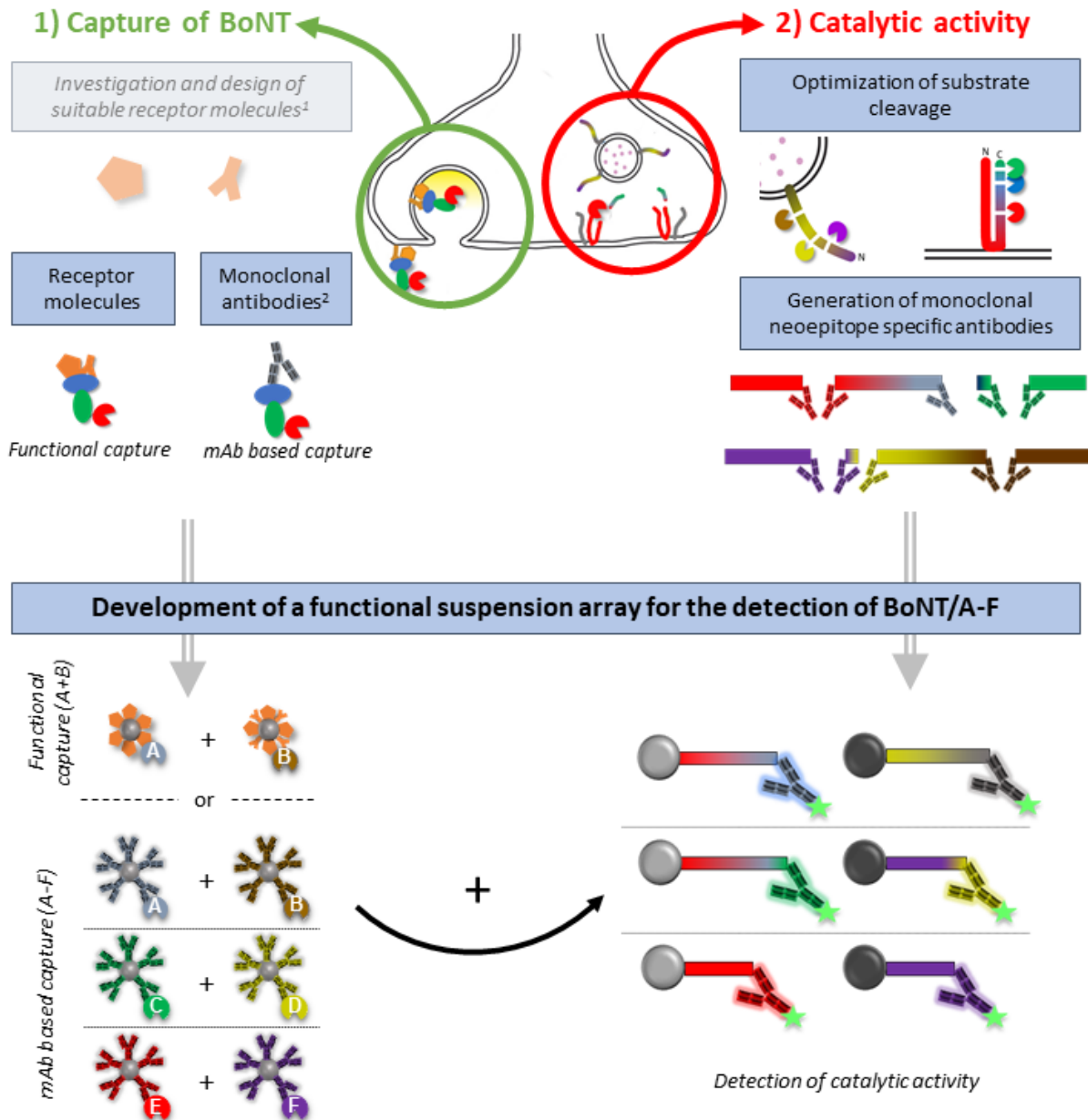


Figure 7: Schematic illustration of BoNTs mode of action (receptor binding and catalytic activity) and aims and results of the FuMiBoNT project and this thesis (depicted in blue boxes). The major goal of this thesis was to develop an innovative *in vitro* approach to detect BoNT/A-F as a routine animal replacement method covering two major steps of BoNT action: receptor binding and catalytic activity. To that aim, suitable receptor molecules were designed by the collaboration partner of the project at MHH for BoNT/A+B. To capture BoNT from solution, receptor molecules were coupled to magnetic beads. As an alternative, monoclonal anti-BoNT antibodies coupled to magnetic beads were used for BoNT capture. To detect BoNTs catalytic activity with high sensitivity, *in vitro* substrate cleavage was optimized by a statistical approach. To monitor substrate cleavage, Neo-mAbs specific for the cleavage sites of BoNT/A-F were generated. Finally, BoNT capture, optimized cleavage conditions, and Neo-mAbs were integrated in a functional multiplex assay based on the Luminex™-platform which enabled the simultaneous detection of one SNAP- and one VAMP-specific serotype. ¹The design of receptor molecules was performed by the collaboration partner of the project at MHH. ²Monoclonal anti-BoNT antibodies were available by the start of the thesis.

4 MATERIAL AND METHODS

4.1 Materials

4.1.1 Chemicals and reagents

All chemicals and reagents not listed in Table 4 were obtained from the following companies: Sigma-Aldrich (Taufkirchen, Germany), Carl Roth GmbH + Co. KG (Karlsruhe, Germany), or Merck KGaA (Darmstadt, Germany).

Table 4: Chemicals and reagents

Chemical/reagent	Manufacturer
10 mM Glycin pH 1.7	GE Healthcare, München, Germany
Acrylamide	Carl Roth, Karlsruhe, Germany
Acrylamide/Bisacrylamide solution (Rotiphorese Gel 30 37.5:1)	Carl Roth, Karlsruhe, Germany
APS (Ammonium persulfate)	Bio-Rad, Munich, Germany
Bacto™ Peptone	BD Biosciences, Heidelberg, Germany
Biotin-NHS (biotinamidohexanoyl-6-aminohexanoic acid N-hydroxysuccinimide ester)	Sigma-Aldrich, Taufkirchen, Germany
Bisacrylamide	Carl Roth, Karlsruhe, Germany
BSA (cell culture)	Serva, Heidelberg, Germany
BSA (Immunoassays)	Carl Roth, Karlsruhe, Germany
Casein	Sigma-Aldrich, Taufkirchen, Germany
CDP-Star	Applied Biosystems, Foster City, CA, USA
CM-dextran (carboxymethyl-dextran)	Sigma-Aldrich, Taufkirchen, Germany
Coomassie Brilliant Blue G-250	Bio-Rad, Munich, Germany
DTT (1,4-Dithiothreitol)	Carl Roth, Karlsruhe, Germany
EDC (1-ethyl-3-(3-dimethylaminopropyl)carbodiimide)	Pierce, Rockford, IL, USA
EDTA (ethylenediaminetetraacetic acid)	Sigma-Aldrich, Taufkirchen, Germany
FCS (fetal calf serum)	Invitrogen, Carlsbad, CA, USA
Freunds Complete Adjuvant	Sigma-Aldrich, Taufkirchen, Germany
Freunds Incomplete Adjuvant	Sigma-Aldrich, Taufkirchen, Germany
Glutathione	Sigma-Aldrich, Taufkirchen, Germany
GST-rSyt-II K51R	Toxogen, Hannover, Germany
gSV2C N565Q	Hannover Medical School (MHH), Hannover, Germany
GT1b	Sigma-Aldrich, Taufkirchen, Germany
HEPES	Carl Roth, Karlsruhe, Germany

MATERIAL AND METHODS

KLH (keyhole limpet hemocyanin)	Sigma-Aldrich, Taufkirchen, Germany
Mag-trypsin (Immobilized TPCK Trypsin Magnetic Beads)	Takara Bio USA, Mountain View, CA, USA
MSP (membrane scaffold protein) 1E3D1	Sigma-Aldrich, Taufkirchen, Germany
N-Ethylmaleimide (NEM)	Sigma-Aldrich, Taufkirchen, Germany
OG (octyl β -D-glucopyranoside)	Sigma-Aldrich, Taufkirchen, Germany
Orthophosphoric acid	Carl Roth, Karlsruhe, Germany
PageRuler Prestained Protein Ladder	Thermo Fisher Scientific, Waltham, MA, USA
PEG 1500	F. Hoffmann-La Roche AG, Basel, Switzerland
POPC (1-palmitoyl-2-oleoyl-sn-glycero-3-phosphocholine)	Sigma-Aldrich, Taufkirchen, Germany
Silver nitrate	Merck KGaA, Darmstadt, Germany
Skimmed milk powder, blotting grade	Carl Roth, Karlsruhe, Germany
Sodium cholate hydrate	Sigma-Aldrich, Taufkirchen, Germany
Streptavidin-R-Phycoerithin PJRS27	ProZyme, Hayward, CA, USA
Streptavidin-R-Phycoerithin PJRS34	ProZyme, Hayward, CA, USA
Sulfo-NHS (sulfo-N-hydroxysulfosuccinimide)	Pierce, Rockford, IL, USA
Sulfo-SMPB (sulfosuccinimidyl 4-(N-maleimidophenyl)butyrate)	Thermo Fisher Scientific, Waltham, MA, USA
Super Signal® West Dura Western blotting substrate	Thermo Fisher Scientific, Waltham, MA, USA
TEMED (tetramethylethylenediamine)	Bio-Rad, Munich, Germany
TMAO (trimethylamine N-oxide dihydrate)	Sigma-Aldrich, Taufkirchen, Germany
TMB (3,3',5,5'-tetramethylbenzidine)	Seramun Diagnostics, Heidesee, Germany
Tween 20	Merck, Darmstadt, Germany
xMAP sheath fluid	Thermo Fisher Scientific, Waltham, MA, USA
ZnCl ₂	Merck, Darmstadt, Germany

4.1.2 Buffers

If not specified else, all buffers were prepared in demineralised water.

Table 5: Buffers

Buffer	Composition	Application
Anode buffer	0.2 M Tris pH 8.9	SDS-PAGE (Peptide gels)
Assay buffer	1 % BSA (w/v) in PBS pH 7.4	Tetraplex-Assay, Duplex-assay
Blocking buffer	2% skimmed milk powder (w/v) in PBS-T	ELISAs, Western blots

MATERIAL AND METHODS

Carbonate buffer	50 mM Carbonate pH 9.6	Endopeptidase-ELISA
Cathode buffer	0.1 M Tris 0.1 M Tricine 0.1% SDS (w/v)	SDS-PAGE (Peptide gels)
Cleavage Buffer	50 mM HEPES 250 μ M ZnCl ₂ 1% Tween 20 (v/v) 0.75 M TMAO 25 mM DTT (freshly added) pH 7	BoNT substrate cleavage
Colloidal Coomassie	0.1% Coomassie G250 (w/v) 10 % Ammonium sulfate (w/v) 3 % ortho-Phosphoric acid (v/v) 20% EtOH (v/v)	SDS-PAGE (Staining)
Electrophoresis running buffer	0.15 M Tris 0.192 M Glycine 0.01% SDS (w/v)	SDS-PAGE
ELISA blocking buffer	5% skimmed milk powder (w/v) in PBS-T	Endopeptidase-ELISA
Evans buffer	50 mM HEPES 20 μ M ZnCl ₂ 1% BSA (w/v) 1 mM DTT (freshly added) pH 7.4	BoNT substrate cleavage (Taguchi DoE analysis)
FACS-PBS	2.5% FCS (v/v) 0.1% NaN ₃ (w/v) in PBS	iFACS
Glutathione buffer	120 mM Glutathione 10 mM EDTA in PBS	Casein-glutathione coupling
HBS-EP+ running buffer	10 mM HEPES 150 mM NaCl 3 mM EDTA 0.05% Tween 20 (v/v) pH 7.4	SPR
Jones buffer	50 mM HEPES 10 μ M ZnCl ₂ 0.5% Tween 20 (v/v) 1 mg/mL BSA 5 mM DTT (freshly added) pH 7	BoNT substrate cleavage (Taguchi DoE analysis)
Laemmli loading buffer (3 x)	150 mM Tris 6% SDS (w/v) 30% Glycerol (v/v) 7.5% β -Mercaptoethanol (v/v) 0.25% Bromophenol blue (w/v) pH 6.8	SDS-PAGE

MATERIAL AND METHODS

MES-buffer	50 mM MES pH 5.0	M270 bead coupling, Luminex-beads coupling
PBS	137 mM NaCl 8.1 mM Na ₂ HPO ₄ 2.7 mM KCl 1.5 mM KH ₂ PO ₄ pH 7.2	Various
PBS/BN	0.1% BSA (w/v) 0.05% NaN ₃ (w/v) in PBS pH 7.4	M280 and M270 bead coupling
PBS/N	0.05 % NaN ₃ (w/v) in PBS	Biotinylation of antibodies
PBS/PenStrep	1% Pen/Strep (v/v) in PBS	Fusion
PBS-T	0.1 % Tween 20 (v/v) in PBS	ELISA
PBS-TBN	0.1% BSA (w/v) 0.02% Tween 20 (v/v) 0.05% NaN ₃ (w/v) in PBS pH 7.4	Luminex-bead coupling
Running buffer	20 mM Sodium phosphate 0.15 M NaCl pH 7.2	mAb purification
Saponin buffer	0.5% Saponin (w/v) in FACS-PBS	iFACS
Silver developing solution	3% K ₂ CO ₃ (w/v) 0.0004% Na ₂ S ₂ O ₃ × 5 H ₂ O (w/v) 0.05% Formaldehyde (w/v)	SDS-PAGE (Staining)
Silver staining solution	0.2% AgNO ₃ (w/v) 0.075 % Formaldehyde (w/v)	SDS-PAGE (Staining)
Sodium phosphate buffer	0.1 M Sodium phosphate pH 7.4	M280 bead coupling
Transfer buffer	48 mM Tris 39 mM Glycin 0.037% SDS (w/v) 20 % MeOH (v/v)	Western blots
Tris-buffer	0.2 M Tris, 0.1 % BSA (w/v) pH 8.5	M280 bead coupling
WB assay buffer	100 mM Diethanolamine 1 mM MgCl ₂ × 6 H ₂ O pH 10	Western blots

MATERIAL AND METHODS

4.1.3 Enzymes and antibodies used in immunological assays

Commercial detection antibodies and enzymes are listed in Table 6. Primary antibodies listed in Table 7 were all generated at RKI.

Table 6: Detection antibodies and enzymes

Antibody/enzyme	Manufacturer
Avidx-AP (streptavidin conjugated alkaline phosphatase)	Thermo Fisher Scientific, Waltham, MA, USA
Goat anti-mouse (Fcy) HRP	Dianova, Hamburg, Germany
Goat anti-mouse (H+L) HRP	Dianova, Hamburg, Germany
goat anti-mouse IgG	SouthernBiotech, Birmingham, AL, USA
goat anti-mouse IgG (H+L)	Dianova, Hamburg, Germany
goat anti-mouse IgG1	SouthernBiotech, Birmingham, AL, USA
goat anti-mouse IgG2a	SouthernBiotech, Birmingham, AL, USA
goat anti-mouse IgG2b	SouthernBiotech, Birmingham, AL, USA
goat anti-mouse IgG3	SouthernBiotech, Birmingham, AL, USA
goat-anti-mouse-IgG-Cy5	Dianova, Hamburg, Germany
Streptavidin peroxidase (SA-POD)	Dianova, Hamburg, Germany
Streptavidin poly-HRP	Diavita, Heidelberg, Germany

Table 7: Primary antibodies

Antibody	Specificity	Species	Isotype	Origin
A1688	BoNT/A H _N	mouse, mAb	IgG1	RKI, D. Pauly [96]
A185	BoNT/A H _C	mouse, mAb	IgG1	RKI, E. Hansbauer [138]
A2807	BoNT/A H _C	mouse, mAb	IgG1	RKI, E. Hansbauer [138]
A778	BoNT/A H _C	mouse, mAb	IgG2a	RKI, E. Hansbauer [138]
B279	BoNT/B LC	mouse, mAb	IgG2a	RKI, D. Pauly [96]
B488	BoNT/B H _C	mouse, mAb	IgG2a	RKI, E. Hansbauer
B710	BoNT/B H _N	mouse, mAb	IgG2a	RKI, D. Pauly [96]
C9	BoNT/C H _C	mouse, mAb	IgG2b	RKI, M. Skiba [139]
D63	BoNT/D LC	mouse, mAb	IgG2b	RKI, J. Wolf [139]
D967	BoNT/D H _C	mouse, mAb	IgG1	RKI, F. Finkenwirth [139]
E1346	BoNT/E H _C	mouse, mAb	IgG1	RKI, E. Hansbauer [138]
E136	BoNT/E H _N	mouse, mAb	IgG2a	RKI, T. Schreiber [140]

MATERIAL AND METHODS

F1726	BoNT/F H _c	mouse, mAb	IgG1	RKI, E. Hansbauer
F757	BoNT/F H _c	mouse, mAb	IgG2b	RKI, E. Hansbauer
KE97	BoNT/E	rabbit, pAb	IgG	RKI, T. Schreiber [140]
SNAP/A/291	Neo BoNT/A (N-terminal fragment)	mouse, mAb	IgG1	RKI, D. Pauly
SNAP/A/305	Neo BoNT/A (N-terminal fragment)	mouse, mAb	IgG1	RKI, D. Pauly
SNAP/C/1844	Neo BoNT/C (N-terminal fragment)	mouse, mAb	IgG2a	RKI, this work
SNAP/C/2207	Neo BoNT/C (C-terminal fragment)	mouse, mAb	IgG1	RKI, this work
SNAP/C/3280	Neo BoNT/C (N-terminal fragment)	mouse, mAb	IgG2b	RKI, this work
SNAP/C/5593	Neo BoNT/C (N-terminal fragment)	mouse, mAb	IgG2a	RKI, this work
SNAP/E/1466	Neo BoNT/E (C-terminal fragment)	mouse, mAb	IgG1	RKI, D. Pauly
SNAP/E/217	Neo BoNT/E (N-terminal fragment)	mouse, mAb	IgG1	RKI, D. Pauly
VAMP/B/1148	Neo BoNT/B (N-terminal fragment)	mouse, mAb	IgG1	RKI, this work
VAMP/B/151	Neo BoNT/B (C-terminal fragment)	mouse, mAb	IgG2b	RKI, this work
VAMP/B/226	Neo BoNT/B (N-terminal fragment)	mouse, mAb	IgG1	RKI, this work
VAMP/B/392	Neo BoNT/B (C-terminal fragment)	mouse, mAb	IgG1	RKI, L. Försterling, D. Stern
VAMP/B/726	Neo BoNT/B (C-terminal fragment)	mouse, mAb	IgG3	RKI, L. Försterling, D. Stern
VAMP/D/27	Neo BoNT/D (C-terminal fragment)	mouse, mAb	IgG2b	RKI, L. Försterling, D. Stern
VAMP/D/29	Neo BoNT/D (C-terminal fragment)	mouse, mAb	IgG2b	RKI, L. Försterling, D. Stern
VAMP/F/1333	Neo BoNT/F (N-terminal fragment)	mouse, mAb	IgG1	RKI, this work
VAMP/F/153	Neo BoNT/F (N-terminal fragment)	mouse, mAb	IgG1	RKI, this work
VAMP/F/425	Neo BoNT/F (N-terminal fragment)	mouse, mAb	IgG1	RKI, this work
VAMP/F/440	Neo BoNT/F (C-terminal fragment)	mouse, mAb	IgG2a	RKI, L. Försterling, D. Stern
VAMP/F/521	Neo BoNT/F (N-terminal fragment)	mouse, mAb	IgG1	RKI, this work

MATERIAL AND METHODS

4.1.4 Toxins

Toxins (purified from *Clostridia* supernatants or recombinantly expressed) and recombinant toxin fragments used in experiments are listed in Table 8. *Clostridia* supernatants used in endopeptidase assays are listed in Table 9.

Table 8: Purified and recombinantly expressed toxins or toxin fragments.

Toxins/Toxin fragments (specific activity ^a)	Comment	Manufacturer
BoNT/A (2.6×10^8 LD/mg)	purified from supernatant	Metabiologics, Madison, WI, USA
BoNT/B (1.2×10^8 LD/mg)	purified from supernatant	Metabiologics, Madison, WI, USA
BoNT/C (3×10^7 LD/mg, and 2.6×10^7 LD/mg ^b)	purified from supernatant	Metabiologics, Madison, WI, USA
BoNT/D	recombinantly expressed	Toxogen, Hannover, Germany
BoNT/DC (9.6×10^7 LD/mg)	purified from supernatant	Metabiologics, Madison, WI, USA
BoNT/E (non-trypsinized: 3×10^5 LD50/mg; trypsinized: 6×10^7 LD50/mg)	purified from supernatant	Metabiologics, Madison, WI, USA
BoNT/F (1.8×10^7 LD/mg)	purified from supernatant	Metabiologics, Madison, WI, USA
HcA1	recombinantly expressed	Toxogen, Hannover, Germany
HcA2	recombinantly expressed	Toxogen, Hannover, Germany
HcA3	recombinantly expressed	Toxogen, Hannover, Germany
HcA4	recombinantly expressed	Toxogen, Hannover, Germany
HcA5	recombinantly expressed	Toxogen, Hannover, Germany
HcA6	recombinantly expressed	Toxogen, Hannover, Germany
HcA7	recombinantly expressed	Toxogen, Hannover, Germany
HcA8	recombinantly expressed	Toxogen, Hannover, Germany
HcB1	recombinantly expressed	Toxogen, Hannover, Germany
HcB2	recombinantly expressed	Toxogen, Hannover, Germany
HcB3	recombinantly expressed	Toxogen, Hannover, Germany
HcB4	recombinantly expressed	Toxogen, Hannover, Germany
HcB5	recombinantly expressed	Toxogen, Hannover, Germany
HcBx	recombinantly expressed	Toxogen, Hannover, Germany
LC-A1	recombinantly expressed	Toxogen, Hannover, Germany
LC-A2	recombinantly expressed	Toxogen, Hannover, Germany
LC-A3	recombinantly expressed	Toxogen, Hannover, Germany
LC-A4	recombinantly expressed	Toxogen, Hannover, Germany
LC-A5	recombinantly expressed	Toxogen, Hannover, Germany
LC-B1	recombinantly expressed	Toxogen, Hannover, Germany
LC-B2	recombinantly expressed	Toxogen, Hannover, Germany

MATERIAL AND METHODS

LC-B3	recombinantly expressed	Toxogen, Hannover, Germany
LC-B4	recombinantly expressed	Toxogen, Hannover, Germany
LC-B5	recombinantly expressed	Toxogen, Hannover, Germany
LC-B7	recombinantly expressed	Toxogen, Hannover, Germany
LC-Bx	recombinantly expressed	Toxogen, Hannover, Germany

^a LD50/mg according to toxin activity as specified by the manufacturer.

^b Different toxin batches were used.

Table 9: *Clostridia botulinum* supernatants used in endopeptidase assays.

Strain	Source ^a	BoNT Subtype	Cultivation media ^b	Reference
NCTC7272	NCTC	A1	TPGY	n.a.
NCTC2916	NCTC	A1(B)	TPGY	[141]
Friedrichshain	RKI	A2	TPGY	[142]
11-013-01	RKI	A2B2	TPGY	n.a.
14-256-01	RKI	A2F4	TPGY	n.a.
Banská Bystrica (15-168-01)	RKI	A3	TPGY	[143]
Eriwan	RKI	A5	TPGY	n.a.
Chemnitz	RKI	A8	TPGY	[32]
NCTC7273	NCTC	B1	RCM	[144]
REB89	TLLV	B2	TPGY	n.a.
15-019-01	RKI	B3	TPGY	n.a.
Templin	RKI	B4	TPGY	[145]
Düsseldorf	RKI	B5F2	TPGY	n.a.
NCTC3807	NCTC	B7	TPGY	[146]
KL34/08	Leipzig	By	TPGY	[145]

^a *Clostridia botulinum* strains used in this work were kindly provided by the following institutions: NCTC, National Collection of Type Culture, London, United Kingdom; TLLV, Thüringer Landesamt für Lebensmittelsicherheit und Veterinärmedizin, Bad Langensalza, Germany; Leipzig, Konsiliarlabor für Anaerobe Bakterien, Leipzig, Germany; RKI, Robert Koch-Institut, Berlin, Germany.

^b TPGY media: 50 g/L tryptone from casein, 5 g/L mix-peptone (BD Biosciences, Heidelberg, Germany), 20 g/L yeast-extract (Carl Roth GmbH + Co. KG, Karlsruhe, Germany), 4 g/L glucose (Merck KGaA, Darmstadt, Germany), 1 g/L sodium thioglycolate (Sigma-Aldrich, Taufkirchen, Germany); RCM media: 38 g/L RCM-powder (Sifin diagnostics GmbH, Berlin, Germany)

^c GenBank accession number

^d 16s rRNA sequence

n.a. = not available

4.1.5 Substrate proteins and peptides

Substrates used for BoNT cleavage are listed in

MATERIAL AND METHODS

Table 10. Peptides used for immunization and antibody characterization are listed in Table 11. All peptides were obtained from Dr. Petra Henklein, Institute of Biochemistry, Charité – Universitätsmedizin Berlin (Berlin, Germany).

Table 10: Substrates used for BoNT cleavage.

Substrate	Manufacturer
H6trVAMP-2	Toxogen, Hannover, Germany
<i>Sequence:</i> MGSSHHHHHH SSGLVPRGSH MSATAATVPP AAPAGEGGPP APPNLTNSR RLQQTQAQVD EVVDIMRVNV DKVLERDQKL SELDDRADAL QAGASQFETS AAKLKRKYWW KNLKMMI	
rSNAP-25 H6	Toxogen, Hannover, Germany
<i>Sequence:</i> MAEDADMRNE LEEMQRRADQ LADESLESTR RMLQLVEESK DAGIRTLVML DEQGEQLDRV EEGMNHINQD MKEAEKNLKD LGKCCGLYIC PCNKLKSSDA YKKAWGNNQD GVVASQPARV VDEREQMAIS GGFIRRVNTD ARENEMDENL EQVSGIIGNL RHMALDMGNE IDTQNRQIDRI MEKADSNKTR IDEANQRATK MLGSGVPPTP GHHHHHH	
SNAP-25	ATGen Co. Ltd., Los Angeles, CA, USA
<i>Sequence:</i> MGSSHHHHHH SSGLVPRGSH MAEDADMRNE LEEMQRRADQ LADESLESTR RMLQLVEESK DAGIRTLVML DEQGEQLERI EEGMDQINKD MKEAEKNLTD LGKFCGLCVC PCNKLKSSDA YKKAWGNNQD GVVASQPARV VDEREQMAIS GGFIRRVNTD RHMALDMGNE IDTQNRQIDR IMEKADSNKT RIDEANQRAT KMLGSGAREN EMDENLEQVS GIIGNL	
SNAP-25-Bio (SNAP-25 ₁₃₇₋₂₀₆)	Dr. Petra Henklein, Institute of Biochemistry, Charité – Universitätsmedizin Berlin, Berlin, Germany
<i>Sequence:</i> (Biotin)- VTND ARENEMDENL EQVSGIIGNL RHMALDMGNE IDTQNRQIDR IMEKADSNKT RIDEANQRAT KMLGSG-K-(Biotin)	
VAMP-2	ProSpec-Tany TechnoGene Ltd., Rehovot, Israel
<i>Sequence:</i> MRGSHHHHHH GMASMTGGQQ MGRDLYDDDD KDRWGSMSA TAATAPPAAP AGEGGPPAPP PNLTNSRRLQ QTQAQVDEVV DIMRVNVDKV LERDQKLEL DDRADALQAG ASQFETSAK LKRKYW	
VAMP-2/B-Bio	Dr. Petra Henklein, Institute of Biochemistry, Charité – Universitätsmedizin Berlin, Berlin, Germany
<i>Sequence:</i> (Biotin)-LDDRADALQAGASQFETSAAKLKRKYWWKNLK-(Biotin)	
VAMP-2/DF-Bio	Dr. Petra Henklein, Institute of Biochemistry, Charité – Universitätsmedizin Berlin, Berlin, Germany
<i>Sequence:</i> (Biotin)-LQQTQAQVDEVVDIMRVNVDKVLERDQKLELDDRADALK-(Biotin)	
VAMP-2-Bio (VAMP-2 ₃₃₋₉₄)	Dr. Petra Henklein, Institute of Biochemistry, Charité – Universitätsmedizin Berlin, Berlin, Germany
<i>Sequence:</i>	

MATERIAL AND METHODS

(Biotin)-QQTQAQVD EVVDIMRVNV DKVLERDQKL SELDDRADAL QAGASQFETS AAKLKRKYWW KNLK-
(Biotin)

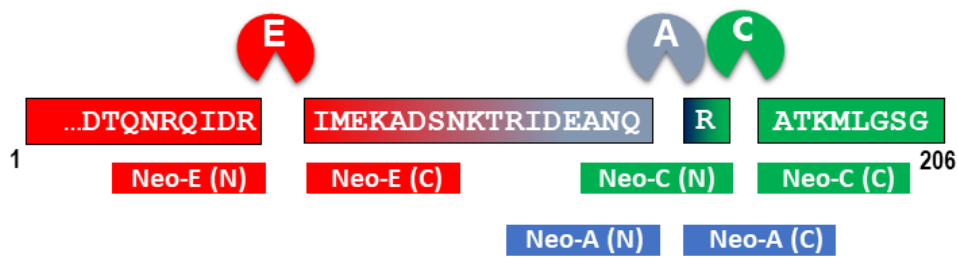
Table 11: Peptides used for immunization of mice and antibody characterization (all obtained from Dr. Petra Henklein, Institute of Biochemistry, Charité – Universitätsmedizin Belin, Germany).

Peptide ^a	Sequence ^b
Neo-A (C)	RATKMLGSC-X
Neo-A (N)	X-CTRIDEANQ
Neo-B (C)	FETSAAKLC-X
Neo-B (N)	X-CALQAGASQ
Neo-C (C)	ATKMLGSGC-X
Neo-C (N)	X-CRIDEANQR
Neo-D (C)	LSELDDRAC-X
Neo-D (N)	X-CDKVLERDQK
Neo-E (C)	IMEKADSNC-X
Neo-E (N)	X-CTQNRQIDR
Neo-F (C)	KLSELDDRC-X
Neo-F (N)	X-CDKVLERDQ

^a as illustrated in Figure 8

^b X = BSA, KLH, or biotin (all peptides were synthesized coupled to different proteins/haptens for immunization and/or screening respectively)

SNAP-25



VAMP-2

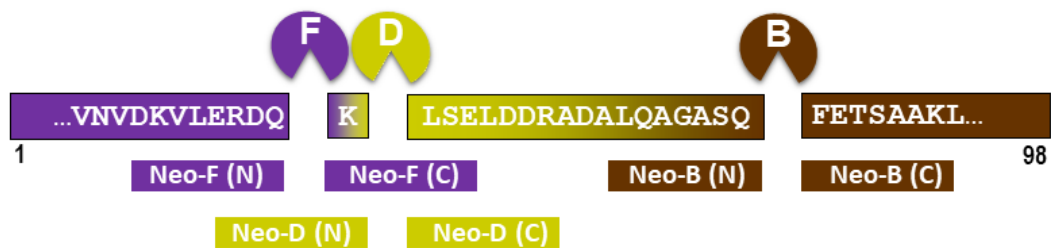


Figure 8: Schematic illustration of peptides used for immunization and screening procedures. For immunization and screening procedures 8mer peptides corresponding to the N- or C-terminal cleavage site of BoNT/A-F were employed.

4.1.6 Animals

To produce monoclonal antibodies, mice of the outbred strain NMRI (Charles River Laboratories, Sulzfeld, Germany) were employed. Thymocytes to support growth of hybridoma cells after fusion were obtained from the inbred strain BALB/c (ibid.). Animals were fed *ad libitum* and checked daily for good health by trained staff of the animal facility. All animal experiments were performed in agreement with the European legislation for the protection of animals used for scientific purposes (Directive 2010/63/EU). Animal experiments were approved by the State Office for Health and Social Affairs in Berlin (LaGeSo Berlin, Germany) under the registration number H109/03 or T0060/03.

4.1.7 Cells, cell culture media, and reagents

Hybridoma cell lines generated in this work were produced by fusing murine myeloma cells P3x63Ag8.653 (American Type Culture Collection, Rockville, MD, USA) with primary murine spleen cells (see section 4.2.3.4). For cultivation of cells, media listed in Table 13 were employed.

MATERIAL AND METHODS

Table 12: Reagents used in cell cultivation media/methods.

Reagent	Comment	Manufacturer
AH 50 x	50 × Azaserine/Hypoxanthine (final concentrations: 5.7 µM Azaserine and 100 µM Hypoxanthine)	Sigma Aldrich, Taufkirchen, Germany
DMSO	Dimethyl sulfoxide, anhydrous	Sigma Aldrich, Taufkirchen, Germany
FCS	Fetal calf serum	Thermo Fisher Scientific, Waltham, MA, USA
IL-6	Interleukin 6, 200,000 U/mL	Hiss Diagnostics, Freiburg im Breisgau, Germany
Pen/Strep 100 ×	10 000 U/mL Penicillin, 10 000 µg/mL Streptomycin	Biochrom, Berlin, Germany
RPMI1640	Roswell Park Memorial Institute Medium	Merck, Darmstadt, Germany
Trypan blue solution	0.81% sodium chloride (w/v) 0.4% trypan blue (w/v) 0.06% potassium phosphate dibasic solution (v/v)	Merck, Darmstadt, Germany
Türks solution	Acetic acid for erythrocyte hemolysis (staining solution for leukocytes)	Merck, Darmstadt, Germany
β-ME	β-Mercaptoethanol 50 mM in PBS	Serva Electrophoresis, Heidelberg, Germany

Table 13: Media used for cell cultivation and cell culture methods.

Name	Composition	Application
ACK lysis buffer	155 M NH ₄ Cl 10 mM KCO ₃ 0.1 mM Na ₂ EDTA pH 7.3	Lysis of erythrocytes
Cell freezing media	80% FCS (v/v) 20% DMSO (v/v)	Freezing of cells
PBS/PenStrep	PBS 1% PenStrep (v/v)	Fusion
R10F ⁻	RPMI1640 with 10% FCS (v/v) 50 µM β-ME	Cultivation of myeloma cells Isolation of thymocytes
R10F ⁺	RPMI1640 with 10% FCS (v/v) 50 µM β-ME 1% Pen/Strep(v/v)	Cultivation of hybridoma cells
R20F ⁻ /AH	RPMI1640 with 20 % FCS (v/v) 50 µM β-ME 50 U/ml IL-6 1 × AH	Selective media for hybridoma cells
R20F ⁺	RPMI1640 with 20% FCS (v/v)	Cultivation of hybridoma cells

MATERIAL AND METHODS

	50 μ M β -ME	
	50 U/ml IL-6	
	1% Pen/Strep (v/v)	
RPMI1640 β -ME	RPMI1640	Fusion
	50 μ M β -ME	

4.1.8 Consumables

Table 14: Consumables

Consumable	Manufacturer
Amicon centrifugal filter units	Merck Millipore, Billerica, MA, USA
Bio-Beads [®] SM-2	Bio-Rad, Munich, Germany
Borosilicate glass tubes with plain end	Fisher Scientific, Pittsburgh, PA, USA
CAP sensor Chip	GE Healthcare, Munich, Germany
Cell culture flasks (Nunclon Delta with filter)	Nunc, Roskilde, DK
Cell culture plates (MicroWell Nunclon Delta)	Nunc, Roskilde, DK
Cell scraper	Nunc, Roskilde, DK
CM5 sensor chip	GE Healthcare, Munich, Germany
Conical centrifugation tubes	TPP Techno Plastic Products, Trasadingen, Switzerland
Cryo Preservation Tube (1.8 mL)	Nunc, Roskilde, DK
Dialysis tubing (8-10 kDa cut-off)	Spectrum Labs, Frankfurt a. M., Germany
Disposable PD-10 Desalting Column	GE Healthcare, München, Germany
Dynabeads [®] M-270 Carboxylic Acid	Thermo Fisher Scientific, Waltham, MA, USA
Dynabeads [®] M-280 Tosylactivated	Thermo Fisher Scientific, Waltham, MA, USA
EMD Millipore™ Steritop™ Sterile Vacuum Bottle-Top Filters	Merck Millipore, Billerica, MA, USA
Greiner flat bottom 96 well plates	Greiner Bio-One, Frickenhausen, Germany
HiTrap MabSelect SuRe column	GE Healthcare, Munich, Germany
HiTrap Protein G HP column	GE Healthcare, Munich, Germany
Hollow needle (StericanR)	B. Braun, Melsungen, Germany
Immobilon [®] -P PVDF Membrane (0.45 μ M)	Merck Millipore, Billerica, MA, USA
MagPlex [®] microspheres	Luminex, Austin, TX, USA
Microtubes	Eppendorf, Hamburg, Germany/Sarstedt, Nümbrecht, Germany
Minivette [®] POCT	Sarstedt, Nümbrecht, Germany
MaxiSorp™ Nunc-Immuno™ MicroWell™ 96 well solid plates	Nunc, Roskilde, DK
Nylon cell strainer (70 μ M)	BD Biosciences, Heidelberg, Germany

MATERIAL AND METHODS

Pipette tips	Nerbe Plus, Winsen/Luhe, Germany
Plastic seal for 96-well microplates	Nunc, Roskilde, DK
Protein LoBind Tubes, 1.5 mL	Eppendorf, Hamburg, Germany
Rubber Caps (type 2)	GE Healthcare, Munich, Germany
Screw cap microtubes	Sarstedt, Nümbrecht, Germany
Serological pipettes	TPP Techno Plastic Products, Trasadingen, Switzerland
Syringes (1 mL, 10 mL, 20 mL)	B. Braun, Melsungen, Germany
Syringes Luer-Lock	BD Biosciences, Heidelberg, Germany
Target2™ PVDF Syringe Filters (0.22 µm)	Fisher Scientific, Pittsburgh, PA, USA
Vacuum bottle-top filter (ExpressR Plus 0,22 µm)	Merck Millipore, Billerica, MA, USA
Whatman filter paper, 3 mm	Thermo Fisher Scientific, Waltham, MA, USA

4.1.9 Kits

Commercial kits listed in Table 15 were employed in this work according to the manufacturer's instructions.

Table 15: Kits

Kit	Manufacturer	Application
Bio-Plex Calibration Kit	Bio-Rad, Munich, Germany	Calibration of Bio-Plex 200
Biotin CAPture Kit	GE Healthcare, München, Germany	SPR
DNeasy Blood and Tissue Kit	Qiagen, Hilden, Germany	Mycoplasma testing
GST Capture Kit	GE Healthcare, Munich, Germany	SPR
Human Antibody Capture Kit	GE Healthcare, Munich, Germany	SPR
Mouse Antibody Capture Kit	GE Healthcare, Munich, Germany	SPR
VenorGeM Mycoplasma Detection Kit	Minerva Biolabs, Berlin, Germany	Mycoplasma testing

4.1.10 Devices

Devices employed in this work are listed in Table 16. Standard laboratory equipment such as centrifuges, water baths, pipettes, or refrigerators are not specified.

MATERIAL AND METHODS

Table 16: Devices

Device	Type	Manufacturer
Anaerobe workstation	MACS 500	Don Whitley, West Yorkshire, UK
Biacore (SPR)	X100	GE Healthcare, München, Germany
Biosafety cabinet (class II)	HeraSafe	Heraeus, Hanau, Germany
Cell dissociation sieve	212 µm	VWR, Darmstadt, Germany
Chromatography system	ÄKTAexplorer100	GE Healthcare, München, Germany
Flow cytometer	LSRII flow cytometer	BD Biosciences, Heidelberg, Germany
Gastight syringe	1710RN, 100 µL	Hamilton, Bonaduz, Switzerland
Gel casting system	Mini-PROTEAN 3 Multi-Casting Chamber	Bio-Rad, Munich, Germany
Gel documentation	ChemiDoc XRS+	Bio-Rad, Munich, Germany
Gel electrophoresis system	Mini-PROTEAN® Electrophoresis System	Bio-Rad, Munich, Germany
Hybridisation oven	OV 3	Biometra, Göttingen, Germany
Incubator	HeraCell 240	Heraeus, Hanau, Germany
Lab blender	BagMixer® 400	Interscience, Saint Nom, France
Magnetic bead separator	DynaMag™-2 Magnet	Thermo Fisher Scientific, Waltham, MA, USA
Microplate reader	Infinite® M200 microplate reader	Tecan, Zurich, Switzerland
Microscope	Leica DMIL 090-135.001	Leica, Wetzlar, Germany
PCR-thermocycler	FlexCycler	Analytik Jena, Jena, Germany
Photometer	NanoPhotometer P300	IMPLEN, Munich, Germany
Plate shaker	IKA® MTS 2/4 multiwell plate shaker	IKA, Staufen, Germany
Plate washer	HydroSpeed™ plate washer	Tecan, Zurich, Switzerland
Semi-dry blotting system	Trans-Blot® Turbo™ Transfer System	Bio-Rad, Munich, Germany
Sonifier	Ultrasonics Sonifier S-450A	Branson, Danbury, CT, USA
Suspension array system	Bio-Plex® 200 instrument	Bio-Rad, Munich, Germany
Test-tube-rotator	34528	Snijders Labs, Tilburg, Netherlands
Thermomixer	Thermomixer compact	Eppendorf, Hamburg, Germany
Vertical shaker	KL-2	Edmund Bühler, Hechingen, Germany
Vortexer	Vortex Genie 2™	Bender & Hobein, Zurich, Switzerland

MATERIAL AND METHODS

4.1.11 Software

For control of technical devices, data analysis and illustration, and writing this dissertation software listed in Table 17 was employed.

Table 17: Software

Software	Manufacturer	Application
Biacore X100 Control Software	GE Healthcare, Munich, Germany	Biacore control software
Biacore X100 Evaluation Software	GE Healthcare, Munich, Germany	Analysis of SPR data
Bio-Plex Manager 6.1	Bio-Rad, Munich, Germany	Bioplex control software
Cell Quest Pro Software 5.1	BD Biosciences, Heidelberg, Germany	FACS control software
Endnote X8	Thomson Reuter, New York, NY, USA	management of references
FlowJo 8.7	FlowJo LLC, Ashland, OR, USA	Analysis of FACS data
GraphPad Prism 7.0	GraphPad Software, Inc., La Jolla, CA, USA	Data analysis/data illustrations
i-control™	Tecan, Zurich, Switzerland	Microplate reader control software
ImageLab 5.2.1	Bio-Rad, Munich, Germany	Illustration/analysis of SDS-PAGE gels and western blots
Microsoft Office 2010	Microsoft Corporation, Redmond, WA, USA	Data analysis/text processing
UNICORN Control	GE Healthcare, Munich, Germany	ÅKTA control software

4.2 Methods

4.2.1 Cell culture

4.2.1.1 *Passaging of myeloma and hybridoma cells*

Myeloma and hybridoma cells were cultivated at 37°C with 5% CO₂ at 98% humidity in an incubator (HeraCell 240). Cells were passaged in R10F⁻, R10F⁺, or R20F⁺ culture media (Table 13) under a biosafety cabinet (HeraSafe). For passaging, cells were suspended using a cell scraper and by pipetting up and down. The desired volume of cell suspension was then diluted in fresh culture media. To count cells and evaluate cell viability, cells were stained with trypan blue solution and analysed microscopically (Leica DMIL). Upon staining, viable cells remain unstained, whereas dead cells appear blue due to a loss of membrane integrity. For staining, cells were diluted in a 1:10 ratio with trypan blue solution (1% (w/v) in PBS). Viable cells were counted using a Neubauer cell counting chamber [147].

4.2.1.2 *Freezing and thawing of cells*

For long term storage cells were frozen in liquid nitrogen at -196°C. Therefore, cells (typically 10 mL cell suspension) were centrifuged (350 × g, 6 min, RT). The cell pellet was suspended in 900 µL cold cell culture media, transferred into a cryo preservation tube, and cooled down for 30 min on ice. Subsequently, cells were supplemented with 900 µL cell freezing medium and gently cooled down for at least 72 h at -80°C in a styrofoam container. Finally, cells were transferred into liquid nitrogen for long term storage. Small cell culture volumes (900 µL cell suspension) were directly transferred into a cryo preservation tube (without centrifugation) and treated as described.

For thawing, cells were quickly warmed up at 37°C in a water bath and immediately transferred into 9 mL fresh cell culture media. Cells were then centrifuged (350 × g, 6 min, RT) and resuspended in fresh cell culture media. Cells were transferred into appropriate cell culture flasks and cultivated as described above.

4.2.2 Handling of botulinum neurotoxins

4.2.2.1 *Safety issues*

Toxins were handled after appropriate supervision wearing adequate personal protective equipment including a back-fastening lab coat, a safety eye shield, two pairs of disposable gloves, and laboratory shoes. Toxins were always handled under a biosafety class II cabinet

MATERIAL AND METHODS

(HeraSafe). Liquid waste was decontaminated by incubation with 5% NaOH overnight. Consumables that got in contact with toxin solutions were decontaminated by flushing with 5% NaOH and treated by autoclave (60 min at 134°C) for toxin inactivation.

4.2.2.2 *Production of Clostridia supernatants*

Toxin containing *Clostridia* supernatants were produced from suspension cultures grown in TPGY or RCM media at 30–37°C under anaerobe conditions in an anaerobe workstation (Don Whitley, A35). *Clostridia* strains used in this work are listed in Table 9. After 1–10 days, suspension cultures were centrifuged (12.000 × g, 15 min, 4°C) and supernatants were subsequently filtered (0.45 µm and 0.22 µM). *Clostridia* supernatants were stored at -80°C.

4.2.3 **Generation of monoclonal antibodies**

4.2.3.1 *Principle of generation of Neo-mAbs*

Monoclonal antibodies were generated as described previously using a dedicated screening approach [96, 139, 140]. The general process of generation of monoclonal antibodies is outlined in Figure 9. Mice were immunized for several weeks with the respective antigen. Antibody titre was monitored by indirect ELISA (see section 4.2.5.3) and finally, mice exhibiting sufficient antibody titres were subjected to fusion. In the latter, murine spleen cells were fused to myeloma cells to produce immortal hybridoma cells. Supernatants of single clones were screened by indirect ELISA and surface plasmon resonance (SPR) techniques. Hybridoma clones producing the desired antibody were subcloned at least twice to ensure monoclonality. Subsequently, clones were cultivated in media supplemented with immunoglobulin (IgG)-free bovine foetal serum and subjected to quality controls including intracellular flow cytometry to demonstrate intracellular IgG antibody production. Finally, hybridoma cultures were expanded and IgG antibodies were purified by affinity chromatography.

Immunization was performed with short 8mer peptides, corresponding to the N- or C-terminal cleavage site. Due to the small sizes of the antigens, 8mer peptides were coupled to BSA as a carrier protein and Freund's complete or incomplete adjuvant was added in the first or the following immunizations, respectively. Antibody titres of mice were controlled on a regular basis for their specificity towards the respective neoepitope by indirect ELISA using corresponding KLH-coupled peptides. Mice exhibiting sufficient antibody titres towards the desired peptide(s) were subjected to fusion and hybridomas were analysed in a rigorous screening procedure involving multiple steps. During screening procedures two major

MATERIAL AND METHODS

challenges had to be tackled. First, clones that specifically recognize the respective BoNT cleavage site on SNARE proteins had to be distinguished from those additionally recognizing uncleaved substrate. This was achieved by testing antibody binding to KLH-coupled peptides (to exclude antibodies binding to BSA used as carrier for immunization) and to uncleaved SNAP-25 or VAMP-2 by indirect ELISA in the initial screening. Highly cross-reactive antibodies were excluded from further characterization. Second, the recognition of neighbouring cleavage sites had to be excluded. This was particularly challenging for antibodies specific for BoNT/A and C neopeptides as well as for BoNT/F and D neopeptides, as cleavage sites of these BoNTs differ in only one amino acid. Thus, KLH-coupled peptides covering neighbouring cleavage sites were including in the screening process.

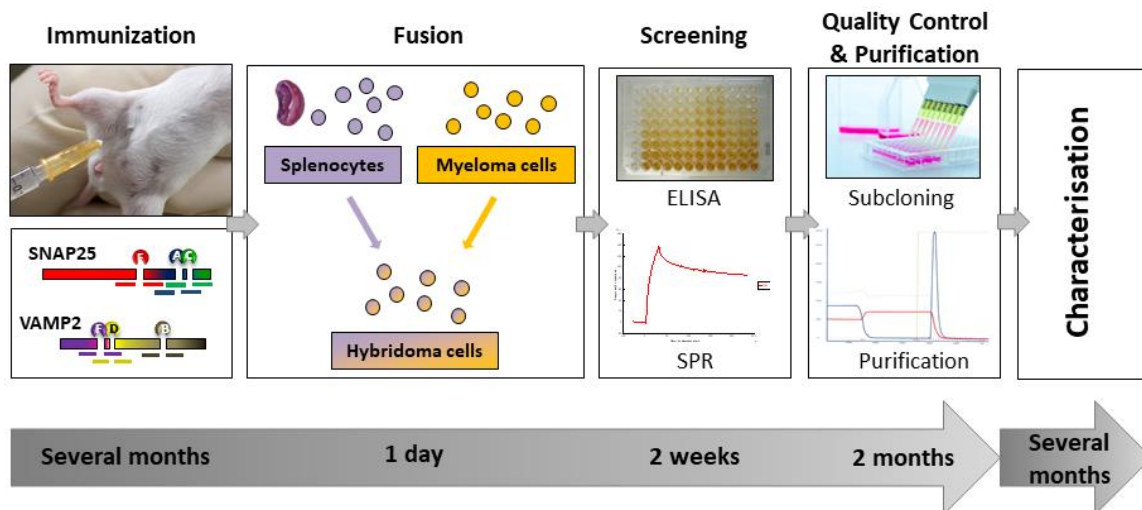


Figure 9: General scheme of the production of neopeptide specific antibodies. Mice were immunized with short BSA-coupled 8-mer peptides corresponding to the respective BoNT cleavage site. Antibody titer was tested by indirect ELISA using corresponding KLH-coupled peptides. For generating monoclonal antibodies, mice exhibiting sufficient antibody titres were selected for fusion. Hereby, murine spleen cells were fused to myeloma cells to generate hybridoma cells. Hybridoma cells were tested for their production of specific antibodies by indirect ELISA and SPR technology. Clones producing highly specific Neo-mAbs were subcloned, expanded, and antibodies were purified. The image was in parts kindly provided by Maren Krüger, RKI.

4.2.3.2 Immunization of mice

To obtain neopeptide specific antibodies, NMRI mice at the age of at least six weeks were immunized with short 8mer peptides corresponding to the respective BoNT cleavage site coupled to BSA as carrier protein. To this end, 100 µg 8mer peptide (either a single peptide or in a mixture of multiple peptides) were diluted in PBS and mixed with Freund's complete (first

MATERIAL AND METHODS

immunization) or incomplete adjuvant (booster immunizations) in a 1:1 ratio. The peptide-adjuvant emulsion was mixed extensively (Vortex Genie 2™) for 10 min and subsequently homogenized by ultrasound treatment for 2 min at 4°C (Ultrasonics Sonifier S-450A: Output Control Level 5, Duty Cycle 50%). Finally, 100–200 µL emulsion was injected intraperitoneally into mice. The last three booster immunizations prior to fusion were performed without adjuvant (peptide in PBS only). Regularly, mice were immunized in three to four-week intervals. Sequences of peptides used for immunizations are outlined in Table 11. Immunization schemes of mice for all fusions performed in this work are summarized in the appendix (Appendix Table 7– Appendix Table 10).

4.2.3.3 Testing of antibody titer

Antibody titer of immunized mice was tested 10-14 days after immunization. A few droplets of blood were collected from the tail vein using a hollow needle (size 16) and a capillary tube (Minivette® POCT). Blood samples were incubated for 1 h at RT to allow for clogging and subsequently centrifuged (5000 × g, 5 min, RT) to separate serum from particles. Serum was tested for antibody titre by indirect ELISA as described below (section 4.2.5.3). Development of antibody titres after immunizations of mice are depicted in Appendix Figure 2.

4.2.3.4 Generation of antibody producing hybridoma cells

To obtain antibody producing hybridoma cells, murine spleenocytes were fused with immortal myeloma cells [148]. Furthermore, to support cellular growth, murine thymocytes were added to the hybridoma cells after fusion.

Preparation of thymocytes

Murine thymi were removed under a biosafety cabinet and incubated in PBS/PenStrep until further processing. To separate cells, thymi were pushed through a cell dissociation sieve (212 µM) with mechanical force and suspended in PBS/PenStrep. Cells were centrifuged (380 × g, 8 min, RT) and suspended in pre-warmed R10F⁻ culture media. Viable cells were counted using trypan blue solution (see section 4.2.1.1) and stored in a water bath at 37°C until further use.

Preparation of myeloma cells

For each fusion, a new vial of myeloma cells (P3X63Ag8.653) was thawed and passaged over 1.5–3 weeks in R10F⁻ culture media (see section 4.2.1). To ensure growth in a logarithmic

MATERIAL AND METHODS

growth phase, cells were passaged daily. Viable cells were counted by staining with trypan blue solution and cell density was adjusted to 2×10^5 cells/mL. Cells were expanded to a total culture volume of 400 mL. Prior to fusion, cells were centrifuged ($380 \times g$, 8 min, RT), and washed twice with 50 mL pre-warmed RPMI1640 β -ME. Finally, cells were suspended in 30 mL RPMI1640 β -ME, counted, and kept in a water bath at 37°C until further application.

Preparation of splenocytes

Murine spleen was removed under a biosafety cabinet and incubated in PBS/PenStrep until further processing. To collect splenocytes located inside the spleen, one end was cut, and the spleen was rinsed with 10 mL PBS/PenStrep by injecting a syringe into the other end. To additionally obtain cells from spleen tissue, fatty components were carefully removed, and spleen tissue was pushed through a cell dissociation sieve (212 μ M) with mild mechanical force. All cells were collected, suspended in PBS/PenStrep and centrifuged ($380 \times g$, 8 min, RT). Subsequently, supernatant was aspirated, cells were washed with 20 mL PBS/PenStrep, and aggregates were removed by passing through a nylon cell strainer (70 μ M) which was subsequently flushed with 20 mL PBS/PenStrep. Then, cells were centrifuged ($380 \times g$, 8 min, RT) and supernatant was aspirated. To lyse erythrocytes, cells were incubated in 4 mL ACK lysis buffer for 1 min under gentle agitation. Lysis was stopped by adding 30 mL PBS/PenStrep and cells were again passed through a nylon cell strainer, which was subsequently flushed with 10 mL PBS/PenStrep. Finally, cells were centrifuged ($380 \times g$, 8 min, RT) and the pellet was suspended in 20 mL pre-warmed RPMI1640 β -ME. Splenocytes were counted by staining with Türks solution. For staining, cells were diluted in a 1:10 ratio with Türks solution and viable cells were counted using a Neubauer cell counting chamber. Splenocytes were kept in a water bath at 37°C until further application.

Fusion of splenocytes and myeloma cells

Splenocytes and myeloma cells were fused to generate hybridoma cells as previously described by Köhler and Milstein [148]. Prepared splenocytes and myeloma cells were pooled at a 2:1 ratio and centrifuged ($380 \times g$, 8 min, RT). To solubilize cellular membranes, PEG solution (1 mL per 100×10^6 splenocytes) was carefully added to the cell pellet under constant gentle agitation in a water bath warmed to 37°C. After 1–3 minutes prewarmed RPMI1640 β -ME (10 mL per 100×10^6 splenocytes) was slowly added to the cells under further agitation. Cells were then incubated for 5 min at 37°C, centrifuged ($500 \times g$, 5 min, RT), and carefully

MATERIAL AND METHODS

suspended in pre-warmed R10F⁻ culture media. Finally, hybridoma cells were supplemented with thymocytes (at a 1:1 ratio to splenocytes), diluted in R20F⁻/AH selective media to a final concentration of 1×10^5 cells/mL, and seeded in sterile 96-well cell culture plates (200 μ L cell suspension/cavity). On days seven and eight post fusion, 100 μ L hybridoma supernatant was replaced by 150 μ L fresh R20F⁻/AH selective media.

4.2.3.5 Screening

Ten days post fusion hybridoma clones were screened for their capacity to produce antibody with the desired specificity. Cell density was controlled visually and supernatants of densely grown hybridoma clones were subjected for screening procedures. Primary screening was performed by indirect ELISA (see section 4.2.5.3), testing specificity towards short KLH coupled 8mer peptides as positive and full-length substrate as negative control. Positive clones were transferred into larger cell culture plates (48-well or 24-well) and subjected to a secondary screening on the next day including indirect ELISA and analysis by SPR techniques (see section 4.2.5.2). Clones passing the secondary screening process were further cultivated in R20F⁺ culture media and subcloned (see section 4.2.3.6). Screening procedure was repeated up to five times to screen approximately 1000-5000 clones (corresponding to 10-50 96-well plates) per fusion.

4.2.3.6 Subcloning

To ensure monoclonality of hybridoma clones used for antibody generation, clones were subcloned at least twice. Serial dilutions of hybridoma cells were prepared in R20F⁺ culture media: 300 cells/mL, 100 cells/mL, 30 cells/mL, 10 cells/mL, and 3 cells/mL. The different dilutions were seeded in 96-well culture plates (100 μ L/well) and incubated for six to seven days. Culture plates were analysed visually for cellular growth and isolated colonies per well, presumably originating from a single clone, were marked. Cells were fed with 150 μ L fresh R20F⁺ culture media. Ten days after seeding, marked clones were analysed by indirect ELISA towards the desired specificity (see section 4.2.5.3). Selected clones were further cultivated and subcloned again if required. Monoclonality was controlled by intracellular FACS staining (see section 4.2.3.7). After subcloning, clones were deprived from IL-6 and FCS and further cultivated in R10F⁺ culture media.

MATERIAL AND METHODS

4.2.3.7 *Quality controls*

To ensure monoclonality as well as to exclude contamination by mycoplasma, hybridoma clones were subjected to quality controls prior to antibody purification.

Intracellular fluorescence-activated cell sorting (iFACS)

To control antibody production and to ensure monoclonality, hybridoma clones were analysed by iFACS. To that aim, cells were fixed, then intracellular IgG antibodies were fluorescently labelled, and finally cells were analysed by flow cytometry. For fixing, cells (usually 200 μ L of a densely grown cell suspension) were centrifuged (400 \times g, 5 min, 4°C) and washed twice with PBS (200 μ L). Then, cells were suspended in 2% (v/v) formaldehyde in PBS (200 μ L) and incubated for 20 min at RT. Cells were subsequently washed twice with PBS (200 μ L) and suspended in saponin buffer (200 μ L) for permeabilization of the cellular membrane. For staining, a goat anti-mouse-IgG-Cy5 antibody was added (50 μ L, 6 μ g/mL diluted in saponin buffer) and incubated for 20 min at RT (in dark). Finally, cells were washed twice with saponin buffer (150 μ L and 200 μ L), suspended in FACS-PBS (200 μ L), and analysed by flow cytometry on a LSRII flow cytometer using Cell Quest Pro Software. Different cell populations were distinguished according to size, granularity, and fluorescence signal by FlowJo software.

Mycoplasma testing

To exclude contaminations by mycoplasma, hybridoma clones were subjected to a mycoplasma PCR. Cells were centrifuged (1 mL of densely grown cell suspension, 350 \times g, 6 min, RT) and suspended in PBS (200 μ L). DNA was extracted using DNeasy Blood and Tissue Kit according to the manufacturer's instructions. The mycoplasma PCR was conducted as instructed in VenorGeM Mycoplasma Detection Kit.

4.2.3.8 *Antibody production and purification*

Hybridoma clones that produced antibodies with the desired specificity, that were subcloned at least twice, and passed all quality controls were expanded in IgG free R10F⁺ GPG culture media to 1.5–2 L suspension cultures. Hybridoma clones were allowed to grow until ~80–90% of the cells died whereupon culture supernatant was harvested by two subsequent centrifugation cycles of cells (2000 \times g, 10 min, 10 °C followed by 8000 \times g, 10 min, 10 °C). Supernatant was neutralized by addition of 2 M Tris pH 8.8 and filtered under sterile

MATERIAL AND METHODS

conditions (0.22 µm sterile vacuum bottle-top filter). IgG antibodies were purified from supernatants by affinity chromatography using a protein A column (HiTrap MabSelect SuRe column) and ÄKTAexplorer100 system. The column was equilibrated with running buffer, loaded with hybridoma supernatant and rinsed with running buffer to remove unbound proteins. IgG antibodies were eluted with 0.1 M sodium citrate pH 3.6 and antibody solutions were immediately neutralized by addition of 3.6 M Tris pH 9. Antibody containing fractions were pooled, dialysed (8-10 kDa cut-off dialysis tubing) against PBS (3 times with 2 h, overnight, 2 h intervals, each with 1 L PBS) and filtered under sterile conditions (0.22 µm PVDF syringe filters). Antibodies were stored at -80°C (long term storage) or 4°C (working aliquots).

4.2.3.9 Isotyping of monoclonal antibodies by sandwich ELISA

Antibody isotypes were determined by sandwich ELISA. To that aim, 5 µg/mL capture antibody goat anti-mouse IgG (50 µL/well diluted in 0.1% BSA/PBS) was immobilized on 96-well MaxiSorp-plates by incubating plates overnight at 4°C. Plates were then washed with PBS-T (4 × with 350 µL/well with plate washer) and blocked with blocking buffer (200 µL/well) for 1 h at RT. Plates were washed again (4 ×), and 500–100 ng/mL purified Neo-mAb was added (50 µL/well diluted in 0.1% BSA/PBS) for 1 h. Then, plates were washed (4 ×) and biotinylated detection antibody (goat anti-mouse IgG1, goat anti-mouse IgG2a, goat anti-mouse IgG2b, goat anti-mouse IgG3) was added (50 µL/well diluted in blocking buffer) for 1 h. After an additional washing step (4 ×) streptavidin conjugated horseradish peroxidase (SA-POD) was added (50 µL/well, 1:2500 diluted in blocking buffer) for 30 min. Finally, plates were washed (8 ×) and signals were detected by the addition of TMB substrate (100 µL/well). Enzymatic reaction was stopped after 15 min by adding 0.25 M H₂SO₄ (100 µL/well) and plates were analysed using a microplate reader measuring absorbance at 450 nm and 620 nm.

4.2.4 Biochemical methods

4.2.4.1 SDS-PAGE

Tris-Glycine SDS-PAGE to separate proteins was performed according to Laemmli et al [149]. Furthermore, a Tricine-SDS-PAGE according to Schägger et al [150] to separate small peptides was applied for separation of cleavage fragments in Taguchi experiments (see section 4.2.6.3). For Tris-Glycine SDS-PAGE, 0.75 mm two-phase polyacrylamide gels consisting of a 16% running gel in the lower part and a 4% stacking gel in the upper part were prepared as indicated in Table 18. After polymerisation, gels were installed in an electrophoresis chamber

MATERIAL AND METHODS

(Mini-PROTEAN® Electrophoresis System) filled with electrophoresis running buffer. Samples were prepared by adding Laemmli loading buffer, boiling for 5 min at 95°C, cooling down and loaded on acrylamide gels. Gels were run for one hour at low voltage (60 V) during accumulation of proteins in the stacking gel. Then voltage was increased (up to 120 V) until the desired protein separation was achieved. Gels were removed from the electrophoresis chamber and stained by colloidal Coomassie [151] or Silver stain [152] as described below. After staining, gels were documented at a ChemiDoc workstation (ChemiDoc XRS+) and analysed using ImageLab software (ImageLab 5.2.1).

Table 18: Composition of stacking gel and running gel for SDS-PAGE

Reagent	Stacking gel (4%)	Running gel (16%)
ddH ₂ O	3.05 mL	2 mL
1.5 M Tris-HCl, pH 8.8	1.25 mL	–
0.5 M Tris-HCl, pH 6.5	–	2.5 mL
10% SDS	50 µL	100 µL
Acrylamide/Bisacrylamide solution	650 µL	5.4 mL
10% APS	25 µL	60 µL
TEMED	6 µL	7 µL

Colloidal Coomassie

For staining with colloidal Coomassie according to Neuhoff et al [151] gels were washed three times with demineralised water (5 min under constant agitation). Gels were then stained overnight with colloidal Coomassie under constant agitation. Finally, gels were thoroughly washed with demineralised water until superfluous stain was removed as desired.

Silver stain

To increase sensitivity, silver stain according to Blum et al [152] was performed after staining gels with colloidal Coomassie. Gels were washed twice with 50% EtOH (20 min under constant agitation) and subsequently sensitized with 0.02 % Na₂S₂O₃ for 1 min (under constant agitation). Gels were then washed three times with demineralised water (20 s under constant agitation) and incubated with silver staining solution for 20 min (under constant agitation). Subsequently, gels were washed again twice with demineralised water (20 s under constant agitation) and developed with silver developing solution for 3–6 min. Development was

MATERIAL AND METHODS

stopped by adding 10% acetic acid. Finally, gels were washed three times with demineralised water (20 s under constant agitation).

4.2.4.2 Determination of protein concentration

Concentration of antibodies was determined spectrophotometrically by measuring absorbance at 280 nm and 320 nm (reference) with a photometer (NanoPhotometer P300). Protein concentration was determined by Beer–Lambert law [153] ($A = c \times \varepsilon \times d$) with an extinction coefficient of $\varepsilon = 210,000 \times \frac{1}{M} \times \frac{1}{cm}$.

4.2.4.3 Assembly of dual-Syt-II-Nanodiscs

Assembly of dual-Syt-II-Nanodiscs (dual-Syt-II-NDs) was performed as described previously [154] with some modifications to the protocol. First, a 1-palmitoyl-2-oleoyl-sn-glycero-3-phosphocholine (POPC) solution in cholate (sodium cholate hydrate) was prepared. POPC lipid stock dissolved in chloroform was transferred into 6 mL borosilicate glass tubes using a gastight syringe and dried under a nitrogen stream followed by vacuumation for 4 h. Then, lipids were dissolved in 400 mM cholate giving a final stock solution of 100 mM POPC and 400 mM cholate by extensive mixing and treatment by ultrasound until the solution appeared clear. For assembly of dual-Syt-II-NDs, a reconstitution mixture consisting of POPC (100 mM), cholate (400 mM), GT1b (10 $\mu\text{g}/\text{mL}$ in PBS), GST-rSyt-II K51R (3–4 mg/mL in TritonX-100/PBS) was added to 100 μL membrane scaffold protein (MSP) 1E3D1 (dissolved in PBS containing 4 mM octyl β -D-glucopyranoside). For the assembly of empty NDs, GT1b and GST-rSyt-II K51R were omitted. Depending on the concentration of the MSP 1E3D1 and the kind of NDs, concentration was adjusted to 120 POPC molecules (11 μL) and 10 molecules of GT1b (19.7 μL) per ND with 30.3 μL concentrated GST-rSyt-II K51R for dual-Syt-II-NDs and 130 POPC molecules per ND for empty NDs. The total volume of the reconstitution mixture was filled to 170 μL with PBS and the mixture was incubated for 30 min at RT. For NDs assembly the mixture was added to 170 μg washed (PBS) and degassed Bio-Beads and incubated for 2 h at 4°C on a vertical shaker at 150 rpm. Then, the mixture was separated from the Bio-Beads, transferred to fresh Bio-Beads (170 μg , washed and degassed) and incubated overnight at 4°C on a vertical shaker at 150 rpm. The ND assembly mixture was then separated from the Bio-Beads, transferred into a glass tube, and stored until use (maximal for one month) at 4°C.

MATERIAL AND METHODS

4.2.4.4 Coupling of glutathione to casein

Coupling of glutathione to casein was performed as described previously [155]. For coupling of glutathione to casein, 0.2 M casein was dissolved in PBS by incubation at 37°C under constant agitation. The casein solution (25 mL) was derivatised with 0.4 mM N-Ethylmaleimide (NEM) by adding 20 mM NEM (in DMSO, 0.5 mL) for 15 min at RT. Subsequently, 50 mg Sulfo-SMPB was added (making a final concentration of 4.36 mM Sulfo-SMPB) and the solution was incubated for 30 min at RT in a rotator (Test-tube-rotator) for crosslinking. To remove precipitate, the solution was centrifuged (5000 × g, 5 min) and supernatant was collected. Unbound Sulfo-SMPB was removed using PD 10 desalting columns equilibrated with PBS. Then, glutathione buffer (6 mL) was added and incubated for 1 h at RT. Finally, unbound glutathione was removed using PD 10 desalting columns equilibrated with PBS. Protein concentration was determined spectrophotometrically, and casein-glutathione was stored at -20°C.

4.2.4.5 Coupling of antibodies or receptor molecules to M270- or M280 paramagnetic dynabeads

Anti-BoNT antibodies were coupled to M280 (Dynabeads® M-280 Tosylactivated) or M270 (Dynabeads® M-270 Carboxylic Acid) dynabeads for toxin enrichment. Casein-glutathione and gSV2C was coupled to M270 dynabeads. For Endopeptidase-ELISA experiments, M280 dynabeads were used. Due to an observed unspecific adherence of some toxins to the M280 dynabeads, M270 dynabeads were applied in the duplex-assay experiments. Coupling was performed according to the manufacturer's instructions with slight modifications of the protocol.

Coupling of M280 dynabeads

For coupling of antibodies to M280 dynabeads, 5×10^8 (250 µL) beads were transferred into low binding 1.5 mL tubes (Protein LoBind Tubes) and supernatant was removed using a magnetic separator (DynaMag™-2 Magnet). Beads were then washed twice with sodium phosphate buffer (800 µL) and incubated with 0.6 mg/mL antibody solution (250 µL diluted in PBS) overnight at 37°C in a rotator. Beads were then washed twice with cold PBS/BN (800 µL), suspended in Tris-buffer (800 µL) and incubated for 4 h at 37°C in a rotator. Finally, beads were washed once with PBS/BN (800 µL) and suspended in PBS/BN (500 µL) for storage. Beads were stored at 4°C and kept for a maximum of three months.

MATERIAL AND METHODS

Coupling of M270 dynabeads

For coupling of antibodies, gSV2C, or casein-glutathion to M270 dynabeads, 5×10^8 (250 μ L) beads were transferred into low binding 1.5 mL tubes and supernatant was removed using a magnetic separator. Beads were then washed twice with MES-buffer (800 μ L) and activated by adding 50 mg/mL EDC (100 μ L diluted in MES-buffer), 50 mg/mL Sulfo-NHS (100 μ L diluted in MES-buffer) and MES-buffer (50 μ L). Beads were then incubated for 30 min at RT in a rotator and washed twice with MES-buffer (800 μ L). Subsequently, beads were incubated with 0.6 mg/mL antibody or casein-glutathion solution (250 μ L diluted in PBS), or 0.1 mg/mL gSV2C (250 μ L) for 4 h at RT (or overnight at 4°C) in a rotator. Beads were then quenched by adding 50 mM Tris pH 7.4 (250 μ L) and incubation for 15 min at RT in a rotator. Finally, beads were washed twice with PBS (800 μ L) and suspended in PBS/BN (500 μ L). Beads were stored at 4°C and kept for a maximum of three months.

Coupling of dual-Syt-II-NDs to M270-casein-glutathion dynabeads

For a directed coupling of dual-Syt-II-NDs to M270 dynabeads a two-step protocol was employed: First, casein-glutathion was covalently coupled to dynabeads as described above. As the second step, dual-Syt-II-NDs were captured by casein-glutathion through GST-tagged Syt-II. To that aim, M270 dynabeads coupled to casein-glutathion (500 μ L) were washed with PBS (800 μ L) and incubated with the dual-Syt-II NDs assembly mixture (see section 4.2.4.3) diluted in a 1:8 ratio with PBS (500 μ L). Beads were incubated for 1 h at RT in a rotator, washed twice with PBS (800 μ L) and suspended in PBS/BN (500 μ L). Beads were stored at 4°C and kept for a maximum of one month.

During NDs assembly a crude mixture of dual-Syt-II-NDs as well as empty NDs or only GT1b containing NDs are produced. As only dual-Syt-II-NDs ensure high affinity binding of BoNT/B, the two-step coupling protocol avoids a time-consuming purification after NDs assembly required to separate the correct dual-Syt-II-NDs from the crude mixture. In addition, this protocol ensures the correct orientation of the receptor molecule for BoNT/B binding.

4.2.4.6 Coupling of substrate molecules to fluorescent magnetic luminex-beads

Substrate molecules were coupled to luminex-beads according to the manufacturer's instructions with some modifications to the protocol. To prevent bleaching of beads, all steps were performed in dark, and exposure to light was kept to a minimum. 1.5×10^6 beads

MATERIAL AND METHODS

(120 μL) were transferred into low binding 1.5 mL tubes and supernatant was removed using a magnetic separator. Beads were suspended in demineralised water, mixed by vortexing, and treated by ultrasound (10 sec). Supernatant was removed, and beads were suspended in 0.1 M NaH_2PO_4 pH 6.2 (80 μL) followed again by mixing and ultrasound treatment. Beads were activated by adding 50 mg/mL EDC (10 μL diluted in demineralised water) and 50 mg/mL Sulfo-NHS (10 μL diluted in demineralised water) and incubation for 20 min in a rotator. After activation, beads were washed twice with MES-buffer (250 μL) with mixing and treatment by ultrasound after each washing step. For coupling of substrate molecules, 20 $\mu\text{g}/\text{mL}$ substrate molecule (500 μL diluted in MES-buffer) was added and beads were incubated for 4 h at RT (or overnight at 4°C) in a rotator. Subsequently, supernatant was removed, and beads were quenched by adding PBS-TBN (500 μL) and incubation for 30 min at RT on a rotator. Finally, beads were washed twice with PBS-TBN (1 mL) and suspended in PBS-TBN (500 μL). Bead concentration was determined microscopically using a Neubauer cell counting chamber and adjusted to 1000 beads/ μL (with PBS-TBN). Beads were stored at 4°C and kept for a maximum of six months.

4.2.4.7 Biotinylation of antibodies

For biotinylation of antibodies, a molar ratio of 20:1 (biotin:antibody) was generally applied. 1 mg/mL antibody (500 μL) was mixed with 1 M NaHCO_3 (50 μL) and 13.4 mM biotin-NHS (dissolved in DMSO, 5 μL) and incubated for 1 h in a rotator. Coupling reaction was stopped by adding 10% NaN_3 (10 μL). Non-bound biotin-NHS was removed using PD 10 desalting columns equilibrated with PBS/N. Protein concentration of biotinylated antibodies was determined as described in section 4.2.4.2. Finally, BSA was added to a final concentration of 0.2%. Biotinylated antibodies were stored at -80°C (long term storage) or 4°C (working aliquots).

4.2.4.8 Trypsin digest of BoNT

Trypsin-activation of BoNT/E or non-proteolytic *Clostridia* supernatants prior to duplex-assay experiments was performed with Mag-trypsin (Immobilized TPCK Trypsin Magnetic Beads) according to the manufacturer's instructions. Mag-trypsin (250 μL) was washed twice with demineralized water (500 μL) and once with 0.1% BSA/PBS (500 μL) using a magnetic separator. Then, toxin solution was added (450 μL) and beads were incubated for 1 h at 37°C in a rotator. The supernatant was collected and applied in the assays.

MATERIAL AND METHODS

4.2.4.9 Preparation of complex matrices for spiking experiments

Human serum was obtained from eight individuals (male and female) and pooled before use. Food matrices (beans, fish, sausage) were prepared by mixing foods with 1% peptone (Bacto™ Peptone) in a 1:1 (beans and sausage) or 1:2 (fish) ratio. Food was then homogenized by hand (fish) or using a bagmixer (BagMixer® 400, beans and sausage). Solid components were removed using a bagfilter. To remove residual particles matrices were centrifuged before usage (5000 × g, 5 min, RT). Matrices were stored at -80°C.

4.2.5 Immunological methods

4.2.5.1 Western blotting to analyse specificity of Neo-mAbs

To test whether Neo-mAbs recognize cleaved, but not uncleaved substrate, Western blots were performed. Substrate cleavage was performed by incubating 6 μM rSNAP-25 H6 or H6trVAMP-2 with 100 nM BoNT/A, B, E, or F, or 40 nM BoNT/DC, or 250 nM BoNT/C in cleavage buffer (total reaction volume 200 μL) for 18 h at 37°C in a thermomixer. Samples were inactivated by heating for 10 min at 95°C and protein fragments were separated by SDS-PAGE using 16% acrylamide gels as described above (see section 4.2.4.1). For Western blotting, PVDF membranes (Immobilon®-P PVDF Membrane) were prepared by soaking in 100% MeOH, washing with demineralised water, and equilibration in transfer buffer for 20 min. Blots were assembled in a blotting system (Trans-Blot® Turbo™ Transfer System) from bottom to top using three sheets of whatman filter paper (soaked in transfer buffer), prepared PVDF membrane, gel from SDS-PAGE (equilibrated in transfer buffer for 5 min), and again three sheets of whatman filter paper (soaked in transfer buffer). For blotting, the low molecular weight program (5 min with 1.3–2.5 A and up to 25 V) was run twice (two cycles of the low molecular weight program turned out to result in complete transfer of cleavage fragments). After blotting, membranes were washed with demineralised water and incubated in blocking buffer for at least 1 h at RT (or overnight at 4°C) under constant agitation. Subsequently, membranes were incubated with 10 μg/mL Neo-mAb (diluted in blocking buffer) for at least 1 h (or overnight at 4°C) under constant agitation. Signal detection was either performed using the Avidx-AP + CDP-Star system or by Dura Western blotting substrate (Super Signal® West Dura Western blotting substrate). For the former, membranes were washed three times for 5 min with blocking buffer, incubated with biotinylated goat anti-mouse IgG (H+L) antibody (diluted 1:10000 in blocking buffer) for 30 min, washed three times

MATERIAL AND METHODS

for 5 min with blocking buffer, and incubated with 0.5 µg/mL Avidx-AP (diluted in PBS-T) for 20 min. Membranes were then washed again three times for 5 min with blocking buffer and signals were detected by adding AP substrate (CDP-Star, diluted 1:50 in WB assay buffer) for 5 min. For signal detection by Dura Western blotting substrate, membranes were washed three times for 5 min with PBS-T (after incubation with primary antibody), incubated with a horseradish peroxidase (HRP) conjugated goat anti-mouse (Fcy) antibody (diluted 1:2500 in blocking buffer) for 30 min, and washed again three times for 5 min with PBS-T. Membranes were then washed once with demineralised water and signals were detected by adding Dura Western blotting substrate according to the manufacturer's instructions. Western blots were documented at a ChemiDoc workstation and analysed using ImageLab software.

4.2.5.2 *Surface plasmon resonance (SPR)*

To analyse antibody affinity and avidity, or affinities of receptor molecules SPR technology using a Biacore X100 (Neo-mAbs and receptor molecules) or Biacore T200 (anti-BoNT antibodies) instrument was employed. The general principle of measuring interactions by SPR technology is outlined in Figure 10. Principally, a ligand (e.g. an antibody) is immobilized on the gold surface of a glass sensor chip, and an interaction partner in solution (analyte) is injected through a microfluidic system. To determine the degree of interaction, polarized light (polarized by a prisma) is directed to the gold surface (incident light), thereby creating an evanescent electromagnetic field, which extends into the ligand containing microfluidic channel below the gold surface. At a specific angle of incident light, interaction of the evanescent electromagnetic field with free oscillating electrons at the gold surface will excite surface plasmons, which creates a dip in the intensity of reflected light. The angle of respective dip is influenced through the evanescent electromagnetic field by changes in optical density of the fluid below the gold surface [156]. Thus, the binding of an analyte to the ligand changes optical density which leads to a change in the angle (Figure 10, A, B). This change can be monitored and is recorded as resonance units (RU) in real time in a sensogram (Figure 10, C, D, E).

All SPR measurements were performed at 25°C. For all measurements ligands and analytes were diluted in HBS-EP+ running buffer.

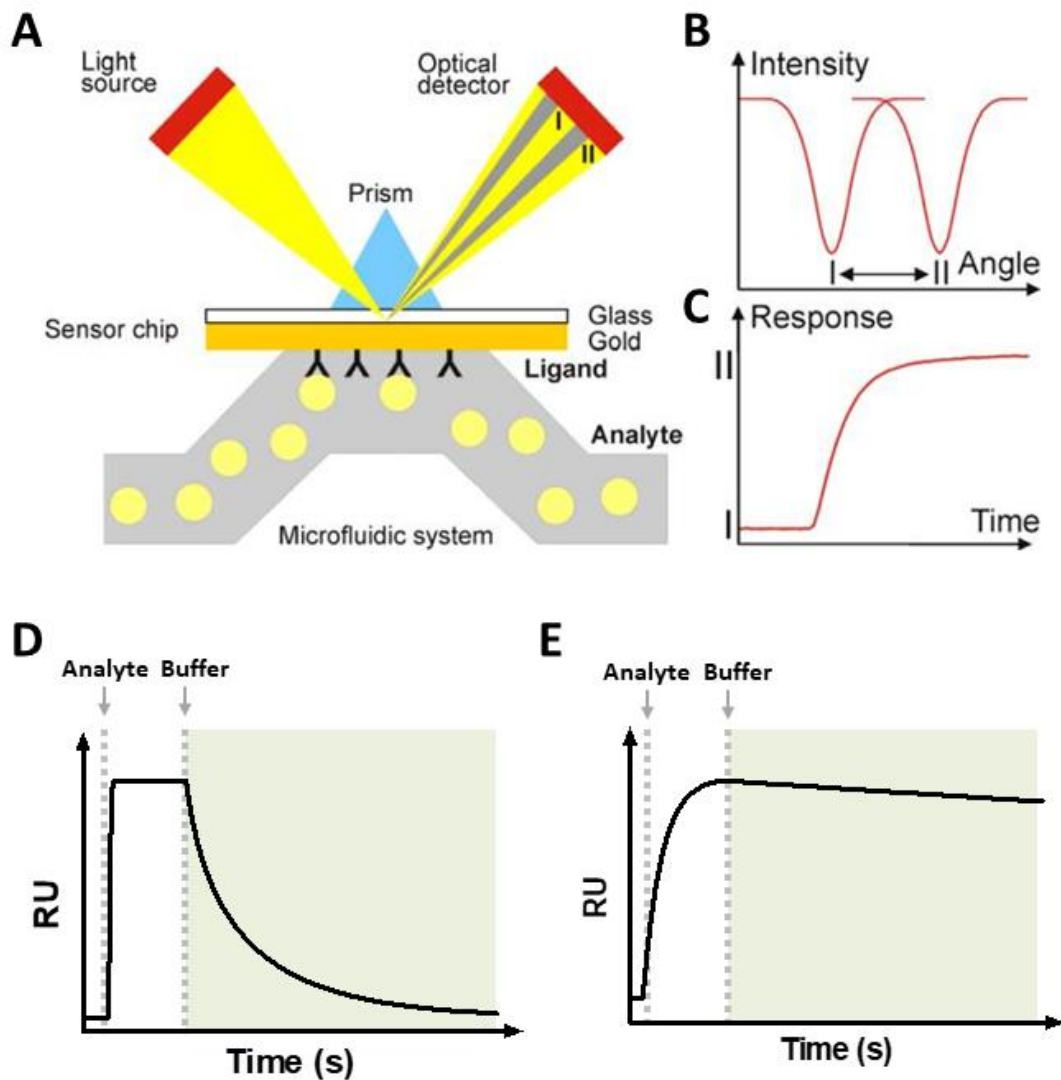


Figure 10: General principle of measuring interactions by SPR. (A+B) Polarized light that is directed to the gold surface of a sensor chip creates an evanescent electromagnetic field, which extends into the ligand-containing microfluidic channel below the gold surface. At a specific angle of incident light, this excites surface plasmons, creating a dip in the intensity of reflected light. The angle of the respective dip changes with changes in the optical density of the fluid below the gold surface, thus binding of an analyte to the ligand changes the angle of the dip. (C) The sensogram depicts the change of the angle of the dip against time. It therefore monitors the interaction of ligand and analyte in real-time. Signals are recorded in resonance units (RUs). Images A, B, and C are taken from [156]. (D+E) Typical sensograms of ligand-analyte interaction depicting an unstable interaction (D) and a stable interaction (E): First, the analyte is injected, which interacts with the immobilized ligand, thus leading to an increase in RUs. Then, buffer is injected, which leads to a quick dissociation of the analyte from the ligand in the unstable interaction (D). In case of a more stable interaction (E), the analyte slowly dissociates from the ligand.

Preparation of CM5 sensor chip

To analyse the affinities of Neo-mAbs, anti-BoNT antibodies, or receptor molecules, anti-mouse IgG, anti-human IgG (Fc), or anti-GST antibody was immobilized on the gold surface of a

MATERIAL AND METHODS

carboxyl-derivatized chip (CM5 sensor chip) through EDC/NHS coupling. The sensor chip was prepared using a mouse antibody/human antibody/GST capture kit and amine coupling kit according to the manufacturer's instructions. Briefly, to activate the carboxyl surface, EDC/NHS was injected for 10 min. Then, 30 µg/mL anti-mouse IgG, 25 µg/mL anti-human IgG (Fc), or 30 µg/mL anti-GST antibody was injected for 7 min, 6 min, or 5 min respectively followed by injection of ethanolamine for 7 min for deactivation. Immobilization was performed at a constant flow rate of 10 µL/min.

Affinity measurements with Neo-mAbs

Affinity measurements with Neo-mAbs were carried out by immobilizing Neo-mAbs on an anti-mouse IgG prepared CM5 sensor chip (see above) and injecting serial dilutions of short biotinylated peptides corresponding to the respective cleavage site. 50 µg/mL Neo-mAb was injected for 120 s at 5 µL/min on Flow cell 2 (Fc2) leading to immobilization levels between 400 and 1500 RUs of captured antibody. Fc1 remained empty (anti-mouse IgG only) and was set as blank control. Binding kinetics and affinities were determined in a multi-cycle kinetic by injecting serial dilutions (1:4 dilutions) of biotinylated peptides over Fc1 and Fc2 for 60 s at 30 µL/min followed by a 300 s dissociation step with HBS-EP+ running buffer (in total five different dilutions were tested for each antibody). Depending on the antibody's affinity dilution series were adjusted accordingly (SNAP/A/291: 80 µg/mL to 313 ng/mL; SNAP/A/305, VAMP/B/1148, VAMP/B/226, VAMP/B/392, SNAP/C/1844, SNAP/C/3280: 100 µg/mL to 391 ng/mL; VAMP/B/726, SNAP/C/5593, SNAP/C/2207, SNAP/E/217: 10 µg/mL to 39 ng/mL; VAMP/B/151, VAMP/D/27, VAMP/F/425, VAMP/F/440, VAMP/F/521, VAMP/F/1333, VAMP/F/153: 500 ng/mL to 1.95 ng/mL; VAMP/D/29, SNAP/E/1466: 20 µg/mL to 78 ng/mL). For sensor chip regeneration, 10 mM Glycin pH 1.7 was injected for 180 s at 10 µL/min. To ensure reproducibility of measurements and stable sensor surface activity the highest analyte concentration was measured in duplicates. In addition, three blank measurements (no analyte) were performed in each run.

Affinity measurements with anti-BoNT antibodies

Affinity measurements with anti-BoNT antibodies were performed analogues to affinity measurements with Neo-mAbs with the following modifications. For antibody immobilization, 5 µg/mL antibody were injected on Fc2 of an anti-mouse IgG prepared CM5 sensor chip for 120 s at 5 µL/min leading to immobilization levels between 50 and 150 RUs of captured

MATERIAL AND METHODS

antibodies. Binding kinetics and affinities were determined by injecting serial dilutions (1:3 dilutions) of 50 kDa BoNT fragments (A2807: HC-A 5 µg/mL to 61.7 ng/mL; B488: HC-B 30 µg/mL to 370 ng/mL; C9: HC-C 30 µg/mL to 370 ng/mL; D967: HC-D 5 µg/mL to 61.7 ng/mL; F1726: HC-F 1 µg/mL to 12.3 ng/mL) over Fc1 and Fc2 for 120 s at 30 µL/min followed by a 600 s injection of running buffer.

Avidity measurements with Neo-mAbs

To measure antibody avidity, cleaved biotinylated substrates were immobilized on a biotin CAP sensor chip using a biotin CAPture kit. For substrate cleavage, 10 µg/mL biotinylated VAMP-2₃₃₋₉₄ (VAMP-2-Bio) or SNAP-25₁₃₇₋₂₀₆ (SNAP-25-Bio) was incubated with 15 µg/mL BoNT in cleavage buffer for 18 h at 37°C with subsequent incubation for 10 min at 95°C for toxin inactivation. As negative control biotinylated substrates were treated analogues without the addition of toxin resulting in uncleaved substrates. Before immobilization, cleaved and uncleaved substrates were diluted 1:10 with HBS-EP+ running buffer. Prior to immobilization of cleaved and uncleaved substrate, the sensor chip was prepared by injecting CAP reagent on Fc1 and Fc2 for 120 s at 2 µL/min. Subsequently, cleaved or uncleaved substrate was injected on Fc2 and Fc1 respectively for 60 s at 2 µL/min. To determine binding avidity, increasing concentrations of Neo-mAb (1:5 dilutions ranging from 96 ng/mL to 60 µg/mL) were injected for 120 s at 30 µL/min over both flow cells in a single-cycle kinetic. Then, HBS-EP+ running buffer was injected for 600 s at 30 µL/min over both flow cells. Finally, sensor surface was regenerated by injecting freshly prepared regeneration buffer (6 M guanidine hydrochloride, 0.25 M NaOH) for 120 s at 10 µL/min over both flow cells.

Affinity measurements with Syt-II

To measure affinity of Syt-II towards different HcB subtypes, isolated Syt-II was immobilized on Fc2 of a CM5 sensor chip. Syt-II harbours a GST-tag and was therefore immobilized on an anti-GST antibody prepared sensor chip (see above). For receptor molecule immobilization, 2.5 µg/mL Syt-II were injected on Fc2 for 30 s at 5 µL/min. Fc1 remained empty (anti-GST antibody only) and was set as blank control. Binding kinetics and affinities were determined by injecting serial dilutions (1:3 dilutions) of 50 kDa BoNT/B HC-fragments (30 µg/mL to 0.37 µg/mL) over Fc1 and Fc2 for 120 s at 30 µL/min followed by a 300 s injection of running buffer. Then, the sensor chip was regenerated by injecting 10 mM Glycin pH 2.1 for 180 s at 10 µL/min over both flow cells.

MATERIAL AND METHODS

Affinity measurements with gSV2C

Affinity of gSV2C towards different HcA subtypes was determined by immobilizing isolated gSV2C on Fc2 of a CM5 sensor chip. gSV2C contains a tag harbouring the Fc part of a human IgG antibody and was immobilized on an anti-human IgG (Fc) prepared CM5 sensor chip (see above). For receptor molecule immobilization 10 µg/mL gSV2C were injected on Fc2 of an anti-human IgG (Fc) prepared CM5 sensor chip for 120 s at 5 µL/min. Fc1 remained empty (anti-human IgG (Fc) only) and was set as blank control. Binding kinetics and affinities were determined by injecting serial dilutions (1:3 dilutions) of 50 kDa BoNT/A HC-fragments (90 µg/mL to 1.11 µg/mL) over Fc1 and Fc2 for 120 s at 30 µL/min followed by a 300 s injection of running buffer. Then, the sensor chip was regenerated by injecting 10 mM Glycin pH 2.1 for 180 s at 10 µL/min over both flow cells.

Data analysis

Data was analysed using Biacore Evaluation Software 2.01. For both, affinity and avidity measurements, the measured binding response on Fc2 was double-referenced by (1) subtracting the RUs of Fc1 (blank control) and (2) subtracting the RUs when buffer only was injected. Binding kinetics were determined by fitting the double referenced binding curves with the heterogeneous (avidity measurements of Neo-mAbs, gSV2C) or the 1:1 Langmuir binding models (affinity measurements with Neo-mAbs and anti-BoNT antibodies, Syt-II) with global R_{max}, with RI set to zero.

4.2.5.3 Indirect ELISA

In the indirect ELISA, the antigen is immobilized on a plastic microtiter plate and detected by a detection antibody and an anti-species antibody coupled to a suitable reporter for signal read-out. Indirect ELISA was applied to determine specificity of Neo-mAbs towards the respective BoNT cleavage site as well as to exclude cross-reactivity towards full-length substrate. In addition, indirect ELISA was applied to determine antibody titer of mouse sera. To that aim, 0.5 µg/mL KLH-coupled peptide (Table 11), KLH, BSA, H6trVAMP-2, or rSNAP-25 H6 (50 µL diluted in 1 µg/mL BSA/PBS) was immobilized on 96-well MaxiSorp-plates (MaxiSorp™ Nunc-Immuno™ MicroWell™ 96 well solid plates) by incubating plates overnight at 4°C. Plates were then washed four times with PBS-T (350 µL/well) using a plate washer (HydroSpeed™ plate washer) and blocked for 1 h with blocking buffer (200 µL/well). Then, 10 µg/mL antibody (50 µL/well), hybridoma supernatant (50 µL/well), or mouse serum

MATERIAL AND METHODS

(50 μL /well diluted 1:1000 in 0.1% BSA/PBS) was added and incubated for 1 h at RT. Plates were washed again (4 \times) and a goat-anti-mouse IgG (Fc- γ -specific)-HRP antibody was added (50 μL /well diluted 1:2500 in blocking buffer) for 30 min. Finally, plates were thoroughly washed (8 \times) and signals were detected by the addition of TMB substrate (100 μL /well). Enzymatic reaction was stopped after 15 min by adding 0.25 M H_2SO_4 (100 μL /well) and plates were analysed using a microplate reader (Infinite[®] M200) measuring absorbance at 450 nm and 620 nm.

4.2.5.4 *Enrichment of toxin with paramagnetic beads*

To detect toxin from complex matrices in Endopeptidase-ELISA (see section 4.2.5.5) and duplex-assay (see section 4.2.5.6) experiments, an enrichment step prior to detection was required. To that aim, paramagnetic dynabeads coupled to anti-BoNT antibodies or receptor molecules (see section 4.2.4.5) were incubated with toxin solutions (200 μL /well) for 1 h under constant agitation for toxin capture. Toxin capture was performed in Greiner flat bottom 96-well plates (Greiner 96 well plates). Beads were then thoroughly washed with PBS-T (4 \times ; 200 μL /well) and demineralised water (4 \times ; 200 μL /well) using a plate washer. Finally, beads were diluted in cleavage buffer (100 μL /well) and applied in the Endopeptidase-ELISA or duplex-assay.

For enrichment from buffer, toxin was directly diluted in 0.1% BSA/PBS. For enrichment from complex matrices (serum, food), prepared matrices (section 4.2.4.9) were diluted in a 1:10 ratio with 0.1% BSA/PBS and subsequently spiked with toxin. *Clostridia* supernatants were diluted with 0.1% BSA/PBS as indicated.

In Endopeptidase-ELISA experiments, a mixture containing 1 μL A2807-, 10 μL B488-, 2.5 μL C9-, 5 μL D63-, 1 μL E136-, and 1 μL F1726-coupled M280 dynabeads were used (total volume of 20.5 μL dynabeads/200 μL sample). In duplex-assay experiments, a mixture of 5 μL A2807-, and 5 μL B488-, or 5 μL gSV2C-, and 5 μL dual-Syt-II-NDs-coupled M270 dynabeads was applied in the duplex-assay for BoNT/A+B. In the duplex-assays for BoNT/D and C or E and F 5 μL C9- and 5 μL D967-, or 5 μL E136- and 5 μL F1726-coupled M270 dynabeads were used respectively (total volume of 10 μL dynabeads/200 μL sample).

MATERIAL AND METHODS

4.2.5.5 *Endopeptidase-ELISA*

The Endopeptidase-ELISA was performed as described previously by Jones et al [110] with some alterations to the protocol. 3 µg/mL of rSNAP-25 H6 or H6trVAMP-2 diluted in carbonate buffer were immobilized on 96-well MaxiSorp-plates (100 µL/well) by incubating plates overnight at 4°C. Then, coating solution was decanted, and plates were blocked with ELISA blocking buffer for 1 h (300 µL/well). Plates were then washed with demineralised water (4 × 350 µL/well with a plate washer) and kept unsealed until wells were completely dry. For substrate cleavage, toxin solutions (or dynabeads with captured toxin) diluted in cleavage buffer (100 µL/well) were added and incubated for 18 h at 37°C in a hybridisation oven under constant back and forth movement. If dynabeads were added, beads were suspended after 1 h incubation. On the next day, toxin solution or dynabeads were removed by pipetting and plates were washed with PBS-T (4 × 350 µL/well). For the detection of cleavage products, Neo-mAbs were added (100 µL/well diluted in blocking buffer) and plates were incubated for 90 min at RT on a multiwell plate shaker at 300 rpm (IKA® MTS 2/4 multiwell plate shaker). For initial experiments an antibody concentration of 1 µg/mL was applied for all Neo-mAbs. For assay evaluation, Neo-mAb concentrations were titrated to 1 µg/mL SNAP/A/291, 0.01 µg/mL VAMP/B/1148, 0.01 µg/mL SNAP/C/5593, 2.5 µg/mL VAMP/D/27, 0.2 µg/mL SNAP/E/217, and 2.5 µg/mL VAMP/F/425. In experiments with previous toxin enrichment by dynabeads, biotinylated Neo-mAbs were applied with 0.5 µg/mL SNAP/A/291, SNAP/C/5593, SNAP/E/217, and VAMP/F/425, 0.005 µg/mL VAMP/B/1148, and 0.05 µg/mL SNAP/C/5593. After incubation with Neo-mAbs, plates were washed with PBS-T (4 × 350 µL/well) and detection antibody goat anti-mouse IgG (H+L) HRP (100 µL/well, diluted 1:2500 in blocking buffer) or, for experiments with biotinylated Neo-mAb, streptavidin coupled HRP (SA poly-HRP, 100 µL/well, diluted 1:5000 in blocking buffer) was added and plates were again incubated for 90 min at RT on a multiwell plate shaker at 300 rpm. Finally, plates were thoroughly washed (8 × 350 µL/well) and signals were detected by adding TMB substrate (100 µL/well) for 15 min and 0.25 M H₂SO₄ (100 µL/well) to stop enzymatic reaction. Plates were analysed using a microplate reader measuring absorbance at 450 nm and 620 nm.

4.2.5.6 *Duplex-assay*

In the duplex-assays recombinant full-length substrate coupled to luminex-beads is cleaved by BoNTs and subsequently cleavage products are detected by biotinylated Neo-mAbs.

MATERIAL AND METHODS

Luminex-bead regions 8 (coupled with VAMP-2 or H6trVAMP-2) and 48 (coupled with SNAP-25 or rSNAP-25 H6) were used in duplex-assay experiments. Three duplex assays for BoNT/A + B, BoNT/C + D, and BoNT/E + F were established. The assays were performed in flat bottom 96-well plates and plates were shielded from light, as luminex-beads may bleach upon exposure to light.

For substrate cleavage, substrate molecules coupled to luminex-beads were incubated with toxin solutions – or captured toxin after enrichment – in cleavage buffer (100 μ L total reaction volume with 2500 Beads/sample when toxin solutions were incubated or 200 μ L total reaction volume with 2500 Beads/sample when captured toxin after enrichment was incubated) for 18 h at 37°C in a hybridisation oven under constant back and forth movement. For BoNT/A + B and BoNT/E + F duplex assays recombinant SNAP-25 and VAMP-2 substrate molecules obtained from ATGen and ProsPec coupled to luminex-beads were used. For the BoNT/C + D duplex-assay, rSNAP-25 H6 and H6trVAMP-2, both obtained from Toxogen, coupled to luminex-beads were applied. This combination of substrate molecules yielded highest sensitivities in respective assays (coupling procedure see section 4.2.4.6).

After one hour incubation at 37°C the beads were suspended thoroughly by pipetting. On the next day, beads were washed with PBS-T (2 \times 200 μ L/well with plate washer) and incubated with 100 μ L/well biotinylated Neo-mAbs diluted in assay buffer (SNAP/A/291 + VAMP/B/1148 for BoNT/A + B duplex-assay, SNAP/C/5593 + VAMP/D/27 for BoNT/C + D duplex-assay, and SNAP/E/217 + VAMP/F/425 for BoNT/E + F duplex-assay) for 90 min at RT on a multiwell plate shaker at 600 rpm. The antibody concentration applied varied for different biotinylation batches and was determined by titration for each batch to achieve signals below 1000 MFI for the blank control and above 20000 MFI as maximum signal intensity. Beads were washed again (2 \times 200 μ L/well) and incubated with 2 μ g/mL SA-PE (PJRS34, 100 μ L/well diluted in assay buffer) for 30 min at RT on a multiwell plate shaker at 600 rpm. Finally, beads were washed (3 \times 200 μ L/well) and resuspended in assay buffer (100 μ L/well). Samples were analysed using a Bio-Plex® 200 suspension array instrument with the following adjustments differing from the default settings: DD gates were set to 8000–22000 and the “run at High PR1 target” option was activated.

MATERIAL AND METHODS

4.2.5.7 Determination of assay performance of endopeptidase assays

Analysis of Endopeptidase-ELISA and duplex-assay experiments was performed using GraphPad Prism software. In titration experiments, data was fitted by the software using a variable slope four-parameter fit (Formula 1). The half maximal effective concentration EC50 marks the turning point of the titration curve. To determine the limits of detection (LODs), the cutoff was calculated by the average mean of blank values plus 3.29 times of the standard deviation (SD, Formula 2) of blank values (Formula 3) and were transferred into pg/mL by interpolation to the standard titration curve. Outliers were cleared prior to calculations using Grubbs' test at a confidence level of 5% [157].

4.2.6 Optimization of cleavage conditions employing multifactorial Design-of-experiments (DoE)

To comprehensively analyse substrate cleavage of BoNT/A-F the Taguchi DoE method was employed. Here, the influence of several factors on cleavage of full-length substrate molecules (rSNAP-25 H6 and H6trVAMP-2) by BoNT/A-F was analysed. The aim of the analysis was to identify optimal cleavage conditions for each serotype that yield maximum substrate cleavage. Thus, for each serotype an individually optimized buffer was identified. In addition, a consensus buffer in which all serotypes exhibit sufficient substrate cleavage was determined. Finally, optimized buffer conditions were compared to previously described cleavage buffers for reference.

4.2.6.1 Principle of the “Taguchi DoE” method

The Taguchi DoE method utilizes orthogonal arrays to design multifactorial experiments testing several factors at the same time. Thus, in contrast to classical “one factor at a time” approaches, several factors are varied simultaneously in the Taguchi DoE method thereby drastically minimizing the number of required experiments. Optimal factor levels as well as the impact of each factor can be calculated by statistical means [158].

The principle work-flow of Taguchi experiments is outlined in Figure 11. It involves four major steps with an additional fifth control step:

First, the overall aim of the experiment, such as “increase cleavage of SNAP-25 by BoNT/A” is formulated.

MATERIAL AND METHODS

Second is the planning phase of the actual experiments. Here, all test parameters must be determined. This includes fixed parameters (consistent throughout all experiments) as well as variable parameters (factors and factor levels to be analysed). As fixed parameters, a short incubation time of 30 min at 37°C and a basal 50 mM HEPES buffer were defined. The only exception from this was BoNT/C, where cleavage duration had to be prolonged to 18 h, due to weak intrinsic substrate cleavage. Variable parameters were chosen according to a known influence on BoNT substrate cleavage (see Table 2 from the introduction). In total seven different factors (pH, ZnCl₂, DTT, NaCl, BSA, TMAO, Tween 20) with three levels each were analysed. In addition, the measured variable, which is determined by the read-out technique of the experiments, was defined in the second step. Here, the percentage of substrate cleavage determined densitometrically by SDS-PAGE and Coomassie Stain was applied. Finally, the array layout, which is specified by standardized orthogonal arrays, was chosen depending on the number of different factors and factor levels to be analysed. As seven different factors with three levels each were analysed here, an L-18 array would have been applicable [158]. However, to facilitate experimental procedures, test factors were separated into buffer components (pH, ZnCl₂, DTT, NaCl) and buffer additives (BSA, TMAO, Tween 20) thus allowing the usage of two consecutive L9-arrays (Table 19).

The third step is the actual experimental phase. Here, data is gathered by conducting all experiments (test conditions) according to the array layout. For each L9-array, nine experiments must be performed, corresponding to nine different test conditions. Hence, for the analysis of one serotype, testing all seven factors, in total 18 experiments (one L9-array for buffer components and a second for buffer additives) are required. Contrary, a full factorial approach, testing the same number of factors and levels, would require 162 experiments. This exemplifies the drastic reduction of experimental effort by the Taguchi DoE approach.

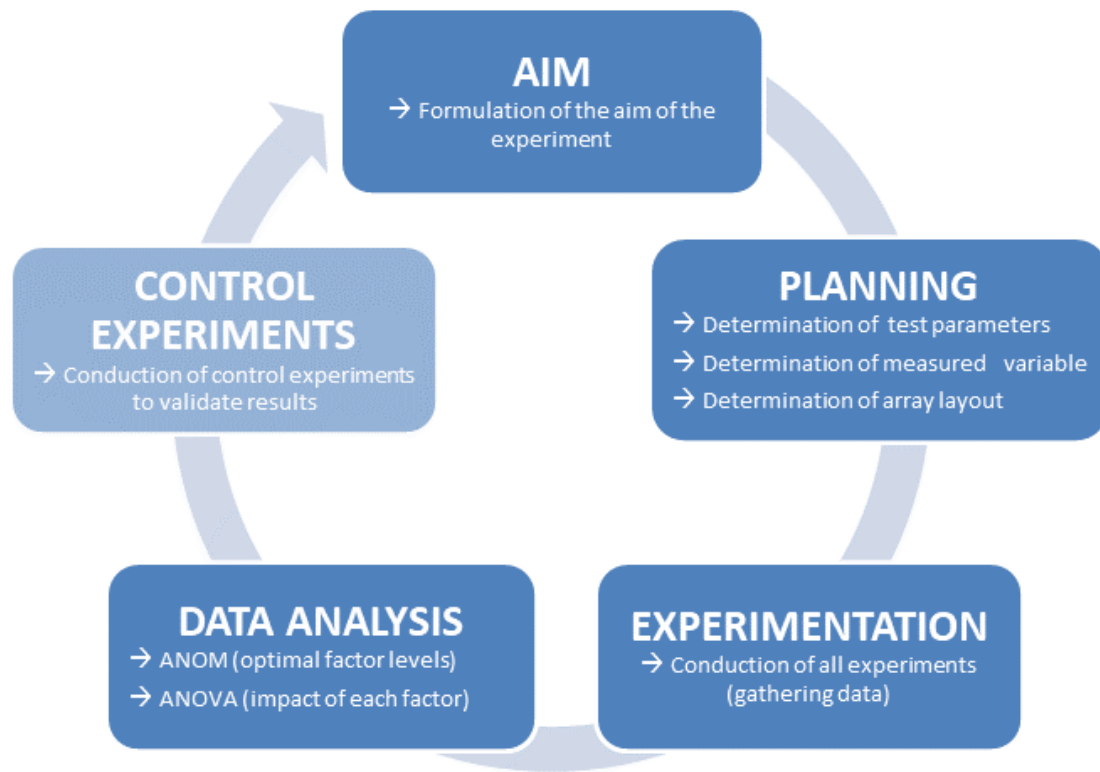


Figure 11: Work-flow of Taguchi experiments. First a specific aim (e.g. “Increase of cleavage of SNAP-25 by BoNT/A”) is formulated. The next step is the determination of fixed and variable test parameters (factors and factor levels to be tested), the determination of the measuring method and therefore measured variable on which the analysis is based on, and the choice of an adequate array layout (depending on the number of factors and levels to be tested). If all parameters have been determined the experimentation phase can be initiated. Finally, the data is analysed by statistical means using ANOM (to determine the optimal factor levels) and ANOVA (to determine the impact of each factor). Eventually, the outcome of Taguchi experiments should be controlled to validate the results.

Finally, as the fourth step of Taguchi experiments, data is analysed by statistical means. Data is transformed into signal-to-noise-ratios (S/N-ratios) using a specific target function, depending on the direction of optimization. As substrate cleavage was sought to be increased, the larger-the-better transformation was applied, in order to transform the percentage of cleavage into S/N-ratios [158]. To determine the optimal level of each factor, analysis of means (ANOM) is performed. In the ANOM, conditions with the same factor level are grouped and mean S/N-ratios are calculated, resulting in three different mean values (one for each test level) for each factor. As in the larger-the-better transformation a maximum in the S/N-ratio marks the optimum, the highest mean value indicates the optimal level for that factor. Eventually, in the analysis of variances (ANOVA) the contribution of each factor is calculated. Thereby, variances of conditions with the same factor (but different factor levels) are

MATERIAL AND METHODS

calculated using the mean S/N-ratios from the ANOM. Strong differences in substrate cleavage between conditions with different factor levels would result in a high variance, thus indicating a high contribution of this factor. In the ANOVA, the variance of each factor is further transformed into a percentage value, representing the impact of each factor.

Eventually, with the results from the ANOM and ANOVA optimal cleavage conditions as well as the relevance of each factor can be deducted. However, to validate results control experiments should be carried out. Hence, the newly optimized buffer conditions resulting from the Taguchi DoE analysis were compared to previously used buffers for reference.

Table 19: Layout of the orthogonal L9-arrays. All buffers were based on 50 mM HEPES.

Condition No.	L9-Array 1: Buffer components				L9-Array 2: Buffer additives		
	pH	ZnCl ₂ [μM]	DTT [mM]	NaCl [mM]	BSA [mg/ml]	TMAO [M]	Tween 20 [%]
1	6.5	10	1	0	0	0	0
2	6.5	50	5	20	0	0.75	0.5
3	6.5	250	25	100	0	1.5	1.0
4	7.0	10	5	100	0.2	0	0.5
5	7.0	50	25	0	0.2	0.75	1.0
6	7.0	250	1	20	0.2	1.5	0
7	7.5	10	25	20	1.0	0	1.0
8	7.5	50	1	100	1.0	0.75	0
9	7.5	250	5	0	1.0	1.5	0.5

4.2.6.2 Substrate cleavage

Prior to Taguchi experiments, toxin concentrations for the first L9-array experiments were adjusted to achieve medium substrate cleavage (20–60%) in a basal HEPES-buffer with 5 mM DTT. Thereby, fully completed (100%) or the lack of substrate cleavage (0%) in the test buffers, was avoided, as this would impede the Taguchi analysis. Concentrations of 0.3 nM BoNT/A, 50 nM BoNT/C, 25 nM BoNT/E (non-trypsinized) for rSNAP-25 H6 cleavage and 100 nM BoNT/B, 80 nM BoNT/DC, or 5 nM BoNT/F for H6trVAMP-2 cleavage were applied. Due to the usage of

MATERIAL AND METHODS

already optimized conditions in the second L9-array experiments, toxin concentrations were reduced to 50 nM BoNT/B, 10 nM BoNT/C, 40 nM BoNT/DC, and 0.625 nM BoNT/F.

For substrate cleavage in the different buffers 3 μ M rSNAP-25 H6 or 20 μ M H6trVAMP-2 was mixed with BoNT in the assigned buffer (Table 19) in a total reaction volume of 30 μ L in thin-walled 0.2 mL PCR vials. Then, samples were incubated for 30 min at 37°C (or for 18 h for BoNT/C) in a PCR-thermocycler and subsequently inactivated by heating to 95°C for 10 min.

4.2.6.3 SDS-PAGE for the analysis of substrate cleavage

Substrate cleavage was analysed by SDS-PAGE. As the resulting cleavage fragments were partially of very small size (<8 kDa), polyacrylamide-peptide gels for Tricine-SDS-PAGE according to Schagger et al [150] were employed. Compared to conventional Tris-Glycine SDS-PAGE, Tricine-SDS-PAGE enables a better separation of peptides.

To that aim, three-phase peptide gels consisting of a 16.5% running gel in the lower part, a 10% spacer gel in the middle, and a 4% stacking gel in the upper part were prepared as outlined in Table 20. After polymerisation, gels were installed in an electrophoresis chamber filled with ice-cold cathode buffer in the inner chamber and ice-cold anode buffer in the outer chamber. Samples (30 μ L) were supplemented with 15 μ L Laemmli loading buffer, heated for 10 min at 70°C and subsequently cooled down. 10 μ L samples were loaded on gels and gels were run for 1 h at 50 V. Then, voltage was increased up to 150 V until the desired separation of proteins was achieved. To visualize cleavage fragments, gels were stained with colloidal coomassie as described above (see section 6.2.4.1) and documented using a ChemiDoc workstation. The percentage of substrate cleavage (0% = uncleaved, 100% = fully cleaved) was analysed densitometrically using ImageLab software. Therefore, band intensities of uncleaved substrate and the larger N-terminal cleavage fragment were determined, and background intensity was subtracted. Then, the N-terminal cleavage product was normalised with regard to the uncleaved negative control (in L9-array experiments, see Formula 4) or to the sum of N-terminal cleavage product and corresponding uncleaved band (control experiments, see Formula 4).

Table 20: Composition of polyacrylamide-peptide gels for Tricine-SDS-PAGE.

Reagent	Stacking gel (4%)	Spacer gel (10%)	Running gel (16.5%)
ddH ₂ O	2.6 mL	1.7 mL	1.7 mL
3 M Tris, 0.3% SDS, pH 8.9	–	1.25 mL	2.5 mL
1 M Tris-HCl, pH 6.8	0.48 mL	–	–
48% Acrylamide/1.5% Bisacrylamide	–	0.75	–
48% Acrylamide/3% Bisacrylamide	–	–	2.5 mL
Acrylamide/Bisacrylamide solution	0.625 µL	–	–
Glycerol (100%)	–	–	0.8 mL
0.2 M EDTA	37.5 µL	–	–
10% APS	30 µL	25 µL	50 µL
TEMED	3.5 µL	2.5 µL	5 µL

4.2.6.4 Statistical analysis of Taguchi experiments

Taguchi experiments were analysed by ANOM and ANOVA as described previously [158]. In ANOM, the optimal level of each factor was determined. The first step of ANOM was to transform the percentage of cleavage of each L9-array experiment (in total 9 test conditions per L9-array) into S/N ratios using the “larger-the-better” log-transformation (Formula 5). Then, mean S/N ratios of conditions with the same factor level (e.g. all conditions with the same pH of 6.5 (Cond. 1, Cond. 2, Cond. 3), or the same DTT concentration of 1 mM (Cond. 1, Cond. 6, Cond. 8) were calculated using the arithmetic mean (see Formula 6). By plotting mean S/N-ratios for each factor level, optimal levels and trends in factor influences could be visualized. Here, a maximum in the mean S/N-ratios of a respective factor indicates the optimal level for maximum substrate cleavage. In the second step of the analysis, the statistical significance of each factor was determined by analysing variances within different test levels of one factor by ANOVA. To that aim, first the mean sum square (Formula 7) and the total error sum square of an L9-array was calculated. With the mean sum square and the sums of S/N-ratios of conditions with the same factor level, the sum square variation of each factor was calculated (Formula 9). Using sum square variation, the impact of each factor in % could be calculated (Formula 10). To determine the significance of each factor, p-values were calculated. Therefore, the F-value was determined (Formula 13) by dividing the variance of each factor (Formula 11) by the estimation of the variation error. The latter was determined with the two factors exhibiting the lowest sum square variation (Formula 12). Finally, the p-

MATERIAL AND METHODS

value was calculated using the F-distribution. Statistical analysis of all Taguchi experiments was performed using Microsoft Excel 2010.

4.2.6.5 Validation of Taguchi-DoE with control experiments

To test if the individually optimized serotype specific buffers as well as the consensus buffers performed better than previously described cleavage buffers (evans buffer [101] and jones buffer [110]), control experiments were carried out. Substrate cleavage with increasing concentrations of BoNT/A-F was analysed in the different buffers. Cleavage was performed and analysed as described above and plotted against the applied concentrations. Data was fitted using Michaelis-Menten kinetics assuming a Michaelis constant (K_m) > 0 and a maximum rate (V_{max}) of 100 (Formula 14).

4.2.7 Formulas used for statistical analysis

Formula 1: Variable slope four-parameter fit [159]

$$Y = \frac{Bottom + (Top - Bottom)}{1 + 10^{LogEC50 - X}} \cdot Hill\ Slope$$

Y: Response (in OD or MFI)

X: Log of concentration (BoNT concentration)

Top and Bottom: Upper and lower plateau of the titration curve

LogEC50: Has the same log unit as X

Hill Slope: Slope factor or Hill Slope (no units)

Formula 2: Standard deviation

$$SD = \sqrt{\frac{\sum(x - \bar{x})^2}{(n - 1)}}$$

x: blank values

\bar{x} : mean of blank values

n: number of blank values

Formula 3: LOD

$$LOD = \bar{x} + 3.29 \cdot SD(x)$$

\bar{x} : mean of blank values

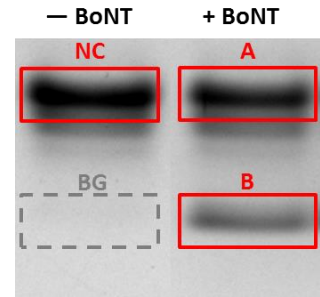
SD(x): Standard deviation of blank values

MATERIAL AND METHODS

Formula 4: Percentage of cleavage in Taguchi experiments

$$\% \text{ cleavage (L9 array experiments)} = \frac{B - BG}{NC - BG}$$

$$\% \text{ cleavage (control experiments)} = \frac{B - BG}{(B - BG) + (A - BG)}$$



NC: uncleaved negative control (no toxin)

A: uncleaved band

B: cleaved band (N-terminal cleavage product)

BG: background

Formula 5: S/N-ratios using the „larger-the-better“ transformation [158]

$$\eta_j = -10 \log_{10} \left(\frac{1}{n} \sum_{i=1}^n \frac{1}{y_i^2} \right)$$

η : S/N ratio in decibel

j : Experiment of L9-array (experiments $j = 1, j = 2, \dots, j = 9$)

n : Number of repetitions (in this work $n = 2$)

i : Count of each experiment

y : Measured variable (percentage of substrate cleavage)

Formula 6: Mean S/N-ratio (exemplified with 1 mM DTT) [158]

$$\bar{\eta}_{DTT_{1mM}} = \frac{1}{3} (\eta_{Exp.1} + \eta_{Exp.6} + \eta_{Exp.8})$$

η : Calculated S/N ratio of specific experiment

Formula 7: Mean sum square [158]

$$SQ_m = \frac{(\sum \eta_i)^2}{n}$$

η : Calculated S/N-ratio for each experiment i

n : Number of experiments (in L9-array $n = 9$)

Formula 8: Total error sum square [158]

$$SQ_{total} = \sum \eta_i^2 - SQ_m$$

η : Calculated S/N-ratio for each experiment i

MATERIAL AND METHODS

Formula 9: Sum square variation [158]

$$SQ_{Factor} = \frac{(\sum \eta_{Level 1})^2}{3} + \frac{(\sum \eta_{Level 2})^2}{3} + \frac{(\sum \eta_{Level 3})^2}{3} - SQ_m$$

η : Calculated S/N-ratio for each experiment (with the same factor level)

Formula 10: Impact of each factor in % [158]

$$p [\%]_{Factor} = \frac{SQ_{Factor}}{SQ_{total}} \cdot 100$$

Formula 11: Variance of each factor [158]

$$V_{Factor} = \frac{SQ_{Factor}}{DF}$$

DF: Degrees of freedom (here $DF = n - 1 = 2$, due to three different test levels (n) for each factor)

Formula 12: Estimation of variation error F2 [158]

$$V_{F2} = \frac{SQ_{low 1} + SQ_{low 2}}{DF_1 + DF_2}$$

SQ_{low} : Two factors with the lowest sum square variation

DF: Degrees of freedom (here $DF_1 + DF_2 = 4$)

Formula 13: F-value [158]

$$F - value = \frac{V_{Factor}}{V_{F2}}$$

Formula 14: Michaelis-Menten kinetics [160]

$$Y = \frac{V_{max} \cdot X}{K_m + X}$$

Y : Amount of cleavage

X : BoNT concentration

V_{max} : maximum rate (maximum enzyme velocity; was set to 100 for fitting)

K_m : Michealis constant

5 RESULTS

5.1 Optimization of BoNT substrate cleavage employing statistical experiments

Sensitive detection of catalytically active BoNT is highly dependent on efficient substrate cleavage. Therefore, one goal of this thesis was to optimize substrate cleavage for BoNT/A-F by varying buffer conditions. Optimal cleavage conditions for each single serotype as well as a consensus buffer in which all serotypes exhibit efficient cleavage were identified. The latter is particularly important for diagnostic purposes as the present serotype cannot be foreseen prior to analysis.

Previous works already demonstrated that substrate cleavage of certain BoNTs can vary depending on buffer components. However, only few serotypes and factors have been analysed and a comprehensive analysis of all relevant serotypes was lacking (Table 2 in the introduction summarizes factors influencing substrate cleavage). Thus, for a comprehensive analysis, factors with a proven positive influence on substrate cleavage were chosen and tested on all serotypes. To reduce experimental efforts, a statistical approach – the Taguchi Design of Experiments (DoE) method – was applied. Here, orthogonal arrays are used to design multifactorial experiments which test several factors at the same time. Thereby experimental effort is greatly reduced compared to classical “one-factor-at-a-time” approaches (the principle of the Taguchi DoE method is explained in more detail in the material and methods section 4.2.6.1). For the analysis, cleavage of full-length SNAP-25 or VAMP-2 in the different buffer conditions was performed in solution, cleavage products were separated by SDS-PAGE, stained, and fragments were analysed densitometrically. By employing this experimental set-up, a broad applicability of results should be ensured, independent of additional factors as antibody affinities.

5.1.1 Influence of buffer components varies between the different BoNT serotypes

To improve BoNT substrate cleavage, two consecutive L9-arrays testing (1) the buffer components pH, ZnCl₂, DTT, and NaCl and (2) the buffer additives BSA, TMAO, and Tween 20 were performed. The different experimental conditions in each L9-array were probed according to the predetermined orthogonal array-layout (Table 19 in the material and

RESULTS

methods section). Toxin concentrations were adjusted prior to the optimization experiments to achieve baseline moderate substrate cleavage.

Results from the first L9-array revealed marked differences between the different conditions (Figure 12, left images of each panel). For example, all serotypes except for BoNT/C exhibited reduced substrate cleavage in experimental condition six (pH 7, 250 μ M ZnCl₂, 1 mM DTT, 20 mM NaCl). Conversely, condition five (pH 7, 50 μ M ZnCl₂, 25 mM DTT, no NaCl) supported cleavage of the respective serotypes. Those results indicate that high DTT concentrations are beneficial for these serotypes, as buffer six contained low (1 mM) and buffer five contained high (25 mM) DTT concentrations.

With the results of the first L9-array optimal buffer conditions for each serotype were determined (see section 5.1.2) and applied in the second L9-array. Akin to the results of the first L9-arrays, clear differences between the different buffer conditions appeared (Figure 12, right images of each panel). Most notably, conditions three, six, and nine, all containing high TMAO concentrations (1.5 M) were detrimental for all serotypes, indicating a negative influence of high TMAO concentrations on substrate cleavage.

Summing up, these results demonstrate that the choice of buffer conditions for BoNT substrate cleavage indeed influenced cleavage efficiency. Without further statistical analysis, tendencies could be observed from the results of the two consecutive L9-arrays such as a strong influence of the factors DTT and TMAO.

RESULTS

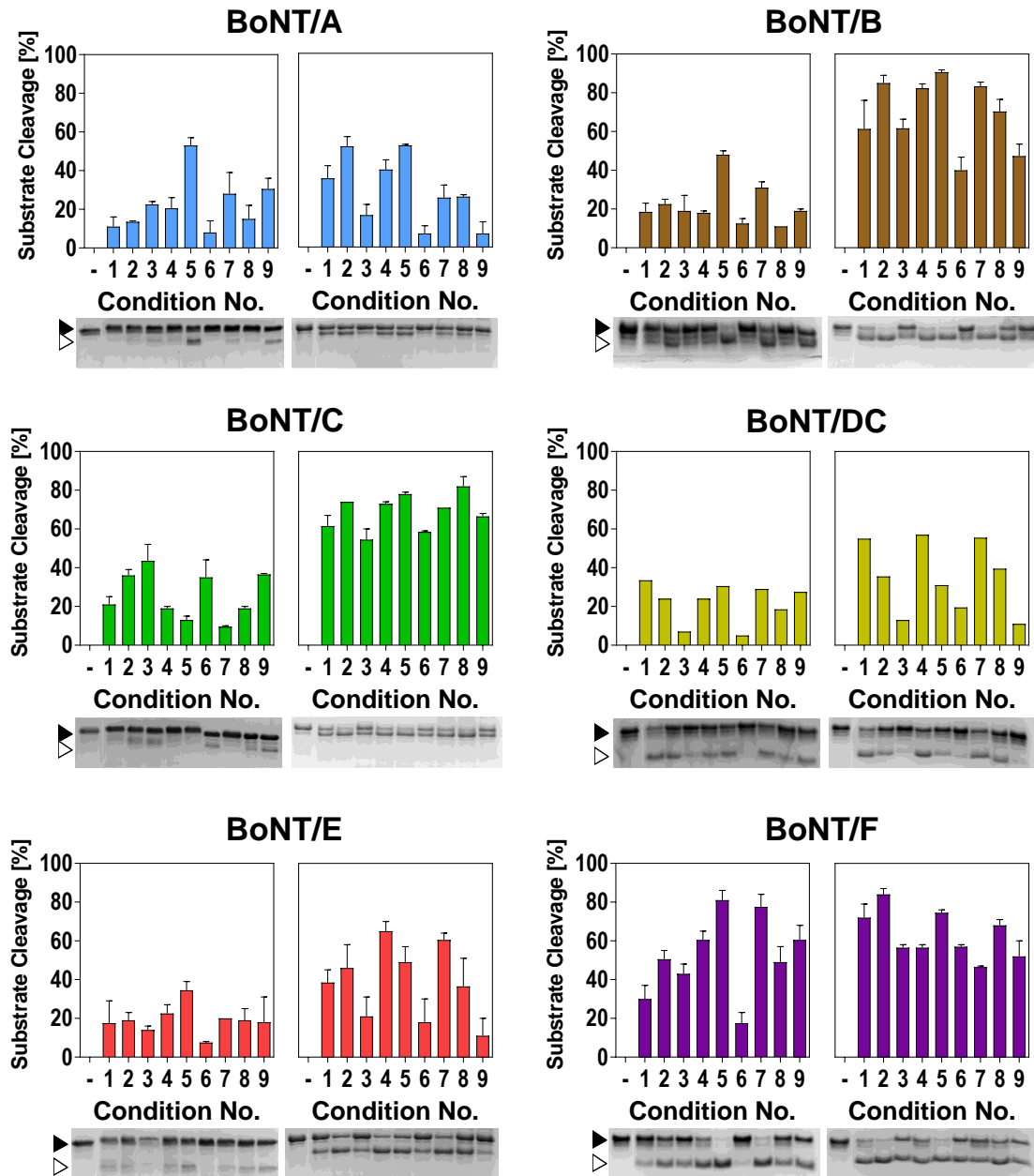


Figure 12: Substrate cleavage of BoNT serotypes A–F in different buffer compositions according to the L9-array 1 (left image of each panel) and L9-array 2 (right image of each panel). Full-length SNAP-25 or VAMP-2, respectively was incubated with BoNT for 30 min (BoNT/A, B, D, E, F) or 18 h (BoNT/C) at 37°C in the assigned buffer (Table 19 in the material and methods section). Nine different buffer conditions were evaluated, and cleavage efficiency was analyzed densitometrically via SDS-PAGE and Coomassie staining. Black triangles indicate uncleaved SNAP-25 or VAMP-2 and white triangles indicate the larger cleavage fragment after cleavage by BoNT. One representative gel image out of two experiments is shown. Bars indicate normalized averaged cleavage (– = no toxin added; n = 2; Mean ± SD).

RESULTS

5.1.2 Statistical analysis of L9 arrays identifies optimal buffer condition for each serotype

With the data gathered from the two consecutive L9-arrays, statistical analysis was carried out according to Klein *et al* [158]. This involved three steps: First, S/N-ratios were calculated from the percentage cleavage in each experiment. Second, in the ANOM, optimal factor levels were identified by a maximum S/N-ratio within each factor. Third, ANOVA was used to determine the percentage impact of each factor.

As expected, results from ANOM exhibited marked differences between the different factor levels tested and clearly confirmed the assumptions made from the matrix experiments. For all serotypes, low DTT concentration (1 mM) and high TMAO concentrations (1.5 M) were unfavourable (Figure 13). Furthermore, results from the first L9-array revealed that most serotypes preferred a neutral pH between 7 and 7.5, modest ZnCl₂ concentrations (50 µM), and high DTT concentrations (25 mM). For BoNT/B and DC an inhibitory effect of NaCl was observed. Interestingly, serotypes DC and particularly C, both pathogenic to animals, differed most from the other serotypes. In contrast to all other serotypes BoNT/C preferred a low pH (6.5) and high ZnCl₂ concentrations (250 µM). Both serotypes, C and DC, exhibited optimal cleavage at 5 mM DTT, but contrary to BoNT/C, high ZnCl₂ concentrations were detrimental for BoNT/D (*ibid.*).

In the second L9-array three, instead of four different factors were analysed. As the statistical analysis of L9-arrays by the Taguchi method assumes the usage of four factors, the “empty factor” served as a control for artefacts caused by interactions between the different factors. Here, except for BoNT/A and E comparably low variations in S/N-ratios of the different control levels were observed (Figure 13). Although variations seemed to be higher for BoNT/A and E, the overall impact of the control factors were low (Table 21, Appendix Table 1, Appendix Table 5).

Results from the second L9-array testing buffer additives showed that Tween 20 slightly enhanced cleavage of most serotypes while BSA had an adverse effect on BoNT/A, E, and to a lesser extent F cleavage, whereas all other serotypes were not affected by varying BSA concentrations. The most prominent effects were observed for TMAO with a strong inhibitory effect on all serotypes at high concentrations. Moderate TMAO concentrations (0.75 M) exhibited, however, a slight stimulatory effect on serotypes A, B, C, and F. The resulting

RESULTS

optimal cleavage conditions for each serotype determined in both L9-arrays are summarized in Table 21.

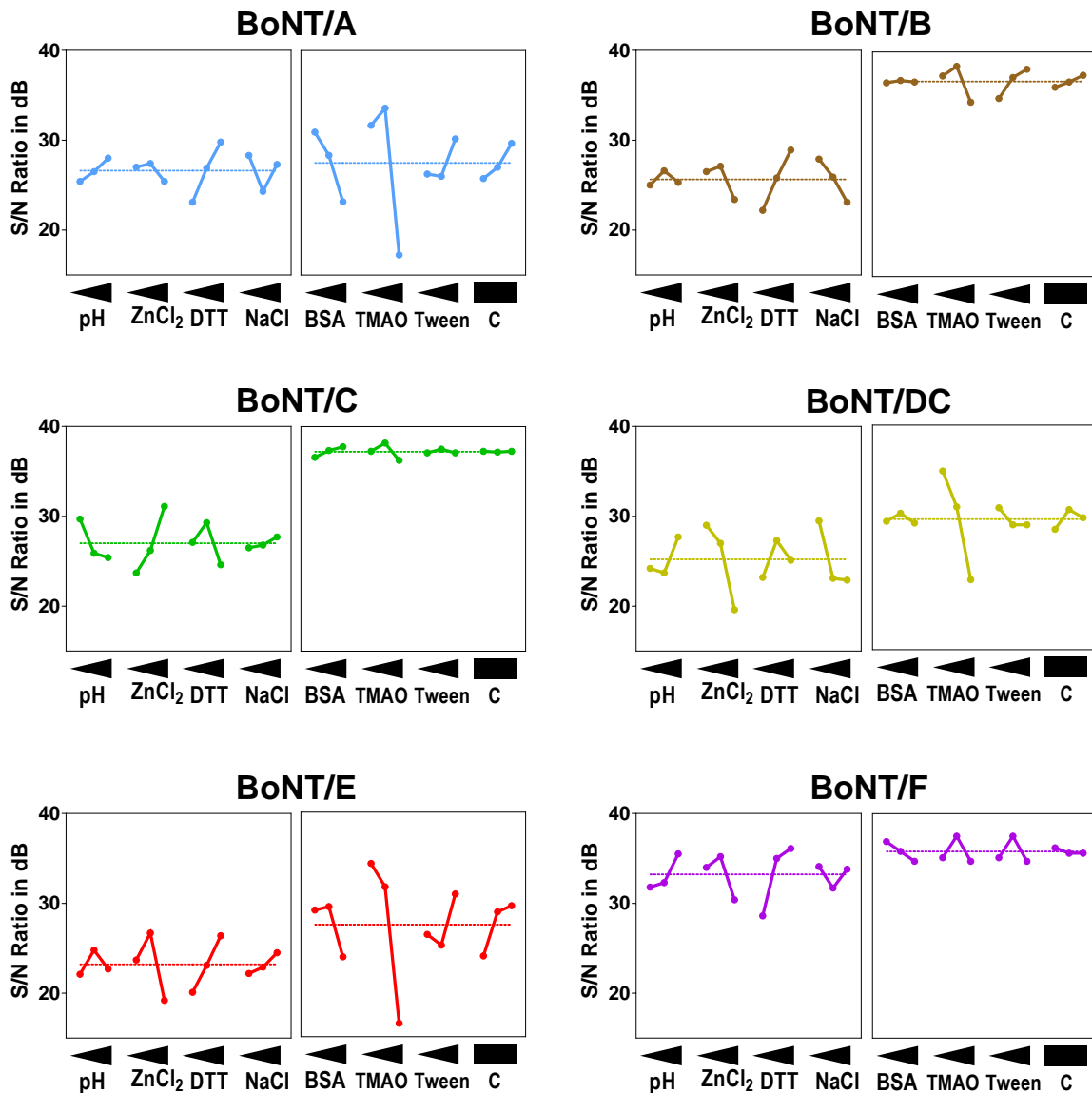


Figure 13: ANOM of L9-array 1 (left image of each panel) and L9-array 2 (right image of each panel). S/N-ratios (larger-the-better) in db (decibel) for each experiment were determined. Graphs display the mean S/N-ratio for each factor level and the overall mean out of two independent experiments. Factor levels (from lowest to highest level as indicated with triangle): pH: 6.5, 7, 7.5; ZnCl₂: 10 μ M, 50 μ M, 250 μ M; DTT: 1 mM, 5 mM, 25 mM; NaCl: 0 mM, 20 mM, 100 mM; BSA: 0 mg/mL, 0.5 mg/mL, 1 mg/mL, TMAO: 0 M, 0.75 mM, 1.5 mM; Tween 20: 0%, 0.5%, 1%; C = control (empty factor). A maximum in each factor indicates the optimal level.

Although factor impacts could be roughly deduced from the results of the ANOM, a more accurate interpretation could be drawn with the ANOVA. Notably, factor impacts determined

RESULTS

in ANOVA do not provide information on the optimal level (which is identified by ANOM) but indicate the contribution of each factor on the observed effects. Hence, deviations from the optimal level of a factor with a high impact will result in a more drastic impairment of substrate cleavage compared to a factor with a negligible impact.

As illustrated in Table 21 and Appendix Figure 1, factors with a high impact on substrate cleavage were ZnCl₂ for BoNT/C, DC, and E (> 51%), DTT for BoNT/A, B, E and F (> 36%), and TMAO for all serotypes (> 60%). Except for BoNT/B, Tween 20 was clearly a negligible factor for all serotypes (< 7%) and BSA was insignificant for serotypes A, B, DC, and E (< 15%). NaCl did not have a strong effect (< 7%) on serotypes C, E, and F and a moderate impact on serotypes A, B, and DC (23–30%). Interestingly, the pH-value had a slightly elevated impact only on BoNT/C (22 %), which was also the only serotype that preferred a lowered pH-value. The low factor impact of the empty control factor (< 8% for all serotypes, Table 4 and Appendix Figure 2) indicated that results of the analysis were reliable and not biased due to interactions (detailed results of the ANOVA are presented in Appendix Table 1–Appendix Table 6).

In summary, the Taguchi DoE analysis to determine optimal buffer conditions for BoNT/A-F revealed that different serotypes favoured different buffer conditions to achieve optimal substrate cleavage. In addition, ZnCl₂, DTT, and TMAO were identified as critical factors that must be adjusted carefully for each serotype.

Table 21: Optimized buffer conditions and factor impact (in %) for each BoNT serotype analysed according to results of ANOM and ANOVA. Numbers in parentheses indicate factor impact.

	BoNT/A	BoNT/B	BoNT/C	BoNT/DC	BoNT/E	BoNT/F
pH	7.5 (10%)	7 (3%)	6.5 (22%)	7.5 (10%)	7 (7%)	7.5 (14%)
ZnCl ₂ [μM]	50 (6%)	50 (18%)	250 (56%)	10 (51%)	50 (52%)	50 (21%)
DTT [mM]	25 (61%)	25 (52%)	5 (21%)	5 (9%)	25 (36%)	25 (58%)
NaCl [mM]	0 (23%)	0 (27%)	<i>100 (2%)^b</i>	0 (30%)	<i>100 (5%)^a</i>	0 (7%)
BSA [mg/ml]	0 (15%)	0.2 (0%)	1 (25%)	0.2 (1%)	0.2 (8%)	0 (32%)
TMAO [M]	0.75 (76%)	0.75 (57%)	0.75 (70%)	0 (93%)	0 (77%)	0.75 (60%)
Tween 20 [%]	1 (5%)	1 (37%)	0,5 (5%)	0 (3%)	1 (7%)	0 (6%)
Control ^b	n.a. (4%)	n.a. (6%)	n.a. (0%)	n.a. (3%)	n.a. (8%)	n.a. (3%)

^a Due to the low impact of NaCl on the cleavage of BoNT/C and BoNT/E, no NaCl was added to the optimized buffer despite a slightly enhanced cleavage by ANOM (depicted in italics).

^b n.a. not applicable.

RESULTS

5.1.3 Comparison of optimized buffers with previously described reference buffer

As the last step of Taguchi experiments the results were validated by control experiments. To test whether optimization indeed improved substrate cleavage, optimized buffers were compared to previously described reference buffers which have been used in enzymatic BoNT assays entitled “Jones buffer” (50 mM HEPES, 10 μ M ZnCl₂, 5 mM DTT, 0.5% Tween 20, 1 mg/ml BSA, pH 7) and “Evans buffer” (50 mM HEPES, 20 μ M ZnCl₂, 1 mM DTT, 1% BSA, pH 7.4). Both buffers have been used in an Endopeptidase-ELISA based method for the detection of catalytically active BoNT/A and E [110] or BoNT/A, B, and F respectively [101].

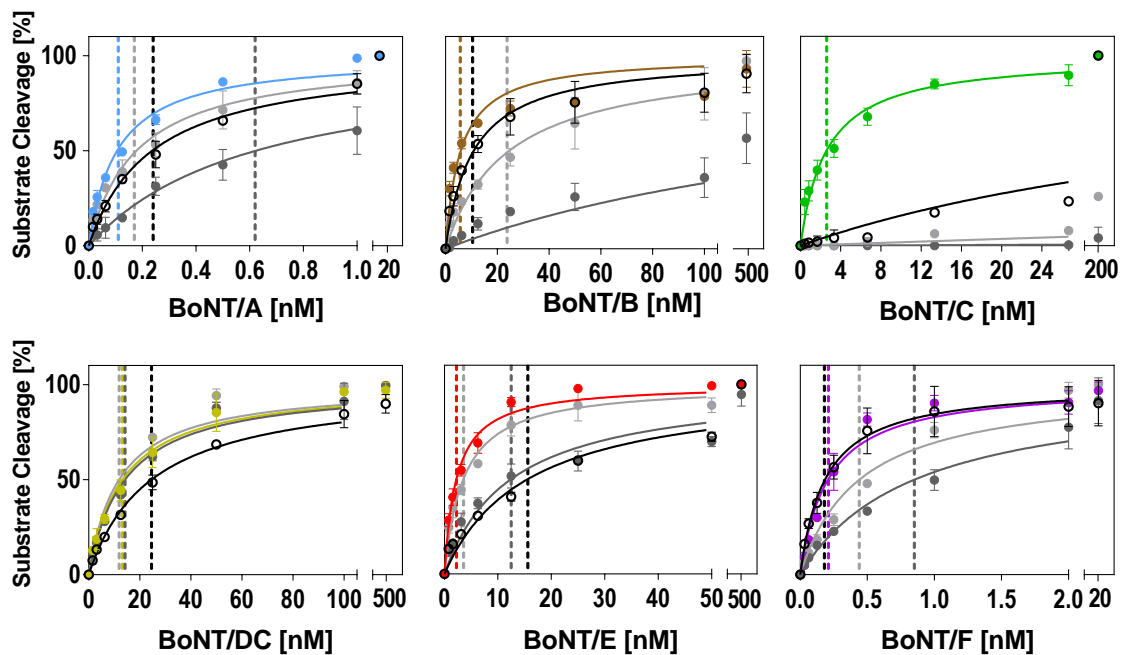


Figure 14: Comparison of optimized buffer conditions for substrate cleavage by each serotype with two reference buffers and the consensus buffer. Full-length SNAP-25 or VAMP-2, respectively, was incubated in a 1:2 dilution series of BoNT for 30 min (BoNT/A, B, D, E, F) or 18 h (BoNT/C) at 37°C in the serotype-optimized buffer (colored circles; see Table 21 for buffer compositions), Jones buffer (light grey circles), Evans buffer (dark grey circles), or consensus buffer (open black circles). Km values (indicated as dashed line) were calculated using Michaelis-Menten kinetics ($Y=V_{max} \times X/(K_m+X)$) assuming a $K_m > 0$ and V_{max} equal to 100. Cleavage was analysed via SDS-PAGE as described in the method section ($n = 2$; Mean \pm SD).

As illustrated in Figure 14, substrate cleavage of all BoNT serotypes was improved in the optimized buffers. Comparing both reference buffers, much better cleavage was obtained with the Jones buffer. Still, optimized buffers further increased cleavage of some serotype.

RESULTS

The most striking improvement regarding cleavage efficiency was achieved for BoNT/C. Here, for 50% substrate cleavage, an at least 206-fold higher toxin concentration was required in the reference buffers compared to the optimal buffer condition (Figure 14 and Table 22). Similarly, improvements could also be achieved for BoNT/B and F, requiring an at least 4- or 2-fold higher toxin concentration, for 50% substrate cleavage in the reference buffers (ibid.). As the only serotype, BoNT/DC seemed to be rather robust towards varying buffer conditions as cleavage was similar in all buffers tested.

Table 22: Comparison of cleavage efficiency of different buffers (determined with graphs of Figure 14).

Serotype	Toxin concentration for 50% cleavage [nM] ^a			
	Evans buffer [101]	Jones buffer [110]	Optimized buffer	Consensus buffer
BoNT/A	0.62 ± 0.05	0.18 ± 0.01	0.11 ± 0.01	0.24 ± 0.01
BoNT/B	193 ± 31.6	23.8 ± 2.29	5.7 ± 0.77	10.5 ± 1.18
BoNT/C	4717 ± 1202	537 ± 37.4	2.6 ± 0.2	53 ± 9.3
BoNT/DC	14.2 ± 1.0	11.9 ± 1.2	13.2 ± 1.1	24.6 ± 1.3
BoNT/E	12.5 ± 1.2	3.6 ± 0.26	2.25 ± 0.15	15.6 ± 1.1
BoNT/F	0.85 ± 0.08	0.44 ± 0.05	0.21 ± 0.02	0.18 ± 0.02

^a Mean ± SEM from n = 2 independent experiments.

5.1.4 Development of a consensus buffer for optimal cleavage of each serotype

The comprehensive analysis of buffer conditions for BoNT serotypes A-F by the Taguchi DoE method revealed optimized buffers for each single serotype. For botulism diagnostics, a consensus buffer, in which all BoNT serotypes exhibit sufficient cleavage, is desirable. From the results of the ANOM and ANOVA such a consensus buffer was designed and compared to the individual optimized buffers as well as two reference buffers (Figure 14 and Table 22).

The design of such consensus buffer is challenging, as optimal conditions for the different serotypes vary (Table 21). Particularly, factors with a high impact such as DTT, ZnCl₂, or TMAO must be adjusted carefully, especially when optimal levels between the different serotypes vary.

RESULTS

As most serotypes favoured high DTT concentrations and moderate TMAO concentrations these factors were adjusted to 25 mM and 0.75 M respectively. Although a high ZnCl₂ concentration was not optimal for most serotypes, 250 µM ZnCl₂ were applied in the consensus buffer, due to the strong beneficial effect on BoNT/C. Tween 20, negligible for almost all serotypes, was adjusted to 1%, as this concentration supported BoNT/B cleavage. Finally, a pH-value of 7 was chosen and NaCl and BSA were completely omitted, due to slightly inhibitory effects of these factors on some serotypes.

As expected, cleavage in the consensus buffer was reduced when compared to the individually optimized buffers for each serotype (Figure 14 and Table 22). However, for serotypes A, B, DC, and F only a slight reduction was observed, and cleavage was still more than or as efficient as in the two reference buffers. A strong reduction was observed for BoNT/C, presumably due to the non-optimal pH-value and elevated DTT concentrations. Yet, cleavage of BoNT/C in the consensus buffer was much better compared to the reference buffers. Similarly, BoNT/E exhibited decreased cleavage. This could be explained by the presence of TMAO and high ZnCl₂ concentrations in the consensus buffer, both having a strong inhibitory effect on BoNT/E substrate cleavage.

Summing up, these results demonstrate that despite the different requirements of different BoNT serotypes, a consensus buffer in which all serotypes exhibited relatively good cleavage could be designed. In addition, with the results of the ANOM and ANOVA, inhibitory effects of specific factors could be anticipated as exemplified by the reduced cleavage of BoNT/C and E in the consensus buffer. Although not optimal for all serotypes, the newly developed consensus buffer (50 mM HEPES, 0.75 M TMAO, 250 µM ZnCl₂, 1% Tween 20, 25 mM DTT, pH 7) represents a valuable tool for assays detecting enzymatically active BoNT and was used in further experiments throughout this thesis.

5.2 Generation and characterisation of monoclonal neoepitope specific antibodies

As a major aim of this work, Neo-mAbs covering the cleavage sites of BoNT/A-F for the detection of catalytically active BoNT were generated. The novel Neo-mAbs were thoroughly characterised to learn more about their unique binding characteristics and draw conclusions for further applications of Neo-mAbs in different assay set-ups.

5.2.1 Generation of Neo-mAbs

Monoclonal Neo-mAbs were generated by immunizing mice with short BSA-coupled 8mer peptides resembling the respective BoNT cleavage site. Mice with sufficient antibody titre were selected for fusion and hybridoma clones producing Neo-mAbs with the desired specificity were selected in a rigorous screening procedure (the process of antibody generation is described in detail in the material and methods section 4.2.3.1).

Provoking a sufficient immune response in mice towards neoepitopes was particularly challenging as antibodies were supposed to only recognize a very specific site on the target protein. In the first attempts immunization was performed with a mixture of multiple peptides (up to six different peptides) to obtain several antibodies from one single mouse. Although this was effective for some serotypes, marked differences were observed in the immune response of mice towards different peptides. For example, peptides corresponding to the cleavage sites of BoNT/B and E provoked an immune response in mice, when immunized in a mixture of six different peptides (Appendix Figure 2). Contrary, peptides corresponding to the cleavage sites of BoNT/C produced very weak antibody titres when immunized in the same mixture of peptides (*ibid.*). Here, mice had to be immunized with larger doses of only one single peptide to obtain a satisfying immune response (*ibid.*). In that respect, the generation of Neo-mAbs targeting the N- and C-terminal cleavage sites of BoNT/C was particularly challenging. Out of three fusions performed and > 8000 clones screened only four Neo-mAbs could be generated, of which only one turned out to perform well in further applications (Table 23, section 5.2.2, section 5.3).

This goes in line with the common observation in all fusions that only few hybridoma clones produced the desired neoepitope-specific antibodies. Out of all hybridomas analysed as few

RESULTS

as 2.6%–8.8% passed the initial screening, and only 0.04%–0.2% were eventually selected to produce purified Neo-mAbs (Table 23).

Table 23: Overview of all successful fusions performed. In total four fusions generating 12 Neo-mAbs were performed during this work.

Fusion target (Neo-mAbs)	BoNT/B, D, F	BoNT/B, C, E	BoNT/B, C, E	BoNT/C
Immunization ^a	6 peptides	6 peptides	6 peptides	1 peptide
Total number of seeded cavities	~4400	~3650	~7900	~8540
Initial screening ^b	2930 (100%)	2674 (100%)	1099 ^e (100%)	5640 (100%)
Secondary screening ^c	257 (8.8%)	70 (2.6%)	38 (3.5%)	158 (2.8%)
Subcloned ^d	8 (0.3%)	4 (0.1%)	2 (0.2%)	14 (0.2%)
Purified Neo-mAbs	4 Neo-F 2 Neo-B (0.2%)	1 Neo-C (0.04%)	1 Neo-B 1 SNAP (0.2%)	3 Neo-C (0.05%)

^a Mice were immunized with 100 µg of short BSA-coupled peptides in a mixture of six different peptides or with one single peptide.

^b Number of hybridoma supernatants tested in initial screening. The initial screening was performed by indirect ELISA with (a mixture of) respective corresponding KLH-coupled peptides and full-length VAMP-2 and/or SNAP-25 as negative control.

^c Number of hybridoma supernatants tested in second screening. Clones from initial screening with a positive signal on the respective KLH-peptide and no cross-reactivity towards full-length substrate were applied to a secondary screening by indirect ELISA, with KLH coupled peptides (single peptides) and VAMP-2 or SNAP-25.

^d Number of clones that were subcloned. Positive clones from secondary screening and/or SPR screening were subcloned at least twice

^e Due to contamination, only very few clones could be screened.

Throughout this thesis a total of four fusions were successfully performed, more than 12,000 hybridomas were screened resulting in three Neo-mAbs targeting BoNT/B cleaved VAMP-2 (both fragments), four Neo-mAbs targeting BoNT/C cleaved SNAP-25 (both fragments), and four Neo-mAbs targeting BoNT/F cleaved VAMP-2 (N-terminal fragment) (Table 23 and Figure 15). Other Neo-mAbs used and characterized in this work were generated previously in the laboratory (Figure 15).

RESULTS

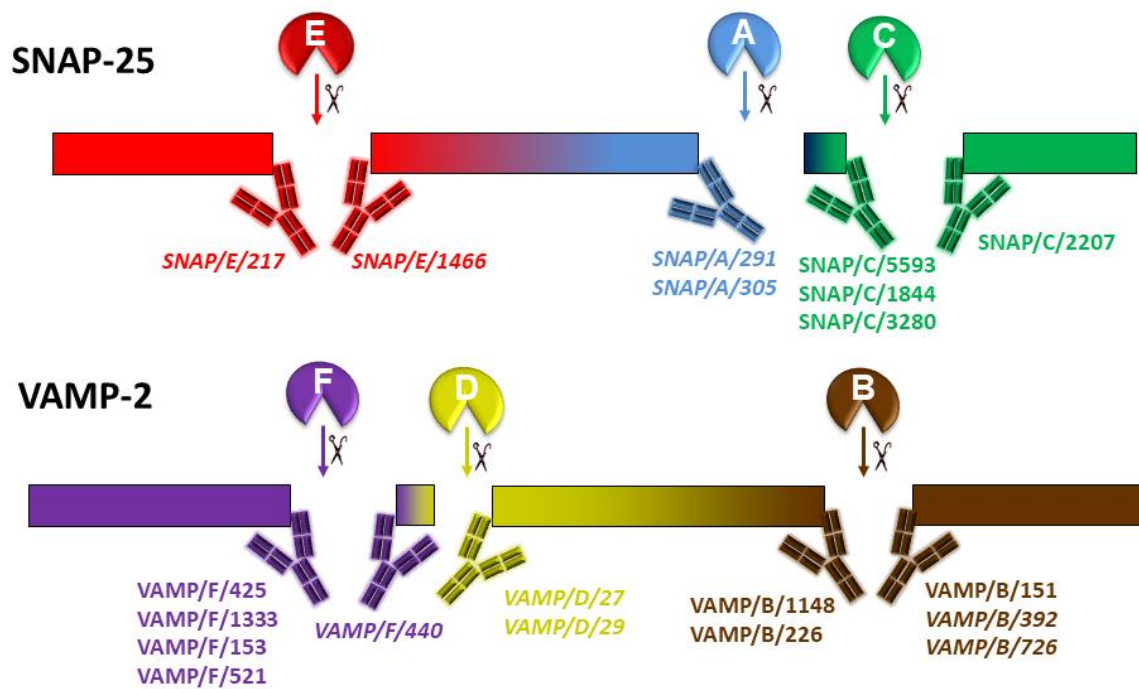


Figure 15: Scheme of all Neo-mAbs that were generated and/or thoroughly characterized by various methods in this work. Neo-mAbs were named according to their target substrate molecule (SNAP or VAMP), their specific target cleavage site (SNAP → A, C, or E; VAMP → B, D, or F), and the clone number assigned during fusion. For BoNT/B, C, E, and F, Neo-mAbs targeting the N- and C-terminal neopeptide were generated and/or characterized. For BoNT/A one Neo-mAb targeting the N-terminal cleavage fragment (and C-terminal neopeptide) was available. For BoNT/D two Neo-mAbs targeting the C-terminal cleavage fragment (N-terminal neopeptide) were characterized. Antibodies shown in italic font were generated in previous works in the laboratory.

To ensure that screening procedures selected antibodies with desired specificity, all available Neo-mAbs were tested by indirect ELISA. Here, all Neo-mAbs exclusively recognized their respective neopeptide and no cross-reactivity towards full-length substrate molecules (SNAP-25 or VAMP-2) or KLH or BSA was observed (Figure 16). Thus, as a starting point for a more in-depth characterisation to identify the best-performing antibodies for detection of BoNT/A-F catalytic activity, a panel of 20 Neo-mAbs specific for the cleavage sites of BoNT/A-F was now available.

RESULTS

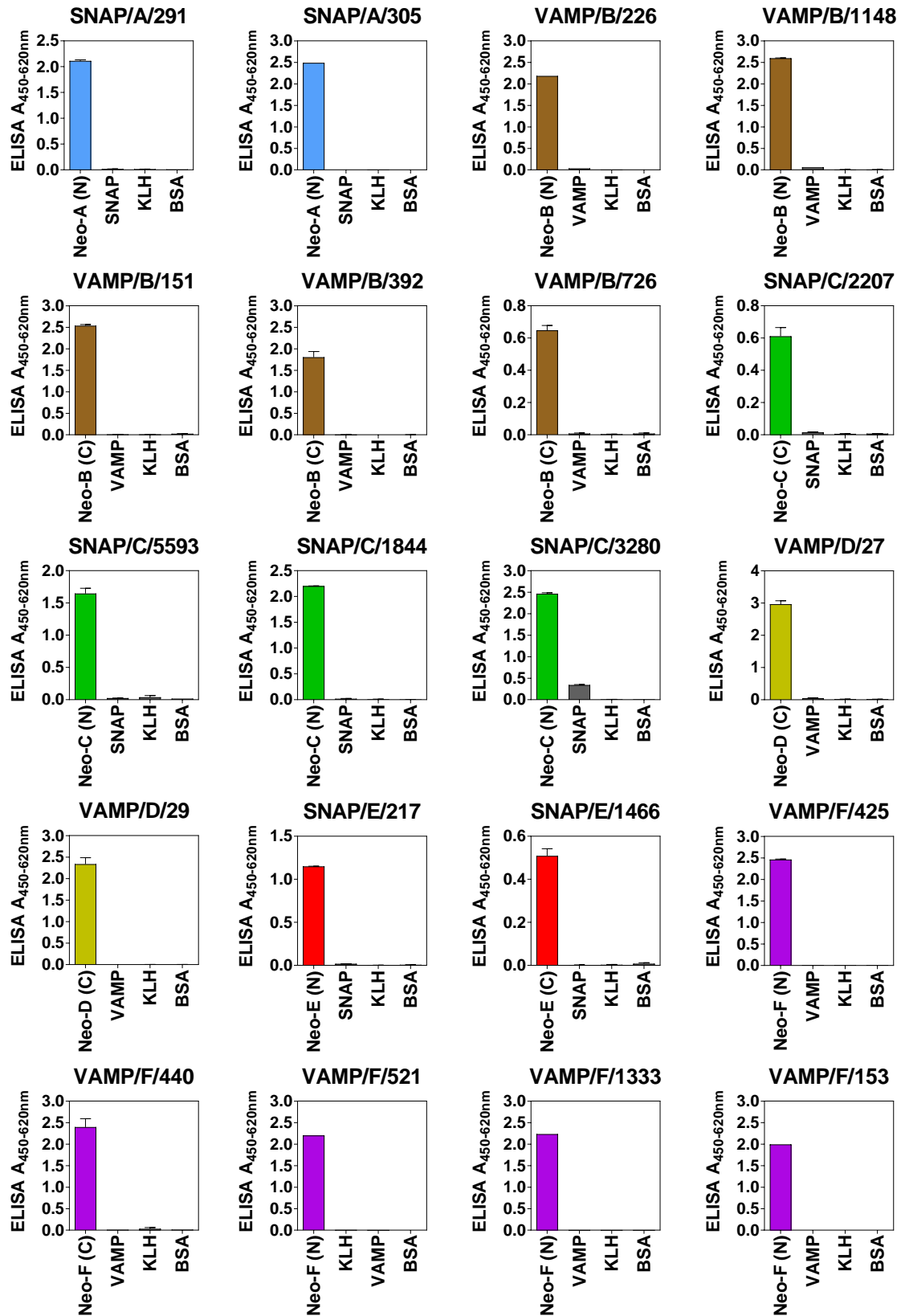


Figure 16: Reactivity of Neo-mAbs towards cleavage site specific short KLH-coupled peptides. Neo-mAbs (as indicated above each image) were characterized by indirect ELISA to analyse exclusive specificity towards the respective neopeptide. Short KLH-coupled peptides corresponding to the respective N- or C-terminal cleavage fragment, KLH, VAMP-2 or SNAP-25, and BSA were coated on

RESULTS

microtiter plates and detected by Neo-mAbs. Results of one experiment performed in technical duplicates are shown ($n = 2$; Mean \pm SD).

5.2.2 Characterisation of purified Neo-mAbs

To identify Neo-mAbs that enable specific and sensitive detection of BoNT/A-F catalytic activity, all purified Neo-mAbs (antibodies generated in this work as well as Neo-mAbs that were previously generated in the laboratory; Figure 15) were thoroughly characterised by various methods.

To determine binding kinetics, all Neo-mAbs were investigated by SPR techniques. Here, binding affinity and avidity provided valuable information regarding assay sensitivity in specific experimental set-ups. Reactivity towards cleaved but not uncleaved substrate was analysed by Western blotting. To exclude reactivity towards cleavage sites of neighbouring BoNT molecules as well as uncleaved substrate, an ELISA based method to detect catalytically active BoNT, termed Endopeptidase-ELISA [110], was employed. Finally, antibody performance of Neo-mAbs targeting the same cleavage site was compared in the Endopeptidase-ELISA by titrating toxin.

5.2.2.1 SPR measurements reveal different binding characteristics of Neo-mAbs

To obtain information on binding characteristics of Neo-mAbs, SPR measurements were carried out. As the antibodies' affinities and/or avidities towards cleaved substrate ultimately dictates the sensitivity achievable in different assay formats this information is a critical determinant in evaluating antibody performance. To determine binding characteristics of Neo-mAbs by SPR, two different experimental set-ups were employed (the principle of SPR technology is explained in more detail in the material and methods section 4.2.5.2).

First, to obtain monovalent affinity data, antibodies were immobilized and short biotinylated peptides (8mers corresponding to the respective cleavage site) were injected in solution.

Here, as a common observation, monovalent binding of most antibodies was characterized by rapid association and dissociation rates (Figure 17) consequently resulting in rather low affinities in the micromolar range (Table 24). However, several antibodies targeting the N-terminal fragment of BoNT/D (VAMP/D/27) or BoNT/F cleaved VAMP-2 (VAMP/F/153, VAMP/F/521, VAMP/F/425, VAMP/F/1333), and one antibody specific for the C-terminal fragment of BoNT/B cleaved VAMP-2 (VAMP/B/151) displayed stable interactions

RESULTS

characterized by decreased binding dissociation resulting in high affinity interactions in the nanomolar range. Finally, two antibodies targeting the N-terminal fragment of BoNT/B cleaved VAMP-2 (VAMP/B/226 and VAMP/B/1148) displayed no binding at all, presumably due to a masked accessibility of the neoepitope in solution, which is unmasked after immobilization, as high signals were achieved in the indirect ELISA with these antibodies (compare with Figure 16).

Second, to obtain bivalent avidity binding, the experimental set-up was turned upside-down: Serotype-specifically cleaved peptide substrate (VAMP-2-Bio or SNAP-25-Bio) was immobilized and serial dilutions of Neo-mAbs were injected. To enable bivalent binding of antibodies, a densely-packed surface of available interaction sites is required. Therefore, high concentrations of cleaved biotinylated peptide substrate were immobilized. This set-up enabled, in contrast to monovalent binding, the binding of Neo-mAbs with both antigen binding sites resulting in a more stable interaction. As antibody-antigen binding was thus mediated by a heterogeneous interaction, two equilibrium binding constants were determined. One of them resembled the very rapid and unstable interaction component from the monovalent binding and the second represented the more stable high avidity binding of the antibody.

Overall, almost all antibodies showed a clear increase in binding avidity with apparent equilibrium binding constants in the nano- to femtomolar range (Figure 18, Table 24). Best results were obtained with antibodies binding to BoNT/B (VAMP/B/151), BoNT/D (VAMP/D/27), or BoNT/F (VAMP/F/425, VAMP/F/440, VAMP/F/521, VAMP/F/1333) cleaved VAMP-2. Thus, an orientation that enables avidity binding of Neo-mAbs clearly improved binding strength. The only exceptions from this are two Neo-mAbs targeting BoNT/C cleaved SNAP-25 (SNAP/C/1844, SNAP/C/3280) which exhibited no binding at all in this assay set-up, despite a weak interaction in the monovalent binding assay. Akin to the results of monovalent antibody binding, no binding was detectable for antibodies recognizing the N-terminal fragment of BoNT/B cleaved VAMP-2 (VAMP/B/226 and VAMP/B/1148).

RESULTS

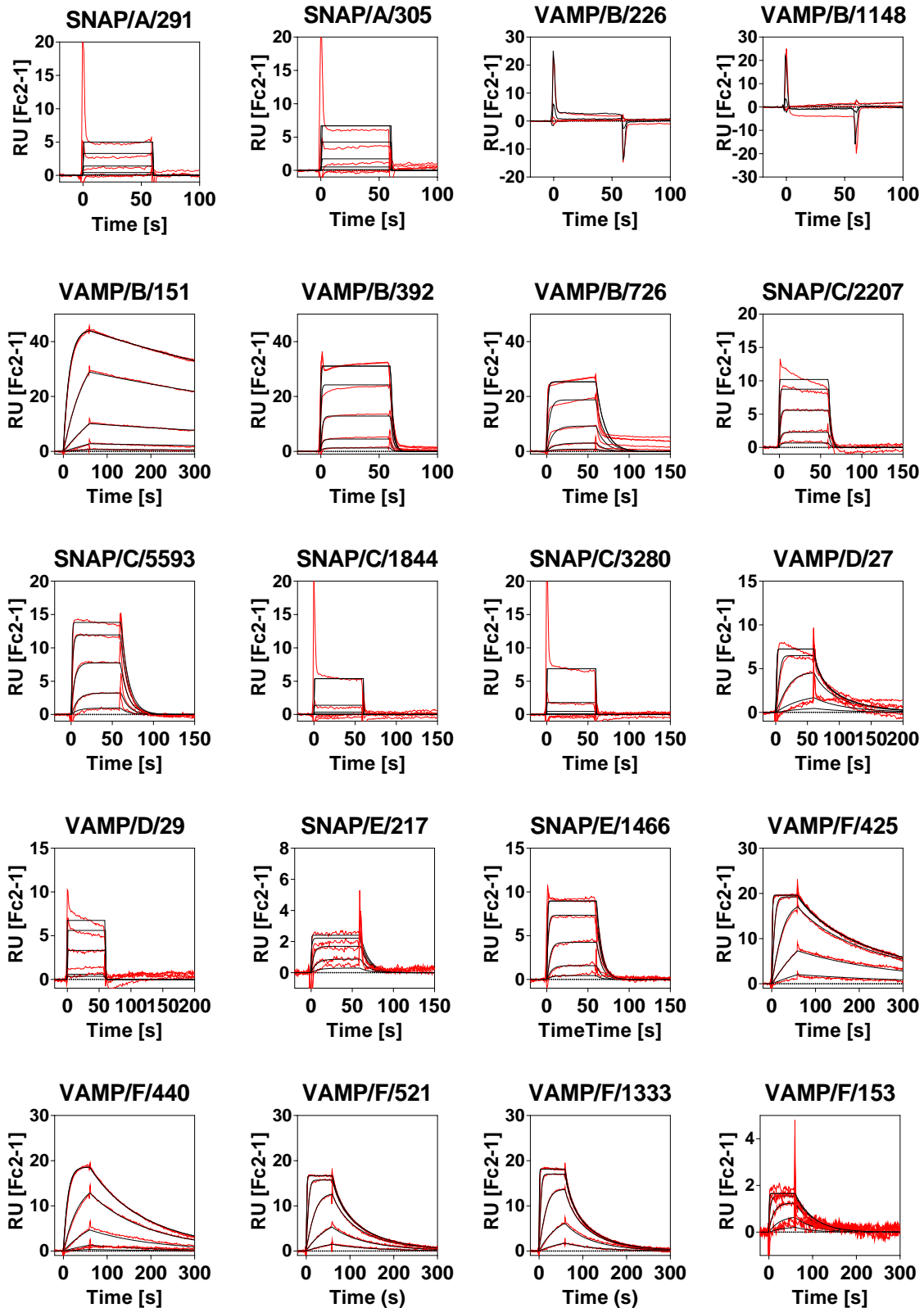


Figure 17: SPR measurements of neopeptide specific antibodies to determine antibody affinity by monovalent binding. Neopeptide specific antibodies were immobilized on a mouse antibody capture kit and serial dilutions of short peptides resembling the respective BoNT cleavage site were injected. Panels depict the binding of peptides to the antibody (red lines = measured RUs). Data was fitted using the 1:1 Langmuir binding model (black lines = fit).

RESULTS

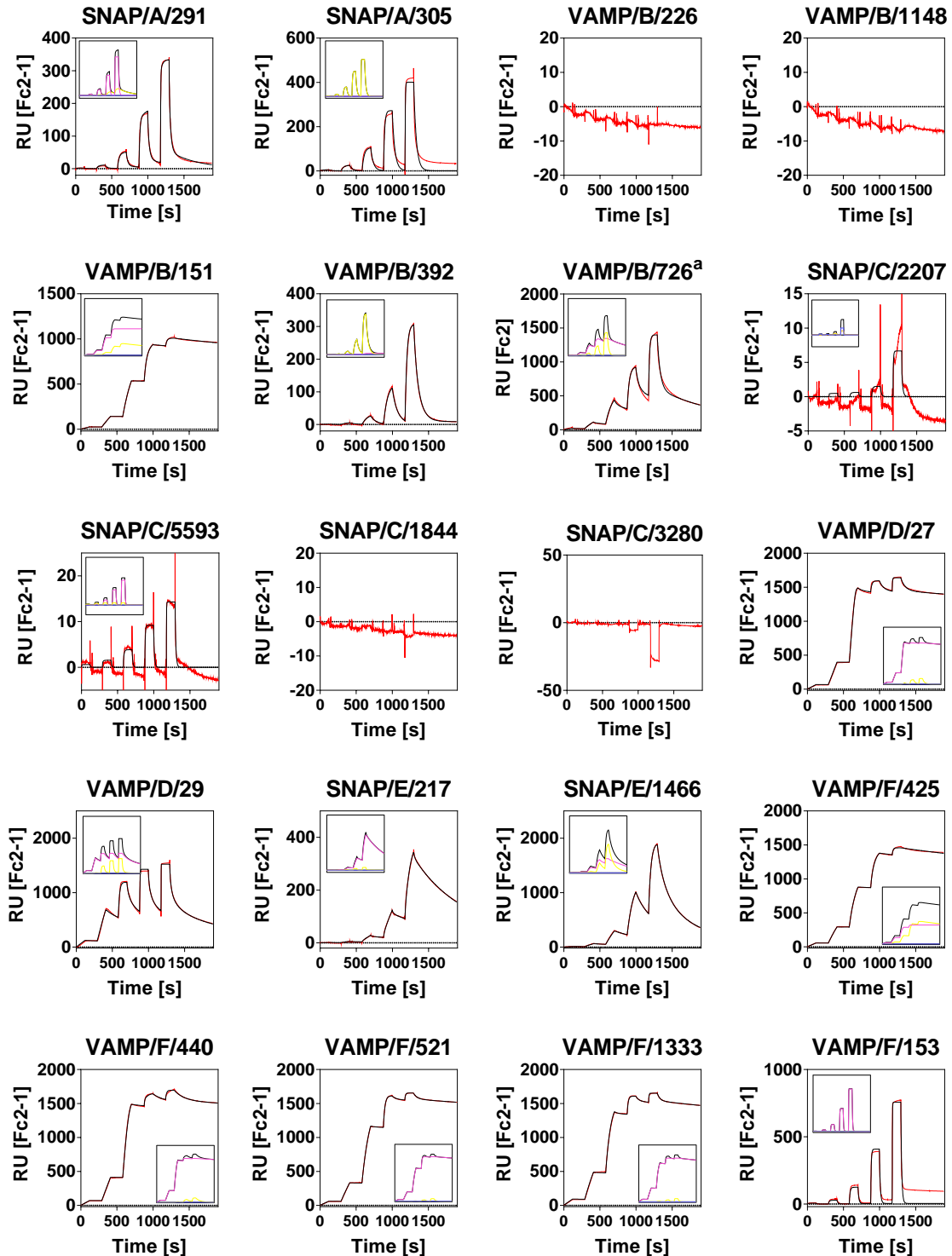


Figure 18: SPR measurements of neopeptide specific antibodies to determine the binding avidity of antibodies by bivalent interactions. BoNT cleaved VAMP-2-Bio or SNAP-25-Bio was immobilized on a biotin CAPture kit sensor chip. Serial dilutions of antibody were injected. Data was fitted using the heterogeneous ligand binding model (red lines = measured; black lines = fit). The inset shows the two components of the heterogeneous interaction (black line = total; pink line = component 1; yellow line = component 2; blue line = bulk and drift). ^a For Neo-mAb VAMP/B/726 the binding to Fc2 only is depicted, as negative signals were observed after referencing, presumably due to strong cross-reactivity against uncleaved substrate

RESULTS

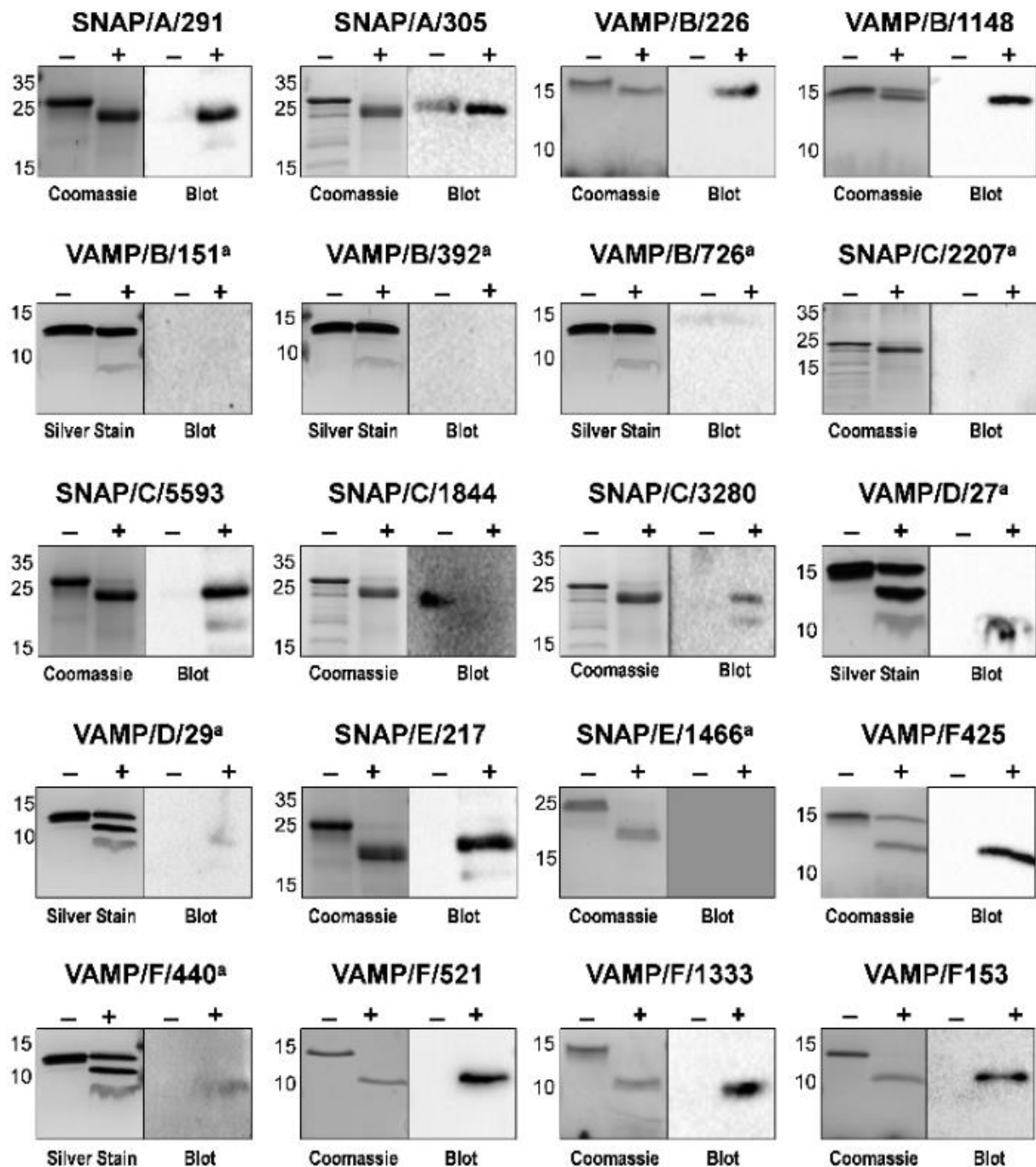
In summary, these data show that kinetic data of antibodies gathered by SPR measurements can provide essential information regarding antibody performance. In addition, it demonstrates that binding strength of antibodies can vary depending on the experimental set-up. Based on these results, an experimental set-up which allows for bivalent binding should yield higher sensitivities with most Neo-mAbs than an assay set-up which solely facilitates monovalent binding. In conclusion, the measurement of avidity binding helps to select from a panel of seemingly similar Neo-mAbs according to ELISA data (Figure 16) those antibodies which show strongest interaction with their respective target. All Neo-mAbs targeting BoNT/F cleaved VAMP-2 for example (VAMP/F/425, VAMP/F/440, VAMP/F/521, VAMP/F/1333, VAMP/F/153) seemed similar according to ELISA data (Figure 16) but avidity data (Figure 18) suggests that VAMP/F/153 would be outperformed by the others.

5.2.2.2 Characterisation by Western blotting and Endopeptidase-ELISA demonstrates exclusive specificity towards cleaved substrate

In indirect ELISA and SPR experiments short peptides or biotinylated peptide substrates were employed to test antibody binding. However, binding to cleaved full-length substrates has not been demonstrated by respective methods. Therefore, further methods were applied to obtain a more comprehensive picture regarding specificity of all Neo-mAbs.

Specificity towards only cleaved but not uncleaved substrate was tested by Western blotting. To that aim, BoNT/A-F were used to cleave full-length VAMP-2 or SNAP-25 and cleaved substrates were loaded on two identical acrylamide gels. To demonstrate sufficient substrate cleavage one gel was stained with Coomassie (or Silver stain), while the second gel was analysed by Western blotting with Neo-mAbs. Here, best results with exclusive recognition of the cleaved substrate were achieved with Neo-mAbs SNAP/A291, VAMP/B/226, VAMP/B/1148, SNAP/C/5593, SNAP/E/217, VAMP/F/425, VAMP/F/521, and VAMP/F/1333 (Figure 19). A very weak signal was achieved with SNAP/C/3280 while cross-reactivity against uncleaved substrate was observed for SNAP/A/305 and SNAP/C/1844. For Neo-mAbs recognizing the smaller C-terminal fragment (VAMP/B/151, VAMP/B/392, VAMP/B/726, SNAP/C/2207, VAMP/D/27, VAMP/D/29, SNAP/E/1466, VAMP/F/440) no clear results were obtained in Western blots as depicting binding to smaller C-terminal cleavage fragments with a size of only 2 to 4.5 kDa is technically challenging.

RESULTS



^a Neo-mAb was raised against the smaller cleavage fragment, which is not/only merely visible after Coomassie or silver stain.

Figure 19: Neopeptide specific monoclonal antibodies exclusively recognize cleaved SNAP-25 or VAMP-2. Full-length SNAP-25 or VAMP-2 was incubated with (+) or without (-) BoNT over night at 37°C in cleavage buffer. Samples were loaded on two identical polyacrylamide gels. One gel was used for Coomassie stain (or silver stain) (left panel), and the second gel was applied for Western blotting using Neo-mAbs (right panel). Numbers on the left side of each panel indicate protein size in kDa according to marker bands. ^a Neo-mAb was raised against the smaller cleavage fragment, which is not/only merely visible after Coomassie or silver stain.

RESULTS

Therefore, specificity was analysed further in an Endopeptidase-ELISA format. Here, as a further criterion, detection of the correct cleavage site was analysed as cross-reactivity towards neighbouring cleavage should be excluded. To that aim, immobilized substrate was cleaved by BoNT on microtiter plates and cleavage products were detected by Neo-mAbs (assay principle see Figure 22). To test cross-reactivity towards neighbouring cleavage sites, binding to substrates cleaved with high concentrations of neighbouring BoNT molecules (10 ng/mL) was analysed (Figure 20). The data clearly showed that most Neo-mAbs (SNAP/A/291, SNAP/A/305, VAMP/B/226, VAMP/B/1148, VAMP/B/151, SNAP/C/5593, VAMP/D/27, VAMP/D/29, SNAP/E/217, SNAP/E/1466, VAMP/F/425, VAMP/F/440, VAMP/F/521, VAMP/F/1333, VAMP/F/153) recognized the correct cleavage fragments, thus demonstrating their exclusive specificity. This was particularly remarkable for Neo-mAbs targeting BoNT/C and A cleaved SNAP-25 as well as BoNT/D and F cleaved VAMP-2 as cleavage sites here differ by only one single amino acid. Interestingly, some Neo-mAbs (VAMP/B/392, VAMP/B/726, SNAP/C/1844, SNAP/C/2207, SNAP/C/3280) that clearly recognized short KLH-coupled or biotinylated peptides in the indirect ELISA and SPR measurements (Figure 16 and Figure 17) did not exhibit any binding for the BoNT cleaved substrate molecule in both methods, the Endopeptidase-ELISA and SPR measurements (Figure 18 and Figure 20). This finding demonstrates that the recognition of short peptides, resembling the respective BoNT cleavage site, is not necessarily transferable to the recognition of BoNT cleaved substrate molecules, although the target neoepitope should be identical.

RESULTS

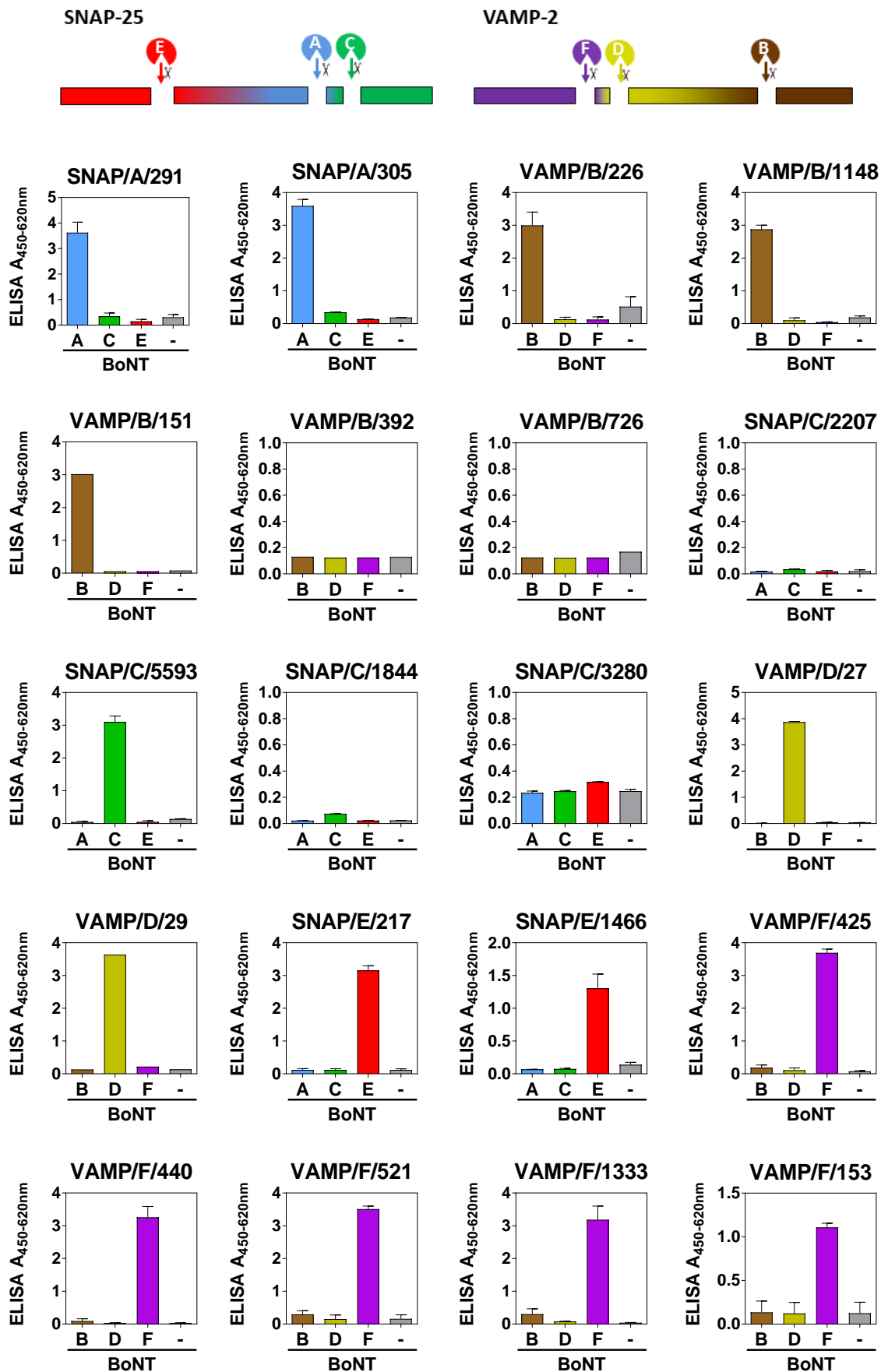


Figure 20: Reactivity of Neo-mAbs towards different cleavage sites as shown by Endopeptidase-ELISA. Full-length VAMP-2 or SNAP-25 coated on microtiter plates was cleaved with 10 ng/mL of different BoNT serotypes targeting the respective substrate molecule: SNAP-25 was cleaved by

RESULTS

BoNT/A, C, and E and VAMP-2 was cleaved by BoNT/B, D, and F (– = no toxin added). Cleavage products were detected with Neo-mAbs as indicated above each panel. Results from two or three independent experiments, each performed in technical duplicates are shown ($n = 4$ or $n = 6$; Mean \pm SD).

5.2.2.3 Comparison of Neo-mAbs in an endopeptidase activity assay

To directly compare the achievable sensitivity of antibodies targeting the same cleavage site, all generated Neo-mAbs were tested in an Endopeptidase-ELISA (Figure 21). Therefore, SNAP-25 or VAMP-2 was immobilized on microtiter plates, cleaved by BoNT, and cleavage products were detected by Neo-mAbs (assay principle see Figure 22).

For BoNT/A, both antibodies targeting the N-terminal cleavage fragment (SNAP/A/291 and SNAP/A/305) exhibited low binding affinity and avidity in SPR measurements and thus comparable sensitivities in the Endopeptidase-ELISA were expected (see Figure 17 and Figure 18). Indeed, equivalent results were achieved for both antibodies with unexpected high sensitivities (Figure 21). High sensitivities in the Endopeptidase-ELISA were most likely achieved due to the highly efficient cleavage of BoNT/A which contributes most to assay sensitivity, thereby compensating the low antibody affinity and avidity.

For BoNT/B, two Neo-mAbs (VAMP/B/226 and VAMP/B/1148) both targeting the larger N-terminal cleavage fragment allowed for highly sensitive detection in the Endopeptidase-ELISA, although a different antibody (VAMP/B/151) which is directed against the shorter C-terminal fragment exhibited a much higher affinity and avidity. The lower sensitivity in the Endopeptidase-ELISA, when detection was performed with the higher affinity/avidity antibody, was presumably caused by inferior accessibility of the very short peptide after cleavage. This was supported by the observation that assay sensitivity of BoNT/B detected with VAMP/B/151 could be improved by increasing the space between substrate molecules by the addition of BSA in coating buffer (Appendix Figure 3).

Likewise, for BoNT/C and E sensitive detection was only achieved with Neo-mAbs directed against the larger N-terminal fragment (SNAP/C/5593 and SNAP/E/217), despite comparable affinities/avidities to the antibodies targeting the shorter C-terminal cleavage fragments.

As expected, for both BoNT/D and F, Neo-mAbs exhibiting highest affinities and avidities achieved best sensitivities in the Endopeptidase-ELISA. Notably, for BoNT/F, satisfactory results were achieved with antibodies against both cleavage fragments, indicating that both

RESULTS

fragments are suitable for immobilization on ELISA plates, probably due to the larger size of the C-terminal fragment.

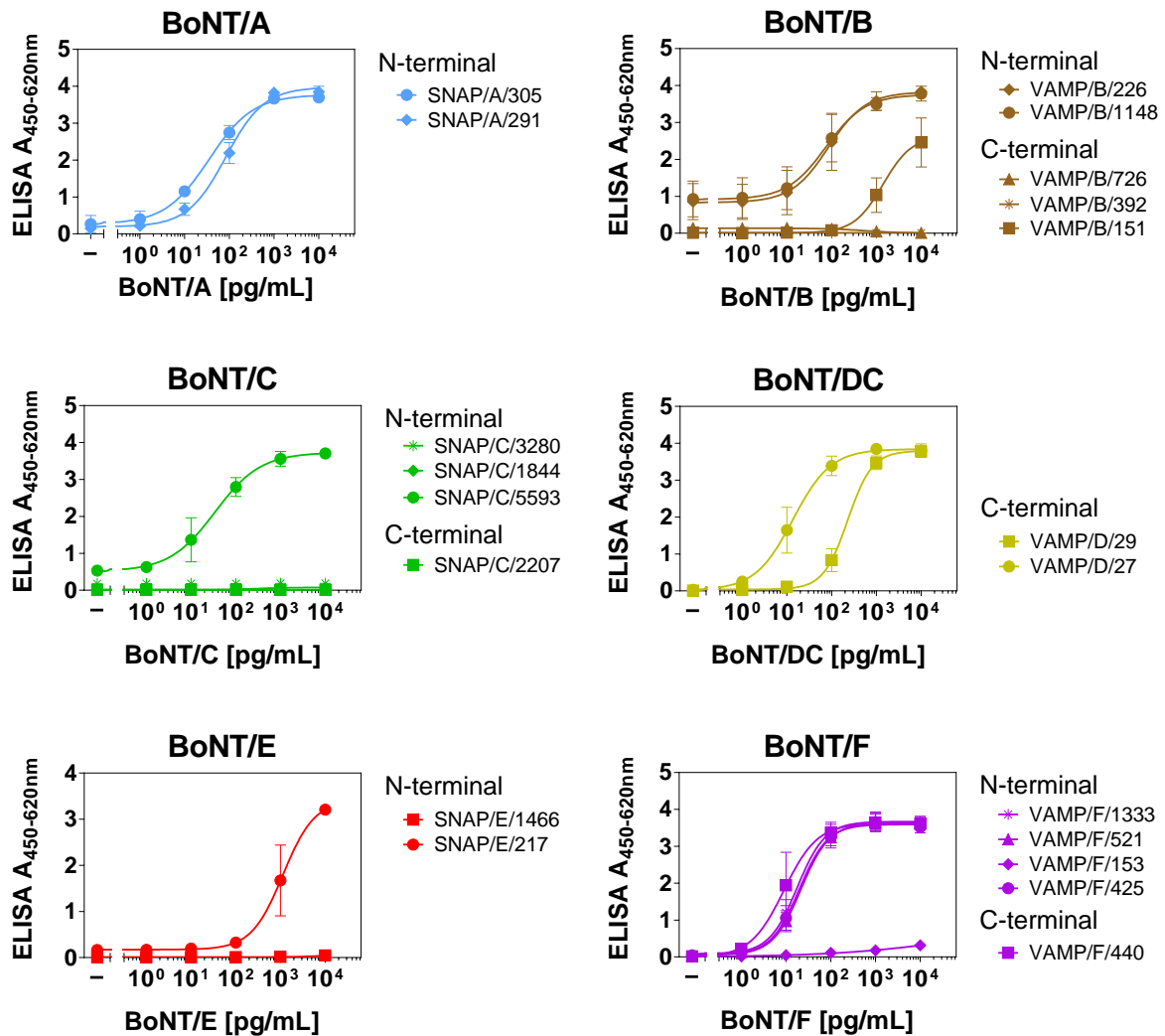


Figure 21: Comparison of performance of Neo-mAbs in an Endopeptidase-ELISA. Full-length VAMP-2 or SNAP-25 was coated on microtiter plates, cleaved by serial dilutions of BoNT as indicated above the figures and cleavage products were detected with Neo-mAbs. Single data points were log-transformed (X axes = Log(X)) and curves were fitted using a four-parameter fit. Results from two independent experiments with each repeat performed in technical duplicates are shown (n = 4; Mean \pm SD).

5.2.2.4 Summary of antibody characterisation

In summary, although all antibodies were selected based on specific binding to KLH-coupled peptides, marked differences were observed, even among Neo-mAbs targeting the same neoepitope. In addition, the presented data show that an in-depth characterization of

RESULTS

antibodies provided valuable information regarding antibody performance in different experimental settings. Here, in most cases, antibodies with good binding properties also yielded good results in an Endopeptidase-ELISA format. However, exceptions clearly showed that kinetic data could not be fully translated into other assays as depending on the experimental setting other factors, such as neoepitope accessibility, might play a role. An overview on all generated data is depicted in Table 24.

Based on the thorough characterization of 20 Neo-mAbs, the following antibodies were selected for further work: SNAP/A/291, VAMP/B/1148, SNAP/C/5593, VAMP/D/27, SNAP/E/217, and VAMP/F/425 (Table 25). For BoNT/A, D, and E SNAP/A/291, VAMP/D/27, and SNAP/E/217 were picked over SNAP/A/305, VAMP/D/29, and SNAP/E/1466 due to their better performance in all assay platforms tested. Even though no binding could be observed in SPR measurements, VAMP/B/1148 was selected for BoNT/B due to its reliable performance in all other assays, particularly in the Endopeptidase-ELISA. As the only BoNT/C cleavage site specific Neo-mAb that yielded good results in all assays tested, SNAP/C/5593 was selected for BoNT/C. For BoNT/F, almost all Neo-mAbs (except for VAMP/F/153) yielded comparable results in all assays tested. For further work VAMP/F/425 was selected.

RESULTS

Table 24: Overview on characterisation data of all Neo-mAbs specifically detecting the cleavage sites of BoNT/A-F in SNAP/VAMP. Antibodies depicted in bold were selected for further work.

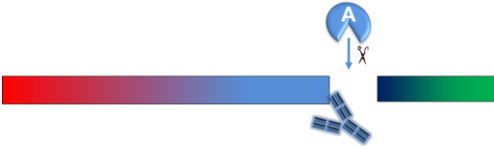
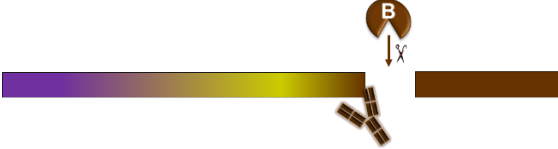

Antibody	Isotype	Specificity ^a	Indirect ELISA ^b	Affinity ^c	Avidity ^d		Western Blot ^e	Endopeptidase-ELISA ^f
				K _D [M]	K _{D1} [M]	K _{D2} [M]		
SNAP/A/291	IgG1	N	+++	1.4×10⁻⁵	1.1×10⁻⁷	3.2×10⁻⁸	+	+++
SNAP/A/305	IgG1	N	+++	2.0×10 ⁻⁵	5.7×10 ⁻⁸	1.8×10 ⁻⁸	+	+++
VAMP/B/226	IgG1	N	+++	n.d.	n.d.	n.d.	+	+++
VAMP/B/1148	IgG1	N	+++	n.d.	n.d.	n.d.	+	+++
VAMP/B/151	IgG2b	C	+++	4.5×10 ⁻⁹	2.3×10 ⁻⁹	1.4×10 ⁻¹³	–	+
VAMP/B/392	IgG1	C	++	5.7×10 ⁻⁶	2.2×10 ⁻⁷	2.4×10 ⁻¹⁰	–	–
VAMP/B/726	IgG3	C	+	7.3×10 ⁻⁷	2.2×10 ⁻⁷	1.9×10 ⁻⁹	–	–
SNAP/C/2207	IgG1	C	+	5.1×10 ⁻⁷	3.1×10 ⁻⁶	3.1×10 ⁻⁶	–	–
SNAP/C/5593	IgG2a	N	++	3.1×10⁻⁷	7.5×10⁻⁸	9.7×10⁻¹⁰	+	+++
SNAP/C/1844	IgG2a	N	+++	1.5×10 ⁻³	n.d.	n.d.	– ^g	–
SNAP/C/3280	IgG2b	N	+++ ^g	1.3×10 ⁻³	n.d.	n.d.	(+)	–
VAMP/D/27	IgG2b	C	+++	1.3×10⁻⁸	3.2×10⁻⁸	6.9×10⁻¹²	(+)	+++
VAMP/D/29	IgG2b	C	+++	8.6×10 ⁻⁷	1.7×10 ⁻⁷	2.5×10 ⁻¹⁰	(+)	++
SNAP/E/217	IgG1	N	++	2.3×10⁻⁷	6.4×10⁻⁸	3.6×10⁻⁸	+	++
SNAP/E/1466	IgG1	C	+	1.3×10 ⁻⁶	1.1×10 ⁻⁷	5.2×10 ⁻⁹	–	–
VAMP/F/425	IgG1	N	+++	2.0×10⁻⁹	9.1×10⁻¹⁰	4.7×10⁻¹³	+	+++
VAMP/F/440	IgG2a	C	+++	2.2×10 ⁻⁸	4.3×10 ⁻⁸	1.7×10 ⁻¹¹	(+)	+++
VAMP/F/521	IgG1	N	+++	6.0×10 ⁻⁹	1.1×10 ⁻⁷	7.8×10 ⁻¹¹	+	+++
VAMP/F/1333	IgG1	N	+++	6.5×10 ⁻⁹	7.1×10 ⁻⁸	7.6×10 ⁻¹¹	+	+++

RESULTS

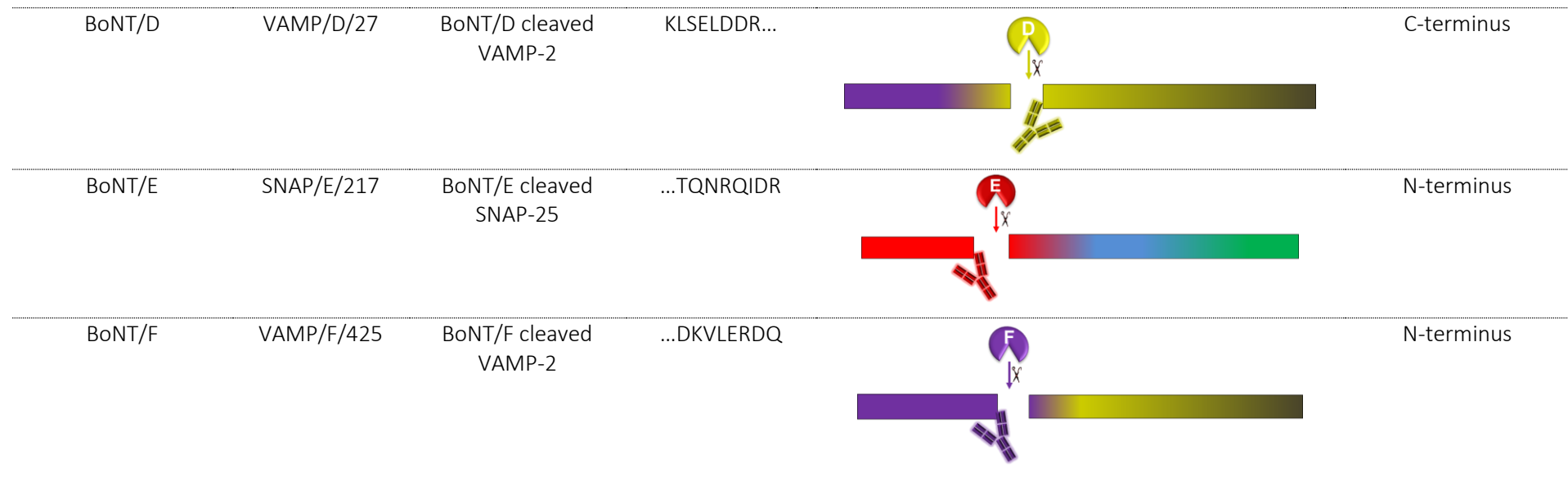
VAMP/F/153	IgG1	N	++	6.5×10^{-9}	1.1×10^{-7}	5.2×10^{-11}	+	0
------------	------	---	----	----------------------	----------------------	-----------------------	---	---

^a Specificity towards N- or C-terminal fragment generated after cleavage.
^b Binding of Neo-mAbs to short immobilized KLH-coupled peptides (+++ = OD > 2; ++ = OD > 1; + = OD > 0.5).
^c Capture of short biotinylated peptides by Neo-mAbs from solution (monovalent binding).
^d Binding of Neo-mAbs to immobilized cleaved substrate (bivalent binding). Due to the use of the heterogeneous binding model, two KD values were obtained for each interaction. n.d. = not detectable; no binding was observed in measurement.
^e Binding of Neo-mAbs to cleaved substrate blotted on membrane (+ = good signal; +) = faint signal; – = no signal detected).
^f Binding of Neo-mAbs to immobilized cleaved substrate in an Endopeptidase-ELISA format (EC50: +++ < 0.1 ng/mL; ++ < 1 ng/mL; + < 10 ng/mL; 0 > 10 ng/mL; – signal too weak for detection).

Table 25: Overview on the six Neo-mAbs that were selected out of a panel of 20 Neo-mAbs for further work.

Detection of catalytic activity	Clone name	Target	Target sequence	Cleavage site	Specificity ^a
BoNT/A	SNAP/A/291	BoNT/A cleaved SNAP-25	...TRIDEANQ		N-terminus
BoNT/B	VAMP/B/1148	BoNT/B cleaved VAMP-2	...ALQAGASQ		N-terminus
BoNT/C	SNAP/C/5593	BoNT/C cleaved SNAP-25	...RIDEANQR		N-terminus

RESULTS



^a Specificity towards N- or C-terminal fragment generated after cleavage.

5.3 Development of different assay formats for the detection of catalytically active BoNT by Neo-mAbs

The major goal of the thesis was to develop a functional method for the detection of all clinically relevant BoNT serotypes A-F. To that aim, Neo-mAbs detecting the exact cleavage site on substrate molecules of each BoNT serotype were generated and thoroughly characterized as described before. Thus, instead of directly detecting the presence of BoNT, the toxin's catalytic activity, which displays the major determinant of BoNT toxicity, is monitored in the different approaches investigated here.

The achievable sensitivity in assay-formats detecting enzymatically active BoNT by Neo-mAbs depends on two major factors: First, sufficient substrate cleavage essentially influences assay sensitivity. Different BoNT serotypes cleave their substrate with different efficiencies. In this context the choice of buffer conditions can tremendously influence substrate cleavage, as demonstrated in section 5.1. Second, assay sensitivity depends on an efficient binding of Neo-mAbs to the cleavage site, which is ultimately dictated by the antibodies' affinity and/or avidity as well as proper accessibility of the respective neoepitope. The latter mainly depends on the experimental set-up and must be determined empirically for each assay system.

Using the panel of Neo-mAbs generated and characterized in this work combined with the optimized consensus buffer for efficient substrate cleavage, different assay formats for sensitive detection of functional active BoNT/A-F were developed: An Endopeptidase-ELISA format for individual toxin detection without the requirement of advanced technical systems and a second assay format for multiplex-detection of all six BoNT serotypes based on the Luminex™ platform.

5.3.1 Evaluation of an Endopeptidase-ELISA for the detection of catalytically active BoNT/A-F

For BoNT detection in routine laboratories easy-to-perform assay systems are required. Therefore, Neo-mAbs were implemented in an Endopeptidase-ELISA format which has previously been described for BoNT/A and E by Jones et al [110]. The Endopeptidase-ELISA is a straightforward assay and only requires a multiplate absorbance reader for sample read-out, commonly present in most diagnostic laboratories. These features ensure a broad

RESULTS

applicability of this assay. Figure 22 illustrates the working principle of the Endopeptidase-ELISA. Briefly, SNAP-25 or VAMP-2 is immobilized on microtiter plates. Then, toxin is added for substrate cleavage and samples are incubated for an overnight digest at 37°C. After thorough washing the newly exposed neoepitopes are detected by Neo-mAbs and a HRP-coupled detection antibody.

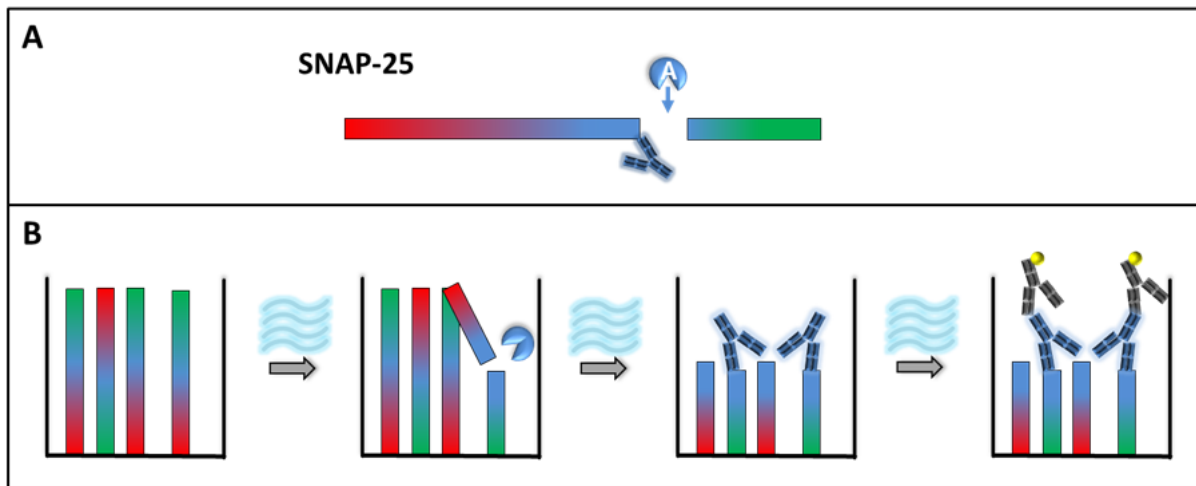


Figure 22: Scheme of the Endopeptidase-ELISA for the detection of BoNT/A. The Endopeptidase-ELISA according to Jones et al was used (among other methods) to determine the catalytic activity of BoNT/A-F (exemplified with BoNT/A in this scheme). (A) Different BoNT serotypes cleave SNAP-25 or VAMP-2 at specific sites. Cleavage sites can be detected by highly specific Neo-mAbs (shown for BoNT/A). (B) In the Endopeptidase-ELISA SNAP-25 (or VAMP-2) is immobilized on microtiter plates. Then, plates are blocked, washed, and toxin containing solution is added for substrate cleavage. Plates are subsequently washed, and cleavage products are detected by adding Neo-mAbs. Finally, plates are washed again and an HRP-coupled anti-mouse IgG detection antibody is added for signal read-out.

5.3.1.1 Endopeptidase-ELISA proves to be a robust assay with high sensitivities for the detection of catalytically active BoNT/A-F

Based on the results of the comparison of Neo-mAbs in the Endopeptidase-ELISA from the antibody characterisation (see section 5.2.2.3, Figure 21) the best performing six Neo-mAbs (SNAP/A/291, VAMP/B/1148, SNAP/C/5593, VAMP/D/27, SNAP/E/217, VAMP/F/425, see Table 25) were selected (one for each serotype) and used for further optimization and evaluation of the assay. To reduce background signals, antibodies were titrated prior to further evaluation of the assay.

To evaluate assay sensitivity and to test its robustness, the Endopeptidase-ELISA as visualized in Figure 22 was performed six times, with each repeat performed in duplicates (Figure 23).

RESULTS

For all serotypes, the assay turned out to be highly sensitive with detection limits in the low pg/mL range (0.3–14 pg/mL, Table 26). Transferred to mouse lethal doses (based on the toxins enzymatic activity specified by the manufacturer) the assay for BoNT/B had a comparable sensitivity to the mouse-bioassay (1.4 LD₅₀/mL), whereas detection limits for all other serotypes clearly outperformed the animal experiment (0.004–0.8 LD₅₀/mL). In addition, all serotypes exhibited low standard deviations, demonstrating the robustness of the assay.

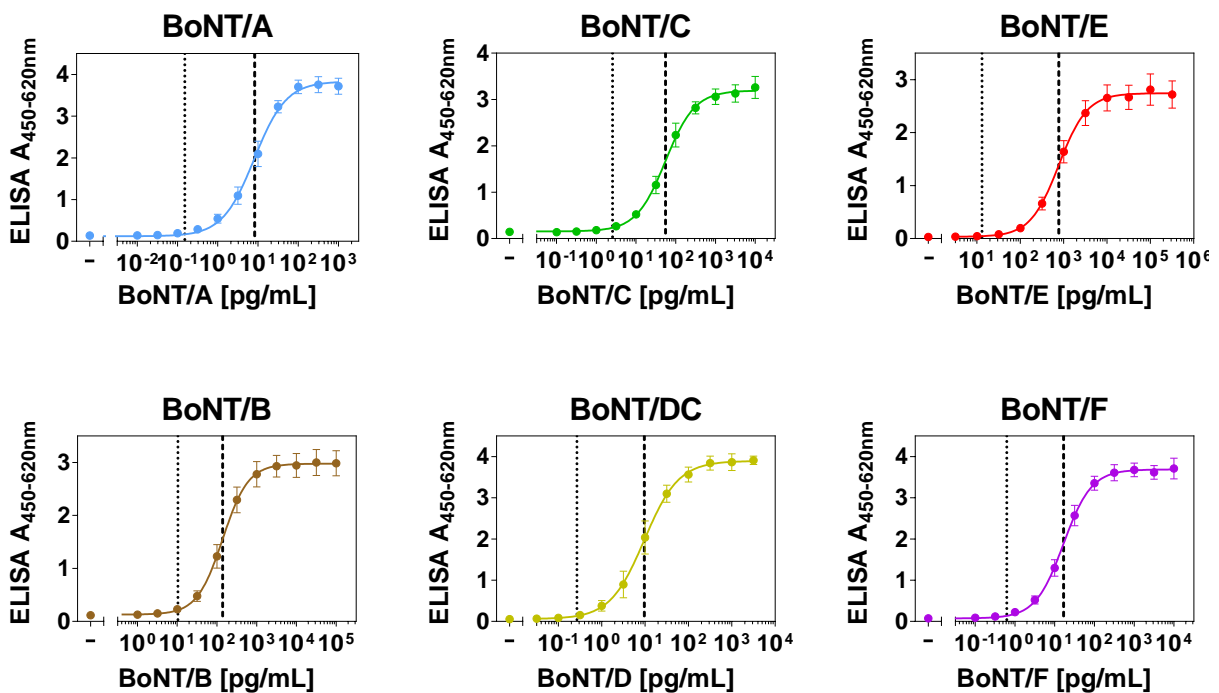


Figure 23: Detection of BoNT/A to F by Endopeptidase-ELISA. VAMP-2 or SNAP-25 was coated on microtiter plates, cleaved by incubation with serial dilutions of BoNT as indicated above each panel, and cleavage products were detected with Neo-mAbs. Curves were fitted over log-transformed toxin concentrations using a four parameter Hill-slope fit. The dashed and dotted lines mark the EC₅₀ and LOD, respectively. Results from six independent experiments (each performed in technical duplicates) are shown (n = 12; Mean ± SD).

RESULTS

Table 26: Assay performance of the Endopeptidase-ELISA for detection of BoNT/A to F substrate cleavage. Results shown in this table were generated using the data from Figure 23.

	BoNT/A	BoNT/B	BoNT/C	BoNT/DC	BoNT/E ^c	BoNT/F
EC50 (pg/mL)	8.1	139	55	9.6	771	17
LOD (pg/mL) ^a	0.3	11	2.7	0.3	14	0.8
	(0.2–0.4)	(8.9–14.9)	(2.1–3.4)	(0.2–0.4)	(9.9–23.3)	(0.7–1)
LOD (LD50/mL) ^b	0.07	1.36	0.08	0.03	0.004	0.02

^a Cutoff: mean + 3.29 × SD of blank values (determined with 32 blank values for each serotype) including lower and upper limit of 95% confidence interval (shown in brackets).

^b LOD calculated to LD50/mL according to toxin activity as specified by the manufacturer (see material and method section).

^c Non-trypsinated BoNT/E was used.

5.3.1.2 Detection of BoNT activity from complex matrices required toxin enrichment

For the detection of BoNT from complex matrices, an enrichment step of the toxin prior to the assay is required for two reasons. First, matrix components might interact with the substrate, the toxin, or the cleavage buffer in an unfavourable way. Along this line, first attempts testing spiked serum samples without prior enrichment failed due to a strong precipitation of samples, presumably caused by interactions between serum immunoglobulins and DTT as essential buffer component. In addition, experiments with toxin containing *Clostridia* supernatants produced inconsistent results with many false positive or negative results, presumably due to degradation of the substrate, the toxin, or both by clostridial proteases. Second, sufficient substrate cleavage strongly depends on optimal buffer conditions as demonstrated in section 5.1. Without enrichment, this could only be achieved with very high sample dilutions, greatly reducing assay sensitivity.

For these reasons, toxin enrichment – or more precisely a buffer exchange step – is indispensable for enzymatic BoNT assays in complex matrices. For enrichment, monoclonal anti-BoNT antibodies were covalently coupled to magnetic dynabeads. Subsequently, dynabeads were incubated with a BoNT containing sample for toxin capture. Beads were then thoroughly washed and diluted in cleavage buffer. Beads with captured toxin were directly used in the endopeptidase assays (Figure 24).

RESULTS

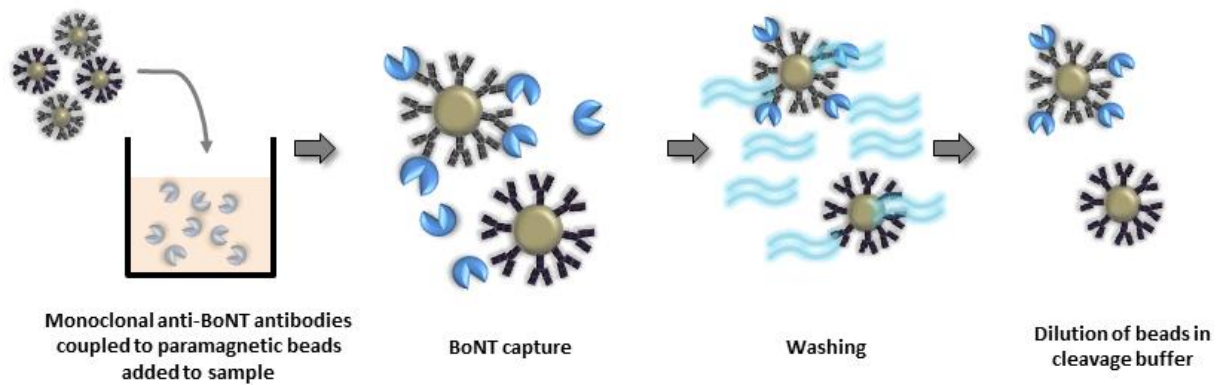


Figure 24: Scheme of toxin enrichment with monoclonal anti-BoNT antibodies. Anti-BoNT antibodies coupled to paramagnetic dynabeads are added to a BoNT containing sample. To allow BoNT capture beads are incubated with the sample for one hour and subsequently thoroughly washed. Finally, beads are diluted in cleavage buffer and applied in the respective assay.

To identify optimal antibodies for toxin enrichment, different antibodies that were previously generated in the laboratory were tested regarding their performance in enrichment independent of the enzymatic assay as well as in combination with an endopep-assay (Table 27, Appendix Figure 4). To test antibody binding to BoNT independent of enzymatic activity, a bead-western was applied, in which enriched toxin was separated from the beads by SDS-PAGE and detected by western blotting. Here, clear differences regarding enrichment efficiency could be observed for the different antibodies. When toxin enrichment was combined with enzymatic activity similar differences regarding enrichment efficiency were observed. Notably, antibodies targeting the toxins' LC or the adjacent translocation domain H_N (e.g. B710, B279, D63) clearly performed worse in the combination of toxin enrichment and enzymatic activity than antibodies targeting the HC (ibid.). Here, antibody binding to the enzymatically active LC or H_N presumably either directly influences catalytic activity in a negative way or causes sterical hindrances thereby reducing cleavage efficiency. Thus, if available, antibodies targeting the toxins HC were preferred for enrichment. For BoNT/A, B, C, and F this could be facilitated (A2807, B488, C9, F1726) and consequently only minor sensitivity losses were observed in the Endopeptidase-ELISA when toxin enrichment was performed prior to the assay (Figure 25). Conversely, for BoNT/DC and E efficient enrichment was only achieved with antibodies recognizing the LC (D63) or the H_N (E136), both leading to a pronounced sensitivity loss in the assay (ibid.).

RESULTS

Table 27: Antibodies tested for toxin enrichment prior to the endopeptidase assay. Antibodies listed in this table were previously available in the laboratory and were not generated in this project. Data shown in this table (Specificity, Isotype, Affinity) were in part previously generated by other scientists in the laboratory [139, 140]. Antibodies depicted in bold were used for further experiments (unless otherwise specified).

Antibody	Species	Serotype	Domain	Isotype	Affinity [KD]	Bead-Western ^a	Endopep-Assay ^b
A1688	mouse (mAb)	BoNT/A	H _N	IgG1	3.4 nM	+	++
A185	mouse (mAb)	BoNT/A	H _C	IgG1	1.0 nM	++	+++
A778	mouse (mAb)	BoNT/A	H _C	IgG2a	1.1 nM	++	+++
A2807	mouse (mAb)	BoNT/A	H_C	IgG1	170 pM	+++	+++
B710	mouse (mAb)	BoNT/B	H _N	IgG2a	n.d.	+	+
B279	mouse (mAb)	BoNT/B	LC	IgG2a	1.7 nM	+++	+
B488	mouse (mAb)	BoNT/B	H_C	IgG2a	9 nM	+++	+++
C9	mouse (mAb)	BoNT/C	H_C	IgG2b	400 pM	n.t.	++
D63^c	mouse (mAb)	BoNT/D	LC	IgG2b	400 pM	n.t.	+
D967^d	mouse (mAb)	BoNT/D	H_C	IgG1	100 pM	n.t.	+++
E136	mouse (mAb)	BoNT/E	H_N	IgG2a	n.d.	+	+++
E1346	mouse (mAb)	BoNT/E	H _C	IgG1	n.d.	+	+
KE97	rabbit (pAb)	BoNT/E	poly	IgG	n.d.	n.t.	+
F757	mouse (mAb)	BoNT/F	H _C	IgG2b	3 nM	+	n.t.
F1726	mouse (mAb)	BoNT/F	H_C	IgG1	70 pM	+++	+++

^a Antibodies coupled to paramagnetic beads were used for enrichment of BoNT. Captured toxin was detected by western blotting with a biotinylated detection antibody and SA-POD. + = weak signal detectable; ++ = good signal detectable; +++ = very good signal detectable. Results of the Bead-Western are shown in Appendix Figure 4 A.

^b Antibodies coupled to paramagnetic beads were used for enrichment of BoNT prior to the Endopeptidase-ELISA or duplex-assay. + = weak signal detectable; ++ = good signal detectable; +++ = very good signal detectable. Results of the Endopeptidase-assays are shown in Appendix Figure 4 B.

^c D63 antibody was used for enrichment of BoNT/DC.

^d D967 antibody was used for enrichment of BoNT/D.

n.t. = not tested

RESULTS

5.3.1.3 Sensitive detection of BoNT/A-F from spiked serum samples with the Endopeptidase-ELISA

To test whether the Endopeptidase-ELISA combined with toxin enrichment via monoclonal antibodies prior to the assay is applicable for routine BoNT diagnostic, the detection of BoNT from a complex matrix was analysed. As the most common matrix in botulism diagnostics human serum was selected as test matrix.

To cover a broad range of concentrations, BoNT concentrations near the EC50 of the six titration curves (medium) as well as near the upper (high) and lower (low) regions were spiked into serum and BSA/PBS as control (compare Figure 23). Overall, no negative effect was observed for the detection of BoNT from spiked serum when compared to spiked BSA/PBS (Figure 25), indicating a negligible effect of matrix interferences from serum on the antibodies used for enrichment. Exceptionally for BoNT/E a clear decrease in sensitivity was observed in serum. Accordingly, when determining recovery rates from spiked serum compared to spiked BSA/PBS, a high recovery was achieved for all serotypes (76–143%), except for BoNT/E, when high or medium toxin concentrations were spiked (Table 28). For BoNT/A, C, and F even the lowest spiked toxin concentration (1, 2, and 6 pg/mL) could almost fully be recovered from spiked serum samples.

Thus, despite a slight sensitivity loss for some serotypes due to toxin enrichment, the Endopeptidase-ELISA still proved to be a useful and sensitive method for the detection of BoNT in a diagnostic setting.

RESULTS

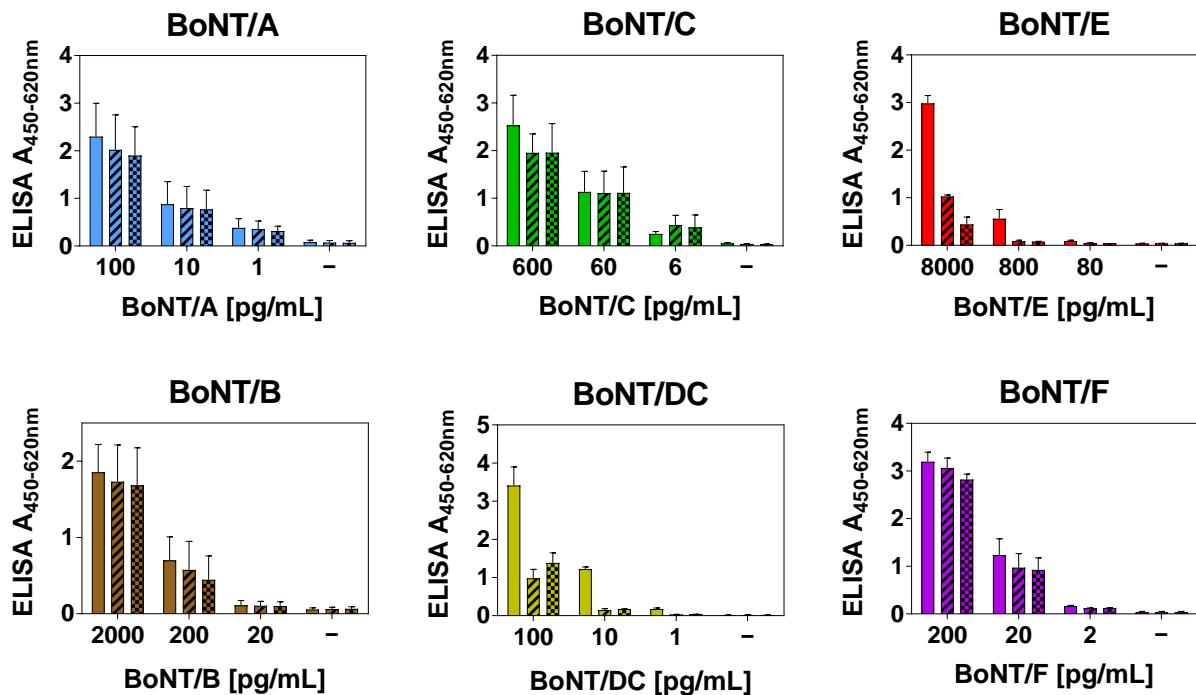


Figure 25: Detection of BoNT from buffer (BSA/PBS) and spiked serum samples after enrichment. Enrichment was performed by incubating toxin solutions (diluted in BSA/PBS or serum) with magnetic dynabeads coupled to different monoclonal BoNT specific antibodies as indicated in Table 27 (followed by several washing steps). Beads were diluted in cleavage buffer and directly used in the Endopeptidase-ELISA. To this end VAMP-2 or SNAP-25 was coated on microtiter plates, cleaved by incubation with enriched/diluted toxin samples and cleavage products were detected with Neo-mAbs. For samples requiring an enrichment step the starting volume was doubled. Plain bars = samples without enrichment (BoNT was directly diluted in cleavage buffer); transversely striped bars = samples with enrichment from buffer spiked with BoNT; squared bars = samples with enrichment from serum spiked with BoNT. Results from three (BoNT/A, BoNT/B, BoNT/C, BoNT/F) or two (BoNT/DC and BoNT/E) independent experiments, each performed in technical duplicate are shown ($n = 6$ or 4 ; Mean \pm SD).

Table 28: Recovery of BoNT from spiked serum samples in the Endopeptidase-ELISA. Recovery was calculated with the results from Figure 25.

Toxin	Low		Medium		High	
	pg/mL ^a	Recovery ^b	pg/mL ^a	Recovery ^b	pg/mL ^a	Recovery ^b
BoNT/A	1	92 \pm 13.4	10	99 \pm 13.0	100	95 \pm 11.2
BoNT/B	20	low signal ^c	200	76 \pm 9.0	2000	97 \pm 3.6
BoNT/C	6	85 \pm 20.7	60	98 \pm 9.6	600	99 \pm 17.2
BoNT/DC	1	low signal ^c	10	124 \pm 24.2	100	143 \pm 17.1
BoNT/E	80	low signal ^c	800	94 \pm 28.8	8000	43 \pm 13.7
BoNT/F	2	101 \pm 8.7	20	96 \pm 5.9	200	92 \pm 12.5

^a Spiked toxin concentrations.

^b Toxin recovery from spiked serum samples compared to spiked BSA/PBS as reference (100%) was calculated. Results from three (BoNT/A, BoNT/B, BoNT/C, BoNT/F) or two (BoNT/DC and BoNT/E) independent experiments, each performed in technical duplicate ($N = 6$ or 4 ; Mean \pm SD).

^c Signals were too low (\leq LOD) for toxin detection.

RESULTS

5.3.2 Development of a novel duplex-assay for the simultaneous detection of two distinct serotypes

In addition to straightforward and fast assay systems as the Endopeptidase-ELISA, approaches covering multiple serotypes from one sample are desired as sample volume is usually limited. By multiplexed detection systems, sample size and number can be drastically reduced saving time and experimental effort.

Therefore, an additional aim of the thesis was to develop a novel enzymatic multiplex suspension array, based on the Luminex™ platform, for functional BoNT detection as an animal replacement method. In an initial approach, Neo-mAbs were coupled to different fluorescently labelled magnetic luminex-bead regions to capture BoNT cleavage products from solution. However, due to an unexpected strong unspecific binding of VAMP-2 to luminex-beads only unsatisfactory sensitivities for BoNT detection were achieved by this approach. To circumvent the undesired interaction between VAMP-2 and luminex-beads, the assay set-up was turned upside down, thereby mimicking the principle of the Endopeptidase-ELISA. Instead of Neo-mAbs, full-length substrate molecules VAMP-2 and SNAP-25 were coupled to different regions of the luminex-beads in the novel approach.

The principle work-flow of the novel duplex-assay is illustrated in Figure 26. Briefly, substrate molecules VAMP-2 and SNAP-25 coupled to fluorescent luminex-beads are cleaved on beads by BoNT. Subsequently, the newly exposed neoepitopes can be detected by biotinylated Neo-mAbs and a fluorescent reporter molecule (SA-PE). Fluorescent signals of the luminex-bead region and the reporter molecule are finally analysed using a Bio-Plex® instrument. SA-PE signals originating from SNAP- or VAMP-coupled beads can be discriminated enabling the detection of one SNAP- and one VAMP-specific BoNT serotype simultaneously. Three duplex-assays for the detection of BoNT/A and B as most frequent serotypes, BoNT/C and D as serotypes causing animal botulism, and BoNT/E and F as rare serotypes, were developed. Detection of BoNT from complex matrices requires a toxin enrichment step prior to the assay, as described in section 5.3.1.2. Therefore, toxin enrichment with monoclonal anti-BoNT antibodies coupled to magnetic dynabeads was included in the novel duplex-assays. Since a loss in sensitivity was observed for BoNT/DC after enrichment with a LC specific antibody in the Endopeptidase-ELISA, recombinantly expressed BoNT/D (see Material and Method section

RESULTS

4.1.4) was used instead in these experiments. This allowed the usage of a H_c specific enrichment antibody (D967, see Table 27), avoiding sensitivity losses due to LC inhibition.

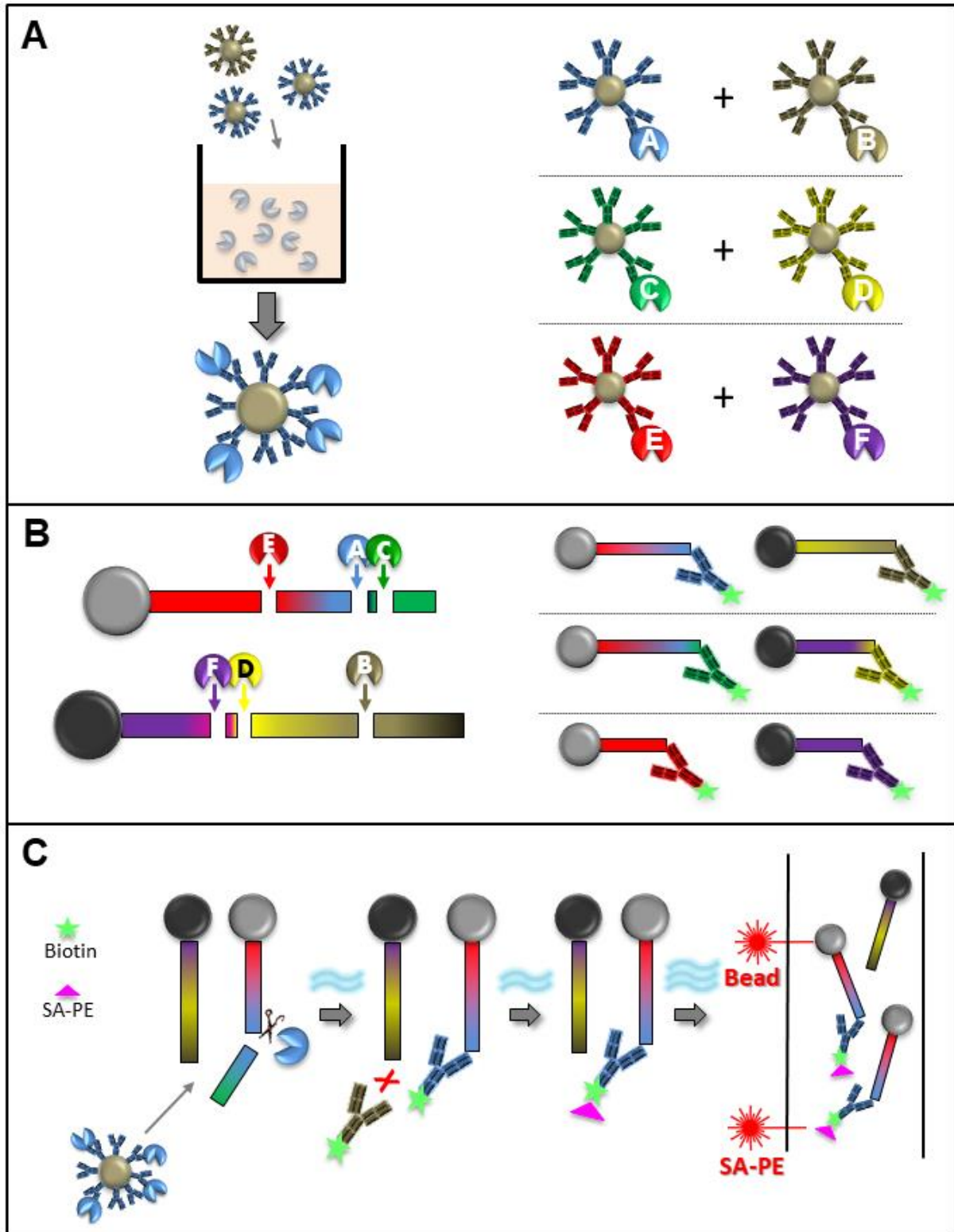


Figure 26: Schematic illustration of the duplex-assay working principle. (A) Paramagnetic dynabeads coupled to monoclonal anti-BoNT antibodies are added to toxin containing sample for toxin

RESULTS

capture. For the duplex-assay, dynabeads coupled with monoclonal anti-A and anti-B, anti-C and anti-D, or anti-E and anti-F antibodies are mixed to enable enrichment of two different serotypes in one sample. **(B)** SNAP-25 and VAMP-2 are coupled to different regions of luminex-beads. Different BoNT serotypes cleave SNAP-25 or VAMP-2 at distinct regions. The resulting serotype-specific neopeptides can be detected by Neo-mAbs. The differently coded luminex-beads for SNAP-25 and VAMP-2 allow for the simultaneous detection of one SNAP- and one VAMP-specific BoNT. **(C)** Work-flow of the duplex-assay: After enrichment, captured toxin is added to VAMP-2 and SNAP-25 coupled luminex-beads. Next, biotinylated Neo-mAbs detecting the specifically cleaved neopeptides are added and subsequently marked by a fluorescence reporter molecule (SA-PE). Finally, the respective luminex-bead region and the fluorescence intensity of the reporter molecule are analysed using the Bio-Plex[®] instrument.

5.3.2.1 Duplex-assay allows for highly sensitive detection of BoNT/A-F

Similar to the Endopep-ELISA, enrichment of BoNT prior to the assay led to a slight loss of assay sensitivity for some serotypes with the most pronounced effects observed for BoNT/A and C (Appendix Figure 5). As expected, the application of a H_C specific antibody avoided sensitivity losses after enrichment for BoNT/D. In all assays, measured signals were specific for the correct SNAP- or VAMP-specific serotype added – no crossreactivity between the two serotypes in one assay was observed.

To evaluate sensitivities and robustness of the three duplex-assays BoNT was titrated (Figure 27). The duplex-assay enabled highly sensitive detection of BoNT/A-F with detection limits in the low pg/mL range. For the most frequent serotypes BoNT/A and B detection limits of 0.8 pg/mL and 1.2 pg/mL were achieved corresponding to 0.211 LD₅₀/mL and 0.147 LD₅₀/mL (Table 29). For serotypes BoNT/C and D, both relevant in cases of animal botulism, LODs of 79.1 pg/mL (corresponding to 2.056 LD₅₀/mL) and 1.1 pg/mL were achieved (ibid.). The less frequent serotypes BoNT/E and F were detected with detection limits of 194 pg/mL and 0.3 pg/mL (corresponding to 0.005 LD₅₀/mL). For BoNT/E, which is a non-proteolytic BoNT thus requiring nicking of the enzymatic LC, activation by trypsin could increase assay sensitivity 15-fold to a detection limit of 13 pg/mL (corresponding to 0.84 LD₅₀/mL). Summing up, for all six serotypes, the duplex-assay achieved comparable or much higher sensitivities than the MBA.

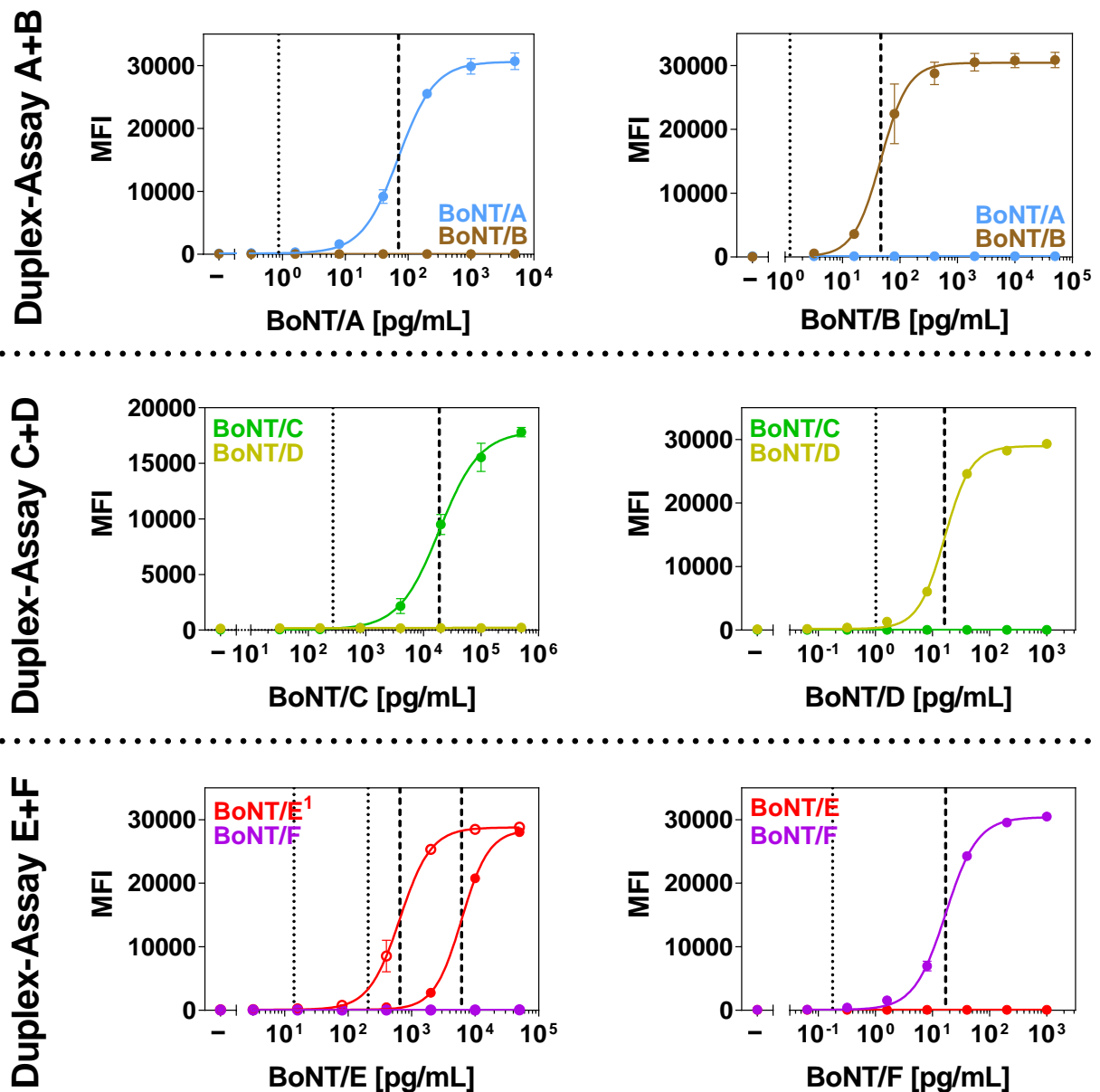


Figure 27: Detection of catalytically active BoNT by three duplex-assays. BoNT was diluted in BSA/PBS and enriched with monoclonal anti-BoNT antibodies (as indicated in Table 27) coupled to paramagnetic dynabeads. Captured toxin was mixed with VAMP-2 and SNAP-25 coupled to luminex-beads for substrate cleavage and cleavage products were subsequently detected by Neo-mAbs. Results from two independent experiments with each repeat performed in technical duplicates are shown ($n = 4$; Mean \pm SD; MFI = Median fluorescent intensity; ¹ open circles: trypsinated BoNT/E; closed circles: non-trypsinated BoNT/E). The dotted and dashed line indicates the LOD and EC50 respectively.

RESULTS

Table 29: Performance of the three different duplex-assays for the detection of catalytically active BoNT/A and B, C and D, or E and F. Results shown in this table were generated with the data depicted in Figure 27.

	<i>BoNT/A</i>	<i>BoNT/B</i>	<i>BoNT/C</i>	<i>BoNT/D</i>	<i>BoNT/E^c</i>	<i>BoNT/F</i>
EC50 [pg/mL]	70	47	18901	16	6108/654	17
LOD [pg/mL] ^a	0.8 (0.6–1.3)	1.2 (0.7–5.4)	79.1 (45–227)	1.1 (0.9–1.3)	194 (171 – 227) /13 (9.2–23.7)	0.3 (0.2–0.4)
LOD [LD50/mL] ^b	0.211	0.147	2.056	n.d. ^d	n.d. ^d /0.84	0.005

^a Cutoff: mean + 3.29 × SD of blank values (determined with 36 blank values for each serotype) including lower and upper limit of 95% confidence interval (shown in brackets).

^b LOD in LD50/mL according to toxin activity as specified by the manufacturer (see material and method section).

^c Non-trypsinated/trypsinated BoNT/E.

^d No data available on toxin activity.

5.3.2.2 Detection of BoNT from spiked serum samples

To validate the utility of the three duplex-assays for botulism diagnostics, detection of BoNT from spiked human serum samples was tested.

Table 30: Recovery of BoNT from spiked serum samples compared to spiked BSA/PBS by the three different duplex-assays. Results shown in this table were generated with the data depicted in Appendix Figure 6.

Toxin	Low		Medium		High	
	pg/mL ^a	Recovery ^b	pg/mL ^a	Recovery ^b	pg/mL ^a	Recovery ^b
BoNT/A	7	67 ± 20.6	70	85 ± 13.4	700	99 ± 1.8
BoNT/B	5	45 ± 4.3	50	50 ± 11.5	500	92 ± 1.7
BoNT/C	2000	156 ± 30.0	20000	100 ± 7.9	200000	98 ± 4
BoNT/D	2	89 ± 11.9	20	89 ± 7.1	200	98 ± 1.9
BoNT/E ^c	70	40 ± 5.0	700	34 ± 7.2	7000	96 ± 1.5
BoNT/F	2	83 ± 4.2	20	81 ± 7.0	200	99 ± 2.7

^a Spiked toxin concentrations.

^b Toxin recovery from spiked serum samples compared to spiked BSA/PBS as reference (100%) was calculated. Results from two independent experiments, each performed in technical duplicates (n = 4; Mean ± SD).

^c Trypsin-activated BoNT/E was used.

Akin to the Endopeptidase-ELISA, toxin concentrations near the EC50 (medium), and upper (high) and lower (low) region of the titrations curves were spiked and recovery from spiked

RESULTS

serum compared to spiked BSA/PBS was determined (Table 30, Appendix Figure 6). For most serotypes, no negative impact for detection from serum compared to BSA/PBS was observed, resulting in almost full recovery (67%–156%) for all toxin concentrations spiked. The only exceptions from this were BoNT/B and E, where recovery rates were considerably lower when medium or low toxin concentrations were spiked (34%–50%). Still, even the lowest spiked toxin concentration could reliably be detected from serum samples for all serotypes.

5.3.2.3 Interlaboratory comparison of the BoNT/A + BoNT/B duplex-assay demonstrates robustness and transferability of the assay

To test whether the newly developed duplex-assays are applicable for routine botulism diagnostics, an interlaboratory comparison was organised. Two key issues were addressed in the comparison: First, it should be tested whether the duplex-assay could be performed by other laboratories equipped with a Bio-Plex® instrument, devoid of intensive experience with the assay protocol. Second, the robustness of the assay across different experimenters, instrumentation, and laboratories was evaluated.

To that aim, reagents and protocols for the duplex-assay for the detection of BoNT/A and B were exchanged between the RKI and Spiez Laboratory (Federal Office for Civil Protection, Spiez Laboratory, Switzerland, URL: <https://www.labor-spiez.ch/en/index.htm>). Experiments conducted in both laboratories for comparison included titration curves for BoNT/A and B as well as the detection of BoNT from spiked serum samples (as described in the previous section 5.3.2.2). Notably, the exact same batches of all reagents (except for washing buffer) were used in both laboratories.

Here, titration curves for BoNT/A and B obtained in the two laboratories agreed almost perfectly (Figure 28, A). Likewise, the serum spike experiments achieved very good agreement between the results of the different laboratories (Figure 28, B). These results demonstrated that the duplex-assay was highly robust and could easily be transferred to other laboratories, both important features for the later exploitation of the assay in routine laboratories.

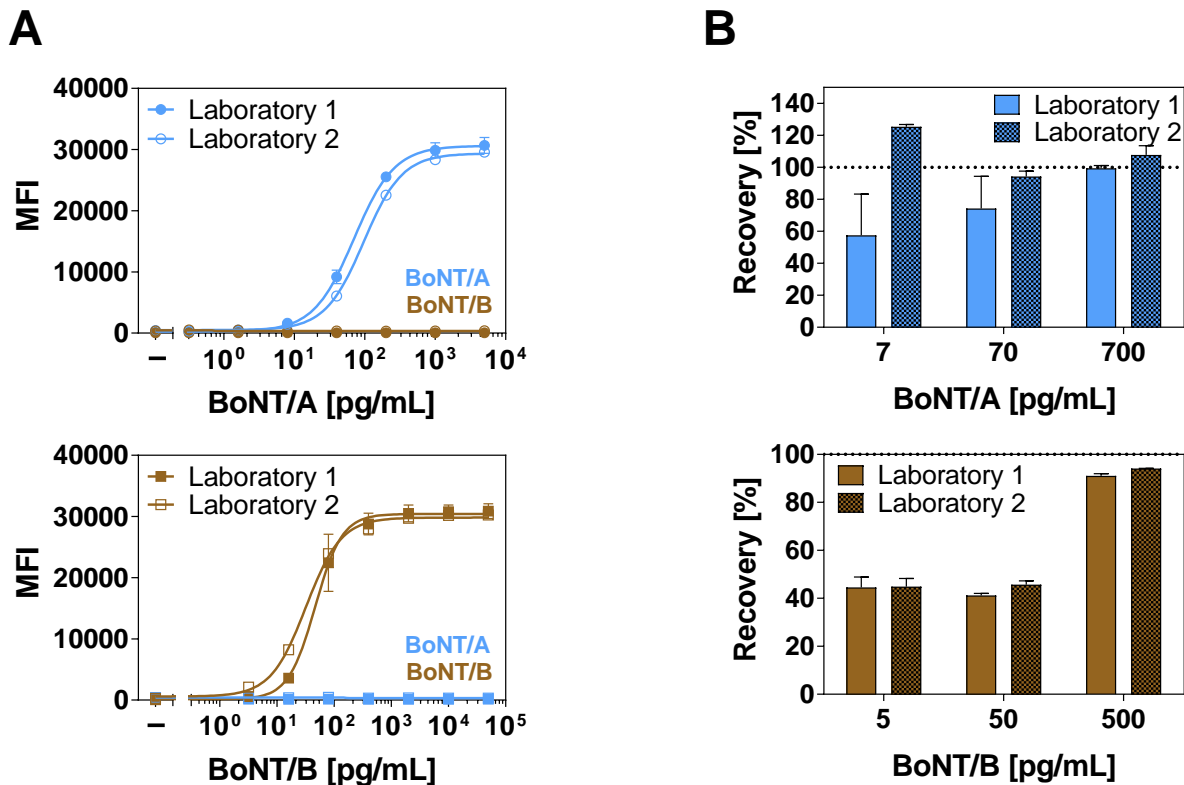


Figure 28: Comparison of results obtained in the duplex-assay with BoNT/A and B in two different laboratories. BoNT was diluted in BSA/PBS or serum and captured via paramagnetic dynabeads coupled to anti-BoNT antibodies. VAMP-2 and SNAP-25 coupled to luminex-baeds were added to captured toxin for substrate cleavage and cleavage products were detected by Neo-mAbs. **(A)** BoNT diluted in BSA/PBS was titrated. **(B)** Toxin recovery of spiked serum samples compared to spiked BSA/PBS as reference (100%) was determined (Laboratory 1: n = 4; Mean \pm SD; Laboratory 2: n = 2; Mean \pm SD).

5.4 Implementation of receptor binding in the duplex-assay for the detection of BoNT/A and B

As addressed earlier (section 5.3.1.2), for the detection of BoNT from complex matrices in enzymatic assays, a toxin enrichment step prior to detection is indispensable as matrix components perturb the assay. In the previous presented assay formats, this was facilitated by toxin enrichment via monoclonal anti-BoNT antibodies coupled to magnetic dynabeads. In doing so, effective toxin enrichment with limited sensitivity losses as well as successful subsequent detection from complex matrices such as serum was achieved. However, using monoclonal antibodies for enrichment also has disadvantages: Due to the large variability among different BoNT subtypes (up to 36% on amino acid level), usage of monoclonal antibodies for enrichment bears the risk of obtaining false negative results, if certain subtypes

RESULTS

are not recognized. Additionally, as exemplified in section 5.4.2, gaining knowledge on subtype recognition of anti-BoNT antibodies is, due to the limited availability of suitable reagents for testing, very complex.

To circumvent this issue, a different enrichment strategy was aspired. Instead of using monoclonal antibodies, enrichment was sought to be performed by the endogenous receptor molecules of the toxins. Besides covering all potentially disease-causing subtypes, this strategy has the advantage of including another crucial functional step of BoNTs mode of action in the assay – the receptor-binding. As a proof of principle, the enrichment by endogenous receptor molecules of the clinically most relevant serotypes A and B was addressed in this thesis and implemented in a novel combined duplex-assay.

5.4.1 Optimized receptor constructs for the enrichment of BoNT/A and B

The interaction of BoNT with its related receptor is based on a double receptor binding mechanisms, involving a proteinaceous receptor in form of synaptic vesicle proteins as well as a ganglioside receptor, both located at the intraluminal region of synaptic membranes. For serotypes A and E it has also been demonstrated that specific glycosylations are crucial for BoNT binding [52, 56, 71, 72].

The design, expression, and testing of BoNT/A and B receptor structures has been performed in the FuMiBoNT project (see section 3.4) in parallel to this work by the collaboration partners from MHH (Dr. A. Rummel, Dr. S. Mahrhold, and Dr. J. Weisemann) and Dr. D. Stern from RKI and the described optimized receptor structures have been implemented in the duplex-assay.

The protein receptor for BoNT/A is synaptic vesicle glycoprotein 2 (SV2). Previous works demonstrated that isoform C and glycosylation at residue N559 increases affinity towards BoNT/A [71, 72]. Thus, to capture BoNT/A, glycosylated human SV2C (gSV2C) was employed (Figure 29, A). Expression of gSV2C was performed in mammalian cells with the protein fused to the Fc part of human IgG antibody for secretion.

The protein receptor for BoNT/B is synaptotagmin II (Syt-II). It has been demonstrated that an Arginine (R) to Lysine (K) mutation at position 51 increases affinity towards BoNT/B [54]. Further increases in affinity can be achieved by additional binding to the ganglioside GT1b [52, 56]. Thus, for BoNT/B capture, Syt-II K51R and GT1b incorporated into phospholipid-bilayer-nanodiscs (NDs) was employed (Figure 29, B). NDs constitute a patch of lipid bilayer stabilized

RESULTS

by a membrane scaffold protein (MSP) which wraps around the lipid membrane, thereby forming a disc-shaped structure. To create Syt-II + GT1b-NDs, Syt-II can be incorporated into NDs through its transmembrane domain, whereas GT1b can bind to lipids through its ceramide moiety. By using these dual-Syt-II-NDs the the dual-receptor binding mechanism of BoNT/B could be mimicked.

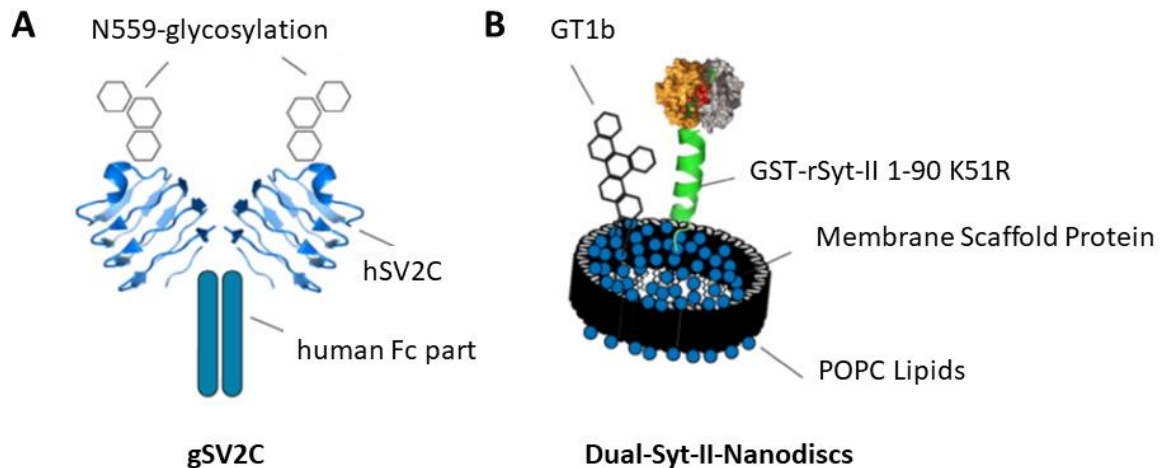


Figure 29: Optimized receptor molecules used for capture of BoNT/A and B. (A) For capture of BoNT/A glycosylated human SV2C fused to human Fc part was employed. hSV2C was glycosylated at position N559. Another disturbing glycosylation at position N565 was removed by introducing a N565Q mutation. (B) For BoNT/B capture, dual-Syt-II-Nanodiscs, mimicking the dual receptor binding mechanism of BoNT/B, were employed. GST tagged rat Syt-II (GST-rSyt-II) was mutated at position 51 (K51R), as this increased affinity towards BoNT/B. Images were designed and kindly provided by Dr. Daniel Stern, RKI.

5.4.2 Sensitive detection of BoNT/A and B in a combined duplex-assay covering receptor binding and enzymatic activity

Optimized receptor constructs were employed to establish a novel combined duplex-assay covering both receptor binding and enzymatic activity. Akin to monoclonal antibodies, gSV2C (Figure 29, A) and dual-Syt-II-NDs (Figure 29, B) were coupled to magnetic dynabeads for enrichment of BoNT/A and B, respectively. As specificity control, an irrelevant antibody or empty NDs were coupled to dynabeads. Here, no signals were detected, demonstrating the specific enrichment of BoNT/A and B by their receptors (Appendix Figure 8).

To evaluate assay sensitivity of the combined duplex-assay combining receptor enrichment with enzymatic activity, toxin was titrated (Figure 30). Here, detection limits of 5.1 pg/mL (corresponding to 1.34 LD₅₀/mL) for BoNT/A and 2.9 pg/mL (corresponding to 0.35 LD₅₀/mL)

RESULTS

for BoNT/B were achieved. Compared to the duplex-assay with antibody enrichment a 6-fold reduction in assay sensitivity was observed for BoNT/A (Table 29 and Table 31). As the receptor gSV2C exhibited a less stable binding towards the H_c of BoNT/A1 than the enrichment antibody A2807 (see Figure 33), a loss in sensitivity was expected. For BoNT/B, a similar sensitivity as in the duplex-assay with antibody enrichment was achieved, demonstrating the high affinity enrichment of BoNT/B by dual-Syt-II-NDs. In summary, despite slight sensitivity losses when compared to antibody enrichment, the combined duplex-assay covering receptor binding and enzymatic activity enabled highly sensitive detection of BoNT/A and B with detection limits in the low pg/mL range which are in the same range as the MBA.

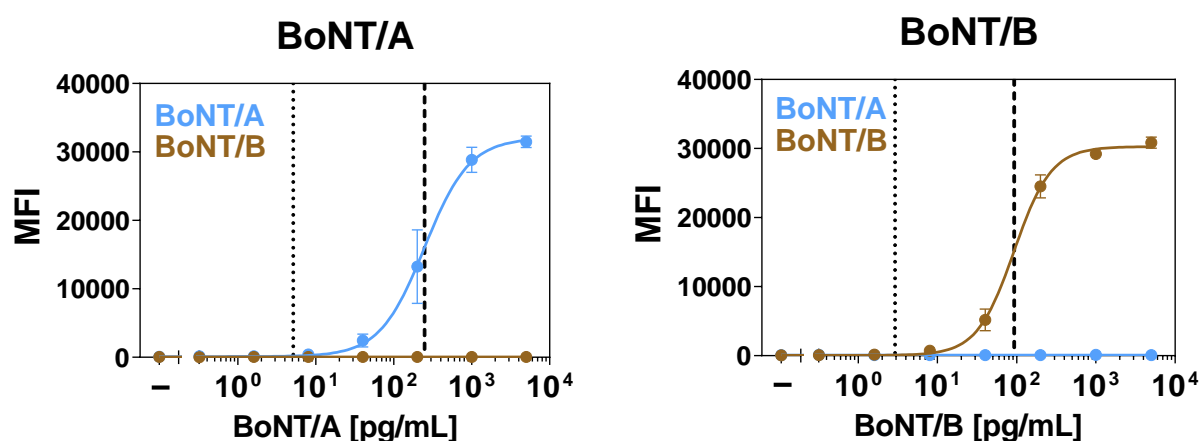


Figure 30: Detection of catalytically active BoNT with previous enrichment via endogenous receptors in the duplex-assay. BoNT was diluted in BSA/PBS and enriched with gSV2C and dual-Syt-II NDs coupled to paramagnetic dynabeads. Captured toxin was mixed with VAMP-2 and SNAP-25 coupled to luminex-beads for substrate cleavage and cleavage products were subsequently detected by Neo-mAbs. Results from three independent experiments with each repeat performed in technical duplicates are shown ($n = 6$; Mean \pm SD; MFI = Median fluorescent intensity). The dotted and dashed lines indicate the LOD and EC₅₀, respectively.

Table 31: Performance of the combined duplex-assay for the detection of functional BoNT/A and B with previous enrichment via endogenous receptor molecules. Results in this table were generated with the data shown in Figure 30.

	BoNT/A	BoNT/B
EC ₅₀ [pg/mL]	249	93
LOD [pg/mL] ^a	5.1 (2.7–19)	2.9 (2.3–4.2)
LOD [LD ₅₀ /mL] ^b	1.34	0.35

^a Cutoff: mean + 3.29 \times SD of blank values (determined with 40 blank values for BoNT/A and 60 blank values for BoNT/B) including lower and upper limit of 95% confidence interval (shown in brackets).

^b LOD in LD₅₀/mL according to toxin activity as specified by the manufacturer (see material and method section).

RESULTS

5.4.2.1 Detection of BoNT/A and B from different sample matrices with the combined duplex-assay (receptor enrichment + enzymatic activity)

To test whether receptor molecules can be used for toxin enrichment from complex matrices, different “typical” sample matrices were tested in the combined duplex-assay. As the most common patient matrix, serum was tested. In addition, food matrices often associated with botulism were applied: fish, sausage, and beans.

All food matrices were dissolved in peptone water, homogenized using a bagmixer, and centrifuged to remove non-soluble particles prior to enrichment. Analogous to previous experiments with spiked serum samples, toxin concentrations near the EC50 (medium), and upper (high) and lower (low) region of the titration curves were spiked and recovery from spiked matrix compared to spiked BSA/PBS was determined. Interestingly, recovery of BoNT/A and B from the different sample matrices varied (Figure 31, Table 32). Good recovery of BoNT/A in medium toxin concentrations could be achieved from fish and beans (> 68%), whereas recovery from serum and sausage was less efficient (< 37%).

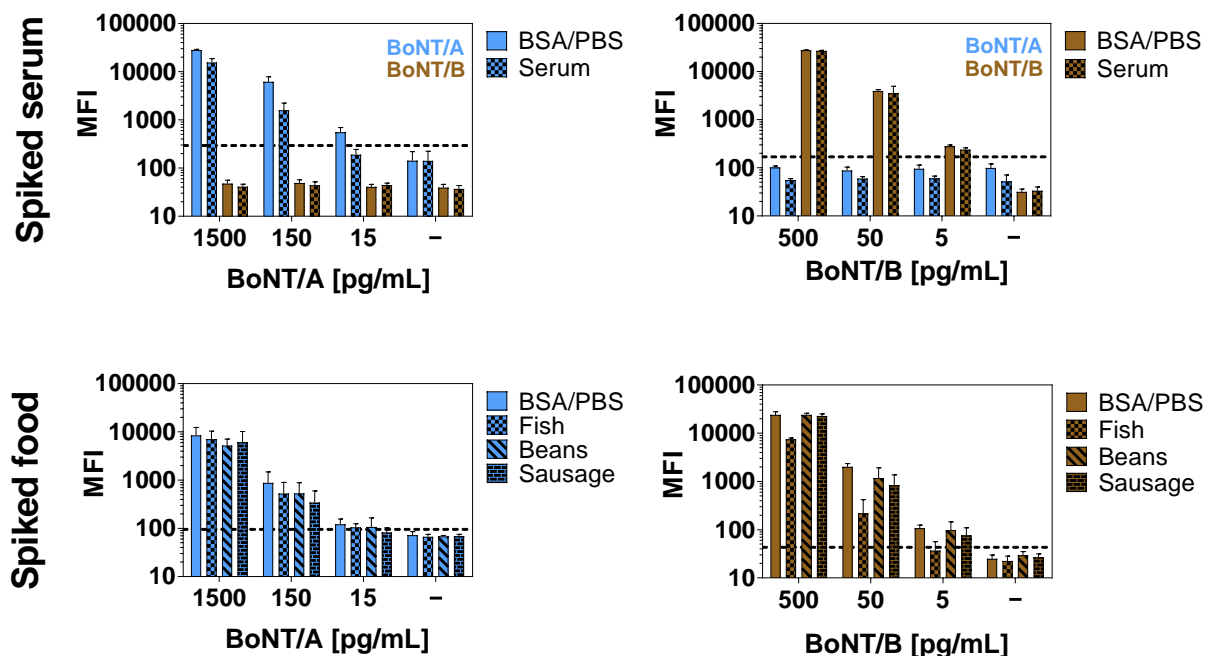


Figure 31. Detection of BoNT/A and B from different sample matrices with the combined duplex assay with previous receptor based toxin enrichment. BoNT/A or B was diluted in BSA/PBS or different sample matrices and enriched with receptor molecules coupled to magnetic dynabeads. Toxin concentrations as indicated were spiked. Captured toxin was mixed with VAMP-2 and SNAP-25 coupled to luminex-beads for substrate cleavage and cleavage products were subsequently detected by Neo-

RESULTS

mAbs. The black dashed line indicates the respective LOD. Results from two independent experiments with each repeat performed in technical duplicates are shown ($n = 4$; Mean \pm SD; MFI = Median fluorescent intensity).

Table 32: Recovery of BoNT/A and B from different sample matrices compared to spiked BSA/PBS by the combined duplex-assay with previous receptor based enrichment. Results shown in this table were generated with the data from Figure 31.

Matrix	Toxin	Low		Medium		High	
		pg/mL ^a	Recovery ^b	pg/mL ^a	Recovery ^b	pg/mL ^a	Recovery ^b
Serum	BoNT/A	15	low signal ^c	150	26 \pm 9.5	1500	55 \pm 11.2
Fish	BoNT/A	15	73 \pm 17.1	150	68 \pm 24.8	1500	84 \pm 22.5
Sausage	BoNT/A	15	low signal ^c	150	37 \pm 13.8	1500	67 \pm 23.5
Beans	BoNT/A	15	low signal ^c	150	74 \pm 38.4	1500	64 \pm 18.3
Serum	BoNT/B	5	83 \pm 6.9	50	90 \pm 33.2	500	97 \pm 2.3
Fish	BoNT/B	5	low signal ^c	50	10 \pm 8.4	500	32 \pm 7.6
Sausage	BoNT/B	5	71 \pm 27.7	50	39 \pm 20	500	97 \pm 16.7
Beans	BoNT/B	5	91 \pm 46.9	50	55 \pm 29	500	101 \pm 9.7

^a Spiked toxin concentrations.

^b Toxin recovery from spiked serum samples compared to spiked BSA/PBS as reference (100%) was calculated. Results from two independent experiments, each performed in technical duplicates ($n = 4$; Mean \pm SD).

^c Signals were too low (\leq LOD) for toxin detection.

Detection of BoNT/B from spiked serum, beans, and sausage was efficient with high toxin recovery (55%–101%). Even BoNT/B concentrations as little as 5 pg/mL were detectable in these matrices. As exception, only in fish pronounced sensitivity losses were observed with recovery rates below 32%.

For comparison, toxin was also enriched with monoclonal anti-BoNT antibodies from the different sample matrices. Generally, a better recovery for BoNT/A and a reduced recovery for BoNT/B was observed when compared to receptor-based enrichment (Figure 32). Notably, differences were more pronounced for BoNT/A. Here, considerably higher recovery rates were achieved with antibody-based enrichment in all matrices tested (e.g. at high toxin concentrations 95%–100% recovery with antibody-based enrichment compared to 55%–84% recovery with receptor-based enrichment) and even the lowest spiked toxin concentration could be recovered from all matrices tested.

RESULTS

In summary, the exemplarily tested sample matrices lead to reduced assay sensitivity, thereby lowering the detection limits. Still, medium toxin concentration could be detected in all matrices tested and even the lowest spiked toxin concentration (near the LOD in buffer) was detectable in some cases. Together, this demonstrates the suitability of the duplex-assay with either antibody- or receptor-based enrichment for botulism diagnostics.

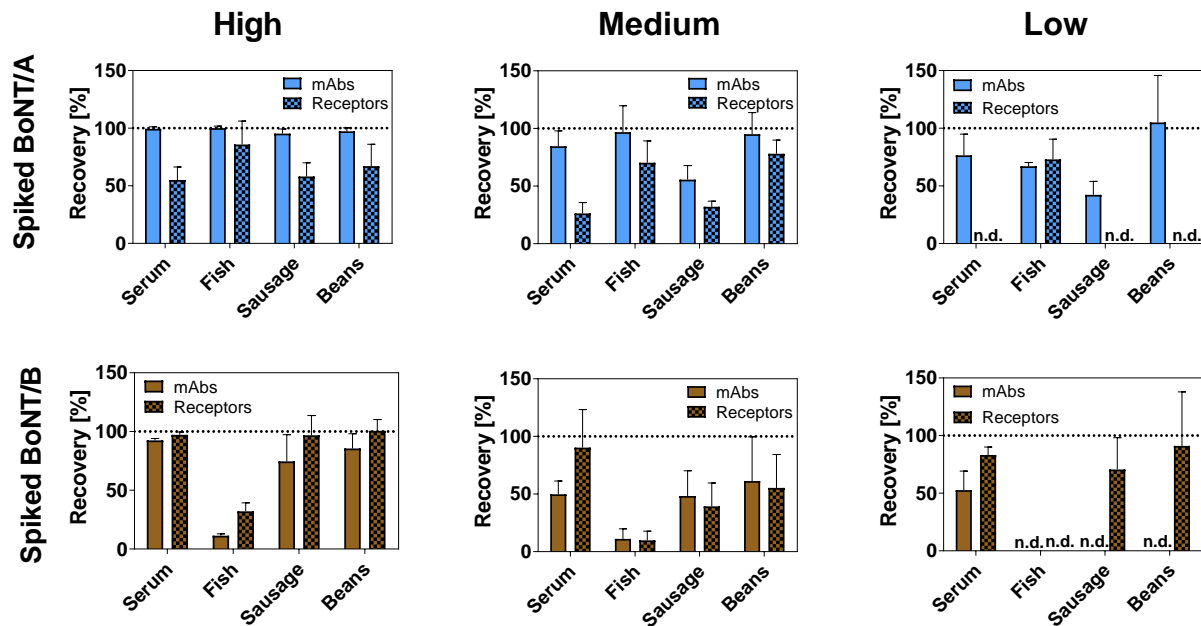


Figure 32: Comparison of antibody-based and receptor-based enrichment in the duplex-assay with different sample matrices. BoNT/A or B was diluted in BSA/PBS or different sample matrices and enriched with antibodies (plain bars) or receptor molecules (chequered bars) coupled to magnetic dynabeads. Toxin concentrations near the EC50 (Medium: 150 pg/mL BoNT/A and 50 pg/mL BoNT/B) the upper (High: 1500 pg/mL BoNT/A and 500 pg/mL BoNT/B) and lower (Low: 15 pg/mL BoNT/A and 5 pg/mL BoNT/B) area of the titration curve were spiked. Captured toxin was mixed with VAMP-2 and SNAP-25 coupled to luminex-beads for substrate cleavage and cleavage products were subsequently detected by Neo-mAbs. Toxin recovery from the different matrices compared to BSA/PBS (set to 100%, highlighted by the black dotted line) was calculated. Results from two independent experiments with each repeat performed in technical duplicates are shown ($n = 4$; Mean \pm SD; n.d. = not detectable, signals were below the LOD).

5.4.3 Subtype recognition of receptor molecules and monoclonal antibodies varies

Toxin enrichment through their endogenous receptors clearly represents an “advanced approach” when compared to the usage of anti-BoNT antibodies, as it reflects the native receptor binding and should be able to display all clinically relevant and functionally active subtypes. For efficient enrichment of BoNT in diagnostics assays, high affinity binding as well as the recognition of all known (and yet unknown) subtypes is crucial. Hence, to test whether receptor binding is advantageous to antibodies regarding high affinity binding and subtype

RESULTS

recognition, the binding of both, optimized receptor molecules as well as anti-BoNT antibodies to recombinant H_C-fragments of all available BoNT/A and B subtypes was analysed by SPR measurements. To that aim, isolated optimized receptor molecules gSV2C or Syt-II (not incorporated into NDs), or enrichment antibodies A2807 or B488 were immobilized on a SPR chip and H_C-fragments were injected in solution.

Generally, both enrichment antibodies (A2807 and B488) build a more stable interaction with the H_C-fragments than the corresponding receptor molecule (gSV2C or Syt-II). As expected, binding of antibodies to the H_C-fragments of different subtypes varied. Antibody A2807, used for enrichment of BoNT/A, recognized all subtypes tested here, albeit with different affinities (Figure 33, A). Contrary, antibody B488, used for BoNT/B enrichment, did not bind to the H_Cs of subtypes B2 and B7, and exhibited clearly reduced affinity towards subtype B_y when compared to the other subtypes tested (Figure 33, B). Interestingly, also binding of receptor molecules to different subtypes varied. For example, gSV2C exhibited only weak binding to the H_C of A4 and showed reduced binding to A2 and A6. Similarly, Syt-II only weakly bound B2, whereas other subtypes were bound with much higher affinities (Figure 33).

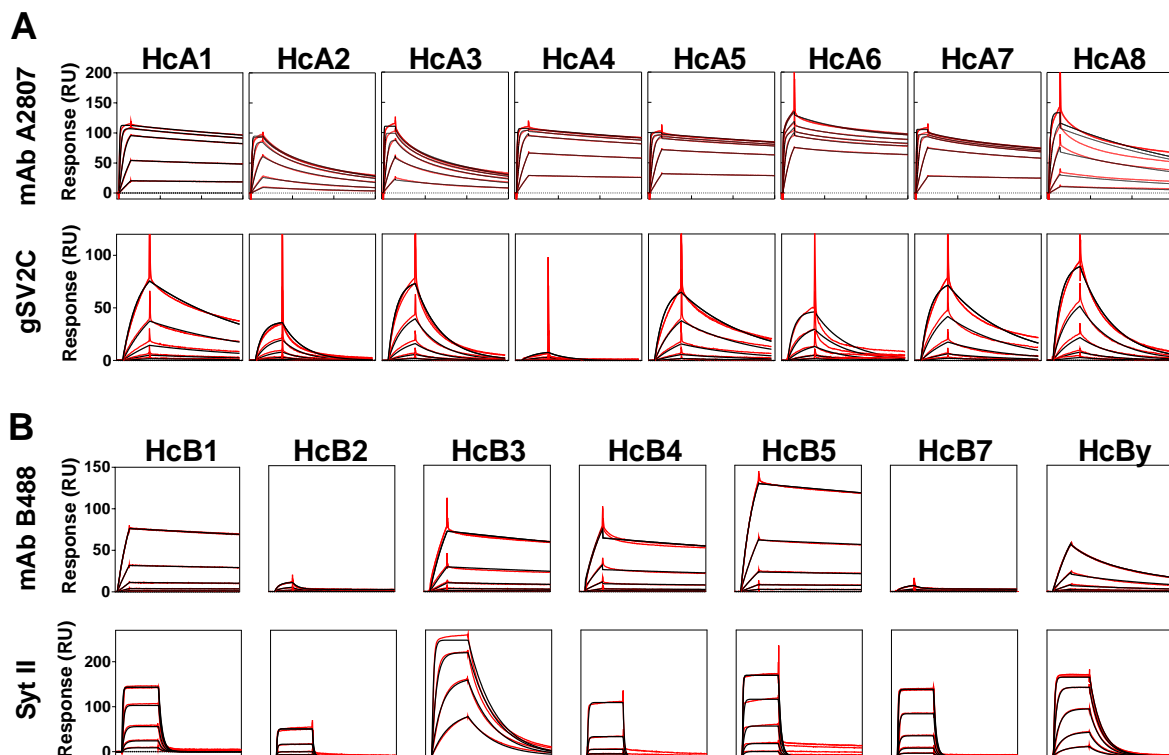


Figure 33: SPR measurements with monoclonal anti-BoNT antibodies A2807 and B488 and BoNT receptor molecules gSV2C and Syt-II to evaluate binding to H_C-fragments of different BoNT/A

RESULTS

and B subtypes. Antibodies or receptor molecules were immobilized on a sensor chip and serial dilutions of recombinant H_C-fragments, corresponding to different BoNT/A or B subtypes, were injected (red lines = measured RUs, x-axis = 600 s). Data was fitted using the 1:1 Langmuir binding model (black lines = fit). Data shown in this figure was generated and kindly provided by Dr. Daniel Stern, RKI.

Taken together, these data demonstrate that both antibodies as well as receptor molecules bind different BoNT subtypes with different strengths. Hence, even the usage of receptor molecules for toxin enrichment cannot ensure that all potential subtypes of one serotype would be detected. However, BoNT subtypes that are not or only weakly recognized by the endogenous receptor presumably are less toxic and are therefore irrelevant in diagnostic assays.

5.4.3.1 Detection of BoNT from Clostridia supernatants with antibody- and receptor-based enrichment

SPR measurements with recombinant H_C-fragments revealed that subtype recognition of anti-BoNT antibodies and receptor molecules varies (section 5.4.2). To further verify these results, *Clostridia* supernatants of different BoNT/A and B subtypes that were available in the laboratory were tested in the duplex-assay with antibody enrichment as well as the combined duplex-assay with receptor enrichment and the approximate toxin concentration in each supernatant was determined. To that aim, well-characterized recombinant BoNT/A1 and BoNT/B1 were used as reference. Notably, it is not possible to determine the precise toxin concentration of different subtypes with the duplex-assay for two reasons: First, receptor or antibody binding as well as cleavage efficiency of different subtypes considerably varies (Appendix Figure 9). Second, toxin standards for different subtypes are not available. Thus, the duplex-assay is intended for qualitative toxin detection and presumably does not allow for precise quantification.

In agreement with the broad subtype-recognition of the monoclonal antibody and receptor molecule, all tested BoNT/A supernatants were detected in the duplex-assay with both antibody- and receptor-based enrichment (Figure 34 and Appendix Figure 7). When the same supernatant dilutions were tested, signals with antibody-based enrichment were much higher compared to enrichment with receptor molecules (Figure 34). This can be explained by the generally lower assay sensitivity after enrichment with receptor molecules (compare Table 29 and Table 31). A remarkable difference in signal intensity was observed for A2 and A5 supernatants, indicating that enrichment with antibodies is much more efficient than with

RESULTS

receptor molecules for these subtypes. This is partly in agreement with the results of the SPR measurements which also exhibited reduced binding of gSV2C to H_C-A2 (Figure 33).

Except for B7, all BoNT/B subtypes were detected by the duplex-assay with receptor- or antibody-based enrichment (Figure 34). Considerable differences in signal intensity were observed for B2 and B_y, with better recognition by the receptor molecule confirming the SPR results. Conversely, B3 seemed to be better recognized by the antibody, as higher signals were achieved here. The low signals obtained for B7 in both approaches is most likely due to a lack of toxin in this supernatant.

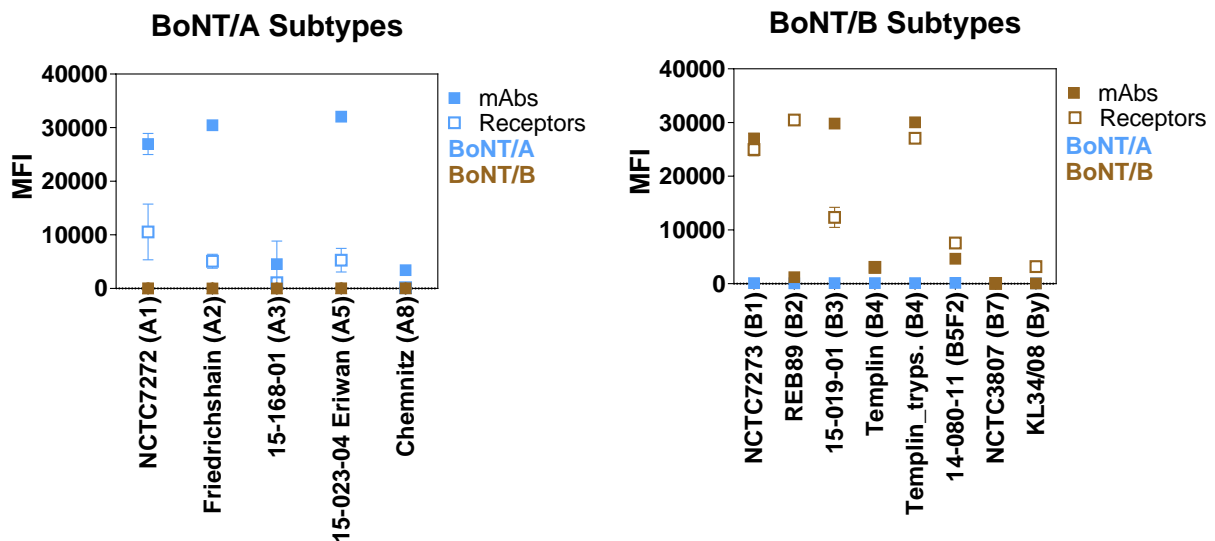


Figure 34: Testing of *Clostridia* supernatants of different BoNT/A and B subtypes in the duplex-assay with antibody-based enrichment (filled squares) or receptor-based enrichment (open squares) prior to the assay. *Clostridia* supernatants were diluted in BSA/PBS and enriched with anti-BoNT antibodies A2807 and B488 or receptor molecules gSV2C and dual-Syt-II-NDs coupled to paramagnetic dynabeads. To allow for comparison of enrichment strategy, the same dilution was applied for antibody- and receptor-based enrichment in each supernatant. Captured toxin was mixed with SNAP-25 and VAMP-2 coupled luminex-beads for substrate cleavage. Cleavage products were subsequently detected with biotinylated Neo-mAbs. Results from two independent experiments with each repeat performed in technical duplicates are shown (n = 4; Mean ± SD; MFI = Median fluorescent intensity).

For determination of the approximate toxin concentration using both arrays, dilutions of supernatants were adjusted to achieve signals in the linear range of the standard curve (see Appendix Figure 7 and Appendix Table 11). Toxin concentrations were determined by interpolation of signals to a standard curve of BoNT/A1 or BoNT/B1 as reference. Generally, for most supernatants, toxin concentrations in a similar concentration range were determined in both assays (Table 33). Exceptions from this are supernatants that exhibited strong

RESULTS

variations in antibody or receptor recognition. Here, the more efficient enrichment strategy yielded much higher concentrations (A2, A5, B2, and B3). However, as mentioned above the determined toxin concentrations with these assays are considered as estimates since reference material for all subtypes is lacking. Nevertheless, these results demonstrate that the duplex-assay with either antibody-based or receptor-based enrichment is suitable to detect a variety of different BoNT subtypes from a complex sample matrix such as bacterial supernatants. Depending on subtype recognition, sensitivity of the duplex-assays with the different enrichment approaches varies and therefore has to be determined individually for each subtype. This underlines the complexity of BoNT quantification in assays displaying one or more functional steps of BoNT action.

Table 33: Determination of toxin concentration in different *Clostridia* supernatants. For determination of toxin concentration different dilutions of *Clostridia* supernatants were tested in the duplex-assay with enrichment by monoclonal anti-BoNT antibodies or receptor molecules. Toxin concentrations were determined by interpolation to a standard curve of BoNT/A1 or BoNT/B1, respectively. MFI values between 1000 and 30000 were considered for calculations. Data shown in this table were generated with the results from Appendix Figure 7 and Appendix Table 11.

	Enrichment with mAbs	Enrichment with receptors
NCTC7272 (A1)	3 µg/mL	1.6 µg/mL
Friedrichshain (A2)	11 µg/mL	588 ng/mL
15-168-01 (A3)	348 ng/mL	147 ng/mL
15-023-04 Eriwan (A5)	> 51 µg/mL	305 ng/mL
Chemnitz (A8)	14 ng/mL	2 ng/mL
NCTC7273 (B1)	15 µg/mL	9 µg/mL
REB89 (B2)	8 ng/mL	2.6 µg/mL
15-019-01 (B3)	138 µg/mL	17 µg/mL
Templin (B4)	43 ng/mL	40 ng/mL
Templin_tryps (B4) ^a	129 µg/mL	52 µg/mL
14-080-11 (B5F2) ^b	7 ng/mL	27 ng/mL
NCTC3807 (B7)	< 0.5 ng/mL	< 0.4 ng/mL
KL34/08 (By)	< 0.5 ng/mL	10 ng/mL

^a The supernatant was trypsinated prior to enrichment.

^b The concentration of BoNT/B is indicated here. The BoNT/F concentration in the supernatant was not determined.

6 DISCUSSION

BoNTs are the most toxic substances known and cause the rare but potentially life-threatening disease botulism. Diagnostics of botulism is highly challenging as minute amounts of different BoNT variants (40 different sero- and subtypes) must be detected reliably from a variety of sample matrices. At the moment, the gold standard method for diagnostics of suspect cases of botulism is the ethically controversial MBA, which has several drawbacks as being time-consuming, requiring trained staff and animal facilities, and inducing pain and distress in mice. The investigation of a functional *in vitro* replacement assay to the MBA was addressed in this thesis. To that aim, optimized cleavage conditions for each BoNT serotype were determined by a statistical DoE approach, to achieve maximum sensitivity in a cleavage-based assay. In addition, Neo-mAbs detecting the exact cleavage sites of different BoNT serotypes on their target SNARE proteins were generated and thoroughly characterised. Both Neo-mAbs and optimal cleavage conditions were employed to develop two highly sensitive assay formats detecting enzymatically active BoNT/A-F: An Endopeptidase-ELISA performed in a 96-well-format and a newly developed enzymatic multiplex Luminex-assay. Furthermore, for the most frequent serotypes BoNT/A and B, a novel approach combining enzymatic activity and receptor binding was developed thereby displaying two major steps of BoNT intoxication *in vitro*. All assays enabled highly sensitive detection with detection limits in the low pg/mL range from buffer as well as complex matrices such as serum, food, or bacteria supernatants.

6.1 Design of optimized buffer conditions for BoNT/A-F employing statistical DoE

To develop highly sensitive enzymatic assays for BoNT detection, an efficient substrate cleavage is crucial. In that sense, the usage of optimal cleavage conditions for the different BoNT serotypes has major implications on the achievable sensitivity in cleavage-based assays.

For the analysis of optimal cleavage conditions for BoNT/A-F, a statistical approach – the Taguchi DoE method – was employed. Thereby, multiple factors could be analysed in a comparably short time frame. Due to its beneficial impact over full-factorial experiments, the Taguchi DoE method has been widely used in the engineering and manufacturing industry for process optimization. Only few applications in the biomedical field are published so far which include, for example, the optimization of protein expression or assay development [161-164].

DISCUSSION

Here, optimal buffer conditions as well as important and negligible factors for BoNT/A-F substrate cleavage were identified by the Taguchi DoE method. Furthermore, a consensus buffer for efficient substrate cleavage of BoNT/A-F was designed.

The improved substrate cleavage in the optimized buffers when compared to reference buffers as well as the agreement of factor effects with previously published data (see section 6.1.1) illustrates the effectiveness of the Taguchi DoE method and validates the obtained results. Both reference buffers have already been optimized for cleavage of SNAP-25 by BoNT/A and E [110] or BoNT/A, B, and F [101] and a substantial improvement of substrate cleavage for these serotypes was unlikely. It is therefore unexpected that further improvements for BoNT/B and F substrate cleavage could be achieved with the optimized buffer. The greatest increase in cleavage efficiency was achieved for BoNT/C, which at the same time was found to differ most from other serotypes regarding preferred cleavage conditions. Interestingly, *Clostridia* producing BoNT/C and DC (and CD and D), both pathogenic to animals, build an individual clade in a genetic dendrogram which is clearly separated from *Clostridia* that produce BoNTs pathogenic to humans [28]. While BoNT/DC was found to be rather robust towards changes in buffer composition, BoNT/C exhibited unique cleavage requirements. Consistently, specially optimized buffers are used for detection of BoNT/C in other assay systems [105, 131].

For multiplex detection approaches of BoNT several serotypes are analysed in one sample, hence only one cleavage buffer can be applied. Furthermore, in the analysis of samples of suspect cases of botulism, the serotype present cannot be foreseen. For these reasons a consensus buffer, in which all serotypes exhibit efficient substrate cleavage is necessary for detection of BoNT in a diagnostic setting. The consensus buffer proposed here achieved, except for BoNT/E and C, comparable sensitivities to the buffers optimized for the individual serotypes. For the analysis of samples presumably containing BoNT/C or E (e.g. cases of botulism in birds for BoNT/C or contaminated fish samples for BoNT/E) buffer conditions may have to be adjusted for a more sensitive detection.

To enable a widespread application of results, the cleavage of full-length SNAP-25 or VAMP-2 in solution was analysed. This implies that results found in the Taguchi analysis may not be 1:1 transferable to other assay systems with different requirements. For example, it has been demonstrated that shortened peptide substrates used in e.g. MS based approaches, are

DISCUSSION

differently influenced by factors such as NaCl concentration compared to full-length substrates [107]. Along this line, optimal cleavage conditions in assays using immobilized substrates such as plate bound ELISAs might differ from cleavage in solution.

Summing up, the comprehensive analysis of multiple factors influencing BoNT/A-F substrate cleavage presented in this work enabled for the first time a direct comparison of different serotypes regarding preferred cleavage conditions. It remains to be tested whether different subtypes of a specific serotype also prefer varying cleavage condition, which is – due to different demonstrated catalytic activities [32, 99, 100] – likely. The optimized buffers designed with the Taguchi DoE method led to enhanced substrate cleavage when compared to previously published buffers as references. Finally, a consensus buffer in which all clinically relevant BoNT serotypes exhibited good substrate cleavage was proposed for the first time.

6.1.1 Previously published results could partially be confirmed by the Taguchi DoE analysis

The comprehensive analysis of several factors affecting BoNT/A-F substrate cleavage revealed positive and negative factors as well as optimal factor levels. Thereby, several observations from previously published works could be confirmed.

NaCl was found to be negligible for most serotypes but negatively influenced cleavage of VAMP-2 by BoNT/B and DC. Consistently, a negative impact of NaCl on BoNT/B cleavage was reported in a previous study, in which cleavage was also performed in solution and analysed by SDS-PAGE [108]. Akin to the results of this study, an enhancing effect of Tween 20 for BoNT/A and E substrate cleavage was observed in a plate bound cleavage assay [110]. In addition, in agreement with the results of the Taguchi analysis, a work analysing substrate cleavage in solution by MS identified high $ZnCl_2$ and a pH at 6.5 optimal for cleavage of SNAP-25 by BoNT/C [105]. Conversely, high $ZnCl_2$ lead to an inhibition of SNAP-25 cleavage by LC/A by an approach detecting cleavage products after cleavage in solution by HPLC [107] which is also in accordance to the results of this study. The same study also found increasing DTT concentrations to support LC/A substrate cleavage. A beneficial impact of high DTT concentrations has also been reported for BoNT/B, when substrate was cleaved in solution and analysed by FRET [106]. In the study presented here, high DTT concentrations (25 mM) were found to increase the activity of BoNT/A, B, E, and F thereby confirming these previous findings.

DISCUSSION

Some observations made in the Taguchi DoE analysis are, however, also deviant from previously published data. For example, with a plate bound endopeptidase assay, optimal DTT concentrations for BoNT/A and E were found at 5 and 2.5 nM, respectively [108], which is lower than the optimal determined concentration of 25 mM in this work. This discrepancy can presumably be explained by the different experimental set-ups and cleavage durations employed. In this work, a short incubation time of 30 minutes was applied, whereas the plate bound assay used an overnight incubation step for substrate cleavage. The long incubation time might allow the usage of lower DTT concentrations for sufficient reduction of BoNT/A and E. In contrast, short incubation times may require much higher DTT concentrations for sufficient reduction and LC release.

The Taguchi analysis identified TMAO as a critical factor with major impact on all serotypes and strong inhibition of substrate cleavage at high concentration (2 M). However, moderate TMAO concentrations (0.75 M) improved cleavage of BoNT/A, B, C, and F. Contrary to these results, another study found concentrations up to 2 M beneficial for LC/A, B, and E substrate cleavage [109]. The beneficial effect of the osmolyte TMAO is thought to be caused by stabilizing proteins by enhancing a more compact protein structure [165, 166]. This might explain the enhancing effect of substrate cleavage by isolated toxin LCs. Conversely, in this work cleavage by full-length toxin was analysed. High TMAO concentration, inducing a compact protein structure, may sterically hinder accessibility of the reducing agent for release of the active LC thereby contributing to the inhibitory effect.

Taken together, observations from previous works analysing BoNT substrate cleavage could be confirmed by this study, demonstrating the effectiveness of the Taguchi DoE method. Deviant results are most likely caused by different experimental set-ups and/or different reagents used.

6.2 Generation and comprehensive characterisation of Neo-mAbs

A major goal of this thesis was to detect the enzymatic activity of all clinically relevant BoNT serotypes *in vitro*. To this end, Neo-mAbs that specifically recognize the newly exposed neopeptide on SNARE proteins after cleavage by BoNT/A to F were employed. So far, monoclonal Neo-Abs were only available for BoNT/A and E cleavage sites [126, 127, 129, 135].

DISCUSSION

Thus, the comprehensive panel of Neo-mAbs generated in this work covers, for the first time, the cleavage sites of the clinically relevant BoNT serotypes A-F.

6.2.1 Special immunization strategies and stringent screening procedure were required to generate a unique panel of Neo-mAbs

For generation of Neo-mAbs, mice were immunized with BSA-coupled peptide antigens corresponding to the respective N- or C-terminal BoNT cleavage site on the target SNARE protein.

Mice with sufficient antibody titers towards the target peptide antigen(s) were subjected to fusion. Hybridoma clones that target the desired neoepitope but do not recognize uncleaved substrate were identified by a stringent screening process by indirect ELISA. Only few clones (< 0.2%) exhibited the desired features, whereas the majority of clones tested either exhibited no reactivity towards the peptide antigen or were cross-reactive towards full-length substrate. Considering these results it seems astonishing that polyclonal antibodies can be generated and used for cleavage site detection [101, 110].

Depending on the cleavage site, complexity of generation of Neo-mAbs differed. Very good immune responses were yielded for peptides resembling the cleavage sites of BoNT/A, D, E (previous works), and F (this work and previous works). Consequently, Neo-mAbs targeting these cleavage sites could be generated with limited efforts within one fusion by immunizing one mouse with a mixture of multiple peptides.

In contrast, peptide antigens corresponding to the cleavage site of BoNT/C were by far less immunogenic. Here, the presence of more immunogenic peptides in the mixture diminished the immune response for those less immunogenic peptides. Consequently, larger doses of a single peptide were required to induce a sufficient antibody titer. Therefore, production of respective antibodies was much more elaborate and required several fusions to find well performing Neo-mAbs. The greater challenge in generating Neo-mAbs towards these neoepitopes is also exemplified by the observation that until now only a single polyclonal Neo-Ab targeting BoNT/C cleaved SNAP-25 exists [131]. Thus, generating Neo-mAbs targeting different BoNT cleavage sites is a complex task as immunogenicity of different peptide antigens is cleavage site dependent and requires an adaptation of the ideal immunization strategy for each target neoepitope. This might explain why until now no comprehensive set of Neo-Abs was available.

DISCUSSION

Despite major challenges, in total, 20 different Neo-mAbs covering the cleavage sites of BoNT/A-F were generated in this and previous works (11 in this and 9 in previous works). For BoNT/A and D Neo-mAbs targeting the N-terminal cleavage fragment were generated, whereas for BoNT/B, C, E, and F Neo-mAbs for both cleavage fragments are now available. To identify candidate Neo-mAbs for implementation in a highly sensitive enzymatic assay, all antibodies were thoroughly characterized.

6.2.2 Thorough characterisation elucidates prominent features of Neo-mAbs

The performance of Neo-mAbs in an enzymatic assay essentially depends on two factors: First, the antibodies' kinetic features dictate the binding strength to the target neoepitope and thus directly influence sensitivity. Second, the accessibility of the neoepitope influences antibody binding and therefore also has major implications on the achievable sensitivity in specific assay set-ups. To elucidate features that characterize well performing Neo-mAbs, various methods were applied. Interestingly, although all Neo-mAbs targeting the same cleavage site were selected using the same screening procedures, marked differences were observed regarding kinetic features and recognition of cleaved substrate.

Regarding kinetic characteristics determined by SPR measurements, most Neo-mAbs followed a common mode of rapid association and rapid dissociation in the monovalent binding approach. Together, this resulted in affinities in the lower micromolar to higher nanomolar range for most Neo-mAbs. This is comparably low for typical interactions between monoclonal antibodies and proteins, which are usually found in the low nanomolar range [167]. However, considering the small interaction surface that can be exploited by Neo-mAbs to bind to the target neoepitope, a low affinity was expected. Indeed, affinities of Neo-mAbs rather resemble those observed for interactions between antibodies and small molecules, such as haptens (*ibid.*). Still, some Neo-mAbs with high affinities in the low nanomolar range could be generated.

The possibility to build two interactions in the bivalent binding approach increased affinity for all Neo-mAbs, due to a more stable interaction. Here, affinities (or rather avidities) in the low nanomolar to low picomolar range could be achieved. This is in good agreement with a previously published Neo-mAb for BoNT/A, which exhibited an affinity in the picomolar range in a bivalent binding approach [126].

DISCUSSION

Despite overall similar kinetic features, pronounced differences regarding affinity and/or avidity between Neo-mAbs targeting the same cleavage site were observed. Neo-mAbs targeting the BoNT/B cleavage site, for example, revealed markedly differing binding profiles. Similarly, different BoNT/C, D, or F Neo-mAbs, all targeting the same respective neoepitope, exhibited remarkable differences regarding binding kinetics. Hence, the kinetic data gathered by SPR helps to decipher the individual binding modes of different antibodies and to make assumptions regarding antibody performance in a specific assay setting. This can facilitate the selection of suitable antibodies for a specific assay.

A comparison of all Neo-mAbs in the Endopeptidase-ELISA detecting cleaved full-length substrate revealed marked differences regarding the achievable assay sensitivity with antibodies targeting the same cleavage site. Although, assay sensitivity generally correlated with antibody affinity, some exceptions to this rule were observed.

Detection of BoNT/B in the Endopeptidase-ELISA, for example, was most sensitive with antibodies that did not exhibit any binding at all in SPR measurements, presumably due to a masked accessibility of the neoepitope in solution. Conversely, a Neo-mAb targeting the C-terminal fragment of BoNT/B cleaved VAMP-2 that exhibited exquisite affinity in SPR measurements performed much worse. One identified reason for this observation was cleavage site accessibility. A generally more sensitive detection was observed in the Endopeptidase-ELISA, when antibodies targeting the larger thus easier accessible N-terminal cleavage fragment were used, regardless of antibody affinities. Other assay set-ups where cleavage products are captured from solutions by Neo-mAbs are less prone to accessibility restrictions and would presumably reflect the kinetic features of Neo-mAbs more accurately.

These observations demonstrate that a selection of different Neo-mAbs targeting the same cleavage site is beneficial, as assay specific requirements influence antibody performance. The comprehensive panel of well-characterised Neo-mAbs presented in this work therefore has the potential to greatly expand the number of detectable serotypes in various previously established assays. In that sense, Neo-mAbs could be easily transferred to a recently introduced highly sensitive SPR based assay, which is so far only available for BoNT/A and E [127, 129]. Furthermore, other enzymatic BoNT assays such as Endopeptidase-ELISAs or cell-based assays could be extended to the detection of all clinically relevant serotypes which was – until now – not possible due to the lack of a suitable Neo-mAbs.

6.2.3 Neo-mAbs exhibit exquisite specificity towards their target cleavage sites

As demonstrated by Western blotting and Endopeptidase-ELISA most Neo-mAbs generated and characterised in this work exhibited exquisite specificity towards their target neopeptide. This includes the recognition of cleaved substrate, whereas cross-reactivity towards full-length substrate and neighbouring cleavage sites is excluded. The latter is particularly remarkable for Neo-mAbs targeting BoNT/A and C or BoNT/F and D neopeptides, as cleavage sites of these serotypes differ by only one amino acid. Surprisingly, this feature has also been demonstrated for polyclonal Neo-Abs targeting BoNT/A or C cleaved SNAP-25, which however required affinity-purification of antibodies [110, 131]. Although a polyclonal Neo-Ab for BoNT/F cleaved VAMP-2 is available [101], the lack of cross-reactivity towards the neighbouring BoNT/D cleavage site has not been shown yet. The exclusive specificity of neopeptide antibodies towards BoNT/F or D cleaved VAMP-2 has therefore been demonstrated for the first time in this work. This feature together with the lack of cross-reactivity against uncleaved substrates hints towards a common binding mode of highly specific Neo-mAbs. This has recently been investigated for a Neo-mAb targeting an N-terminal epitope on amyloid beta peptide (Bapineuzumab). By analysing the crystal structure of the antibody-antigen complex, the study revealed that binding of the Neo-mAb seems to be based on burying the newly exposed neopeptide in deep binding pockets of the antibody with critical contribution of the terminal amino acids [168].

6.2.4 Suitability of Neo-mAbs for enzymatic detection of BoNT

Compared to assays solely analysing substrate cleavage, such as FRET based approaches, the exact identification of each cleavage site by Neo-mAbs is clearly the more powerful method. In FRET based cleavage assays, a discrimination of serotypes targeting the same SNARE protein is not possible, as all cleavage sites are located between fluorescent donor and quencher molecule. Thus, the exact cleavage site is not relevant for signal generation. This limitation could only be overcome by shortened peptides allowing for discrimination between BoNT/E and A/C and BoNT/B and F/D [119], presumably causing pronounced sensitivity losses due to hindered substrate recognition. On top, serotypes A and C or F and D cannot be differentiated without further substrate modifications. Furthermore, assays that solely rely on substrate cleavage and do not detect the exact cleavage site are more prone to generate false positive results as any cleavage of the substrate away from the BoNT specific cleavage site would result

DISCUSSION

in a positive signal. This is particularly critical when complex matrices that might contain proteases are analysed, as unspecific substrate cleavage is likely. In contrast, assays employing Neo-mAbs allow for the exact determination of the present serotype and will only result in positive signals if the correct substrate is cleaved at the exact serotype specific position. However, a false positive result could potentially be generated by the presence of proteases that cleave SNARE proteins at the same position as BoNTs. In this context, a sample containing trypsin would be positively tested for BoNT/C, as trypsin cleaves SNAP-25 at the BoNT/C cleavage site [131]. This could be controlled by including BoNT-non-cleavable control substrates that do harbour a trypsin cleavage site but cannot be cleaved by BoNT/C as proposed by Bagramyan et al [169]. In addition, the presence of multiple proteases in a sample resulting in complete substrate degradation would provoke false negative results. Still, these conditions are, for most sample matrices tested so far, less likely and can be circumvented by sample dilutions and toxin enrichment approaches.

6.3 Development of different approaches for the functional detection of BoNT

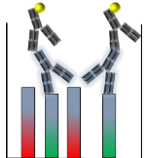
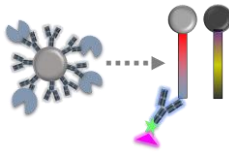
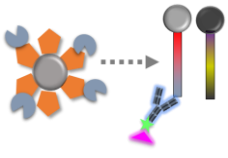
As major goal of this work a functional assay detecting BoNT should be established. Hereby, the focus lay in the sensitive detection of BoNTs' enzymatic activity. To that aim both the well-characterized Neo-mAbs and the newly developed consensus cleavage buffer were implemented in different experimental approaches. In doing so, highly sensitive detection methods for BoNT serotypes A-F were developed emphasizing the usefulness of the broad panel of generated Neo-mAbs and knowledge on optimal substrate cleavage requirements. Until now, detection of enzymatically active BoNT by monoclonal Neo-Abs was only possible for BoNT/A and E [126-129]. The different approaches presented in this work therefore enable, for the first time, a detection of all clinically relevant BoNT serotypes by Neo-mAbs. For straightforward and sensitive toxin detection, an Endopeptidase-ELISA was employed. To enable multiplex toxin detection a bead-based assay using the Luminex™ xMAP technology was established.

In order to display an additional functional step, the endogenous receptor structures of BoNT/A and B were explored and optimized receptors were recombinantly expressed (cooperation with MHH) and used to enrich BoNT/A and B. Combined with the display of

DISCUSSION

catalytic activity by Neo-mAbs, two essential steps of BoNT's activity were successfully displayed *in vivo* and integrated in a combined functional assay. Hereby, sensitive detection of the clinically most relevant serotypes BoNT/A and B could be achieved from buffer and a variety of complex matrices. The different assay systems established in this work are summarized in Table 34.

Table 34: Overview on different assay platforms developed in this thesis.

	Endopeptidase-ELISA	Duplex-assay	Combined duplex-assay
			
Serotypes	BoNT/A-F	BoNT/A-F	BoNT/A, BoNT/B
Enrichment	anti-BoNT mAbs	anti-BoNT mAbs	recombinant receptors
Depicted BoNT action	enzymatic activity	enzymatic activity	receptor binding + enzymatic activity
Sensitivity (LOD)	(0.3–14 pg/mL) ^a	0.3–79.1 pg/mL ^b	2.9–5.1 pg/mL ^c
Sensitivity (LD50/mL)	(0.004–1.36) ^d	0.005–2.056 ^e	0.35–1.34 ^f
Assay duration	3 days	2 days	2 days
Sample volume	200 µL	200 µL	200 µL
Matrix-compatibility ^g	Serum, <i>Clostridia</i> supernatants ^h	Serum, <i>Clostridia</i> supernatants	Serum, <i>Clostridia</i> supernatants, food
Technical equipment required ⁱ	low	medium	medium
Possibility for automatization	high	high	high

^a Sensitivity in buffer without enrichment: BoNT/A: 0.3 pg/mL; BoNT/B: 11 pg/mL; BoNT/C: 2.7 pg/mL; BoNT/DC: 0.3 pg/mL; BoNT/E (non-trypsinated): 14 pg/mL; BoNT/F: 0.8 pg/mL

^b Sensitivity in buffer with enrichment: BoNT/A: 0.8 pg/mL; BoNT/B: 1.2 pg/mL; BoNT/C: 79.1 pg/mL; BoNT/D: 1.1 pg/mL; BoNT/E (trypsinated): 13 pg/mL; BoNT/F: 0.3 pg/mL

^c Sensitivity in buffer with enrichment: BoNT/A 5.1 pg/mL; BoNT/B: 2.9 pg/mL

^d Sensitivity in buffer without enrichment in LD50/mL: BoNT/A: 0.07; BoNT/B: 1.36; BoNT/C: 0.8; BoNT/DC: 0.03; BoNT/E (non-trypsinated): 0.004; BoNT/F: 0.02

^e Sensitivity in buffer with enrichment in LD50/mL: BoNT/A: 0.211; BoNT/B: 0.147; BoNT/C: 2.056; BoNT/D: not determined; BoNT/E (trypsinated): 0.84; BoNT/F: 0.005

^f Sensitivity in buffer with enrichment in LD50/mL: BoNT/A: 1.34; BoNT/B: 0.35

^g Matrices tested in respective assay.

^h data not shown

ⁱ low = ELISA reader, medium = Bioplex®-instrument

DISCUSSION

6.3.1 Detection of BoNT/A-F enzymatic activity

6.3.1.1 *Highly sensitive detection of BoNT/A-F by a straightforward Endopeptidase-ELISA*

For simple toxin detection, an Endopeptidase-ELISA as previously described by Jones *et al* [110] was established. This approach has the advantage of having a straightforward assay protocol without the requirement of special technical equipment or expert laboratory staff for data analysis. For sample read-out, a microplate reader is sufficient ensuring a broad applicability of the method in routine laboratories such as local food or health authorities. The Endopeptidase-ELISA therefore represents a useful method for broad application in laboratory diagnostics. Accordingly, the majority of endopeptidase assays employing Neo-Abs is based on an Endopeptidase-ELISA (see Table 3 from the introduction). Different Endopeptidase-ELISAs, most of them employing polyclonal Neo-Abs, have been described for the detection of BoNT/A, B, C, E, and F in different studies [101, 110, 131, 132, 170]. However, most of these approaches only address one or selected serotypes and were optimized for the specific requirements of the serotype tested, thereby limiting their usage for diagnostic purposes. The Endopeptidase-ELISA developed in this work overcomes this limitation as all relevant BoNT serotypes A-F were detected with high sensitivity. For all serotypes, detection limits in the low pg/mL range were achieved, which are in the same range or much lower than the previously published Endopeptidase-ELISAs (see Table 3). Accordingly, sensitivity of the Endopeptidase-ELISA also matches or greatly exceeds the MBA as well as other enzymatic approaches such as Endopep-MS or FRET [120, 171]. In the future, the Endopeptidase-ELISA could therefore be employed to replace the MBA for serotyping of diagnostic samples.

6.3.1.2 *Implementation of the Luminex™ platform enables multiplex toxin detection*

To enable multiplex toxin detection to save experimental effort and sample consumption the Luminex™ xMAP technology was employed. Here, three different duplex-assays simultaneously detecting BoNT/A+B, BoNT/C+D, or BoNT/E+F were developed. Thus, by combining BoNT/A and B as well as BoNT/E and F, all BoNTs pathogenic to humans can be analysed in only two tests. Otherwise, the combination of BoNT/C and D allows for the analysis of BoNTs pathogenic to animals. Thus, depending on sample origin the most suitable assay can be applied, thereby reducing sample size. A further advantage of the duplex-assay is that beads can be prepared in advance and stored over several months. Thereby an overnight coating step, as required in the Endopeptidase-ELISA, can be spared thus shortening assay

DISCUSSION

duration to two days. A one-day protocol with a shortened substrate cleavage step would also be possible, but presumably reduces assay sensitivity. However, even with the two days assay protocol, the duplex-assay is considerably faster than the MBA, which requires up to four days, particularly when toxin concentration in a sample is low. Akin to the Endopeptidase-ELISA, the duplex-assay is easy to perform and data analysis is straightforward. This is exemplified by the fact that another laboratory in Switzerland could easily perform the duplex-assay achieving almost identical results in a small interlaboratory comparison performed as part of this work. Furthermore, the Luminex™ system is commonly used for diagnostics of pathogens as demonstrated by the fact that a widely used FDA approved method is commercially available (xTAG® gastrointestinal pathogen panel, Luminex Corporation, Austin, USA). Thus, the system is available in many public health laboratories thereby potentially allowing a wide distribution of the duplex-assay.

Limits of detection of the three different duplex-assays are for most serotypes in the same range as the Endopeptidase-ELISA and therefore similar to or much more sensitive than the MBA or other enzymatic approaches [120, 171]. The only exception from this is BoNT/C, which exhibited a markedly reduced sensitivity in the duplex-assay. BoNT/C seems, however, to tend to reduced cleavage efficiency caused by varying experimental conditions, also observed in the Taguchi DoE analysis of this work and previous studies [105, 131]. Nevertheless, sensitivity for BoNT/C is in the same range as the MBA and previously published enzymatic assays (ibid.). The application of individually optimized buffer conditions would presumably be capable of further enhancing sensitivity of specific serotypes. Summing up, the newly developed duplex-assays presented in this work enable detection of functional BoNT/A-F with exquisite sensitivity. The simple experimental set-up ensures a broad applicability of the assay thereby representing a major step towards a replacement method to the MBA.

6.3.1.3 Detection of BoNT from human serum

To demonstrate that the assays established in this work can be employed for routine botulism diagnostics, detection of BoNT from spiked human serum samples, as the most common sample matrix, was tested.

Generally, sensitivities for detection of BoNT from serum with both presented assay formats are in the same range as other enzymatic approaches, such as Endopep-MS or FRET [121, 172, 173]. Only few studies employing Neo-Abs for BoNT detection demonstrated sufficient

DISCUSSION

detection from human serum so far. In respective studies BoNT/A, B, and F were detected from human serum samples with similar sensitivities to the assays developed in this work [101, 133, 134]. Exceptionally an SPR based approach yielded higher sensitivities in the femto- to picomolar range for the detection of BoNT/A and E from serum using monoclonal Neo-Abs [128, 129]. The enzymatic detection of the veterinary relevant serotypes C and D from serum has not been demonstrated with Neo-Abs before. To draw a more accurate conclusion and determine the exact limits of detection a more thorough investigation including validation of the different assays will be required. Still, the available data demonstrates efficient and sensitive detection of all serotypes from serum, thereby proving the usability of the assays for botulism diagnostics.

6.3.2 Duplex assay combining receptor binding and enzymatic activity for BoNT/A and B

To overcome the limitation of subtype recognition as well as to depict an additional functional step of BoNT action, a novel assay for BoNT/A and B combining receptor binding and enzymatic activity was established. Hereby, instead of anti-BoNT antibodies, recombinant receptor molecules were coupled to paramagnetic dynabeads and used for toxin enrichment in the duplex-assay. The idea of using the endogenous neuronal receptors for toxin enrichment combined with detection of catalytic activity has been demonstrated by very few studies before. In respective studies toxin was captured by synaptosomes prepared from rat brain extracts, functionalized liposomes, or recombinant receptor molecules and cleavage products were detected by Neo-Abs with an Endopeptidase-ELISA, FRET, or ultra-performance liquid chromatography (UPLC) [101, 137, 174-176]. Compared to synaptosomes or liposomes, recombinant receptor molecules are clearly more suitable for a diagnostic assay as they are easier to produce and to handle and usually more stable. In addition, they constitute defined molecules with a known amino acid sequence that can be produced in unlimited amounts with consistent quality. Consequently, in this study recombinantly expressed receptor molecules either directly coupled to paramagnetic dynabeads or incorporated into membrane-mimicking nanodiscs were employed and integrated in a novel duplex-assay detecting BoNT/A and B from buffer and a variety of complex matrices with high sensitivity.

DISCUSSION

6.3.2.1 Suitability of receptor molecules for BoNT enrichment

For BoNT/A and B enrichment in the combined duplex-assay, glycosylated SV2C or dual-Syt-II-NDs were employed. The usage of recombinant SV2C for BoNT/A enrichment has only been demonstrated in one approach before [176]. This is mainly due to the highly complex interaction of BoNT/A with its receptor requiring specific glycosylations that could be resolved by the cooperation partner MHH in during the course of this work [71, 72]. The usage of nanodiscs for BoNT enrichment has never been demonstrated before. In this work, dual-Syt-II-NDs were employed for the first time to capture BoNT/B from different sample matrices.

SPR measurements with isolated receptor molecules and recombinant H_C-fragments of different BoNT/A and B subtypes revealed a broad recognition of subtypes with the receptors. This could further be verified by testing different *Clostridia* supernatants in the combined duplex-assay. Particularly for BoNT/B subtypes, which were not all recognized by antibody-based enrichment, a broader coverage of subtypes was achieved by using receptors. However, also marked differences regarding subtype recognition of receptors were observed. BoNT/A4, for example, was barely recognized by its natural neuronal receptor, while all other subtypes exhibited clear binding, although to different extents. Interestingly BoNT/A4, exhibits a 1000-fold reduced toxicity in mice as well as different neuronal cell lines [99, 177] while *in vivo* toxicity of A1, A2, A3, and A5 is comparable [178-180]. As substrate cleavage of A4 is similar to other subtypes, as demonstrated in this work and others [99], the reduced *in vivo* toxicity is most likely caused by the weak receptor interaction. This example demonstrates that subtypes that are not or only weakly recognized by the neuronal BoNT receptors are presumably also less clinically relevant, as high toxin concentrations are required for intoxication. A reduced sensitivity in combined functional assays is therefore not relevant.

6.3.2.2 Sensitive detection of BoNT/A and B from buffer and complex matrices

The combined duplex-assay presented in this work covers two essential steps of BoNT action: receptor binding and enzymatic activity. Thereby high sensitivities, which are in the range of the MBA, were achieved for BoNT/A and B. Compared to the antibody-based duplex-assay, the combined duplex-assay is slightly less sensitive for BoNT/A, and achieves a similar sensitivity for BoNT/B. The sensitivity loss for BoNT/A is mainly due to a less efficient enrichment with the recombinant receptor molecule compared to the antibody. However,

DISCUSSION

one has to keep in mind, that sensitivities were only determined for one subtype (BoNT/A1 and BoNT/B1). For other subtypes, considerable differences might be observed.

A previously published enzymatic assay employing recombinant Syt-II for enrichment of BoNT/B yielded similar sensitivities to the combined duplex-assay presented in this work [137]. Conversely, another assay, putatively displaying all three steps of BoNT/B action using functionalized liposomes was less sensitive and presented inconclusive results [175]. Regarding detection of BoNT/A, only one study demonstrated enrichment with recombinant SV2C so far with subsequent detection of cleavage products by FRET [176]. In this approach, a 10-fold reduced sensitivity compared to the combined duplex-assay developed in this work was achieved.

The usage of synaptosomes for toxin enrichment combined with an Endopeptidase-ELISA demonstrated detection of BoNT/A, B (and F) from buffer and spiked serum samples [101] with comparable sensitivities to this work. In respective study, however, much larger sample volumes than in this work (5 mL compared to 200 μ L) were employed. Although synaptosomes may be a useful tool for enrichment as they represent the natural membrane environment, they also have considerable drawbacks and are less suitable to use in a routine diagnostic assay. Generation of synaptosomes is tedious and still requires a considerable number of animals. Also, consistent quality can hardly be assured possibly causing lot-to-lot variations. In addition, compatibility with different matrices might be problematic, as the authors of the study claimed that only a maximum of 10% serum could be applied, while higher concentrations disturbed the assay.

With the recombinant receptors employed in the combined duplex-assay, sensitive detection of BoNT/A and B was demonstrated from a variety of different complex matrices including serum, *Clostridia* supernatants, and different foods. Although detection from complex matrices led to sensitivity losses in most cases, medium toxin concentrations (150 pg/mL BoNT/A and 50 pg/mL BoNT/B) could be detected from all matrices tested from a 200 μ L sample volume. Larger sample volumes would further increase assay sensitivity due to a higher concentration of toxin through enrichment.

In summary, the combined duplex-assay established in this work is the first approach described that combines receptor enrichment and enzymatic activity enabling sensitive and simultaneous detection of the clinically most relevant BoNT serotypes A and B. Furthermore,

DISCUSSION

the assay sufficiently detects BoNT from different complex matrices which has not been demonstrated in any system employing receptor-based enrichment before. The usage of receptor molecules for BoNT enrichment ensures a reliable detection of all clinically relevant subtypes by the assay. For these reasons, the combined duplex-assay represents a promising tool capable of fully replacing the MBA in the future.

6.4 Conclusion and outlook

The well characterized Neo-mAbs generated in this work as well as the optimized cleavage conditions are of great benefit for botulism diagnostics exemplified by two different assay systems detecting functionally active BoNT/A-F with high sensitivity. For simple toxin detection, an Endopeptidase-ELISA was established. The development of a novel Luminex™ duplex-assay enabled simultaneous detection of two serotypes thereby reducing experimental effort and sample consumption. Both assays detect BoNT/A-F with sensitivities in the range of the MBA or higher from buffer and – after toxin enrichment by monoclonal antibodies – spiked serum samples. To include an additional functional step of BoNT action and enable reliable detection of all possible BoNT subtypes, natural neuronal receptors were integrated in a combined duplex-assay for BoNT/A and B, which enabled sensitive toxin detection from a variety of different complex matrices. The results presented in this work therefore demonstrate that the assay systems established together with the large panel of Neo-mAbs and optimized substrate cleavage conditions are a great step forward towards a replacement method to the MBA.

Nevertheless, more research efforts should be undertaken in the future to overcome limitations of the presented as well as other functional assays. A fully valid replacement method to the MBA should detect all known sero- and subtypes from a variety of different matrices with high sensitivity. Therefore, the following issues must be addressed in future research attempts.

In this work, Neo-mAbs targeting BoNT/A-F were generated and used for toxin detection, as they are clinically most relevant. Neo-Abs covering the cleavage sites of BoNT/G and HA and the novel serotypes BoNT/X and BoNT/En were not addressed, as for these serotypes no or very few natural cases of botulism in humans (or animals) have been reported so far. With the experience from this work such Neo-mAbs could be generated in the future and easily

DISCUSSION

implemented in the presented assays thereby expanding them to all known serotypes. For the detection from complex matrices, the anti-BoNT/A antibody could be used for enrichment of BoNT/HA, as BoNT/A and HA share the same receptor binding domain (HC). For enrichment of BoNT/G, X, or En, however, novel antibodies would be required.

Regarding toxin enrichment, a thorough investigation on subtype recognition of antibodies used for enrichment will be required. Ideally, only antibodies that cover all known subtypes should be implemented in a diagnostic assay. However, due to the limited availability of test reagents such as *Clostridia* supernatants or recombinant toxins, this can hardly be evaluated soon. Therefore, as an alternative to antibody-based toxin enrichment, a strong focus should be set on the investigation of receptor molecules for the so far missing serotypes. As BoNT-receptor interactions are highly complex, and knowledge for most serotypes is limited, this will require further intense basic research efforts. The achievements regarding BoNT/A receptor interaction gathered in the FuMiBoNT project (addressed by the collaboration partner at MHH) promise that also receptor interactions of other serotypes will be elucidated in the future.

Finally, thorough validation studies of the presented assays, including a broad set of different sample matrices and clinical and food samples should be undertaken. Thereby, matrix compatibility must be evaluated, and exact detection limits have to be determined.

As overall goal, the presented assays should fully replace the MBA for botulism diagnostics in the future. Thus, they will have to be evaluated against the MBA sooner or later. Until then, they constitute a valuable tool for basic research purposes. Furthermore, they already can support botulism diagnostics by e.g. serotyping samples that have been tested positively in the MBA, thereby considerably reducing the number of required animals.

7 REFERENCES

1. Rummel, A., *The long journey of botulinum neurotoxins into the synapse*. *Toxicon*, 2015. **107**(Pt A): p. 9-24.
2. Kerner, J., *Das Fettgift oder die Fettsäure und ihre Wirkungen auf den thierischen Organismus. Ein Beytrag zur Untersuchung des in verdorbenen Würsten giftig wirkenden Stoffes*. Cotta, 1822.
3. van Ermengem, E., *Classics in infectious diseases. A new anaerobic bacillus and its relation to botulism. E. van Ermengem. Originally published as "Ueber einen neuen anaeroben Bacillus und seine Beziehungen zum Botulismus" in Zeitschrift für Hygiene und Infektionskrankheiten 26: 1-56, 1897*. *Rev Infect Dis*, 1979. **1**(4): p. 701-19.
4. Burgen, A.S., F. Dickens, and L.J. Zatman, *The action of botulinum toxin on the neuromuscular junction*. *J Physiol*, 1949. **109**(1-2): p. 10-24.
5. Kumar, R., H.P. Dhaliwal, R.V. Kukreja, and B.R. Singh, *The Botulinum Toxin as a Therapeutic Agent: Molecular Structure and Mechanism of Action in Motor and Sensory Systems*. *Semin Neurol*, 2016. **36**(1): p. 10-19.
6. Gart, M.S. and K.A. Gutowski, *Overview of Botulinum Toxins for Aesthetic Uses*. *Clin Plast Surg*, 2016. **43**(3): p. 459-471.
7. Rotz, L.D., A.S. Khan, S.R. Lillibridge, S.M. Ostroff, and J.M. Hughes, *Public health assessment of potential biological terrorism agents*. *Emerg Infect Dis*, 2002. **8**(2): p. 225-230.
8. Sobel, J., *Botulism*. *Clin Infect Dis*, 2005. **41**(8): p. 1167-1173.
9. Gilsdorf, D.A., *Infektionsepidemiologisches Jahrbuch meldepflichtiger Krankheiten für 2015*. 2016, Robert Koch-Institut.
10. Rosow, L.K. and J.B. Strober, *Infant botulism: review and clinical update*. *Pediatr Neurol*, 2015. **52**(5): p. 487-492.
11. Yuan, J., G. Inami, J. Mohle-Boetani, and D.J. Vugia, *Recurrent wound botulism among injection drug users in California*. *Clin Infect Dis*, 2011. **52**(7): p. 862-866.
12. Gonzales y Tucker, R.D. and B. Frazee, *View from the front lines: an emergency medicine perspective on clostridial infections in injection drug users*. *Anaerobe*, 2014. **30**: p. 108-15.
13. Bakheit, A.M., C.D. Ward, and D.L. McLellan, *Generalised botulism-like syndrome after intramuscular injections of botulinum toxin type A: a report of two cases*. *J Neurol Neurosurg Psychiatry*, 1997. **62**(2): p. 198.
14. *World Health Organization, Botulism* (December 2016), Available from: <http://www.who.int/mediacentre/factsheets/fs270/en/> [cited May 31, 2017]
15. Dembek, Z.F., L.A. Smith, and J.M. Rusnak, *Botulism: cause, effects, diagnosis, clinical and laboratory identification, and treatment modalities*. *Disaster Med Public Health Prep*, 2007. **1**(2): p. 122-134.
16. Smith LD, S.H., *Botulism. The Organism, Its Toxins, The Disease*. American Lecture Series in Clinical Microbiology. Vol. 42. 1988: Charles C Thomas.
17. Smith, T.J., K.K. Hill, and B.H. Raphael, *Historical and current perspectives on Clostridium botulinum diversity*. *Res Microbiol*, 2015. **166**(4): p. 290-302.
18. Barash, J.R. and S.S. Arnon, *A novel strain of Clostridium botulinum that produces type B and type H botulinum toxins*. *J Infect Dis*, 2014. **209**(2): p. 183-191.
19. Kalb, S.R., J. Baudys, B.H. Raphael, J.K. Dykes, C. Luquez, S.E. Maslanka, and J.R. Barr, *Functional characterization of botulinum neurotoxin serotype H as a hybrid of known serotypes F and A (BoNT F/A)*. *Anal Chem*, 2015. **87**(7): p. 3911-3917.

REFERENCES

20. Maslanka, S.E., C. Luquez, J.K. Dykes, W.H. Tepp, C.L. Pier, S. Pellett, B.H. Raphael, S.R. Kalb, J.R. Barr, A. Rao, and E.A. Johnson, *A Novel Botulinum Neurotoxin, Previously Reported as Serotype H, Has a Hybrid-Like Structure With Regions of Similarity to the Structures of Serotypes A and F and Is Neutralized With Serotype A Antitoxin*. J Infect Dis, 2016. **213**(3): p. 379-85.
21. Yao, G., K.H. Lam, K. Perry, J. Weisemann, A. Rummel, and R. Jin, *Crystal Structure of the Receptor-Binding Domain of Botulinum Neurotoxin Type HA, Also Known as Type FA or H*. Toxins (Basel), 2017. **9**(3): p. e93.
22. Brunt, J., A.T. Carter, S.C. Stringer, and M.W. Peck, *Identification of a novel botulinum neurotoxin gene cluster in Enterococcus*. FEBS Lett, 2018. **592**(3): p. 310-317.
23. Zhang, S., F. Lebreton, M.J. Mansfield, S.I. Miyashita, J. Zhang, J.A. Schwartzman, L. Tao, G. Masuyer, M. Martinez-Carranza, P. Stenmark, M.S. Gilmore, A.C. Doxey, and M. Dong, *Identification of a Botulinum Neurotoxin-like Toxin in a Commensal Strain of Enterococcus faecium*. Cell Host Microbe, 2018. **23**(2): p. 169-176.e6.
24. Zhang, S., G. Masuyer, J. Zhang, Y. Shen, D. Lundin, L. Henriksson, S.I. Miyashita, M. Martinez-Carranza, M. Dong, and P. Stenmark, *Identification and characterization of a novel botulinum neurotoxin*. Nat Commun, 2017. **8**: p. 14130.
25. Rossetto, O., M. Pirazzini, and C. Montecucco, *Botulinum neurotoxins: genetic, structural and mechanistic insights*. Nat Rev Microbiol, 2014. **12**(8): p. 535-549.
26. Lindstrom, M., J. Myllykoski, S. Sivela, and H. Korkeala, *Clostridium botulinum in cattle and dairy products*. Crit Rev Food Sci Nutr, 2010. **50**(4): p. 281-304.
27. Sonnabend, O., W. Sonnabend, R. Heinzle, T. Sigrist, R. Dirnhofner, and U. Krech, *Isolation of Clostridium botulinum type G and identification of type G botulinum toxin in humans: report of five sudden unexpected deaths*. J Infect Dis, 1981. **143**(1): p. 22-27.
28. Hill, K.K. and T.J. Smith, *Genetic diversity within Clostridium botulinum serotypes, botulinum neurotoxin gene clusters and toxin subtypes*. Curr Top Microbiol Immunol, 2013. **364**: p. 1-20.
29. Peck, M.W., T.J. Smith, F. Anniballi, J.W. Austin, L. Bano, M. Bradshaw, P. Cuervo, L.W. Cheng, Y. Derman, B.G. Dorner, A. Fisher, K.K. Hill, S.R. Kalb, H. Korkeala, M. Lindstrom, F. Lista, C. Luquez, C. Mazuet, M. Pirazzini, M.R. Popoff, O. Rossetto, A. Rummel, D. Sesardic, B.R. Singh, and S.C. Stringer, *Historical Perspectives and Guidelines for Botulinum Neurotoxin Subtype Nomenclature*. Toxins (Basel), 2017. **9**(1): p. 38.
30. Montecucco, C. and M.B. Rasotto, *On botulinum neurotoxin variability*. MBio, 2015. **6**(1): p. e02131-14.
31. Dover, N., J.R. Barash, K.K. Hill, G. Xie, and S.S. Arnon, *Molecular characterization of a novel botulinum neurotoxin type H gene*. J Infect Dis, 2014. **209**(2): p. 192-202.
32. Kull, S., K.M. Schulz, J. Weisemann, S. Kirchner, T. Schreiber, A. Bollenbach, P.W. Dabrowski, A. Nitsche, S.R. Kalb, M.B. Dorner, J.R. Barr, A. Rummel, and B.G. Dorner, *Isolation and functional characterization of the novel Clostridium botulinum neurotoxin A8 subtype*. PLoS One, 2015. **10**(2): p. e0116381.
33. Chen, Y., H. Korkeala, J. Aarnikunnas, and M. Lindstrom, *Sequencing the botulinum neurotoxin gene and related genes in Clostridium botulinum type E strains reveals orfx3 and a novel type E neurotoxin subtype*. J Bacteriol, 2007. **189**(23): p. 8643-8650.
34. Raphael, B.H., M. Lautenschlager, S.R. Kalb, L.I. de Jong, M. Frace, C. Luquez, J.R. Barr, R.A. Fernandez, and S.E. Maslanka, *Analysis of a unique Clostridium botulinum strain from the Southern hemisphere producing a novel type E botulinum neurotoxin subtype*. BMC Microbiol, 2012. **12**: p. 245.

REFERENCES

35. Woudstra, C., H. Skarin, F. Anniballi, L. Fenicia, L. Bano, I. Drigo, M. Koene, M.H. Bayon-Auboyer, J.P. Buffereau, D. De Medici, and P. Fach, *Neurotoxin gene profiling of clostridium botulinum types C and D native to different countries within Europe*. Appl Environ Microbiol, 2012. **78**(9): p. 3120-3127.
36. Macdonald, T.E., C.H. Helma, Y. Shou, Y.E. Valdez, L.O. Ticknor, B.T. Foley, S.W. Davis, G.E. Hannett, C.D. Kelly-Cirino, J.R. Barash, S.S. Arnon, M. Lindstrom, H. Korkeala, L.A. Smith, T.J. Smith, and K.K. Hill, *Analysis of Clostridium botulinum serotype E strains by using multilocus sequence typing, amplified fragment length polymorphism, variable-number tandem-repeat analysis, and botulinum neurotoxin gene sequencing*. Appl Environ Microbiol, 2011. **77**(24): p. 8625-8634.
37. Gu, S. and R. Jin, *Assembly and function of the botulinum neurotoxin progenitor complex*. Curr Top Microbiol Immunol, 2013. **364**: p. 21-44.
38. Lam, K.H. and R. Jin, *Architecture of the botulinum neurotoxin complex: a molecular machine for protection and delivery*. Curr Opin Struct Biol, 2015. **31**: p. 89-95.
39. Benefield, D.A., S.K. Dessain, N. Shine, M.D. Ohi, and D.B. Lacy, *Molecular assembly of botulinum neurotoxin progenitor complexes*. Proc Natl Acad Sci U S A, 2013. **110**(14): p. 5630-5635.
40. Lee, K., S. Gu, L. Jin, T.T. Le, L.W. Cheng, J. Strotmeier, A.M. Krueel, G. Yao, K. Perry, A. Rummel, and R. Jin, *Structure of a bimodular botulinum neurotoxin complex provides insights into its oral toxicity*. PLoS Pathog, 2013. **9**(10): p. e1003690.
41. Amatsu, S., Y. Sugawara, T. Matsumura, K. Kitadokoro, and Y. Fujinaga, *Crystal structure of Clostridium botulinum whole hemagglutinin reveals a huge triskelion-shaped molecular complex*. J Biol Chem, 2013. **288**(49): p. 35617-35625.
42. Ohishi, I., S. Sugii, and G. Sakaguchi, *Oral toxicities of Clostridium botulinum toxins in response to molecular size*. Infect Immun, 1977. **16**(1): p. 107-109.
43. Lee, K., X. Zhong, S. Gu, A.M. Krueel, M.B. Dorner, K. Perry, A. Rummel, M. Dong, and R. Jin, *Molecular basis for disruption of E-cadherin adhesion by botulinum neurotoxin A complex*. Science, 2014. **344**(6190): p. 1405-1410.
44. Sugawara, Y., T. Matsumura, Y. Takegahara, Y. Jin, Y. Tsukasaki, M. Takeichi, and Y. Fujinaga, *Botulinum hemagglutinin disrupts the intercellular epithelial barrier by directly binding E-cadherin*. J Cell Biol, 2010. **189**(4): p. 691-700.
45. Matsumura, T., Y. Jin, Y. Kabumoto, Y. Takegahara, K. Oguma, W.I. Lencer, and Y. Fujinaga, *The HA proteins of botulinum toxin disrupt intestinal epithelial intercellular junctions to increase toxin absorption*. Cell Microbiol, 2008. **10**(2): p. 355-364.
46. Swaminathan, S. and S. Eswaramoorthy, *Structural analysis of the catalytic and binding sites of Clostridium botulinum neurotoxin B*. Nat Struct Biol, 2000. **7**(8): p. 693-699.
47. Gill, D.M., *Bacterial toxins: a table of lethal amounts*. Microbiol Rev, 1982. **46**(1): p. 86-94.
48. Arnon, S.S., R. Schechter, T.V. Inglesby, D.A. Henderson, J.G. Bartlett, M.S. Ascher, E. Eitzen, A.D. Fine, J. Hauer, M. Layton, S. Lillibridge, M.T. Osterholm, T. O'Toole, G. Parker, T.M. Perl, P.K. Russell, D.L. Swerdlow, and K. Tonat, *Botulinum toxin as a biological weapon: medical and public health management*. Jama, 2001. **285**(8): p. 1059-1070.
49. Pantano, S. and C. Montecucco, *The blockade of the neurotransmitter release apparatus by botulinum neurotoxins*. Cell Mol Life Sci, 2014. **71**(5): p. 793-811.
50. Brunger, A.T., R. Jin, and M.A. Breidenbach, *Highly specific interactions between botulinum neurotoxins and synaptic vesicle proteins*. Cell Mol Life Sci, 2008. **65**(15): p. 2296-2306.

REFERENCES

51. Lam, K.H., G. Yao, and R. Jin, *Diverse binding modes, same goal: The receptor recognition mechanism of botulinum neurotoxin*. Prog Biophys Mol Biol, 2015. **117**(2-3): p. 225-231.
52. Rummel, A., *Double receptor anchorage of botulinum neurotoxins accounts for their exquisite neurospecificity*. Curr Top Microbiol Immunol, 2013. **364**: p. 61-90.
53. Montecucco, C., *How Do Tetanus and Botulinum Toxins Bind to Neuronal Membranes*. Trends Biochem Sci, 1986. **11**(8): p. 314-317.
54. Stern, D., J. Weisemann, A. Le Blanc, L. von Berg, S. Mahrhold, J. Piesker, M. Laue, P.B. Lupp, M.B. Dorner, B.G. Dorner, and A. Rummel, *A lipid-binding loop of botulinum neurotoxin serotypes B, DC and G is an essential feature to confer their exquisite potency*. PLoS Pathog, 2018. **14**(5): p. e1007048.
55. Aureli, M., S. Grassi, S. Prioni, S. Sonnino, and A. Prinetti, *Lipid membrane domains in the brain*. Biochim Biophys Acta, 2015. **1851**(8): p. 1006-16.
56. Rummel, A., *Two Feet on the Membrane: Uptake of Clostridial Neurotoxins*. Curr Top Microbiol Immunol, 2016.
57. Fernandez-Chacon, R., A. Konigstorfer, S.H. Gerber, J. Garcia, M.F. Matos, C.F. Stevens, N. Brose, J. Rizo, C. Rosenmund, and T.C. Sudhof, *Synaptotagmin I functions as a calcium regulator of release probability*. Nature, 2001. **410**(6824): p. 41-49.
58. Nishiki, T., Y. Kamata, Y. Nemoto, A. Omori, T. Ito, M. Takahashi, and S. Kozaki, *Identification of protein receptor for Clostridium botulinum type B neurotoxin in rat brain synaptosomes*. J Biol Chem, 1994. **269**(14): p. 10498-10503.
59. Dong, M., D.A. Richards, M.C. Goodnough, W.H. Tepp, E.A. Johnson, and E.R. Chapman, *Synaptotagmins I and II mediate entry of botulinum neurotoxin B into cells*. J Cell Biol, 2003. **162**(7): p. 1293-1303.
60. Rummel, A., T. Eichner, T. Weil, T. Karnath, A. Gutcaits, S. Mahrhold, K. Sandhoff, R.L. Proia, K.R. Acharya, H. Bigalke, and T. Binz, *Identification of the protein receptor binding site of botulinum neurotoxins B and G proves the double-receptor concept*. Proc Natl Acad Sci U S A, 2007. **104**(1): p. 359-364.
61. Peng, L., R.P. Berntsson, W.H. Tepp, R.M. Pitkin, E.A. Johnson, P. Stenmark, and M. Dong, *Botulinum neurotoxin D-C uses synaptotagmin I and II as receptors, and human synaptotagmin II is not an effective receptor for type B, D-C and G toxins*. J Cell Sci, 2012. **125**(Pt 13): p. 3233-3242.
62. Chang, W.P. and T.C. Sudhof, *SV2 renders primed synaptic vesicles competent for Ca²⁺-induced exocytosis*. J Neurosci, 2009. **29**(4): p. 883-897.
63. Bartholome, O., P. Van den Ackerveken, J. Sanchez Gil, O. de la Brassinne Bonardeaux, P. Leprince, R. Franzen, and B. Rogister, *Puzzling Out Synaptic Vesicle 2 Family Members Functions*. Front Mol Neurosci, 2017. **10**: p. 148.
64. Dong, M., F. Yeh, W.H. Tepp, C. Dean, E.A. Johnson, R. Janz, and E.R. Chapman, *SV2 is the protein receptor for botulinum neurotoxin A*. Science, 2006. **312**(5773): p. 592-596.
65. Dong, M., H. Liu, W.H. Tepp, E.A. Johnson, R. Janz, and E.R. Chapman, *Glycosylated SV2A and SV2B mediate the entry of botulinum neurotoxin E into neurons*. Mol Biol Cell, 2008. **19**(12): p. 5226-5237.
66. Mahrhold, S., A. Rummel, H. Bigalke, B. Davletov, and T. Binz, *The synaptic vesicle protein 2C mediates the uptake of botulinum neurotoxin A into phrenic nerves*. FEBS Lett, 2006. **580**(8): p. 2011-2014.
67. Mahrhold, S., J. Strotmeier, C. Garcia-Rodriguez, J. Lou, J.D. Marks, A. Rummel, and T. Binz, *Identification of the SV2 protein receptor-binding site of botulinum neurotoxin type E*. Biochem J, 2013. **453**(1): p. 37-47.

REFERENCES

68. Fu, Z., C. Chen, J.T. Barbieri, J.J. Kim, and M.R. Baldwin, *Glycosylated SV2 and gangliosides as dual receptors for botulinum neurotoxin serotype F*. *Biochemistry*, 2009. **48**(24): p. 5631-5641.
69. Rummel, A., K. Hafner, S. Mahrhold, N. Darashchonak, M. Holt, R. Jahn, S. Beermann, T. Karnath, H. Bigalke, and T. Binz, *Botulinum neurotoxins C, E and F bind gangliosides via a conserved binding site prior to stimulation-dependent uptake with botulinum neurotoxin F utilising the three isoforms of SV2 as second receptor*. *J Neurochem*, 2009. **110**(6): p. 1942-1954.
70. Peng, L., W.H. Tepp, E.A. Johnson, and M. Dong, *Botulinum neurotoxin D uses synaptic vesicle protein SV2 and gangliosides as receptors*. *PLoS Pathog*, 2011. **7**(3): p. e1002008.
71. Mahrhold, S., T. Bergstrom, D. Stern, B.G. Dorner, C. Astot, and A. Rummel, *Only the complex N559-glycan in the synaptic vesicle glycoprotein 2C mediates high affinity binding to botulinum neurotoxin serotype A1*. *Biochem J*, 2016. **473**(17): p. 2645-2654.
72. Yao, G., S. Zhang, S. Mahrhold, K.H. Lam, D. Stern, K. Bagramyan, K. Perry, M. Kalkum, A. Rummel, M. Dong, and R. Jin, *N-linked glycosylation of SV2 is required for binding and uptake of botulinum neurotoxin A*. *Nat Struct Mol Biol*, 2016. **23**(7): p. 656-662.
73. Karalewitz, A.P., Z. Fu, M.R. Baldwin, J.J. Kim, and J.T. Barbieri, *Botulinum neurotoxin serotype C associates with dual ganglioside receptors to facilitate cell entry*. *J Biol Chem*, 2012. **287**(48): p. 40806-40816.
74. Strotmeier, J., S. Gu, S. Jutzi, S. Mahrhold, J. Zhou, A. Pich, T. Eichner, H. Bigalke, A. Rummel, R. Jin, and T. Binz, *The biological activity of botulinum neurotoxin type C is dependent upon novel types of ganglioside binding sites*. *Mol Microbiol*, 2011. **81**(1): p. 143-156.
75. Fischer, A. and M. Montal, *Crucial role of the disulfide bridge between botulinum neurotoxin light and heavy chains in protease translocation across membranes*. *J Biol Chem*, 2007. **282**(40): p. 29604-29611.
76. Sudhof, T.C., *The synaptic vesicle cycle*. *Annu Rev Neurosci*, 2004. **27**: p. 509-547.
77. Binz, T., *Clostridial neurotoxin light chains: devices for SNARE cleavage mediated blockade of neurotransmission*. *Curr Top Microbiol Immunol*, 2013. **364**: p. 139-157.
78. Kalb, S.R., J. Baudys, R.P. Webb, P. Wright, T.J. Smith, L.A. Smith, R. Fernandez, B.H. Raphael, S.E. Maslanka, J.L. Pirkle, and J.R. Barr, *Discovery of a novel enzymatic cleavage site for botulinum neurotoxin F5*. *FEBS Lett*, 2012. **586**(2): p. 109-115.
79. Rawlings, N.D. and A.J. Barrett, *Evolutionary families of metallopeptidases*. *Methods Enzymol*, 1995. **248**: p. 183-228.
80. Binz, T., S. Sikorra, and S. Mahrhold, *Clostridial neurotoxins: mechanism of SNARE cleavage and outlook on potential substrate specificity reengineering*. *Toxins (Basel)*, 2010. **2**(4): p. 665-682.
81. Breidenbach, M.A. and A.T. Brunger, *Substrate recognition strategy for botulinum neurotoxin serotype A*. *Nature*, 2004. **432**(7019): p. 925-929.
82. Dorner, M.B., K.M. Schulz, S. Kull, and B.G. Dorner, *Complexity of botulinum neurotoxins: challenges for detection technology*. *Curr Top Microbiol Immunol*, 2013. **364**: p. 219-255.
83. Lindstrom, M. and H. Korkeala, *Laboratory diagnostics of botulism*. *Clin Microbiol Rev*, 2006. **19**(2): p. 298-314.
84. Stern, D., L. von Berg, M. Skiba, M.B. Dorner, and B.G. Dorner, *Replacing the mouse bioassay for diagnostics and potency testing of botulinum neurotoxins – progress and challenges*. *Berl Muench Tieraerztl Wochenschr*, 2018.

REFERENCES

85. Solomon, H. and T. Lilly, *Clostridium botulinum*, in *Bacteriological Analytical Manual, 8th Edition*. 2001, US Food and Drug Administration: Silver Spring MD, USA
86. Sugiyama, H., *Clostridium botulinum* neurotoxin. *Microbiol Rev*, 1980. **44**(3): p. 419-448.
87. Strotmeier, J., G. Willjes, T. Binz, and A. Rummel, *Human synaptotagmin-II is not a high affinity receptor for botulinum neurotoxin B and G: increased therapeutic dosage and immunogenicity*. *FEBS Lett*, 2012. **586**(4): p. 310-313.
88. Sesardic, D., T. Leung, and R. Gaines Das, *Role for standards in assays of botulinum toxins: international collaborative study of three preparations of botulinum type A toxin*. *Biologicals*, 2003. **31**(4): p. 265-276.
89. Bigalke, H. and A. Rummel, *Botulinum Neurotoxins: Qualitative and Quantitative Analysis Using the Mouse Phrenic Nerve Hemidiaphragm Assay (MPN)*. *Toxins (Basel)*, 2015. **7**(12): p. 4895-905.
90. Shin, N.R., S.Y. Yoon, J.H. Shin, Y.J. Kim, G.E. Rhie, B.S. Kim, W.K. Seong, and H.B. Oh, *Development of enrichment semi-nested PCR for Clostridium botulinum types A, B, E, and F and its application to Korean environmental samples*. *Mol Cells*, 2007. **24**(3): p. 329-337.
91. Lindstrom, M., R. Keto, A. Markkula, M. Nevas, S. Hielm, and H. Korkeala, *Multiplex PCR assay for detection and identification of Clostridium botulinum types A, B, E, and F in food and fecal material*. *Appl Environ Microbiol*, 2001. **67**(12): p. 5694-5699.
92. Fach, P., L. Fencia, R. Knutsson, P.R. Wielinga, F. Anniballi, E. Delibato, B. Auricchio, C. Woudstra, J. Agren, B. Segerman, D. de Medici, and B.J. van Rotterdam, *An innovative molecular detection tool for tracking and tracing Clostridium botulinum types A, B, E, F and other botulinum neurotoxin producing Clostridia based on the GeneDisc cyclor*. *Int J Food Microbiol*, 2011. **145 Suppl 1**: p. 145-151.
93. Anniballi, F., B. Auricchio, E. Delibato, M. Antonacci, D. De Medici, and L. Fencia, *Multiplex real-time PCR SYBR Green for detection and typing of group III Clostridium botulinum*. *Vet Microbiol*, 2012. **154**(3-4): p. 332-338.
94. Capek, P. and T.J. Dickerson, *Sensing the deadliest toxin: technologies for botulinum neurotoxin detection*. *Toxins (Basel)*, 2010. **2**(1): p. 24-53.
95. Singh, A.K., L.H. Stanker, and S.K. Sharma, *Botulinum neurotoxin: where are we with detection technologies?* *Crit Rev Microbiol*, 2013. **39**(1): p. 43-56.
96. Pauly, D., S. Kirchner, B. Stoermann, T. Schreiber, S. Kaulfuss, R. Schade, R. Zbinden, M.A. Avondet, M.B. Dorner, and B.G. Dorner, *Simultaneous quantification of five bacterial and plant toxins from complex matrices using a multiplexed fluorescent magnetic suspension assay*. *Analyst*, 2009. **134**(10): p. 2028-2039.
97. Braeckmans, K., S.C. De Smedt, M. Leblans, R. Pauwels, and J. Demeester, *Encoding microcarriers: present and future technologies*. *Nat Rev Drug Discov*, 2002. **1**(6): p. 447-456.
98. Sikorra, S., T. Henke, T. Galli, and T. Binz, *Substrate recognition mechanism of VAMP/synaptobrevin-cleaving clostridial neurotoxins*. *J Biol Chem*, 2008. **283**(30): p. 21145-21152.
99. Whitmarsh, R.C., W.H. Tepp, M. Bradshaw, G. Lin, C.L. Pier, J.M. Scherf, E.A. Johnson, and S. Pellett, *Characterization of botulinum neurotoxin A subtypes 1 through 5 by investigation of activities in mice, in neuronal cell cultures, and in vitro*. *Infect Immun*, 2013. **81**(10): p. 3894-3902.

REFERENCES

100. Henkel, J.S., M. Jacobson, W. Tepp, C. Pier, E.A. Johnson, and J.T. Barbieri, *Catalytic properties of botulinum neurotoxin subtypes A3 and A4*. *Biochemistry*, 2009. **48**(11): p. 2522-2528.
101. Evans, E.R., P.J. Skipper, and C.C. Shone, *An assay for botulinum toxin types A, B and F that requires both functional binding and catalytic activities within the neurotoxin*. *J Appl Microbiol*, 2009. **107**(4): p. 1384-1391.
102. Yamamoto, H., T. Ida, H. Tsutsuki, M. Mori, T. Matsumoto, T. Kohda, M. Mukamoto, N. Goshima, S. Kozaki, and H. Ihara, *Specificity of botulinum protease for human VAMP family proteins*. *Microbiol Immunol*, 2012. **56**(4): p. 245-253.
103. Kumar, R., R.V. Kukreja, S. Cai, and B.R. Singh, *Differential role of molten globule and protein folding in distinguishing unique features of botulinum neurotoxin*. *Biochim Biophys Acta*, 2014. **1844**(6): p. 1145-1152.
104. Park, S., Y.M. Shin, J.J. Song, and H. Yang, *Facile electrochemical detection of botulinum neurotoxin type E using a two-step proteolytic cleavage*. *Biosens Bioelectron*, 2015. **72**: p. 211-217.
105. Moura, H., R.R. Terilli, A.R. Woolfitt, M. Gallegos-Candela, L.G. McWilliams, M.I. Solano, J.L. Pirkle, and J.R. Barr, *Studies on botulinum neurotoxins type /C1 and mosaic/DC using Endopep-MS and proteomics*. *FEMS Immunol Med Microbiol*, 2011. **61**(3): p. 288-300.
106. Wang, H.H., S. Riding, P. Lindo, and B.R. Singh, *Endopeptidase activities of botulinum neurotoxin type B complex, holotoxin, and light chain*. *Appl Environ Microbiol*, 2010. **76**(19): p. 6658-6663.
107. Mizanur, R.M., R.G. Stafford, and S.A. Ahmed, *Cleavage of SNAP25 and its shorter versions by the protease domain of serotype A botulinum neurotoxin*. *PLoS One*, 2014. **9**(4): p. e95188.
108. Shone, C.C. and A.K. Roberts, *Peptide substrate specificity and properties of the zinc-endopeptidase activity of botulinum type B neurotoxin*. *Eur J Biochem*, 1994. **225**(1): p. 263-270.
109. Nuss, J.E., L.M. Wanner, L.E. Tressler, and S. Bavari, *The osmolyte trimethylamine N-oxide (TMAO) increases the proteolytic activity of botulinum neurotoxin light chains A, B, and E: implications for enhancing analytical assay sensitivity*. *J Biomol Screen*, 2010. **15**(8): p. 928-936.
110. Jones, R.G., M. Ochiai, Y. Liu, T. Ekong, and D. Sesardic, *Development of improved SNAP25 endopeptidase immuno-assays for botulinum type A and E toxins*. *J Immunol Methods*, 2008. **329**(1-2): p. 92-101.
111. Schmidt, J.J. and K.A. Bostian, *Endoproteinase activity of type A botulinum neurotoxin: substrate requirements and activation by serum albumin*. *J Protein Chem*, 1997. **16**(1): p. 19-26.
112. Ferracci, G., S. Marconi, C. Mazuet, E. Jover, M.P. Blanchard, M. Seagar, M. Popoff, and C. Leveque, *A label-free biosensor assay for botulinum neurotoxin B in food and human serum*. *Anal Biochem*, 2011. **410**(2): p. 281-288.
113. Anne, C., F. Cornille, C. Lenoir, and B.P. Roques, *High-throughput fluorogenic assay for determination of botulinum type B neurotoxin protease activity*. *Anal Biochem*, 2001. **291**(2): p. 253-61.
114. Dong, M., W.H. Tepp, E.A. Johnson, and E.R. Chapman, *Using fluorescent sensors to detect botulinum neurotoxin activity in vitro and in living cells*. *Proc Natl Acad Sci U S A*, 2004. **101**(41): p. 14701-14706.

REFERENCES

115. Rasooly, R. and P.M. Do, *Development of an in vitro activity assay as an alternative to the mouse bioassay for Clostridium botulinum neurotoxin type A*. Appl Environ Microbiol, 2008. **74**(14): p. 4309-4313.
116. Bagramyan, K., J.R. Barash, S.S. Arnon, and M. Kalkum, *Attomolar detection of botulinum toxin type A in complex biological matrices*. PLoS One, 2008. **3**(4): p. e2041.
117. Shine, N.R., Crawford, K. R., and Eaton, L. J. A., *Substrate peptides and assays for detecting and measuring proteolytic activity of serotype A neurotoxin from clostridium botulinum*, U.S. Patent 6,504,006, July 1, 2003
118. Rasooly, R., L.H. Stanker, J.M. Carter, P.M. Do, L.W. Cheng, X. He, and D.L. Brandon, *Detection of botulinum neurotoxin-A activity in food by peptide cleavage assay*. Int J Food Microbiol, 2008. **126**(1-2): p. 135-139.
119. Ouimet, T., S. Duquesnoy, H. Poras, and M.C. Fournie-Zaluski, *Comparison of Fluorogenic Peptide Substrates PL50, SNAPtide, and BoTest A/E for BoNT/A Detection and Quantification: Exosite Binding Confers High-Assay Sensitivity (vol 18, pg 726, 2013)*. J Biomol Screen, 2014. **19**(8): p. 1231-1231.
120. Boyer, A.E., H. Moura, A.R. Woolfitt, S.R. Kalb, L.G. McWilliams, A. Pavlopoulos, J.G. Schmidt, D.L. Ashley, and J.R. Barr, *From the mouse to the mass spectrometer: detection and differentiation of the endoprotease activities of botulinum neurotoxins A-G by mass spectrometry*. Anal Chem, 2005. **77**(13): p. 3916-3924.
121. Kalb, S.R., H. Moura, A.E. Boyer, L.G. McWilliams, J.L. Pirkle, and J.R. Barr, *The use of Endopep-MS for the detection of botulinum toxins A, B, E, and F in serum and stool samples*. Anal Biochem, 2006. **351**(1): p. 84-92.
122. Wang, D., J. Baudys, S.R. Kalb, and J.R. Barr, *Improved detection of botulinum neurotoxin type A in stool by mass spectrometry*. Anal Biochem, 2011. **412**(1): p. 67-73.
123. Kalb, S.R., J. Lou, C. Garcia-Rodriguez, I.N. Geren, T.J. Smith, H. Moura, J.D. Marks, L.A. Smith, J.L. Pirkle, and J.R. Barr, *Extraction and inhibition of enzymatic activity of botulinum neurotoxins/A1, /A2, and /A3 by a panel of monoclonal anti-BoNT/A antibodies*. PLoS One, 2009. **4**(4): p. e5355.
124. Kalb, S.R., W.I. Santana, I.N. Geren, C. Garcia-Rodriguez, J. Lou, T.J. Smith, J.D. Marks, L.A. Smith, J.L. Pirkle, and J.R. Barr, *Extraction and inhibition of enzymatic activity of botulinum neurotoxins /B1, /B2, /B3, /B4, and /B5 by a panel of monoclonal anti-BoNT/B antibodies*. BMC Biochem, 2011. **12**: p. 58.
125. Hu, X., S. Kang, C. Lefort, M. Kim, and M.M. Jin, *Combinatorial libraries against libraries for selecting neoepitope activation-specific antibodies*. Proc Natl Acad Sci USA, 2010. **107**(14): p. 6252-6257.
126. Fernandez-Salas, E., J. Wang, Y. Molina, J.B. Nelson, B.P.S. Jacky, and K.R. Aoki, *Botulinum Neurotoxin Serotype a Specific Cell-Based Potency Assay to Replace the Mouse Bioassay*. Plos One, 2012. **7**(11): p. e49516.
127. Leveque, C., G. Ferracci, Y. Maulet, C. Grand-Masson, M.P. Blanchard, M. Seagar, and O. El Far, *A substrate sensor chip to assay the enzymatic activity of Botulinum neurotoxin A*. Biosens Bioelectron, 2013. **49**: p. 276-281.
128. Leveque, C., G. Ferracci, Y. Maulet, C. Mazuet, M. Popoff, M. Seagar, and O. El Far, *Direct biosensor detection of botulinum neurotoxin endopeptidase activity in sera from patients with type A botulism*. Biosens Bioelectron, 2014. **57**: p. 207-212.
129. Leveque, C., G. Ferracci, Y. Maulet, C. Mazuet, M.R. Popoff, M.P. Blanchard, M. Seagar, and O. El Far, *An optical biosensor assay for rapid dual detection of Botulinum neurotoxins A and E*. Sci Rep, 2015. **5**: p. e17953.

REFERENCES

130. Gray, B., V. Cadd, M. Elliott, and M. Beard, *The in vitro detection of botulinum neurotoxin-cleaved endogenous VAMP is epitope-dependent*. *Toxicol In Vitro*, 2018. **48**: p. 255-261.
131. Jones, R.G., Y. Liu, and D. Sesardic, *New highly specific botulinum type C1 endopeptidase immunoassays utilising SNAP25 or Syntaxin substrates*. *Journal of Immunological Methods* 2009. **343**(1): p. 21-27.
132. Wictome, M., K. Newton, K. Jameson, B. Hallis, P. Dunnigan, E. Mackay, S. Clarke, R. Taylor, J. Gaze, K. Foster, and C. Shone, *Development of an in vitro bioassay for Clostridium botulinum type B neurotoxin in foods that is more sensitive than the mouse bioassay*. *Appl Environ Microbiol*, 1999. **65**(9): p. 3787-3792.
133. Liu, Y.Y., P. Rigsby, D. Sesardic, J.D. Marks, and R.G. Jones, *A functional dual-coated (FDC) microtiter plate method to replace the botulinum toxin LD50 test*. *Anal Biochem*, 2012. **425**(1): p. 28-35.
134. Jones, R.G.A. and J.D. Marks, *Use of a new functional dual coating (FDC) assay to measure low toxin levels in serum and food samples following an outbreak of human botulism*. *J Med Microbiol*, 2013. **62**: p. 828-835.
135. Rheume, C., B.B. Cai, J. Wang, E. Fernandez-Salas, K.R. Aoki, J. Francis, and R.S. Broide, *A Highly Specific Monoclonal Antibody for Botulinum Neurotoxin Type A-Cleaved SNAP25*. *Toxins (Basel)*, 2015. **7**(7): p. 2354-2370.
136. Hallis, B., B.A. James, and C.C. Shone, *Development of novel assays for botulinum type A and B neurotoxins based on their endopeptidase activities*. *J. Clin. Microbiol.*, 1996. **34**(8): p. 1934-8.
137. Wild, E., U. Bonifas, J. Klimek, J.H. Troschmeier, B. Kramer, B. Kegel, and H.A. Behrendorf-Nicol, *In vitro potency determination of botulinum neurotoxin B based on its receptor-binding and proteolytic characteristics*. *Toxicol In Vitro*, 2016. **34**: p. 97-104.
138. Hansbauer, E., *Stationäre und mobile Verfahren zur Detektion und Differenzierung biologischer Toxine*. 2016, Freie Universität Berlin: Berlin.
139. Hansbauer, E.M., M. Skiba, T. Endermann, J. Weisemann, D. Stern, M.B. Dorner, F. Finkenwirth, J. Wolf, W. Luginbuhl, U. Messelhauser, L. Bellanger, C. Woudstra, A. Rummel, P. Fach, and B.G. Dorner, *Detection, differentiation, and identification of botulinum neurotoxin serotypes C, CD, D, and DC by highly specific immunoassays and mass spectrometry*. *Analyst*, 2016. **141**(18): p. 5281-5297.
140. Simon, S., U. Fiebig, Y. Liu, R. Tierney, J. Dano, S. Worbs, T. Endermann, M.C. Nevers, H. Volland, D. Sesardic, and M.B. Dorner, *Recommended Immunological Strategies to Screen for Botulinum Neurotoxin-Containing Samples*. *Toxins (Basel)*, 2015. **7**(12): p. 5011-5034.
141. Hall, I.C., *A COLLECTION OF ANAEROBIC BACTERIA*. *Science*, 1928. **68**(1754): p. 141-2.
142. Ringe, H., M. Schuelke, S. Weber, B.G. Dorner, S. Kirchner, and M.B. Dorner, *Infant botulism: is there an association with thiamine deficiency?* *Pediatrics*, 2014. **134**(5): p. e1436-40.
143. Mad'arova, L., B.G. Dorner, L. Schaade, V. Donath, M. Avdicova, M. Fatkulina, J. Strharsky, I. Sedliacikova, C. Klement, and M.B. Dorner, *Reoccurrence of botulinum neurotoxin subtype A3 inducing food-borne botulism, Slovakia, 2015*. *Euro Surveill*, 2017. **22**(32).
144. Hutson, R.A., D.E. Thompson, P.A. Lawson, R.P. Schocken-Itturino, E.C. Bottger, and M.D. Collins, *Genetic interrelationships of proteolytic Clostridium botulinum types A, B,*

REFERENCES

- and F and other members of the *Clostridium botulinum* complex as revealed by small-subunit rRNA gene sequences. *Antonie Van Leeuwenhoek*, 1993. **64**(3-4): p. 273-83.
145. Kirchner, S., K.M. Kramer, M. Schulze, D. Pauly, D. Jacob, F. Gessler, A. Nitsche, B.G. Dorner, and M.B. Dorner, *Pentaplexed quantitative real-time PCR assay for the simultaneous detection and quantification of botulinum neurotoxin-producing clostridia in food and clinical samples*. *Appl Environ Microbiol*, 2010. **76**(13): p. 4387-4395.
146. Meyer, K.F. and B.J. Dubovsky, *The Distribution of the Spores of B. botulinus in the United States. IV*. *The Journal of Infectious Diseases*, 1922. **31**(6): p. 559-594.
147. Absher, M., *CHAPTER 1 - Hemocytometer Counting*, in *Tissue Culture*. 1973, Academic Press. p. 395-397.
148. Kohler, G. and C. Milstein, *Continuous cultures of fused cells secreting antibody of predefined specificity*. *Nature*, 1975. **256**(5517): p. 495-497.
149. Laemmli, U.K., *Cleavage of structural proteins during the assembly of the head of bacteriophage T4*. *Nature*, 1970. **227**(5259): p. 680-685.
150. Schagger, H. and G. von Jagow, *Tricine-sodium dodecyl sulfate-polyacrylamide gel electrophoresis for the separation of proteins in the range from 1 to 100 kDa*. *Anal Biochem*, 1987. **166**(2): p. 368-379.
151. Neuhoff, V., N. Arold, D. Taube, and W. Ehrhardt, *Improved staining of proteins in polyacrylamide gels including isoelectric focusing gels with clear background at nanogram sensitivity using Coomassie Brilliant Blue G-250 and R-250*. *Electrophoresis*, 1988. **9**(6): p. 255-262.
152. Blum, H., H. Beier, and H.J. Gross, *Improved silver staining of plant proteins, RNA and DNA in polyacrylamide gels*. *Electrophoresis*, 1987. **8**(2): p. 93-99.
153. Lambert, J.H. and E. Anding, *Lamberts Photometrie: (Photometria, sive De mensura et gradibus luminis, colorum et umbrae) (1760)*. 1892: W. Engelmann.
154. Ritchie, T.K., Y.V. Grinkova, T.H. Bayburt, I.G. Denisov, J.K. Zolnerciks, W.M. Atkins, and S.G. Sligar, *Chapter 11 - Reconstitution of membrane proteins in phospholipid bilayer nanodiscs*. *Methods Enzymol*, 2009. **464**: p. 211-231.
155. Waterboer, T., *Multiplex-Serologie - Simultane Analyse von Antikörper-Antworten gegen humane Papillomviren (HPV) mit Protein-Arrays* 2005, Ruprecht-Karls-Universität Heidelberg Heidelberg.
156. Hodnik, V. and G. Anderluh, *Toxin detection by surface plasmon resonance*. *Sensors (Basel)*, 2009. **9**(3): p. 1339-1354.
157. Grubbs, F.E., *Sample Criteria for Testing Outlying Observations*. *Ann Math Statist*, 1950. **21**: p. 27-58.
158. Klein, B., *Versuchsplanung - DoE: Einführung in die Taguchi/Shainin-Methodik*. 2007: Oldenbourg.
159. GraphPad Software, I., *Equation: log(inhibitor) vs. response -- Variable slope*, Available from: https://www.graphpad.com/guides/prism/7/curve-fitting/index.htm?reg_dr_inhibit_variable.htm [cited June, 02 2018]
160. GraphPad Software, I., *Equation: Michaelis-Menten model*, Available from: https://www.graphpad.com/guides/prism/7/curve-fitting/index.htm?reg_michaelis_menten_enzyme.htm [cited June, 02 2018]
161. Augustine, S.A., K.J. Simmons, T.N. Eason, S.M. Griffin, C.L. Curioso, L.J. Wymer, G.S. Fout, A.C. Grimm, K.H. Oshima, and A. Dufour, *Statistical approaches to developing a multiplex immunoassay for determining human exposure to environmental pathogens*. *J Immunol Methods*, 2015. **425**: p. 1-9.

REFERENCES

162. Ramakrishna, U.S., J.J. Kingston, M. Harishchandra Sripathi, and H.V. Batra, *Taguchi optimization of duplex PCR for simultaneous identification of Staphylococcus aureus and Clostridium perfringens alpha toxins*. FEMS Microbiol Lett, 2013. **340**(2): p. 93-100.
163. Savari, M., S.H. Zarkesh Esfahani, M. Edalati, and D. Biria, *Optimizing conditions for production of high levels of soluble recombinant human growth hormone using Taguchi method*. Protein Expr Purif, 2015. **114**: p. 128-135.
164. Yari, K., S.S. Fatemi, and M. Tavallaei, *Optimization of the BoNT/A-Hc expression in recombinant Escherichia coli using the Taguchi statistical method*. Biotechnol Appl Biochem, 2010. **56**(1): p. 35-42.
165. Auton, M. and D.W. Bolen, *Predicting the energetics of osmolyte-induced protein folding/unfolding*. Proc Natl Acad Sci U S A, 2005. **102**(42): p. 15065-15068.
166. Ma, J., I.M. Pazos, and F. Gai, *Microscopic insights into the protein-stabilizing effect of trimethylamine N-oxide (TMAO)*. Proc Natl Acad Sci U S A, 2014. **111**(23): p. 8476-8481.
167. Houk, K.N., A.G. Leach, S.P. Kim, and X. Zhang, *Binding affinities of host-guest, protein-ligand, and protein-transition-state complexes*. Angew Chem Int Ed Engl, 2003. **42**(40): p. 4872-4897.
168. Feinberg, H., J.W. Saldanha, L. Diep, A. Goel, A. Widom, G.M. Veldman, W.I. Weis, D. Schenk, and G.S. Basi, *Crystal structure reveals conservation of amyloid-beta conformation recognized by 3D6 following humanization to bapineuzumab*. Alzheimers Res Ther, 2014. **6**(3): p. 31.
169. Bagramyan, K., B.E. Kaplan, L.W. Cheng, J. Strotmeier, A. Rummel, and M. Kalkum, *Substrates and controls for the quantitative detection of active botulinum neurotoxin in protease-containing samples*. Anal Chem, 2013. **85**(11): p. 5569-76.
170. Hallis, B., B.A. James, and C.C. Shone, *Development of novel assays for botulinum type A and B neurotoxins based on their endopeptidase activities*. J Clin Microbiol, 1996. **34**(8): p. 1934-1938.
171. Ruge, D.R., F.M. Dunning, T.M. Piazza, B.E. Molles, M. Adler, F.N. Zeytin, and W.C. Tucker, *Detection of six serotypes of botulinum neurotoxin using fluorogenic reporters*. Anal Biochem, 2011. **411**(2): p. 200-209.
172. Bjornstad, K., A. Tevell Aberg, S.R. Kalb, D. Wang, J.R. Barr, U. Bondesson, and M. Hedeland, *Validation of the Endopep-MS method for qualitative detection of active botulinum neurotoxins in human and chicken serum*. Anal Bioanal Chem, 2014. **406**(28): p. 7149-7161.
173. Dunning, F.M., D.R. Ruge, T.M. Piazza, L.H. Stanker, F.N. Zeytin, and W.C. Tucker, *Detection of botulinum neurotoxin serotype A, B, and F proteolytic activity in complex matrices with picomolar to femtomolar sensitivity*. Appl Environ Microbiol, 2012. **78**(21): p. 7687-7697.
174. Rosen, O., E. Ozeri, A. Barnea, A.B. David, and R. Zichel, *Development of an Innovative in Vitro Potency Assay for Anti-Botulinum Antitoxins*. Toxins (Basel), 2016. **8**(10): p. 276.
175. Weingart, O.G. and M.J. Loessner, *Nerve cell-mimicking liposomes as biosensor for botulinum neurotoxin complete physiological activity*. Toxicol Appl Pharmacol, 2016. **313**: p. 16-23.
176. Gregory, R.W., W.E. Werner, and C. Ruegg, *A quantitative bifunctional in vitro potency assay for botulinum neurotoxin serotype A*. J Pharmacol Toxicol Methods, 2014. **69**(2): p. 103-107.
177. Bradshaw, M., W.H. Tepp, R.C. Whitemarsh, S. Pellett, and E.A. Johnson, *Holotoxin Activity of Botulinum Neurotoxin Subtype A4 Originating from a Nontoxigenic*

REFERENCES

- Clostridium botulinum* Expression System. Appl Environ Microbiol, 2014. **80**(23): p. 7415-7422.
178. Tepp, W.H., G. Lin, and E.A. Johnson, *Purification and characterization of a novel subtype a3 botulinum neurotoxin*. Appl Environ Microbiol, 2012. **78**(9): p. 3108-3113.
179. Lin, G., W.H. Tepp, C.L. Pier, M.J. Jacobson, and E.A. Johnson, *Expression of the Clostridium botulinum A2 neurotoxin gene cluster proteins and characterization of the A2 complex*. Appl Environ Microbiol, 2010. **76**(1): p. 40-47.
180. Jacobson, M.J., G. Lin, W. Tepp, J. Dupuy, P. Stenmark, R.C. Stevens, and E.A. Johnson, *Purification, modeling, and analysis of botulinum neurotoxin subtype A5 (BoNT/A5) from Clostridium botulinum strain A661222*. Appl Environ Microbiol, 2011. **77**(12): p. 4217-4222.

8 PUBLICATIONS

von Berg, L., D. Stern, D. Pauly, S. Mahrhold, J. Weisemann, L. Försterling, E.M. Hansbauer, C. Müller, M.A. Avondet, M.B. Dorner, A. Rummel, B.G. Dorner, *Bead-based duplex-assays for functional detection of botulinum neurotoxin serotypes A to F by novel monoclonal neoepitope-antibodies*. Scientific Reports, Submitted

Stern, D., L. von Berg, M. Skiba, M.B. Dorner, B.G. Dorner, *Replacing the mouse bioassay for diagnostics and potency testing of botulinum neurotoxins – progress and challenges*. Berl Muench Tieraerztl Wochenschr, 2018. DOI: 10.2376/0005-9366-17110

Stern, D., J. Weisemann, A. Le Blanc, L. von Berg, S. Mahrhold, J. Piesker, M. Laue, P.B. Lupp, M.B. Dorner, B.G. Dorner, and A. Rummel, *A lipid-binding loop of botulinum neurotoxin serotypes B, DC and G is an essential feature to confer their exquisite potency*. PLoS Pathog, 2018. 14(5): p. e1007048. DOI: 10.1371/journal.ppat.1007048

von Berg, L., D. Stern, J. Weisemann, A. Rummel, M.B. Dorner, B.G. Dorner, *Optimization of SNAP-25 and VAMP-2 cleavage by Botulinum Neurotoxin Serotypes A to F employing Taguchi Design-of-Experiments*. In preparation

9 POSTERS AND TALKS

von Berg, L., D. Stern, D. Pauly, S. Mahrhold, J. Weisemann, L. Försterling, E.M. Hansbauer, C. Müller, M.A. Avondet, M.B. Dorner, A. Rummel, B.G. Dorner, *Neoepitope specific monoclonal antibodies to detect the catalytic activity of botulinum neurotoxin serotypes A to F*. 2nd German Pharm-Tox Summit and 83rd Annual Meeting of the German Society for Experimental and Clinical Pharmacology and Toxicology (DGPT) 2017, Heidelberg, Germany. Talk (the talk was awarded by the DGPT with the price for the best short talk)

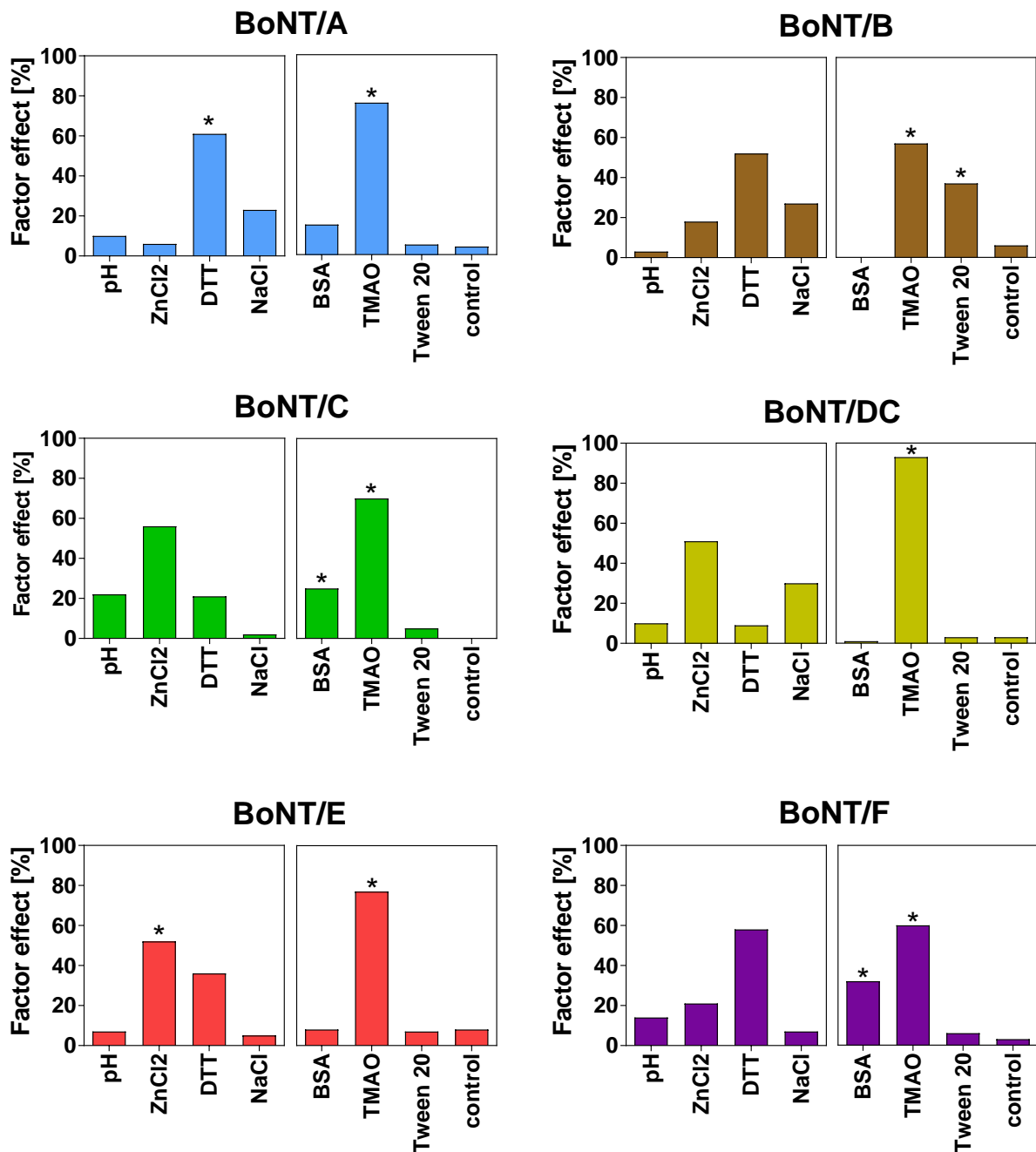
von Berg, L., D. Stern, D. Pauly, L. Försterling, J. Weisemann, S. Mahrhold, A. Rummel, M.B. Dorner, B.G. Dorner, *Functional Detection of Botulinum Neurotoxin Serotypes A–F using Neoepitope-Specific Monoclonal Antibodies*. Junior Scientist Zoonoses Meeting 2016, Göttingen, Germany. Poster and Short Talk

von Berg, L., D. Stern, A. Rummel, M.B. Dorner, B.G. Dorner, *Optimization of Botulinum Neurotoxin Synaptic Protein Cleavage by the Taguchi Design-of-Experiment Method*. German Symposium on Zoonoses Research 2014 and 7th International Conference on Emerging Diseases, Hamburg, Germany. Poster

10 CURRICULUM VITAE

For reasons of data protection,
the curriculum vitae is not included in the online version.

11 APPENDIX



Appendix Figure 1: Factor effects of factors analysed in L9-array 1 (left image of each panel) and L9-array 2 (right image of each panel). The effect of each factor (in %) was determined by ANOVA. Bars marked with an asterisk indicate significant factors ($p < 0.05$).

Detailed results of ANOVA of L9-array experiments 1 and 2

DF = degrees of freedom; SQ = sumsquares; V = variance. *Italic numbers indicate values used for error estimation; bold numbers indicate significant factors ($p < 0.05$)*

Appendix Table 1: Results of ANOVA of L9-array experiments 1 and 2 of BoNT/A.

Factor	DF	SQ	V	F-Value	p [%]	<i>p value</i>
pH	2	<i>11</i>	5.4	1.23	10	0.38
ZnCl ₂	2	<i>7</i>	3.4	0.77	6	0.52
DTT	2	69	34.3	7.86	61	0.04
NaCl	2	26	12.8	2.93	23	0.16
BSA	2	134	67	3	15	0.14
TMAO	2	688	344	17	76	0.01
Tween 20	2	47	23	1	5	0.41
empty (control)	2	35	18	1	4	0.49

Appendix Table 2: Results of ANOVA of L9-array experiments 1 and 2 of BoNT/B.

Factor	DF	SQ	V	F-Value	p [%]	<i>p value</i>
pH	2	<i>4</i>	2	0	3	0.75
ZnCl ₂	2	<i>24</i>	12	2	18	0.29
DTT	2	68	34	5	52	0.09
NaCl	2	35	17	2	27	0.12
BSA	2	<i>0</i>	0	0	0	0.95
TMAO	2	38	19	18	57	0.01
Tween 20	2	24	12	12	37	0.02
empty (control)	2	<i>4</i>	2	2	6	0.26

Appendix Table 3: Results of ANOVA of L9-array experiments 1 and 2 of BoNT/C.

Factor	DF	SQ	V	F-Value	p [%]	<i>p value</i>
pH	2	34	17	2	22	0.25
ZnCl ₂	2	86	43	5	56	0.08
DTT	2	32	16	2	21	0.27
NaCl	2	2	1	0	2	0.88
BSA	2	3	1	10	25	0.03

APPENDIX

TMAO	2	8	4	27	70	0.005
Tween 20	2	1	0	2	5	0.26
empty (control)	2	0	0	0	0	0.96

Appendix Table 4: Results of ANOVA of L9-array experiments 1 and 2 of BoNT/DC.

Factor	DF	SQ	V	F-Value	p [%]	<i>p</i> value
pH	2	28	14	1	10	0.43
ZnCl ₂	2	147	74	5	51	0.07
DTT	2	26	13	1	9	0.45
NaCl	2	85	42	3	30	0.15
BSA	2	2	1	0	1	0.673
TMAO	2	229	115	48	93	0.002
Tween 20	2	7	4	2	3	0.32
empty (control)	2	7	4	2	3	0.32

Appendix Table 5: Results of ANOVA of L9-array experiments 1 and 2 of BoNT/E.

Factor	DF	SQ	V	F-Value	p [%]	<i>p</i> value
pH	2	12	6	1	7	0.40
ZnCl ₂	2	87	43	9	52	0.04
DTT	2	60	30	6	36	0.06
NaCl	2	8	4	1	5	0.50
BSA	2	58	29	1	8	0.431
TMAO	2	557	279	10	77	0.03
Tween 20	2	54	27	1	7	0.45
empty (control)	2	56	28	1	8	0.44

Appendix Table 6: Results of ANOVA of L9-array experiments 1 and 2 of BoNT/F.

Factor	DF	SQ	V	F-Value	p [%]	<i>p</i> value
pH	2	24	12	1	14	0.35
ZnCl ₂	2	36	18	2	21	0.24
DTT	2	99	50	6	58	0.07
NaCl	2	11	6	1	7	0.58
BSA	2	7	4	7	32	0.05

APPENDIX

TMAO	2	14	7	13	60	0.02
Tween 20	2	1	1	1	6	0.35
empty (control)	2	1	0	1	3	0.58

Immunization schemes and development of antibody titres of all fusions performed

Fusion #1

Target neopeptides: Neo-B, Neo-D, Neo-F (C-terminal neopeptides)

Mouse Strain: NMRI

Isolated Neo-mAbs: VAMP/F/153, VAMP/F/425, VAMP/F/521, VAMP/F/1333, VAMP/B/226, VAMP/B/1148

Appendix Table 7: Immunization scheme of mouse subjected to fusion #1.

Immunization	Day ^a	Antigen ^b	Adjuvant ^c
1	0	Neo-F (C), Neo-B (C), Neo-D (C), 33.3 µg each	FCA
2	25	Neo-F (C), Neo-B (C), Neo-D (C), 33.3 µg each	FIA
3	53	Neo-F (C), Neo-B (C), Neo-D (C), 33.3 µg each	FIA
4	330	Neo-F (C), Neo-B (C), Neo-D (C), 33.3 µg each	FIA
5	358	Neo-F (C), Neo-B (C), Neo-D (C), 33.3 µg each	FIA
6	386	Neo-F (C), Neo-B (C), Neo-D (C), 66.6 µg each	–
7	387	Neo-F (C), Neo-B (C), Neo-D (C), 66.6 µg each	–
8	388	Neo-F (C), Neo-B (C), Neo-D (C), 66.6 µg each	–
	389	Fusion	

^a The first three immunizations (shown in grey) were performed before the start of the thesis.

^b see Table 11 in Material and Method section 4.1.5

^c FCA = Freund's complete adjuvant; FIA = Freund's incomplete adjuvant

Fusion #2

Target neopeptides: Neo-B, Neo-C, Neo-E (N- and C-terminal neopeptides)

Mouse Strain: NMRI

Isolated Neo-mAbs: SNAP/C/2207

Appendix Table 8: Immunization scheme of mouse subjected to fusion #2.

Immunization	Day	Antigen ^a	Adjuvant ^b
1	0	Neo-B (C), Neo-B (N), Neo-C (C), Neo-C (N), Neo-E (C), Neo-E (N), 16.7 µg each	FCA
2	28	Neo-B (C), Neo-B (N), Neo-C (C), Neo-C (N), Neo-E (C), Neo-E (N), 16.7 µg each	FIA
3	56	Neo-C (C), Neo-C (N), Neo-E (C), Neo-E (N), 25 µg each	FIA
4	85	Neo-C (C), Neo-C (N), Neo-E (C), Neo-E (N), 25 µg each	FIA

APPENDIX

5	111	Neo-C (C), Neo-C (N), Neo-E (C), Neo-E (N), 50 µg each	–
6	112	Neo-C (C), Neo-C (N), Neo-E (C), Neo-E (N), 50 µg each	–
7	113	Neo-C (C), Neo-C (N), Neo-E (C), Neo-E (N), 50 µg each	–
	114	Fusion	

^asee Table 11 in Material and Method section 4.1.5

^b FCA = Freund's complete adjuvant; FIA = Freund's incomplete adjuvant

Fusion #3

Target neopeptides: Neo-B, Neo-C, Neo-E (N- and C-terminal neopeptides)

Mouse Strain: NMRI

Isolated Neo-mAbs: VAMP/B/151, SNAP/33

Appendix Table 9: Immunization scheme of mouse subjected to fusion #3.

Immunization	Day	Antigen ^a	Adjuvant ^b
1	0	Neo-B (C), Neo-B (N), Neo-C (C), Neo-C (N), Neo-E (C), Neo-E (N), 16.7 µg each	FCA
2	28	Neo-B (C), Neo-B (N), Neo-C (C), Neo-C (N), Neo-E (C), Neo-E (N), 16.7 µg each	FIA
3	56	Neo-C (C), Neo-C (N), Neo-E (C), Neo-E (N), 25 µg each	FIA
4	169	Neo-B (N), Neo-E (C), 50 µg each	FIA
5	213	Neo-B (N), Neo-E (C), 50 µg each	FIA
6	246	Neo-B (N), Neo-E (C), 50 µg each	–
7	247	Neo-B (N), Neo-E (C), 50 µg each	–
8	248	Neo-B (N), Neo-E (C), 50 µg each	–
	249	Fusion	

^asee Table 11 in Material and Method section 4.1.5

^b FCA = Freund's complete adjuvant; FIA = Freund's incomplete adjuvant

Fusion #4

Target neopeptide: Neo-C (C-terminal neopeptide)

Mouse Strain: NMRI

Isolated Neo-mAbs: SNAP/C/5593

Appendix Table 10: Immunization scheme of mouse subjected to fusion #4.

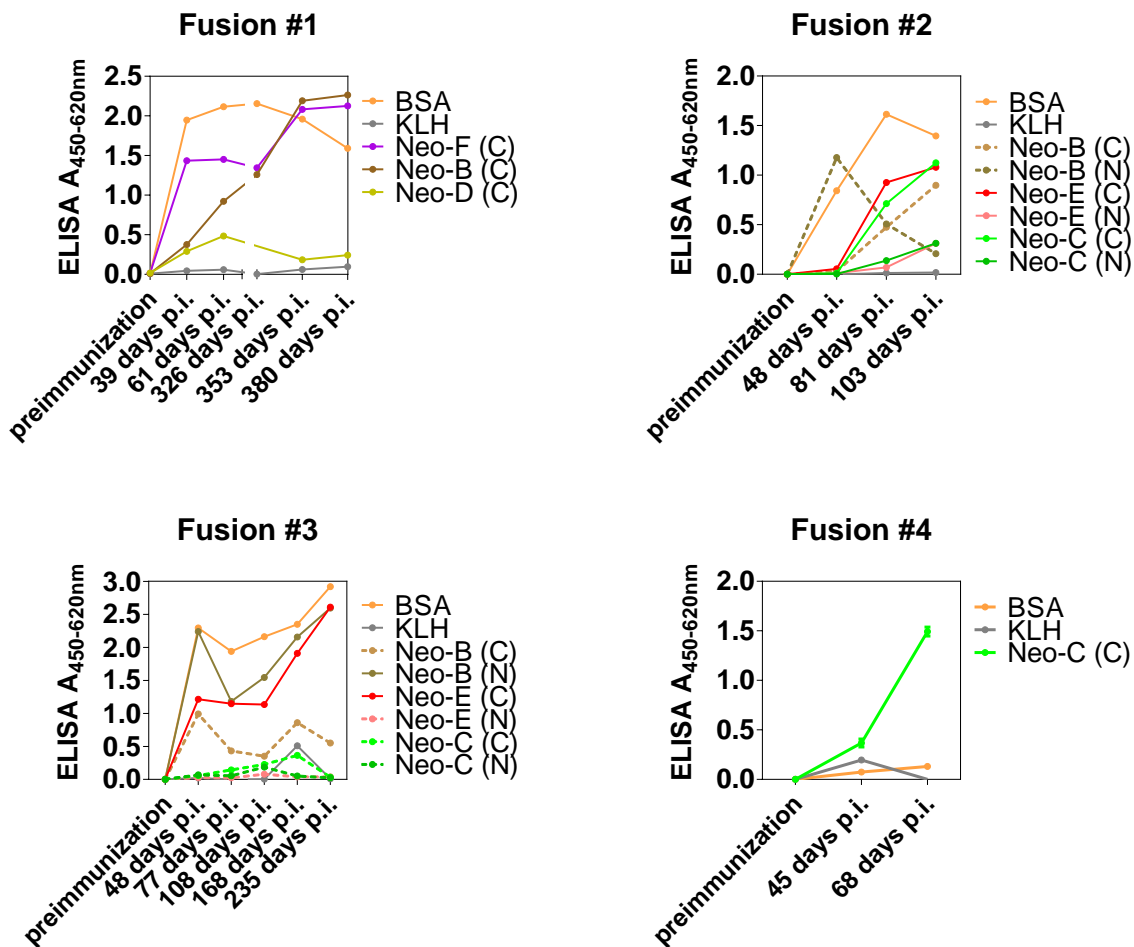
Immunization	Day	Antigen ^a	Adjuvant ^b
1	0	Neo-C (C), 100 µg	FCA
2	20	Neo-C (C), 100 µg	FIA

APPENDIX

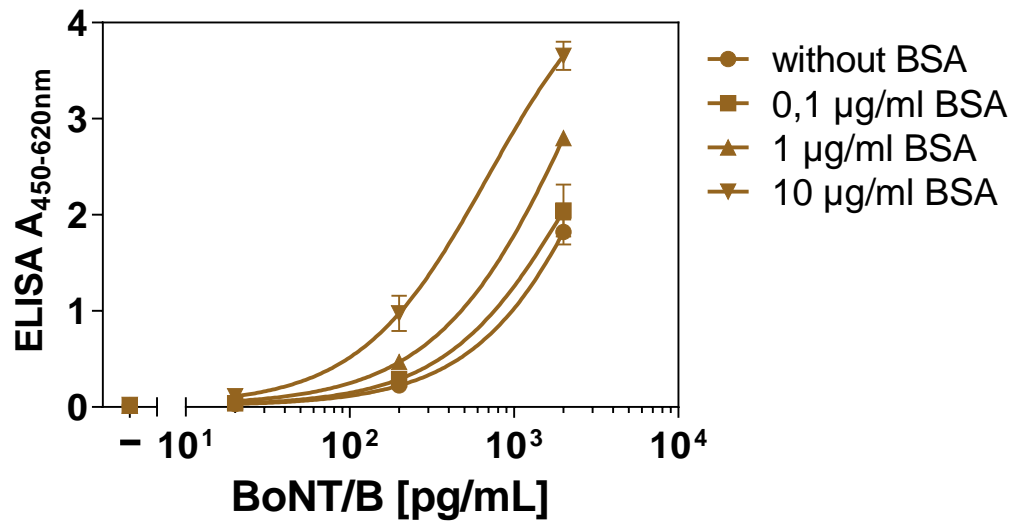
3	48	Neo-C (C), 100 µg	FIA
4	110	Neo-C (C), 100 µg	—
5	111	Neo-C (C), 100 µg	—
6	112	Neo-C (C), 100 µg	—
	113	Fusion	

^asee Table 11 in Material and Method section 4.1.5

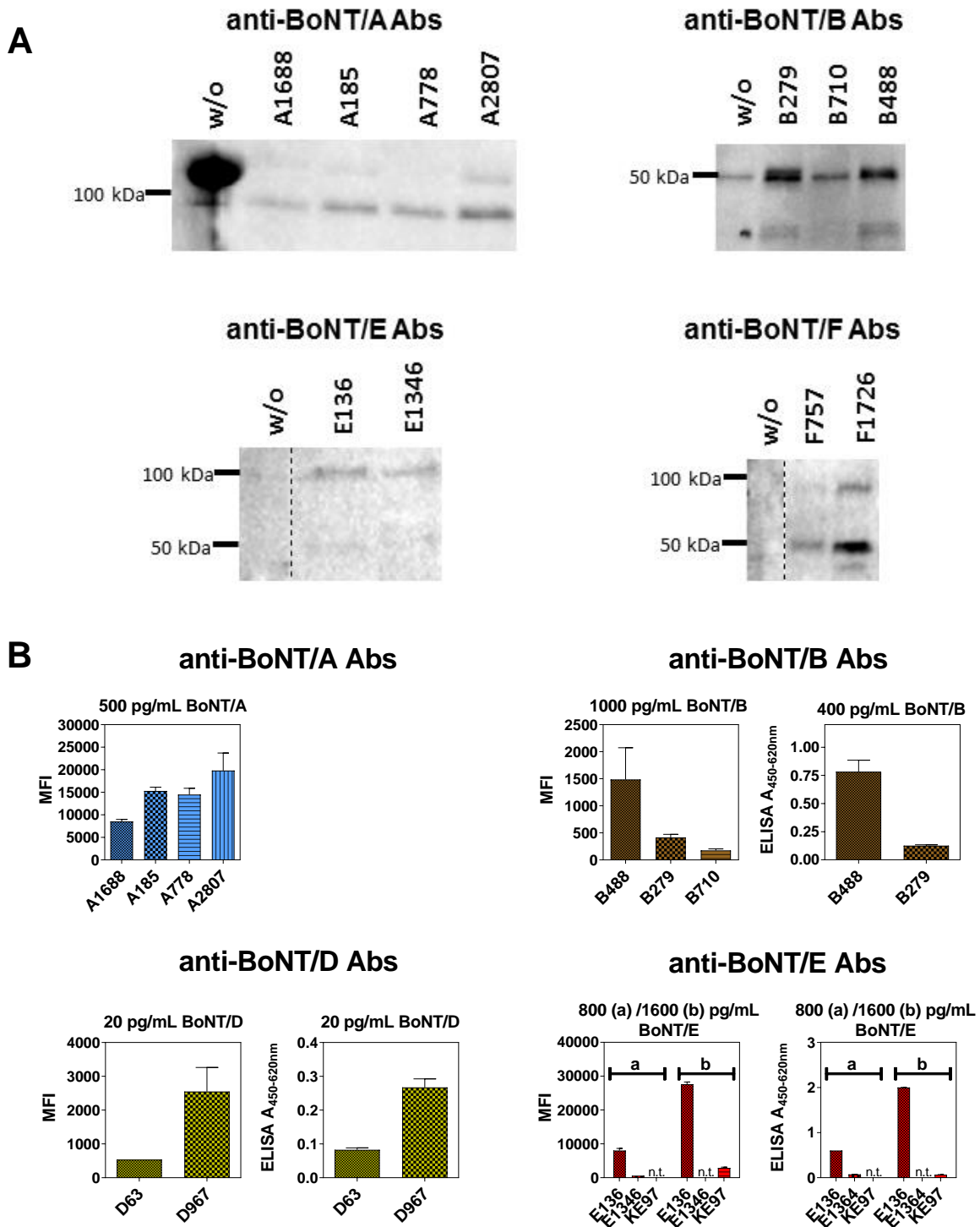
^b FCA = Freund’s complete adjuvant; FIA = Freund’s incomplete adjuvant



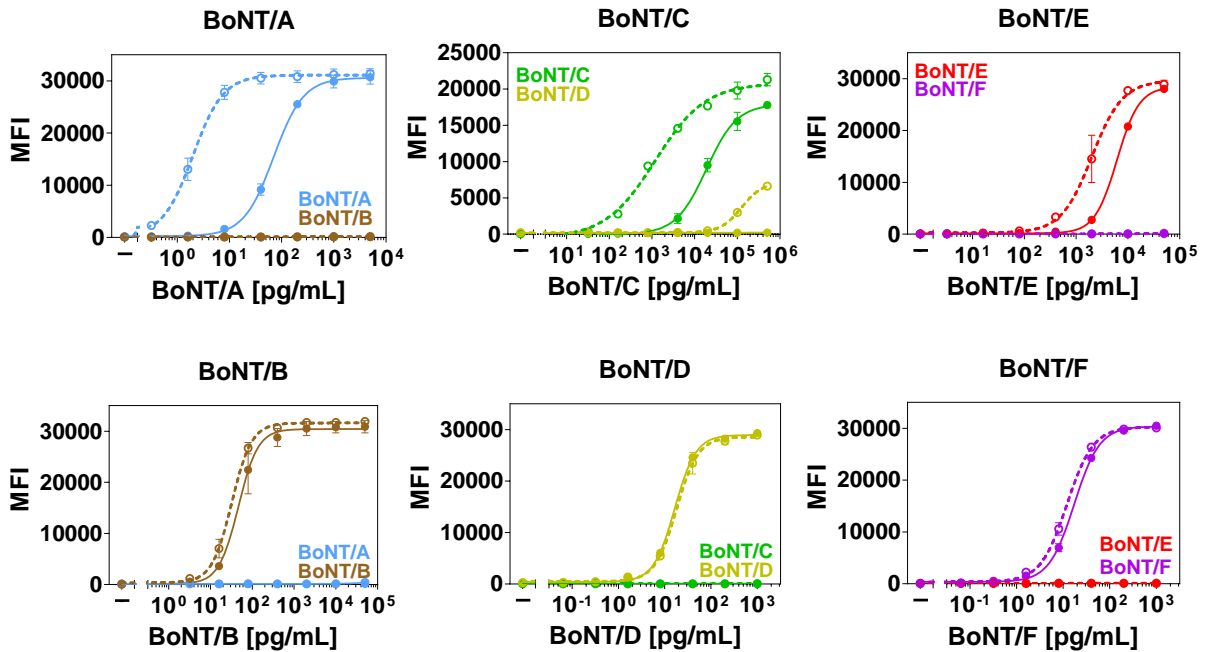
Appendix Figure 2: Development of antibody titres after immunization with short BSA-coupled 8 mer peptides. For immunizations, 100 µg short BSA-coupled 8mer peptides corresponding to the respective N- or C-terminal neopeptide of different BoNT cleavage sites were used as indicated. Antibody titres were determined by indirect ELISA. (p.i. = post immunization; n = 2; Mean ± SD).



Appendix Figure 3: Addition of BSA to coating buffer increases the sensitivity of the Endopeptidase-ELISA with Neo-mAb VAMP/B/151 for BoNT/B detection. VAMP-2 was coated on microtiter plates with the addition of different concentrations BSA (as indicated) to the coating mixture. Substrate was then cleaved by serial dilutions of BoNT/B and cleavage products were detected with VAMP/B/151. Single data points were log-transformed ($X = \text{Log}(X)$) and curves were fitted using a four-parameter fit ($n = 2$; Mean \pm SD).

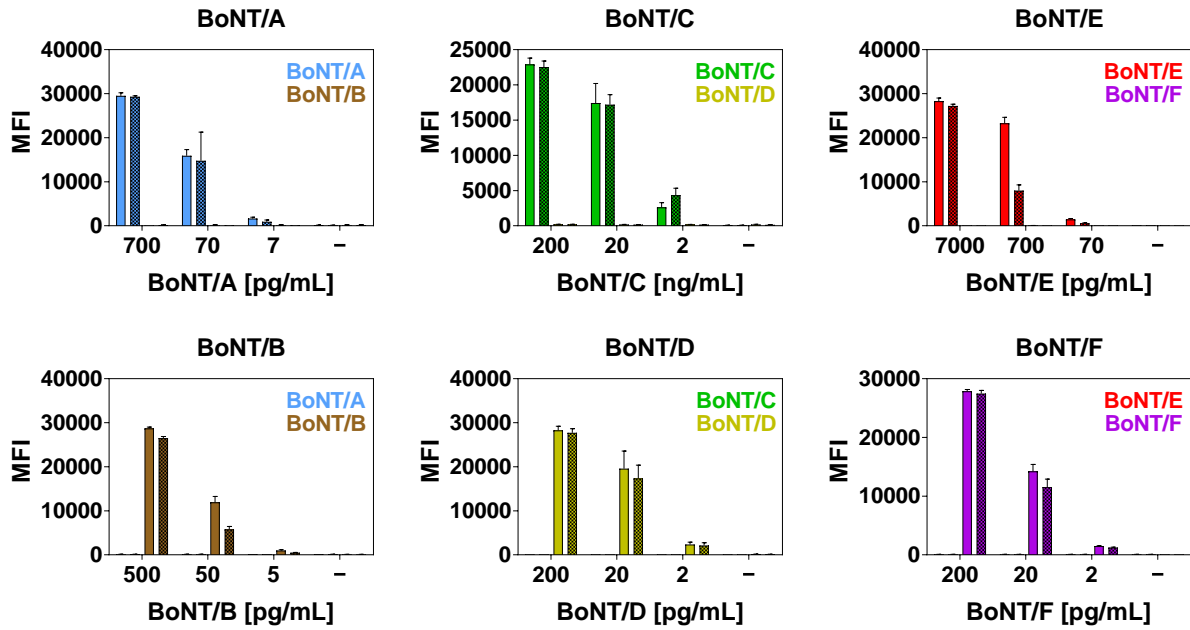


Appendix Figure 4: Comparison of anti BoNT antibodies in Bead-Western (A) or endopep-assays (B). (A) BoNT was enriched with anti-BoNT antibodies coupled to paramagnetic dynabeads as indicated and detected via western blotting. For detection, biotinylated detection antibodies (anti-BoNT/A: A360 (HC-specific); anti-BoNT/B: B335 (LC-specific); anti-BoNT/E: KE97 (polyclonal); anti-BoNT/F: KF98 (polyclonal) and SA-POD were used. This data was generated by Daniel Stern. (B) BoNT was enriched as above with anti-BoNT antibodies coupled to paramagnetic dynabeads and beads were used in the duplex-assay (left image of each panel) or Endopeptidase-ELISA (right image of each panel, for BoNT/A, the duplex-assay was performed only).

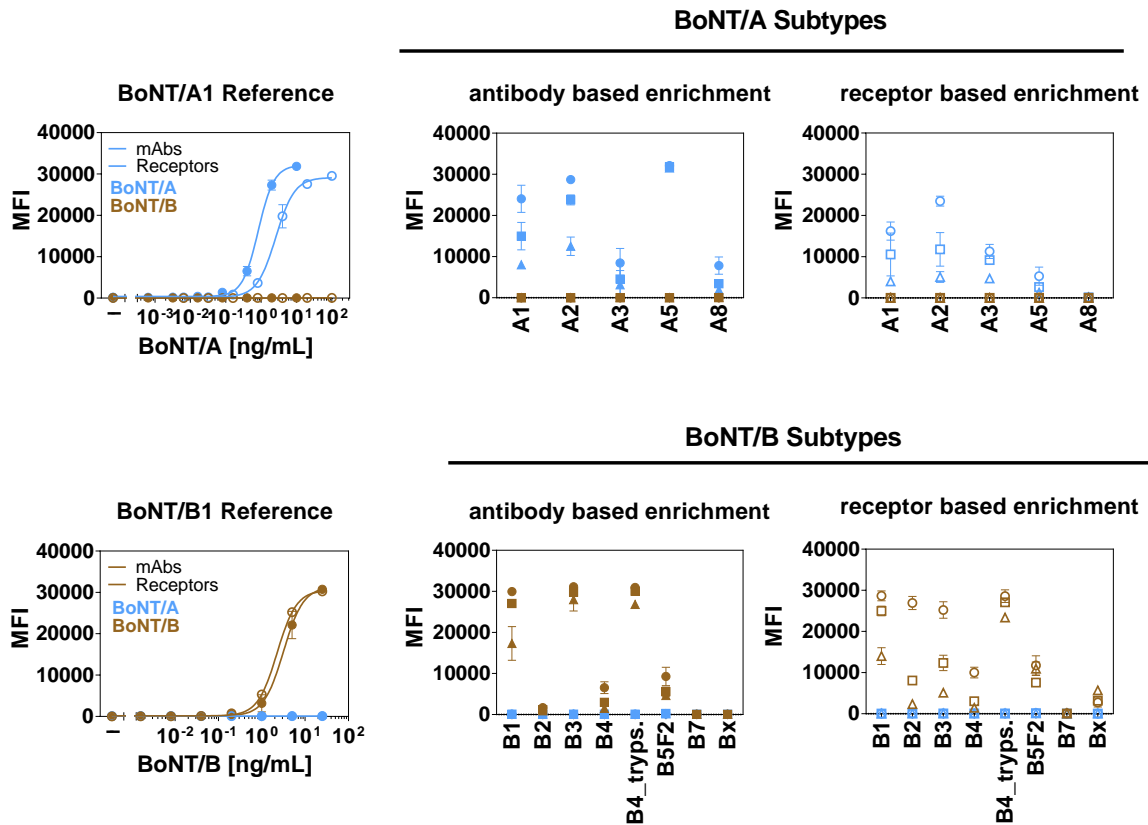


Appendix Figure 5: Detection of catalytically active BoNT/A-F with the duplex-assay. For enrichment (closed circles, continuous line) BoNT was diluted in BSA/PBS and enriched with monoclonal anti-BoNT antibodies (as indicated in Table 27) coupled to paramagnetic dynabeads. Samples without enrichment (open circles, dashed line) were directly diluted in cleavage buffer. For samples with an enrichment step the starting volume was doubled. Captured/diluted toxin was mixed with VAMP-2 and SNAP-25 coupled to luminex-beads for substrate cleavage and cleavage products were subsequently detected by Neo-mAbs. Results from two independent experiments with each repeat performed in technical duplicates are shown ($n = 4$; Mean \pm SD; MFI = Median fluorescent intensity).

APPENDIX



Appendix Figure 6: Detection of catalytically active BoNT/A-F from spiked BSA/PBS and spiked serum samples by three duplex-assay. BoNT was diluted in BSA/PBS (plain bars) or serum (chequered bars) and enriched with monoclonal anti-BoNT antibodies coupled to magnetic dynabeads. Captured toxin was mixed with VAMP-2 and SNAP-25 coupled to luminex-beads for substrate cleavage and cleavage products were subsequently detected by Neo-mAbs. Results from two independent experiments with each repeat performed in technical duplicates are shown (n = 4; Mean ± SD; MFI = Median fluorescent intensity).



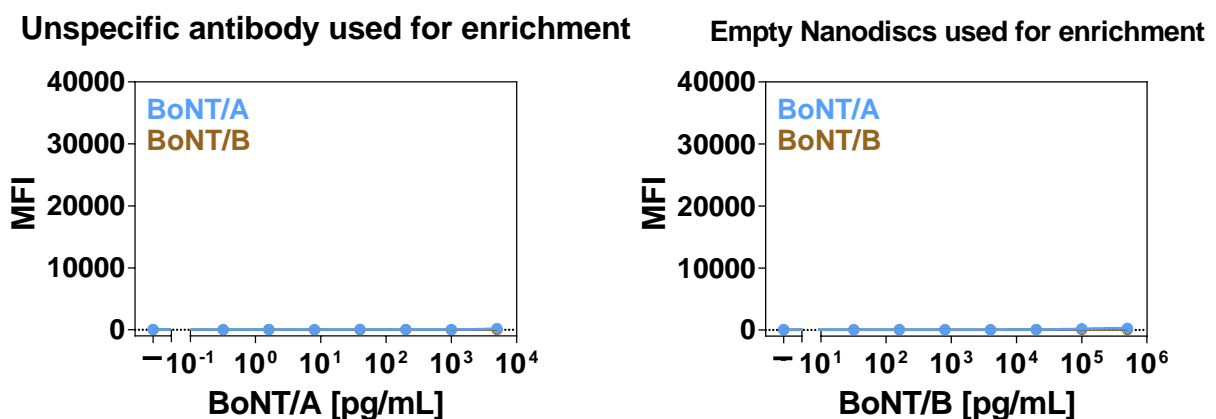
Appendix Figure 7: Testing of different *Clostridia* supernatants of different BoNT/A and B subtypes in the duplex-assay with antibody-based or receptor-based enrichment. *Clostridia* supernatants were diluted in 0.1%BSA/PBS as indicated in Appendix Table 11 and enriched with antibodies or receptor molecules. Captured toxin was mixed with VAMP-2 and SNAP-25 coupled to luminex-beads for substrate cleavage and cleavage products were subsequently detected by Neo-mAbs. Results from two independent experiments with each repeat performed in technical duplicates are shown (n = 4; Mean ± SD; MFI = Median fluorescent intensity). The following *Clostridia* strains were used: A1: NCTC7272, A2: Friedrichshain, A3: 15-168-01, A5: 15-023-04 Eriwan, A8: Chemnitz, B1: NCTC7273, B2: REB89, B3: 15-019-01, B4: Templin, B5F2: 14-080-11, B7: NCTC3807, Bx: KL34/08.

Appendix Table 11: Applied dilutions of *Clostridia* supernatants for determination of toxin concentration with the duplex-assay with antibody-based or receptor-based enrichment. Results of the duplex-assay are shown in Appendix Figure 7. Determined toxin concentrations are shown in Table 33.

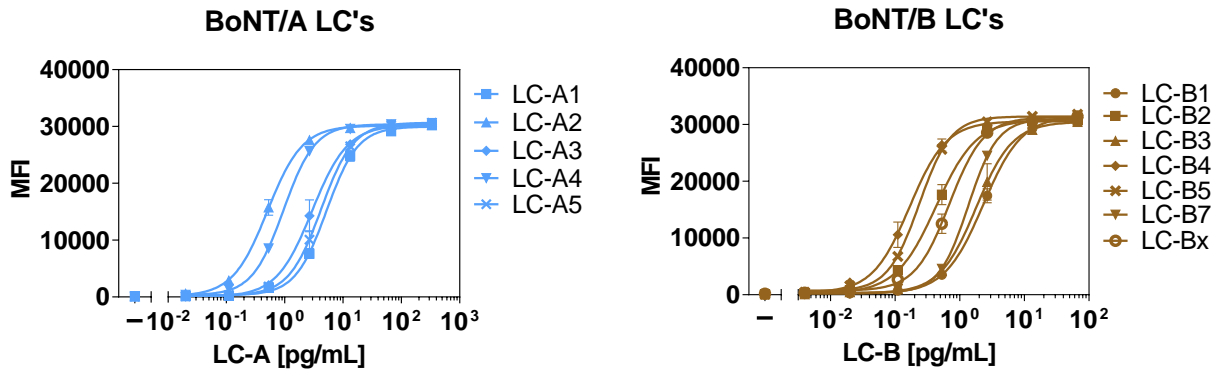
	Enrichment with mAbs			Enrichment with receptors		
	Dilution 1 ^a ● ●	Dilution 2 ^a ■ ■	Dilution 3 ^a ▲ ▲	Dilution 1 ^a ○ ○	Dilution 2 ^a □ □	Dilution 3 ^a △ △
NCTC7272 (A1)	1:2000	1:4000	1:8000	1:500	1:1000	1:2000
Friedrichshain (A2)	1:4000	1:8000	1:16000	1:125	1:250	1:500
15-168-01 (A3)	1:500	1:1000	1:2000	1:50	1:100	1:200
15-023-04 Eriwan (A5)	1:4000	1:8000	1:16000	1:250	1:500	1:1000
Chemnitz (A8)	1:25	1:50	1:100	1:1	1:2	1:4
NCTC7273 (B1)	1:1000	1:2000	1:4000	1:1000	1:2000	1:4000
REB89 (B2)	1:5	1:10	1:20	1:400	1:2000	1:10000
15-019-01 (B3)	1:4000	1:8000	1:16000	1:4000	1:8000	1:16000
Templin (B4)	1:25	1:50	1:100	1:25	1:50	1:100
Templin_tryps (B4) ^b	1:4000	1:8000	1:16000	1:4000	1:8000	1:16000
14-080-11 (B5F2)	1:2	1:4	1:8	1:4	1:8	1:16
NCTC3807 (B7)	1:2	1:4	1:8	1:2	1:4	1:8
KL34/08 (Bx)	1:5	1:10	1:20	1:5	1:10	1:20

^aSymbols refer to Appendix Figure 7.

^b Supernatant was trypsinated prior to the assay.



Appendix Figure 8: Usage of unspecific molecules coupled to dynabeads for enrichment in the duplex-assay. Dynabeads coupled to an unspecific antibody (left panel) or empty Nanodiscs (right panel) were added to BoNT diluted in BSA/PBS. Beads were then washed and mixed with VAMP-2 and SNAP-25 coupled to luminex-beads for substrate cleavage. Cleavage products were subsequently detected by Neo-mAbs. Results from one experiment performed in technical duplicates is shown (n = 2; Mean ± SD; MFI = Median fluorescent intensity).



Appendix Figure 9: Comparison of recombinant LC's of different BoNT/A and B subtypes in the duplex-assay. Serial dilutions of different light chains were incubated with VAMP-2 and SNAP-25 coupled to luminex-beads for substrate cleavage. Cleavage products were subsequently detected by Neo-mAbs. Results from two independent experiment with each repeat performed in technical duplicates are shown (n = 4; Mean ± SD; MFI = Median fluorescent intensity).